THEORETICAL STUDIES IN CONDENSATION ON BANKS OF PLAIN TUBES

by

MUDATHER IBRAHIM

MUDATHER

ZEINELABDEEN

in part of fullfilment

of the requirements for the degree of

DOCTOR OF PHILOSPHY

in the

School of Engineering and Materials Science

Queen Mary and Westfield College

University of London

Mile End Road

London E1 4NS

UK

Abstract

Condensation on banks of tubes is of considerable interest in the power, refrigeration and process industries, where large scale condensers form a significant proportion of plant capital costs. Since the pioneering paper by Nusselt in 1916, numerous investigations, both experimental and theoretical, have made great inroads into the understanding of the important physical factors effecting performance, including effects of vapour shear and condensate inundation on heat-transfer performance. Despite this there are still significant gaps in the knowledge and no single recognised design approach exists for condensers under all conditions. Purely theoretical models have shown some success in modelling condensation on single tubes under high shear regimes, but these have not been successfully extended to full tube banks.

The present work begins by drawing together a comprehensive data base of experimental results from those available in the literature. This includes assessing the experimental accuracy of the data and organising it into a consistent format to allow detailed comparison with existing and future models. The resulting data base comprises 13 tube bank geometries, 7 test fluids and over 4000 individual data points.

The data base was used to evaluate existing theoretical and empirical models, and highlighted the weaknesses therein. In particular, it was found that empirical approaches were limited to application (ie refrigeration or steam condensers), with development and validation being based on experimental data for single fluids or groups of fluids. When these models were compared to the more comprehensive data base described above their performance was poor. Consequently there is limited confidence in their extension to applications outside those they were developed for.

A new empirical based model was then developed. The approach involved identifying relevant dimensionless groups to account for the various physical factors which may affect heat transfer during condensation on a bank of tubes and formulating these into an equation involving a number of initially unknown but empirically obtainable constants. An iterative scheme was then employed to eliminate those groups having little effect on the result while retaining those which proved to be more important. The resulting model predicted the majority of the experimental data base to around 12%. A subsequent parametric study

showed the correct dependence of heat transfer coefficient on factors such as vapour velocity and tube row. The thesis concludes with some suggestions for future work.

ACKNOWLEDGEMENTS

First and foremost I would like to express my greatest thanks to my parents ; Nayla Osman and Ibrahim Mudather, and my older brother Mohammed, without them I could not have achieved this as they have endlessly supported me and motivated me to be positive in all my difficult and challenging moments.

I would like to convey my sincere appreciation to Dr Adrian Briggs, who has always inspired me to push myself when the road ahead became difficult and who was always keen to assist and advise me without hesitation. His guidance was the catalyst in my achievement of this endeavour.

I would like to express my thanks to my friends and colleagues at Queen Mary and Westfield College. It was a challenging period of my life to undertake this research and PhD, but it has been greatly enjoyable and rewarding.

Finally, a very special thanks to my friends Mohammed Kardaman, Mohammed Ismael, Ismael Jumaa, Anwar Mohamed and Ahmed Hassan for their support and friendship over these past years.

School of Engineering and Materials Science
Queen Mary and Westfield College
University of London
Mile End Road
London E1 4NS

List of Contents

List of Figures

Chapter 1

Chapter 3

Chapter 4

List of Tables

Chapter 1

Chapter 2

Chapter 3

Chapter 4

Nomenclature

Symbols

c_p - specific isobaric heat capacity, J/ kg K

c_{Pw} - specific isobaric heat capacity evaluated at the wall surface, J/ kg K

d - diameter of plain tube, m

G - mass velocity, $\rho_v U_\infty$, equation (1.79), kg / m^2s

g - specific force of gravity, m/s^2

h_{fg} - specific enthalpy of evaporation, J/kg

$h_{fg(N)}$ - specific enthalpy of evaporation at N_{th} row, evaluated at T_v, J/kg

k - thermal conductivity, W/m K

k_w - thermal conductivity evaluated at the wall surface, W/m K

L - length of tube , m

$m_{condensate}$ - local condensation mass flux, kg / m^2s

$m_{v(N)}$ - vapour mass flow rate to N_{th} row , kg/s

$m_{v(N+1)}$ - vapour mass flow rate to $(N+1)_{th}$ row, kg/s

P_t - horizontal tube pitch , m

P_l - vertical tube pitch , m

P_∞ - vapour pressure , Pa

P - pressure in equations 1.2 and 1.5, Pa

Q_N - heat-transfer rate to the tubes in N_{th} row, W

q - local heat flux, $\frac{k\Delta T}{\delta}$, W/m^2

$\bar{q}$ - mean heat flux, $\frac{1}{\pi}\int_0^{\pi}\frac{k\Delta T}{\delta}d\varphi$, W/m^2

R - radius of tube , m

R_v - specific ideal gas constant , J/ kg K

T - absolute temperature, K

T_{sat} - vapour saturation temperature, K

T_v - vapour temperature, K

T_w - local wall temperature, K

$\overline{T}_w$ - mean wall temperature, $\frac{1}{\pi}\int_0^{\pi}T_W d\varphi$, K

T_δ - temperature at condensate-vapour interface , K

U - x- wise condensate velocity, m/s

U_δ - vapour velocity at the vapour-liquid interface, m/s

U_∞ - free stream vapour velocity, m/s

U_{max} - vapour velocity just upstream of the Nth tube row based on the minimum flow area in tube bundle, m/s

U_{min} - vapour velocity just upstream of the Nth tube row based on the maximum flow area in tube bundle, m/s

$U_{mean-void}$ - vapour velocity just upstream of the Nth tube row based on the mean flow area in tube bundle , m/s

u - x- wise condensate velocity, m/s

V - y -wise vapour velocity, m/s

v - y- wise condensate velocity, m/s

x - coordinate in stream-wise direction, m

y - coordinate normal to the surface of the tube, m

Greek symbols

α - mean vapour-side heat-transfer coefficient, W/m^2 K

α_1 - mean vapour-side heat-transfer coefficient for the top tube in the bank, W/m^2 K

α_{gr} - gravity controlled heat-transfer coefficient , W/m^2 K

α_N - mean vapour-side heat-transfer coefficient for Nth tube (or tube row), W/m^2 K

α_{Nu} - mean vapour-side heat-transfer coefficient for horizontal plain tube, using Nusselt model (equation 1.15), W/m^2 K

α_{Nu-q} - mean vapour-side heat-transfer coefficient for horizontal plain tube from uniform heat flux theory, W/m^2 K

α_{sh} - shear controlled heat-transfer coefficient, W/m^2 K

$\overline{\alpha}_N$ - mean vapour-side heat-transfer coefficient for N tubes (or tube rows) , W/m^2 K

$\overline{\alpha}_{Nu}$ - mean vapour-side heat-transfer coefficient for N tubes (or tube rows) in a bank, using Nusselt uniform surface temperature model, W/m^2 K

Γ_N - the mass flow rate of the condensate per unit length drained from Nth tube, (or tube row) , kg / ms

γ_N - the condensation rate per unit length on the Nth tube , kg / ms

ΔP_1 - pressure difference given by equation 1.63, Pa

ΔP_2 - pressure difference given by equation 1.64, Pa

ΔT - temperature difference across the condensate film, $T_\delta - T_W$, K

$\overline{\Delta T}$ - mean temperature difference across the condensate film, K

δ - condensate film thickness, m

μ - dynamic viscosity, kg/ ms

μ_w - dynamic viscosity evaluated at the wall surface, kg / ms

ρ - density, kg/m^3

τ_δ - shear stress at the condensate surface, Pa

φ - angle from top of horizontal tube, radians

φ_c - angle at which, $\frac{d\delta^*}{d\varphi} \to \infty$,radians

Dimensionless groups

A - the wall temperature variation amplitude, $\frac{a}{\overline{\Delta T}}$

$A(\varphi)$ - defined by equation 1.33 or 1.35.

a - constant in equation 1.26.

a_1 - constant in equation 1.63.

a_2 - constant in equation 1.64.

B_1 - constant in equation 1.48.

B_2 - constant in equation 1.48.

F - dimensionless quantity, $\frac{\mu h_{fg} gd}{k\Delta T U_\infty{}^2}$

G - dimensionless quantity, $\frac{k\Delta T}{\mu h_{fg}}\left[\frac{\mu\rho}{\rho_v \mu_v}\right]^{\frac{1}{2}}$

H - dimensionless quantity, $\frac{c_P \Delta T}{h_{fg}}$

H_N - dimensionless quantity, $\frac{c_P \Delta T}{h_{fg}}$, for Nth tube.

J - dimensionless quantity, $\frac{k \Delta T}{\mu h_{fg}}$

J_v - dimensionless quantity, $\frac{xG}{\sqrt{dg\rho_v(\rho - \rho_v)}}$, in equation 1.79.

N - number of tube rows in a bank.

Nu- Nusselt number, $\frac{\alpha d}{k}$

Nu_{gr} - gravity-controlled Nusselt number.

Nu_{sh} - shear-controlled Nusselt number.

$Nu_{\pi/2}$ -Nusselt Number for a half tube, $\frac{\alpha_{\pi/2} d}{k}$

P - dimensionless number, $\frac{\rho_v h_{fg} \mu}{\rho k \overline{\Delta T}}$

Pr - dimensionless quantity, $\frac{c_P \mu}{k}$

Re_{eq} - Reynolds number, see equation (1.62).

Re_f - Reynolds number of film.

$Re_{f,gr}$ - Reynolds number of film based on gravity drained flow.

$Re_{f,u}$ - Reynolds number of film based on uniformly distributed flow.

$Re_{l,max}$ - Reynolds number of liquid flowing alone through the bundle and based on the maximum velocity (i.e.through minimum cross-sectional area between the tubes).

Re_v - vapour Reynolds number for horizontal tube, $\frac{\rho_v U_\infty d}{\mu_v}$

$Re_{v,max}$ - maximum vapour Reynolds number for horizontal tube, $\frac{\rho_v U_{max} d}{\mu_v}$

$\tilde{Re}$ - two-phase Reynolds number for horizontal tube, $\frac{\rho U_\infty d}{\mu}$

$\tilde{Re}_{max}$ - maximum two-phase Reynolds number for horizontal tube, $\frac{\rho U_{max} d}{\mu}$

x - vapour mass quality in equation 1.82.

z - dimensionless film thickness, $\frac{g\rho(\rho-\rho_v)h_{fg}}{\mu dk\overline{\Delta T}}\delta^4$

α_{1-3} - } coefficients in equations 1.22 and 1.23.

β_{1-3} - } coefficients in equations 1.22 and 1.23.

γ_{1-3} - } coefficients in equations 1.22 and 1.23.

γ - ratio of specific heat capacity at constant pressure to that of constant volume for a flowing vapour, $c_{p-v}/(c_{p-v}-R_v)$

δ^* - dimensionless film thickness, $\delta\left(\frac{U_\infty}{R\nu}\right)^{\frac{1}{2}}$

ε - void fraction (free volume divided by total volume)

ξ - fraction of the condensate drained from the Nth tube (tube row), which impinges the (N+1)th tube, (or tube row).

Subscripts

None - property of condensate.

B - h_{fg} corrected using equation 1.16.

gr - gravity-controlled region.

Nu - calculated from Nusselt Theory .

R - h_{fg} corrected using equation 1.17

sh - shear-controlled region .

v - property of vapour.

w - wall surface.

1. Introduction

1.1. Basic Knowledge.

Condensers are important and costly pieces of equipment, which play key roles in the power, air conditioning and refrigeration industries. Continuous research in the area of the condensation heat-transfer has aimed to minimise this capital cost while maximising efficiency. Condensation occurs on a surface when the saturation temperature of a vapour is higher than the temperature of the surface. Generally, there are two types of the condensation: drop-wise or film-wise. Drop-wise condensation takes place when the condensate does not wet the surface and accumulates to form the droplets, whereas film-wise condensation occurs when the solid surface is wetted by the condensate and forms a continuous film. Dropwise condensation produces vapour-side, heat-transfer coefficients up to 20 times higher than this for filmwise, but it has only ever been maintained consistently under laboratory conditions and even then only for high surface tension fluids such as water. Because of this, in practical condensers it is always assumed filmwise condensation will occur as this produces a conservative design.

For filmwise condensation of a saturated pure vapour, it is safe to assume that the vapour-side heat-transfer coefficient is controlled by the thermal resistance of the condensate film, and hence the thickness of this film is critical to the heat-transfer resistance and a thinner film will result in higher vapour-side coefficients. In 1916, Nusselt obtained theories for determining the heat-transfer coefficients in the case of filmwise condensations of a pure vapour on single tubes. Over the years, developments have been made to the Nusselt theory to account for effects which were originally neglected in the original model.

In the case of a single tube, increasing the vapour velocity leads to vapour shear stress at the surface of the condensate film which can result in a decrease of the average condensate film thickness, which in turn causes the heat-transfer rate to the surface to be increased.

Shell and tube condensers which consist of banks of plain tubes are usually arranged in the in-line or staggered form. An accurate estimation of the vapour-side heat transfer coefficient during condensation within a bank requires an understanding of the physical processes involved, which are more complex than that of single tubes, since they involve complex interactions between the vapour and the condensate film and inundation (condensate

from higher tubes impinging on lower tubes). In most studies, a reduction of the vapour-side heat transfer coefficient has been observed as the condensation of vapour takes place through the bank. This reduction is due to the drop-off in the vapour shear effect, which leads to the increase of the condensate film's thickness and the effect of the inundation.

Many researchers have conducted theoretical and experimental studies, and recommended models and empirical correlations to determine the heat-transfer coefficient for tube banks, but there are still uncertainties in estimating the heat-transfer coefficient for tube banks. The work described in this thesis is aimed at developing a simple and reliable empirical model for predicting the heat-transfer performance of shell-and-tube condensers which accounts for the effects of vapour shear and inundation. The model will be semi-empirical in nature and will be developed and validated using an existing experimental data base extracted from numerous earlier studies and including data for a wide range of test fluids, tube bank geometries and operating conditions.

1.2. Theory and Physical Problem.

1.2.1. Basic equations governing condensation on horizontal tubes.

Figure 1.1 shows the physical model and nomenclature for condensation of a saturated vapour on a horizontal tube. The governing equations for steady, two-dimensional incompressible laminar flow with constant properties are as follows,

Condensate film,

$$\frac{\partial u}{\partial x}+\frac{\partial v}{\partial y}=0 \tag{1.1}$$

$$\rho\left(u\frac{\partial u}{\partial x}+v\frac{\partial u}{\partial y}\right)=\mu\frac{\partial^2 u}{\partial y^2}-\frac{dP}{dx}+\rho g\sin\varphi \tag{1.2}$$

$$\rho c_P\left(u\frac{\partial T}{\partial x}+v\frac{\partial T}{\partial y}\right)=k\frac{\partial^2 T}{\partial y^2} \tag{1.3}$$

Vapour,

$$\frac{\partial U}{\partial x}+\frac{\partial V}{\partial y}=0 \tag{1.4}$$

$$\rho_v\left(U\frac{\partial U}{\partial x}+V\frac{\partial U}{\partial y}\right)=\mu_v\frac{\partial^2 U}{\partial y^2}-\frac{dP}{dx} \tag{1.5}$$

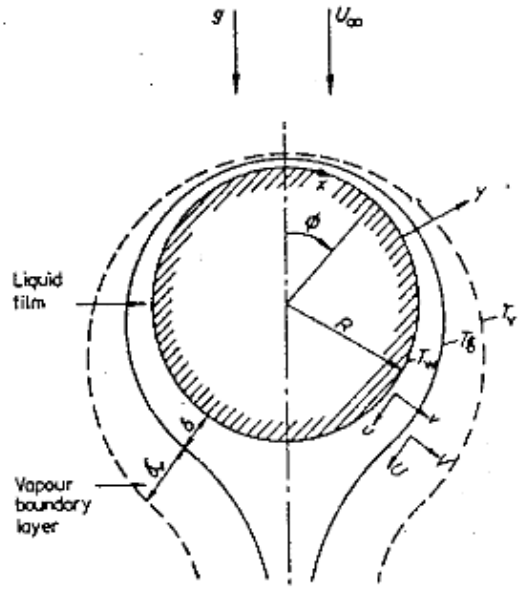

Figure 1.1. Coordinate system for condensation on horizontal plain tube (after Fujii (1972a)).

If the vapour is assumed saturated, then its temperature is uniform and the energy equation for the vapour boundary layer is not needed. The boundary conditions are:

At $y=0$ (solid surface)

$$u=v=0 \tag{1.6}$$

In addition, if it is assumed that the tube wall temperature is constant

$$T=T_W=\text{constant} \tag{1.7}$$

Alternatively, if it is assumed that the heat flux was constant at the tube wall, the temperature gradient at the wall would be:

$$\left(\frac{\partial T}{\partial y}\right)_{y=0}=\quad\text{constant} \tag{1.8}$$

At $y=\delta$ (liquid-vapour interface)

$$\rho\left(v-u\frac{d\delta}{dx}\right)=\rho_v\left(V-U\frac{d\delta}{dx}\right) \tag{1.9}$$

$$u=U \tag{1.10}$$

$$\mu \frac{\partial u}{\partial y} = \mu_v \frac{\partial U}{\partial y} \tag{1.11}$$

$$T = T_\delta = T_v = \text{constant} \tag{1.12}$$

Where equation (1.12) represents continuity of temperature at the liquid-vapour interface and neglects interfacial resistance, which would result in a temperature jump at the boundary. Equations (1.9)-(1.11), represent the continuity of mass transfer, velocity and shear stress at the interface. The problem is closed by introducing either continuity of mass or energy in the film.

$$k\left(\frac{\partial T}{\partial y}\right)_\delta = \rho h_{fg} \frac{d}{dx}\left(\int_0^\delta u dy\right) \tag{1.13}$$

$$k\left(\frac{\partial T}{\partial y}\right)_0 = \rho \frac{d}{dx}\left(\int_0^\delta \left(h_{fg} + c_p\left(T_\delta - T\right)\right) u dy\right) \tag{1.14}$$

There are two possible types of the flow during film-wise condensation on the surface of a plain tube; these are free convection and forced convection. Free convection condensation is where the vapour is stationary, in other words, if the effect of shear stress at the surface of the condensate is negligible compared to the effect of gravity $(U \to 0)$ as $y \to \infty$. On the other hand, forced convection condensation (higher vapour velocities) takes place when the effect of shear stress is comparable to or outweighs the effect of gravity $(U \to U_\infty)$ as $y \to \infty$.

1.3. Condensation on a Single, Horizontal Tube-Theoretical Treatments.

1.3.1. Free-Convection Condensation.

Nusselt (1916) derived analytical solutions for the condensation of stationary vapour on a horizontal plain tube. The assumptions were:

1. The condensate film is laminar.
2. The temperature of the surface where the condensation occurs is uniform.
3. The thickness of the condensate film is small compared to the radius of the tube.
4. The properties of the condensate are constant through the film.

5. Convective heat transfer across the condensate film is negligible compared to conduction.
6. The stationary vapour does not apply a shear force on the surface of the condensate film.
7. The inertia of the flowing condensate is negligible.
8. Sub-cooling in the condensate film is negligible.

Nusselt's analytical solution for a horizontal tube is given by the following equation:

$$\alpha_{Nu} = 0.728\left[\frac{\rho(\rho-\rho_v)gh_{fg}k^3}{\mu d\Delta T}\right]^{\frac{1}{4}} \tag{1.15}$$

(Note that in Nusselt's original paper, the coefficient in equation (1.15) was given as 0.725 due to an inaccuracy in Nusselt's original calculation). The result for the tube assumes $\delta << R$, which is not true for the bottom of the tube where $\delta \to \infty$, but the error is negligible since most of the heat transfer occurs in the thin film region at the top of the tube.

Bromley (1952) studied the effect of the sub-cooling of the condensate film on the Nusselt Theory, where the non-linear temperature gradient effect in the film was included in the analysis, resulting in a correction for h_{fg} in the Nusselt equation (equation 1.15), as follows:

$$h_{fg,B} = h_{fg}(1+0.4H) \tag{1.16}$$

Where

$$H = \frac{c_p\Delta T}{h_{fg}} \tag{1.17}$$

Rohsenow (1956) modified equation (1.16) by including the effect of cross-flow in the condensate film (i.e. flow-normal to the solid surface), which gave rise to a different correction term as follows:

$$h_{fg,B} = h_{fg}(1+0.68H) \tag{1.18}$$

Chen (1961) analysed condensation of stationary vapour on a horizontal tube using the boundary-layer approximations including the effects of the inertia, convection in the film

and interfacial shear stress, the latter using the asymptotic infinite condensation rate approximation, given by:

$$\tau_\delta = -mU_\delta \tag{1.19}$$

The corrected heat-transfer coefficient given by Chen is

$$\frac{\alpha}{\alpha_{Nu}} = \left(\frac{1+H(0.68+0.02J)}{1+J(0.95-0.15H)}\right)^{\frac{1}{4}} \tag{1.20}$$

Where

$$J = \frac{k\Delta T}{\mu h_{fg}} \tag{1.21}$$

Equation (1.20) fits the numerical results of Chen (1961) to within 1% in the following ranges, $H \le 2$ and $J \le 20$ for $Pr > 1$ or $Pr < 0.051$. Figure 1.2 represents the numerical results for condensation on a horizontal tube for different values of Prandtl numbers. For the high values of Prandtl numbers ($Pr > 1$), the effect of the surface shear stress on the heat transfer is negligible.

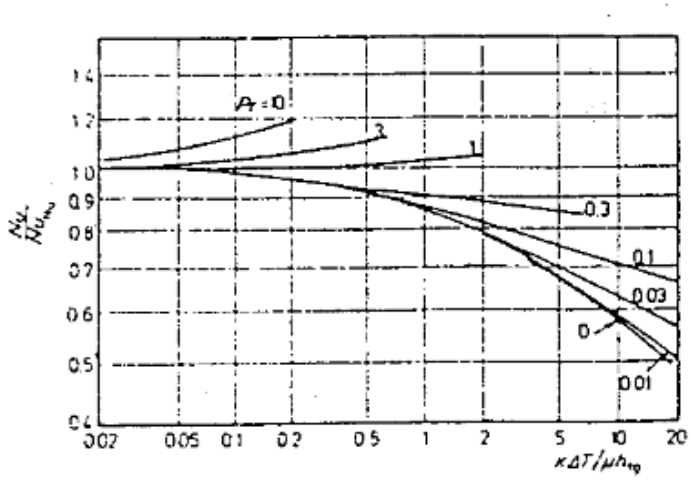

Figure 1.2. Numerical results for free-convection condensation on a horizontal plain tube (after Chen (1961a, 1961b)).

Maekawa and Rose (2015) replicated the method of Chen (1961), using a similarity solution for the liquid boundary layer in preference to the integral solution used by Chen, to obtain the following expression:

$$\frac{\alpha_v}{\alpha_{Nu}} = 1 + \left[\alpha_1 + \frac{\beta_1}{Pr}\right]H + \left[\alpha_1 + \frac{\gamma_1}{Pr} + \frac{\beta_2}{Pr^2}\right]H^2 + \left[\alpha_3 + \frac{\gamma_2}{Pr} + \frac{\gamma_3}{Pr^2} + \frac{\beta_3}{Pr^3}\right]H^3 \qquad (1.22)$$

or alternatively

$$\frac{\alpha_v}{\alpha_{Nu}} = 1 + \left[\alpha_1 Pr + \beta_1\right]J + \left[\alpha_1 Pr^2 + \gamma_1 Pr + \beta_2\right]J^2 + \left[\alpha_3 Pr^3 + \gamma_2 Pr^2 + \gamma_3 Pr + \beta_3\right]J^3 \qquad (1.23)$$

Where

$$Pr = \frac{c_P \mu}{k} \qquad (1.24)$$

and

$$\begin{aligned} \alpha_1 &= 0.1680 & \beta_1 &= -0.2418 & \gamma_1 &= 0.03577 \\ \alpha_2 &= -0.03250 & \beta_2 &= 0.1476 & \gamma_2 &= -0.006218 \\ \alpha_3 &= 0.005716 & \beta_3 &= -0.06092 & \gamma_3 &= -0.01980 \end{aligned}$$

Equation (1.22) is applicable for all Pr and for $H \le 1$ and $J \le 1$, and gives the numerical results to within 0.01% in most cases with a maximum error of 0.1% for $Pr = 1$ and H or J near unity.

In all the above treatments the constant wall temperature assumption was made (equation 1.7). Fujii et al. (1972b) obtained the following equation for the heat-transfer coefficient for a horizontal tube, assuming a uniform heat flux rather than uniform wall temperature, but otherwise based on the assumptions of the Nusselt (1916) theory:

$$\alpha_{Nu-q} = 0.695\left[\frac{\rho(\rho - \rho_v)g h_{fg} k^3}{\mu d \Delta T}\right]^{\frac{1}{4}} \qquad (1.25)$$

The heat-transfer coefficient in equation (1.25) is 5% lower than that of the original Nusselt analysis (equation 1.15). Lee and Rose (1982) pointed out that the solution for

uniform heat flux is strongly dependent on the lower half of the tube, where the assumption of $\delta << d$ is not applicable.

Memory and Rose (1991) included the variation of wall temperature around the tube for free convection laminar film condensation on a horizontal tube, using the following wall temperature profile:

$$T_w = a\cos\phi + \overline{T}_W \tag{1.26}$$

In equation (1.26), a is a constant, which depends on the ratio of the condensate heat-transfer coefficient (vapour-side) to the coolant heat-transfer coefficient. If the heat-transfer coefficient of the coolant is large compared to that of the condensate, the wall temperature will be fairly close to uniform (where a is close to zero). In other words, the equation of the surface temperature would be:

$$T_W = \overline{T}_W \tag{1.27}$$

If the heat-transfer coefficient of the vapour-side is large compared to the heat-transfer coefficient of the coolant, a is large and the surface temperature is more strongly dependent on the angle ϕ. For a saturated vapour (constant temperature), a temperature difference across the condensate film is given by the following equation:

$$\Delta T = \overline{\Delta T}(1 - A\cos\phi) \tag{1.28}$$

Where the value of A is in the range $(0 < A < 1)$, and $A = 0$ represents uniform temperature at the surface of the tube. The following table represents the key to curves in figure 1.3, where the measurements for condensation of ethylene glycol under certain conditions are compared with the distribution of cosine functions (Memory and Rose (1991)).

Table 1.1. Condensation of the steam on single plain tube-Experimental data base.

	T_{sat}/K	U_∞ / ms^{-1}	$\overline{\Delta T}$/K	A
a	425	3.6	109.8	0.048
b	425	3.6	105.3	0.051
c	425	8.9	96.3	0.1
d	398	22.0	64.6	0.133
e	398	22.0	53.5	0.163
f	398	49.0	40.5	0.242

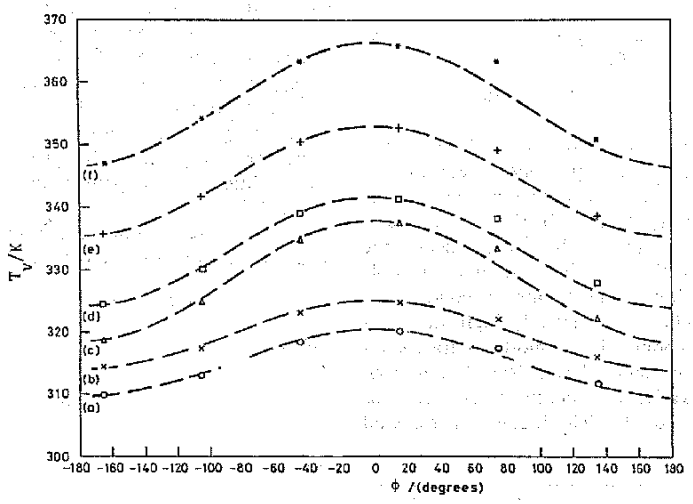

Figure 1.3. Distribution of the wall's surface temperature for condensation of Ethylene Glycol (Memory and Rose (1991)).

By using the conservation of mass, momentum and energy, the non-dimensionalized local heat flux would be as follow:

$$q^* = q\left\{\frac{\mu d}{\rho(\rho-\rho_v)gh_{fg}k^3\overline{\Delta T}^3}\right\} = (1-A\cos\varphi)z^{-\frac{1}{4}} \tag{1.29}$$

Where

$$z = \frac{g\rho(\rho-\rho_v)h_{fg}}{\mu dk\overline{\Delta T}}\delta^4 \tag{1.30}$$

A relationship between q^* and ϕ for different values of A is demonstrated in figure 1.4. In the case of uniform temperature (where $A=0$), the heat flux decreases with increasing angle around the tube. For A only slightly greater than zero however, the heat flux increases with increasing ϕ, where the effect on the heat transfer due to the rise in ΔT initially overcomes the increase of the film thickness. On the lower side of the tube, the effect of increasing film thickness eventually begins to dominate, which causes the heat flux to decrease with increasing angle around the tube for all values of A. The following equation demonstrates the mean Nusselt number around the tube:

$$\overline{Nu} = C\left[\frac{\rho_l(\rho_l-\rho_v)gh_{fg}d^3}{\mu k\overline{\Delta T}}\right]^{\frac{1}{4}} \tag{1.31}$$

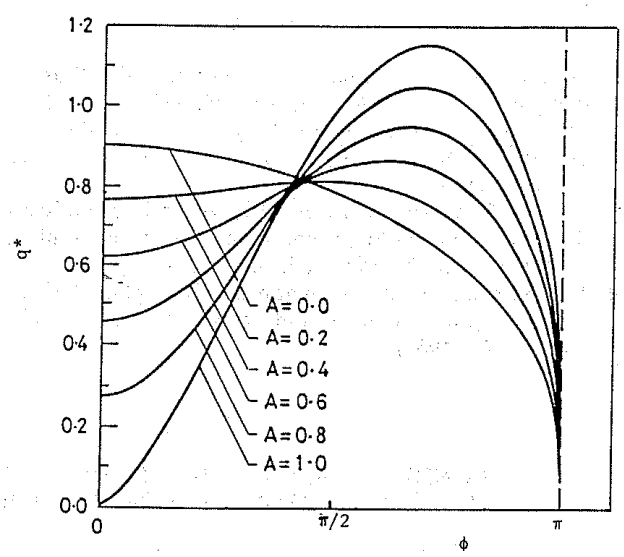

Figure 1.4. Heat flux against angle for free-convection condensation (Memory and Rose (1991)).

Where

$$C = \frac{1}{\pi}\int_0^{\pi}\left\{\frac{(1-A\cos\phi)\sin^{\frac{1}{3}}\phi}{\left[2\int_0^{\phi}\sin^{\frac{1}{3}}\phi d\phi - \frac{3A}{2}\sin^{\frac{4}{3}}\phi\right]}\right\}d\phi \qquad (1.32)$$

The value of C was obtained numerically from equation (1.32) for various values of A and found to be constant to four significant figures with a value of 0.7280 for all values of A. Therefore, despite large differences in the local heat flux for different values of A, the mean heat flux is independent of A.

1.3.2. Forced-Convection Condensation

For the analysis of forced convection condensation, many of the basic assumptions of the simple Nusselt theory for free-convection condensation can be retained, except that of neglecting the shear stress at the surface of the condensate film. Sugawara et al. (1956) proposed a theory that approximates the shear stress of a vapour boundary layer at any given point for forced convection flow over a dry, impermeable cylinder, given by the following equation:

$$\tau_{\delta} = \frac{\rho_v U_{\infty}^{\ 2}}{2\sqrt{Re_v}} A(\phi) \qquad (1.33)$$

Where

$$Re_v = \frac{\rho_v U_\infty d}{\mu_v} \tag{1.34}$$

$$A(\phi) = 6.0222\phi - 2.1114\phi^3 - 0.4053\phi^5 \tag{1.35}$$

ϕ is the angle around the tube in radians, measured from the forward stagnation point. Sugawara assumed that this equation can be applied at the surface of the condensate film when forced-convection condensation takes place. This equation predicts that the vapour boundary layer separates at $\phi = 83.3^\circ$, when $\tau_\delta = 0$. Figure 1.5 demonstrates the effect of vapour velocity on the local condensation heat-transfer coefficient for a horizontal plain tube up to the separation point. The condensation beyond this point was assumed to take place under Nusselt conditions, with zero vapour shear stress at the condensate surface. In the theory, the mean heat transfer was found to be higher than that predicted by Nusselt theory due to the effect of the vapour shear stress which thins the film over the forward part of the tube (before the point of separation).

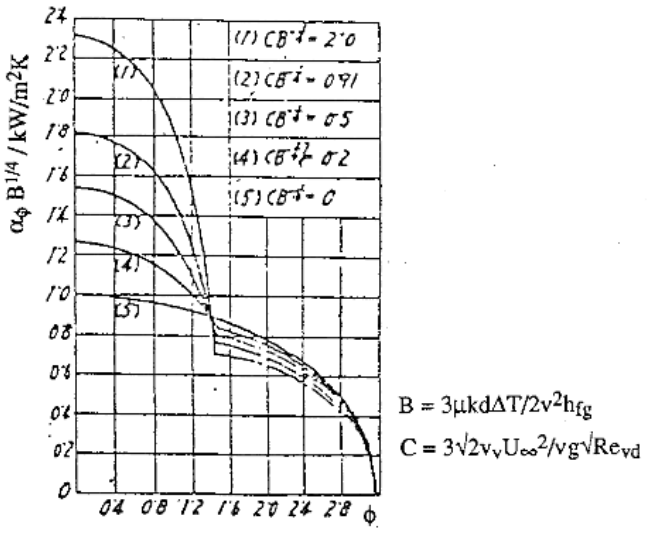

Figure 1.5. Effect of vapour velocity on the local condensation heat-transfer coefficient for a horizontal plain tube (after Sugawara et.al. (1956)).

Schlichting (1974) came up with a theory for the distribution of the shear stress at the surface of the film as expressed in equation (1.33), using the first five terms of the Blasius power series, given in the following expression:

$$A(\phi) = 6.973\phi - 2.732\phi^3 + 0.29\phi^5 - 0.018\phi^7 + 0.000043\phi^9 \qquad (1.36)$$

This theory predicts that separation occurs at an angle $\phi = 108.8^\circ$ from the forward stagnation point of the tube. Using equation (1.36), Nicol and Wallace (1974) showed the variation of the condensate film thickness around a horizontal plain tube for forced-convection of steam, their result are shown in figure 1.6, corresponding to the given velocities and its variation of the local heat-transfer coefficient is shown in figure 1.7.

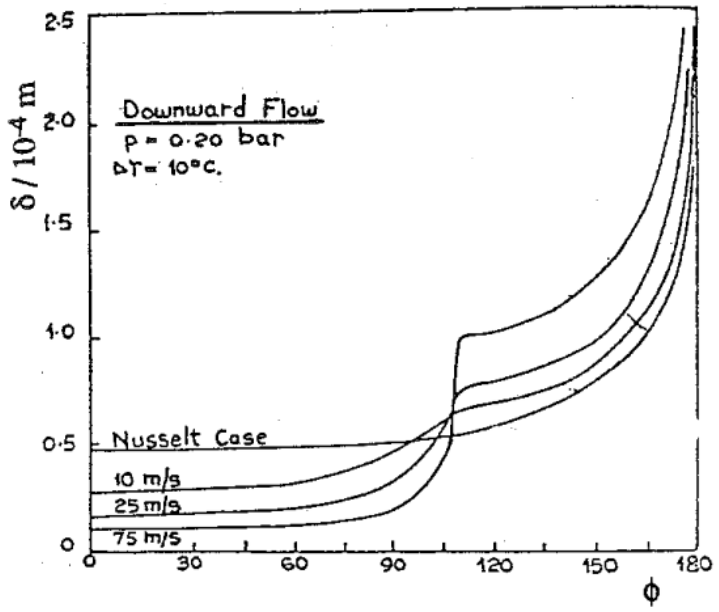

Figure 1.6. Variation of condensate film thickness around a horizontal plain tube for forced-convection condensation of steam (after Nicol and Wallace (1974)).

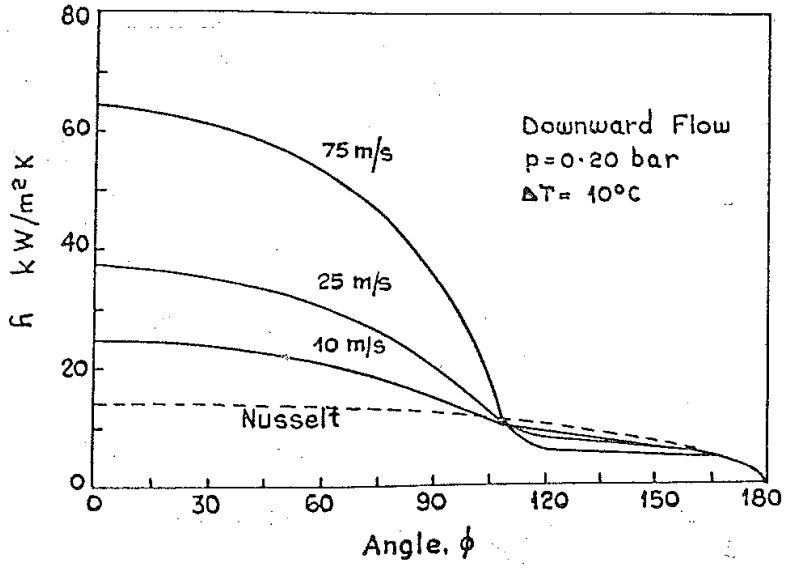

Figure 1.7. Variation of local heat-transfer coefficient around a horizontal plain tube for forced-convection condensation of steam (after Nicol and Wallace (1974)).

Shekriladze and Gomelauri (1966) recommended that the interfacial surface shear stress be given by the following equation:

$$\tau_\delta = m\left(U_\phi - U_\delta\right) \tag{1.37}$$

Where $U_\phi = 2U_\infty \sin\phi$ (assuming potential flow), and U_δ represents a velocity at the vapour-liquid interface. Equation (1.37) indicates that there is no boundary-layer separation. They determined the following expression for the vapour flowing over a tube in the absence of the effects of gravity, inertia, pressure drop, and convection in the film, and by assuming that $U_\phi >> U_\delta$,

$$Nu\,\tilde{Re}^{-\frac{1}{2}} = 0.9 \tag{1.38}$$

Where

$$\tilde{Re} = \frac{\rho U_\infty d}{\mu} \tag{1.39}$$

To include the effect of the gravity, Shekriladze and Gomelauri (1966) suggested the following equation:

$$Nu\,\tilde{Re}^{-\frac{1}{2}} = 0.64\left(1+\left(1+1.69F\right)^{\frac{1}{2}}\right)^{\frac{1}{2}} \tag{1.40}$$

Where

$$F = \frac{\mu h_{fg} g d}{k U_\infty{}^2 \Delta T} \tag{1.41}$$

With F indicating the relative importance of gravity and vapour velocity on the motion of the condensate film. If the value of this parameter is low, the flow is forced convection, while if it is high, the flow would be free convection. Equation (1.40) satisfies both gravity and vapour-shear controlled extremes, and gives values of Nu within 2% of the numerical solutions.

Shekriladze and Zhorzholiani (1973) approached the problem using the same assumptions as Shekriladze and Gomelauri (1966), but by treating the circumference of the

horizontal tube as a large number of flat plates. The numerical results obtained from this method are compared with equation (1.40) and demonstrated in figure 1.8. It can be seen that the obtained values of $\mathrm{Nu}\,\tilde{\mathrm{R}}\mathrm{e}^{-\frac{1}{2}}$ from this method satisfy with that in equation (1.40).

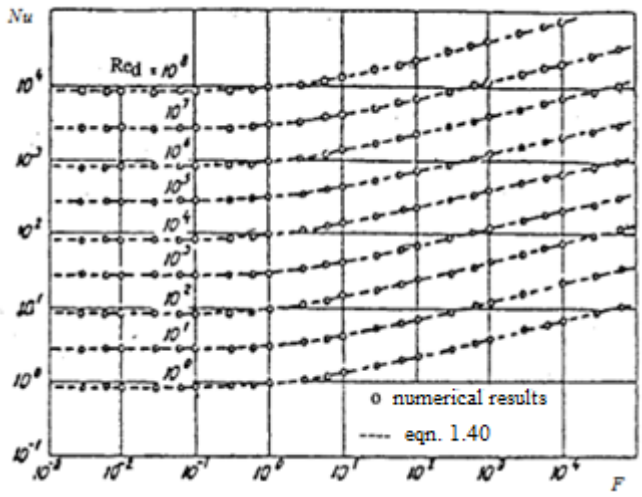

Figure 1.8. Comparison of the numerical results of Shekriladze and Gomelauri with equation (1.33) (after Shekriladze and Gomelauri (1966)).

For free convection flow $(\mathrm{F} \to \infty)$, equation (1.15), which has been derived analytically by Nusselt (1916) for a uniform temperature can be expressed as follows:

$$\mathrm{Nu}\,\tilde{\mathrm{R}}\mathrm{e}^{-\frac{1}{2}} = 0.728\mathrm{F}^{\frac{1}{4}} \quad (\text{assuming } \mathrm{U}_{\infty} \to 0) \tag{1.42}$$

As $\mathrm{F} \to \infty$, equation (1.40) tends to equation (1.42), while at low F, it tends to equation (1.38).

To account for vapour-boundary-layer separation Shekriladze and Gomelauri considered the earliest point at which separation could occur at $\phi = 82^{\circ}$, and neglected heat transfer beyond this position. They arrived at the following expression:

$$\mathrm{Nu}\,\tilde{\mathrm{R}}\mathrm{e}^{-\frac{1}{2}} = 0.42\left(1+\left(1+1.69\mathrm{F}^{\frac{1}{2}}\right)\right)^{\frac{1}{2}} \tag{1.43}$$

Lee and Rose (1982) improved equation (1.43) to blend with the Nusselt theory at low velocity, to give the following expression:

$$\mathrm{Nu}\,\tilde{\mathrm{Re}}^{-\frac{1}{2}} = 0.42\left(1+\left(1+9.47\mathrm{F}^{\frac{1}{2}}\right)\right)^{\frac{1}{2}} \tag{1.44}$$

Fujii et al. (1972a) provided an expression which satisfied the Nusselt result (free convection) at low velocity (equation (1.42)) and the high velocity (forced convection) extremes, giving a close fit to numerically-obtained solutions to within 5% by matching the vapour-shear stress at the vapour-condensate interface and using the integral treatment of the vapour boundary-layer. They assumed a quadratic velocity profile in the vapour, where the shear stress at the interface would always be positive, which avoids the separation problem. Figure 1.9 shows the variation of the local heat-transfer coefficient around the tube obtained using this method, for condensation of steam.

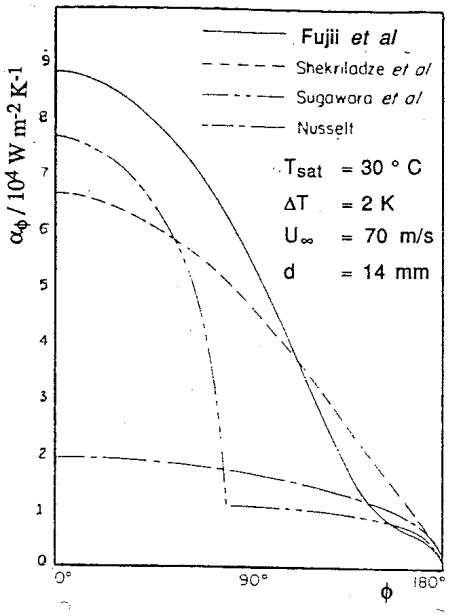

Figure 1.9. Comparison of the numerical results of Shekriladze and Gomelauri with equation (1.33) (after Shekriladze and Gomelauri (1966)).

The solution of Fujii et al. (1972a) gives higher heat-transfer coefficients for most of the tube compared to the Shekriladze and Gomelauri (1966) model, due to the fact that the actual vapour shear stress at the condensate surface is larger than either the zero or infinite

condensation rate asymptotes. Fujii et al. (1972a) gave the following approximate equation for the average Nusselt number:

$$\mathrm{Nu}\,\tilde{\mathrm{Re}}^{-\frac{1}{2}} = 0.9\left(1+\mathrm{G}^{-1}\right)^{\frac{1}{3}}\left[1+\frac{0.421\mathrm{F}}{\left(1+\mathrm{G}^{-1}\right)^{\frac{4}{3}}}\right]^{\frac{1}{4}} \tag{1.45}$$

Where

$$\mathrm{G} = \frac{\mathrm{k}\Delta\mathrm{T}}{\mu\mathrm{h}_{\mathrm{fg}}}\left[\frac{\mu\rho}{\rho_{\mathrm{v}}\mu_{\mathrm{v}}}\right]^{\frac{1}{2}} \tag{1.46}$$

For pure forced convection $(\mathrm{F}\to 0)$, equation (1.45) simplifies to the following,

$$\mathrm{Nu}\,\tilde{\mathrm{Re}}^{-\frac{1}{2}} = 0.9\left(1+\mathrm{G}^{-1}\right)^{\frac{1}{3}} \tag{1.47}$$

Fujii et al. (1979) presented a correlation, which approximates $\mathrm{Nu}\,\tilde{\mathrm{Re}}^{-\frac{1}{2}}$ using their data for steam, in terms of the film-condensate's properties and the conditions of the flowing vapour, which is given in the following expression:

$$\mathrm{Nu}\,\tilde{\mathrm{Re}}^{-\frac{1}{2}} = \mathrm{B}_1\left(\frac{\mathrm{g}^2\mathrm{d}\rho\mu\mathrm{h}_{\mathrm{fg}}}{\mathrm{U}_\infty{}^3\mathrm{q}^2}\right)^{\mathrm{B}_2} \tag{1.48}$$

The values of B_1 and B_2 ,which are 0.91 and 0.13 ,were obtained by a fit to the experimental data, using the earlier data of Fujii et al. (1979) for steam, which is shown in Figure 1.10. Fujii et al. (1979) used his same earlier data and assumed a uniform heat flux takes place, where he proposed the following empirical correlation et al. (1981), which is applicable in a given range of F:

$$\mathrm{Nu}\,\tilde{\mathrm{Re}}^{-\frac{1}{2}} = 0.96\mathrm{F}^{\frac{1}{5}} \quad (0.03 < \mathrm{F} < 600) \tag{1.49}$$

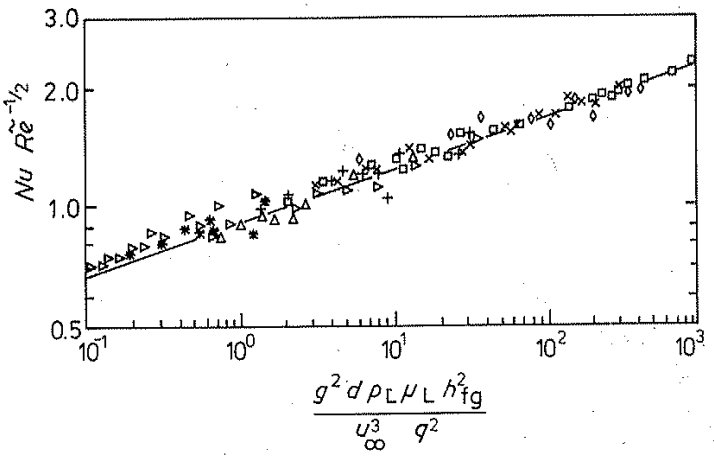

Figure 1.10. Comparison of the pure vapour data of Fujii et al. (1979) with equation (1.49).

Equation (1.49) illustrates that the heat-transfer coefficient increases with the vapour velocity at a rate $U_\infty^{0.1}$. For the lower vapour velocities (high F), Fujii et al. (1979) suggested the Nusselt theory (1916) (equation 1.42). There is a good agreement between their data and equation (1.49) as shown in figure 1.11.

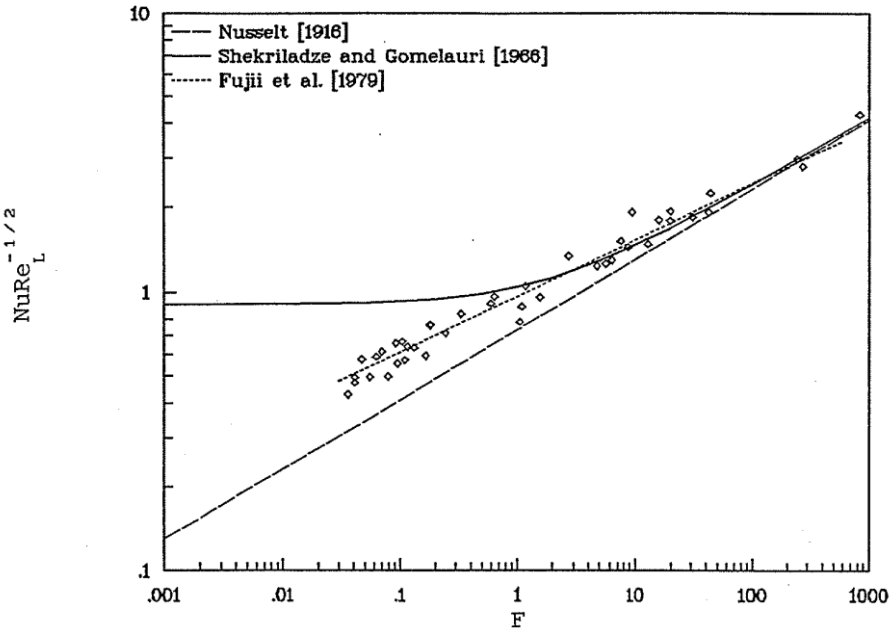

Figure 1.11. Data of Fujii et al. (1979) for steam.

Lee and Rose (1982) recommended the following conservative equation, which ignores the heat transfer beyond the separation position, rather than continuing the calculation with the shear stress set to zero:

$$\mathrm{Nu}\tilde{\mathrm{Re}}^{-\frac{1}{2}} = \xi\left[1+\frac{0.281\mathrm{F}}{\xi^4}\right]^{\frac{1}{4}} \tag{1.50}$$

Where

$$\xi = 0.88\left[1+\frac{0.74}{\mathrm{G}}\right]^{\frac{1}{3}} \tag{1.51}$$

Rose (1984) repeated the theoretical analysis of Shekriladze and Gomelauri (1966) and suggested the following equation.

$$\mathrm{Nu}\tilde{\mathrm{Re}}^{-\frac{1}{2}} = \frac{0.9+0.728\mathrm{F}^{\frac{1}{2}}}{\left(1+3.44\mathrm{F}^{\frac{1}{2}}+\mathrm{F}\right)^{\frac{1}{4}}} \tag{1.52}$$

Equation (1.52) is a more accurate version of equation (1.40), which gives the values of $\mathrm{Nu}\tilde{\mathrm{Re}}^{-\frac{1}{2}}$ to within 0.4% of the numerically obtained values for all the ranges of F. At low vapour velocity $(\mathrm{F}\to\infty)$, it approaches the Nusselt (1916) theory (equation (1.42)), and at high vapour velocity $(\mathrm{F}\to 0)$, it tends to equation (1.38).

Rose (1984) also repeated the solution of Fujii et al. (1972a) in equation (1.45), which includes a small correction that accounts the vapour shear stress more accurately, from which for the large values of F, it satisfies with Nusselt (1916) theory (equation (1.42)), while for the low values of F, it satisfies with equation (equation (1.47)). The result of this analysis is given by the following equation:

$$\mathrm{Nu}\tilde{\mathrm{Re}}^{-\frac{1}{2}} = \frac{0.9\left(1+\mathrm{G}^{-1}\right)^{\frac{1}{3}}+0.728\mathrm{F}^{\frac{1}{2}}}{\left(1+3.44\mathrm{F}^{\frac{1}{2}}+\mathrm{F}\right)^{\frac{1}{4}}} \tag{1.53}$$

Finally Rose (1984) also modified the Shekriladze and Gomelauri (1966) model to take account of the effect of pressure variation around the tube. The insertion of a pressure term to the momentum balance for the condensate film added a new dimensionless parameter to the solution, i.e.

$$P = \frac{\rho_v h_{fg} \mu}{\rho k \overline{\Delta T}} \tag{1.54}$$

It was shown that for $P > \frac{F}{8}$, the thickness of a condensate film increases with position around the tube and becomes infinite at some position on the lower half of the tube. Figure 1.12 shows the calculated film thickness profiles with and without the pressure term. The insertion of the pressure term causes a thinner condensate film on the top-side of the tube, and a thicker film on the bottom-side.

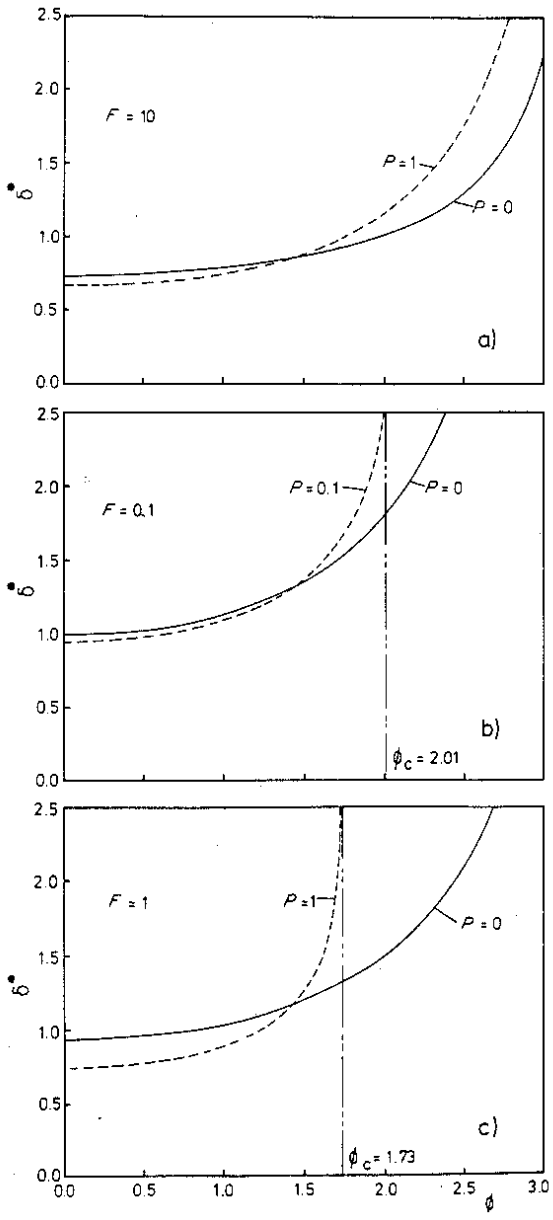

Figure 1.12. Variation of the calculated dimensionless condensate film thickness around a horizontal plain tube (after Rose (1984)).

These two effects counteract each other and the overall heat-transfer coefficient agrees to within 1% of that found when the pressure gradient term was neglected ($P = 0$). Angle ϕ_c represents the angle from the top of the tube to the location where $\frac{d\delta^*}{d\varphi} \to \infty$. An expression for ϕ_c was obtained for the given range of $P > \frac{F}{8}$, by minimizing the sum of the squares of the residuals of ϕ_c, which agrees with the numerical results to within 0.6% , and is given as follows:

$$\phi_c = \cos^{-1}\left\{\frac{-\left(1+21.5\theta(P)^{1.05}\right)}{\left(1+21.5(P)^{1.05}\right)}\right\} \tag{1.55}$$

Where

$$\theta = \frac{F}{8P} = \frac{\rho g d}{8\rho_v U^2{}_\infty} \le 1 \tag{1.56}$$

The following equation represents the adjustment of equation (1.53) including the effect of pressure variation.

$$Nu\,\tilde{Re}^{-\frac{1}{2}} = \frac{0.64(1+1.81P)^{0.209}\left(1+G^{-1}\right)^{\frac{1}{3}} + 0.728F^{\frac{1}{2}}}{\left(1+3.51F^{0.53}+F\right)^{\frac{1}{4}}} \tag{1.57}$$

A low vapour velocity $(F \to \infty)$, equation (1.57) approaches towards Nusselt theory (equation (1.42)). At high vapour velocity $(F \to 0)$, equation (1.57) neglects the heat transfer to the rear half of the tube, which generates the following equation:

$$Nu_{(\pi/2)}\,\tilde{Re}^{-\frac{1}{2}} = \frac{1.273(1+1.81P)^{0.209}\left(1+G^{-1}\right)^{\frac{1}{3}} + 0.866F^{\frac{1}{2}}}{\left(1+3.51F^{0.53}+F\right)^{\frac{1}{4}}} \tag{1.58}$$

The Honda (1986) model was based on experimental data for a refrigerant-113 condensing on a single tube, in which they performed a number of dye injection tests to determine the onset of turbulence. Honda et al. (1986) correlated their experimental data using the following semi-empirical model:

$$\alpha = \left(\alpha_{gr}^4 + \alpha_{sh}^4\right)^{\frac{1}{4}} \tag{1.59}$$

Where

$$\alpha_{gr} = 0.725\left(\frac{k}{d}\right)\left(F + 2.38\left(1 + G^{-1}\right)^{\frac{4}{3}}\right)^{\frac{1}{4}} \tilde{Re}^{\frac{1}{2}} \tag{1.60}$$

and

$$\alpha_{sh} = 0.11\left(\frac{k}{d}\right) Re_{eq}^{\ 0.8}\, Pr^{0.4} \tag{1.61}$$

Re_{eq} indicates an equivalent Reynolds number, which is defined by the following expression:

$$Re_{eq} = Re_f + \tilde{Re}\left(\frac{\rho_v}{\rho}\right)^{\frac{1}{2}} \tag{1.62}$$

Where Re_f is the condensate film Reynolds number, defined as $\frac{2\pi dq}{h_{fg}\mu}$. Equation (1.59) predicts the experimental data of Honda et al. (1986) for refrigerant-113 to within $\pm 15\%$.

1.4. Condensation on Single, Horizontal Tubes-Experimental Studies.

1.4.1. Measurements with steam.

Table 1.2 summarizes the experimental data for flowing steam condensing on horizontal tubes.

Berman and Tumanov (1962) performed condensation experiments with low pressure steam flowing vertically downward over a horizontal tube with a tube outside diameter of 19mm. The heat flux was obtained from the mass flow rate and temperature rise of the coolant water. The surface temperature was evaluated using a resistance thermometer mounted in a groove in the tube wall.

Fujii et al. (1972a) studied condensation of steam at low pressure flowing at an angle of 3º to a horizontal across single brass tube positioned in a circular duct, with outside diameter of 92mm. The heat flux was calculated from the mass flow rate and temperature rise of the coolant water. The outside tube was instrumented with eight thermocouples fitted in

the tube wall at intervals of 45º.The experiments were performed at pressures lower than atmospheric, while the vapour pressure and the velocity were controlled by the power input to the boilers and the coolant flow rate through the dump condenser. The vapour velocity was calculated from the power input to the boilers using a steady flow energy balance.

Table 1.2. Condensation of the steam on single plain tube-Experimental data base.

Reference	Tube Material	Outside diameter / mm	Length / mm	U_∞/(m/s)	T_{sat}/°C	ΔT/K
Berman and Tumanov (1962)	Not available	19	Not available	25.0	0.97-17.6	0.56-5.3
				31.5	0.96-13.0	0.71-6.5
				43.0	0.84-7.2	1.50-9.8
				80.0	0.26-1.5	2.10-12.1
Fujii et al. (1972a)	Brass	14	92	55.8-71.3	22.1-22.3	1.01-1.23
				35.4-36.3	20.3-20.8	1.00-1.05
				26.1-37.1	25.5-26.5	1.11-1.37
				22.5-24.8	21.5-22.0	1.42-1.97
Nicol and Wallace (1974, 1976) and Wallace (1975)	Aluminium Brass	19.05	143	10.3-148	21.7-64.9	9.60-20.4
Nobbs (1975) and Nobbs and Mayhew (1976)	Copper	19.1	500	0.58-7.96	99.1-102	13.6-29.4
	Copper	19.1	500	0.05-8.77	99.4-104	8.70-34.8
Fujii et al. (1979)	Copper	37.7	500	0.64-15.1	23.4-36.1	1.77-7.18
		37.7	97.5	0.70-79.9	30.5-38.3	2.04-8.05
	Brass	18.6	197	21.6-34.8	32.1-35.8	5.06-6.80
		18.6	96.5	4.40-64.2	31.2-38.8	3.15-5.56
Lee (1982) and Lee and Rose (1984)	Copper	25.25	109.5	0.44-15.2	30.3-102	3.21-41.5
		12.5	109.5	0.39-18.0	34.0-104	1.05-39.8

Nicol and Wallace (1974, 1976) and Wallace (1975) performed condensation experiments with low pressure steam flowing vertically downwards on an alloy single tube, which consists of aluminium and brass, located in a rectangular duct, of length 143mm and width 92.2 mm. The wall temperature was measured by groups of three thermocouples, at intervals of 120º and at four locations along the tube. The heat flux was calculated from the mass flow rate and the temperature rise of the coolant water. All the experiments were carried out at a vapour pressure of 18 kPa.

Nobbs (1975) and Nobbs and Mayhew (1976) obtained data for steam flowing vertically downwards over a single horizontal copper tube with outside diameter of 19.1mm and tube length of 500mm, positioned in a rectangular duct with a length of 500 mm and a

width of 95.3 mm. Since the working fluid was supplied from a steam main, the vapour velocity was evaluated from the total condensate accumulated from the test-tube and dump condenser. The heat flux was calculated from the flow rate and temperature rise of the coolant water. The vapour-side heat-transfer coefficient was calculated using two methods. In the first method, an instrumented tube was used to measure the wall temperature directly. In the second method, an un-instrumented tube was used, and the vapour-side heat-transfer coefficient was obtained using a modified version of the method of Wilson (1915). The vapour-side coefficient was evaluated from the coolant and the vapour conditions by assuming expressions for the inside and outside heat-transfer coefficients of the tube, containing constants, which were obtained by a least squares fit of the experimental data.

Fujii et al. (1979) carried out condensation of low pressure steam on a single horizontal tube with different diameters and lengths, situated in a rectangular duct with a width of 500mm. The width of the duct was varied by inserting acylic blocks which also changed the effective length of the tube. These gave higher vapour velocities while decreasing the working length of the test-tube. The tube was instrumented with eight thermocouples fitted in the tube wall and the heat flux was calculated from the coolant temperature rise and flow rate.

Lee (1982) and Lee and Rose (1984) carried out experiments with steam flowing vertically downwards over two different single copper tubes, with tube outside diameters of 25.25mm and 12.5mm and, tube length of 109.5mm. The tubes were located within a circular duct of diameter 152.4mm.The vapour velocity was evaluated from the power input to the boilers using a steady flow energy balance (including a small correction for losses to the atmosphere). Each tube had four thermocouples inserted in the tube wall at intervals of 90º with a 45º offset at the top of the tube. The heat flux was calculated from the coolant flow rate and temperature rise, which was checked by gathering the condensate flowing from the tube. The two methods agreed to within 5%.

1.4.2. Measurements with other Fluids.

The following table demonstrates the experimental databases that have been obtained by some of the investigators based on the flowing non-steam vapours over a horizontal tube.

Table 1.3. Condensation of the non-steam vapours on single plain tube-experimental data base.

Reference	Fluid	Tube Material	Outside diameter / mm	Length / mm	U_∞/(m/s)	T_{sat}/°C	ΔT/K
Gogonin and Dorokhov (1976)	R-21	Titanium	17.0	547	1.3	40-60	Not available
		Nickel	6.0	528	3.0	40-90	
			2.5	548	5.0	40-60	
Goto (1979)	Various	Not available	15.85	616	Low	Not available	Not available
Honda et al. (1982)	R-113	Copper	37.1	100	0.19-3.17	36.9-53.1	9.48-20.1
			8		0.19-7.73	41.9-50.8	4.96-25.3
Lee (1982) and Lee and Rose (1984)	R-113	Copper	12.5	109.5	0.47-2.77	24.7-51.1	7.80-36.4
Rahbar and Rose (1984) and Rahbar (1989)	R-113	Copper	12.5	109.5	0.1-8.60	19.4-50.7	4.07-37.7
	Ethylene Glycol				1.5-127	77.0-140	15.3-102
Honda et al. (1986)	R-113	Copper	19	100	0.34-8.50	48.0-52.0	3.0-29.0
			8		0.36-15.6	53.0-54.0	3.0-32.0
Memory and Rose (1986) and Memory (1989)	Ethylene Glycol	Copper	25.25	110	7-55	86.7-108	20-70
			12.50	76.2	1.20-139	86.7-152	11.3-114

Gogonin and Dorokhov (1976) obtained data for condensation of low velocity refrigerant R-21 vapour flowing vertically downwards over three different single horizontal tubes, placed between parallel plates. The vapour velocity was determined from the power input to the boilers and checked against the total heat-transfer to the test-tube and the auxiliary condenser. The two methods agreed to within 5%. The heat flux to the test-tube was calculated from the temperature rise and flow rate of the cooling water.

Goto et al. (1979) condensed quiescent vapours of seven refrigerants on a horizontal tube of diameter 15.85mm and length 616mm. The heat flux was obtained from the temperature rise and the flow-rate of the coolant, from which it was compared with the values obtained by collecting and measuring the condensate from the tube. The two methods agreed to within 5%. The wall temperature was measured by six thermocouples inserted in the tube wall.

Honda et al. (1982) carried out experiments with refrigerant R-113 flowing vertically downwards over two different single copper tubes, with outside diameters of 37.1mm and 8mm and tube length of 100mm. The tubes were located within a rectangular duct, with a

length of 110mm and a width of 100 mm. The heat flux to the test-tube was calculated from the mass flow rate and temperature rise of the cooling water, which was kept within the range 1-3K by a refrigeration unit and a heater on the coolant inlet line, and measured using thermocouples placed in mixing boxes at the coolant entrance and exit.

Lee (1982) and Lee and Rose (1984) used the same apparatus as described earlier for their steam data for refrigerant R-113, with the tube outside diameter of 12.5mm, tube length of 109.5mm.

Rahbar and Rose (1984) and Rahbar (1989) conducted experiments with downward flowing refrigerant R-113 using the same apparatus as Lee (1982), but with a smaller diameter test section of 76.2mm, giving higher velocities. The tube outside diameter was 12.5mm.

Rahbar and Rose (1984) and Rahbar (1989) also performed experiments with downward flowing low pressure ethylene glycol. The apparatus was the same as that used for refrigerant-113 discussed above. The low density of ethylene glycol at these low pressures allows very high vapour velocities to be achieved.

Honda et al. (1986) performed experiments with refrigerant R-113 flowing vertically downwards (with higher velocities compared to that of Honda et al. (1982)) over two different single copper tubes, with tube outside diameters of 19mm and 8mm and tube length of 100mm. They used the same apparatus as Honda et al. (1982), using plates made of glass and polyvinyl-chloride to narrow the test-section and extend the range of vapour velocities.

Memory and Rose (1986) and Memory (1989) investigated the effect of inter-phase mass transfer resistance further with ethylene glycol and obtained more data for two copper tubes, with the tube outside diameter of 25.25mm and 12.5mm, tube length of 76.2mm.

1.5. Condensation on Single, Horizontal Tubes-Comparison of Theory and Experimental Data.

Figure 1.13 represents the comparison between the measured Nusselt Numbers for Berman and Tumanov (1962) and Fujii et al. (1972a) with those obtained from the theory of Fujii et al. (1972b) given by equation (1.45). As can be observed in Figure 1.25, most of the data of Berman and Tumanov (1962) falls above equation (1.45) by 20%, while the data of Fujii et al. (1972a) takes place within +20% and -20% of theory.

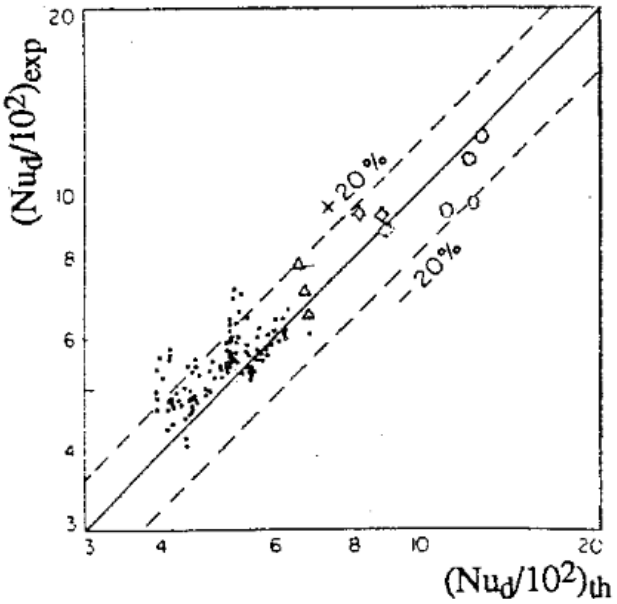

Figure 1.13. Variation of the calculated dimensionless condensate film thickness around a horizontal plain tube (after Rose (1984)).

The experimental data of Nicol and Wallace (1974), Wallace (1975) and Nicol and Wallace (1976) for steam are plotted in Figure 1.14. It can be seen that at the high velocity, the heat-transfer coefficients are twice that of Nusselt Theory (equation (1.42)), but well below the theoretical heat-transfer coefficient of Shekriladze and Gomelauri (equation (1.40)).

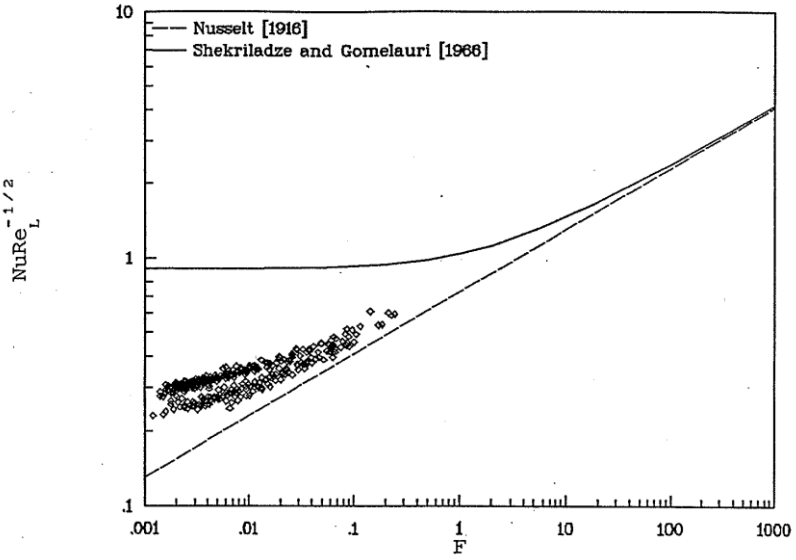

Figure 1.14. Data of Nicol and Wallace (1974), Wallace (1975) and Nicol and Wallace (1976) for steam.

Figure 1.15 illustrates good agreement between the Shekriladze and Gomelauri theory (equation (1.40)) and the experimental data of Nobbs (1975) and Nobbs and Mayhew (1976) for high heat flux (high suction) (shown on figure 1.15 as black diamonds), while for the medium and the low heat fluxes, Shekriladze and Gomelauri theory (equation (1.40)) over-estimates the data, mainly at high velocity (illustrated as white diamonds in figure 1.15). It was thought that this could be due to the separation of the vapour-boundary layer. At high heat flux, boundary layer separation would not occur due to the increased suction, while at the medium and low heat fluxes, separation could occur, which would cause the thickness of the condensate film to increase beyond the separation point, resulting in lower heat-transfer coefficients.

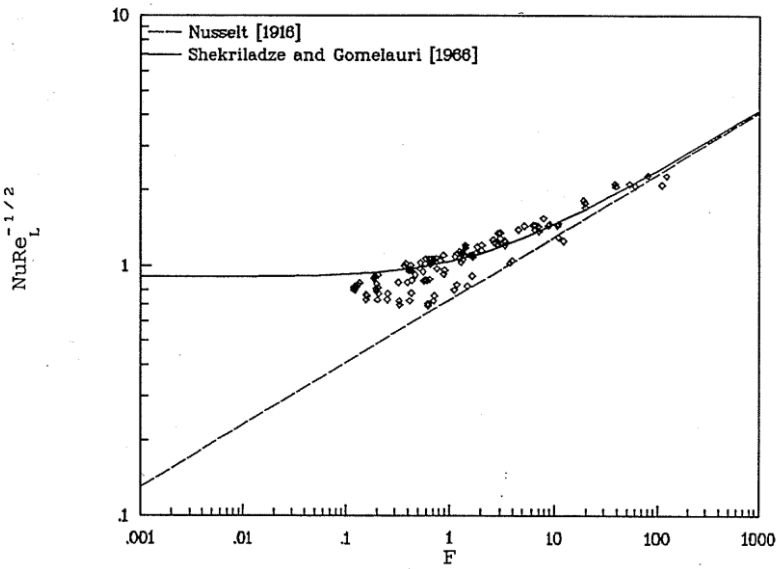

Figure 1.15. Data of Nobbs (1975) and Nobbs and Mayhew (1976) for steam.

Figure 1.16 compares the experimental results of Goto et al. (1979) for refrigerants with the Nusselt theory (equation 1.16). As can be observed in this figure, there is good agreement for refrigerants R-12, R-22, R-114 and R-502, while the data for R-11, R-113 and R-500 were approximately 10% below theory.

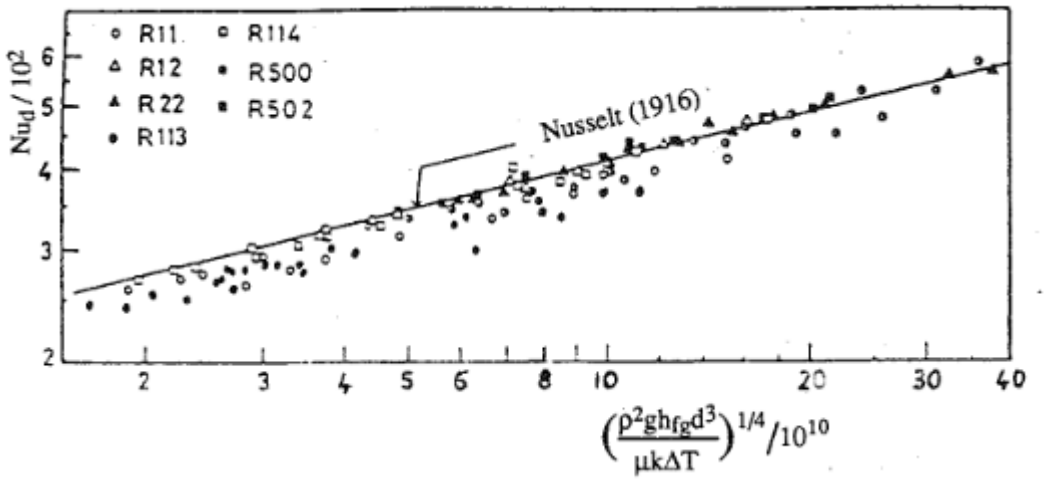

Figure 1.16. Experimental results for free-convection condensation for various refrigerants (after Goto et al (1979)).

Figure 1.17 shows the comparison between the data of Lee (1982) and Lee and Rose (1984) and the theories of Nusselt (1916) and Shekriladze and Gomelauri (1966). Agreement between the Shekriladze and Gomelauri (1966) model and the data of Lee (1982) and Lee and Rose (1984) is good in the range of $F < 1$, while in a range of $F > 1$ (low velocity), the Shekriladze and Gomelauri (1966) model over-predicts the data.

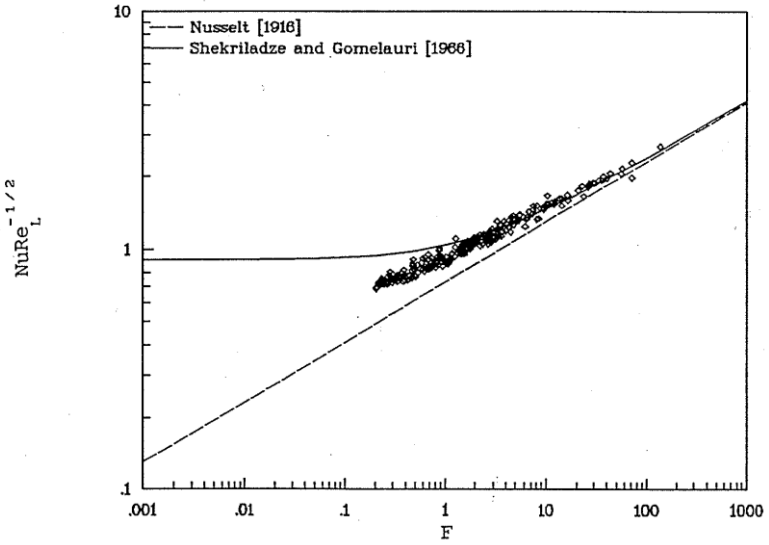

Figure 1.17. Data of Lee (1982) and Lee and Rose (1984) for steam.

It can be seen in figure 1.18 that at low vapour velocity, the refrigerant R-21, the data of Gogonin and Dorokhov (1976), were found to be somewhat higher than that given by the Nusselt (1916) theory. Gogonin and Dorokhov (1976) suggested that this may be due to the effects of surface tension on the condensate film at low velocity.

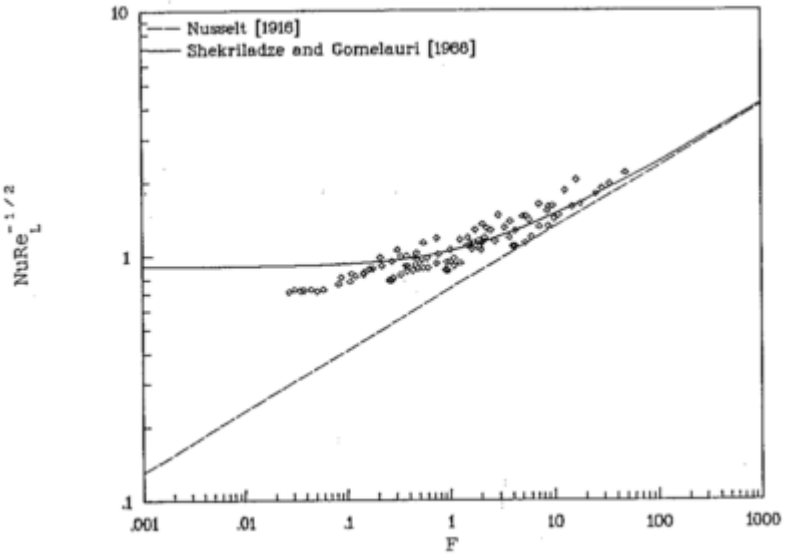

Figure 1.18. Data of Gogonin and Dorokhov (1976) for refrigerant-21.

Good agreement is seen between the data of Honda et al. (1982) for refrigerant-113 and the theories given by Nusselt (1916) and Shekriladze and Gomelauri (1966) at low velocity (figure 1.19). The data shows an increase in $\mathrm{Nu}\,\tilde{\mathrm{R}}\mathrm{e}^{-\frac{1}{2}}$ as F decreases for a range of $\mathrm{F}<1$. It was suggested that this was due to the onset of turbulence.

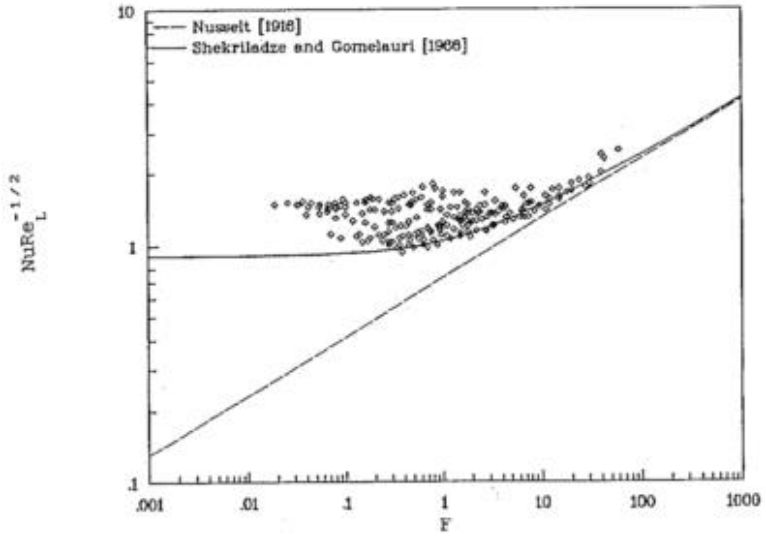

Figure 1.19. Data of Honda et al. (1982) for refrigerant-113.

The experimental data of Lee (1982) and Lee and Rose (1984) for R-113 given in table 1.2 are plotted in figure 1.20. It can be seen that there is an agreement between the experimental data and the theories of Nusselt (1916) and Shekriladze and Gomelauri (1966).

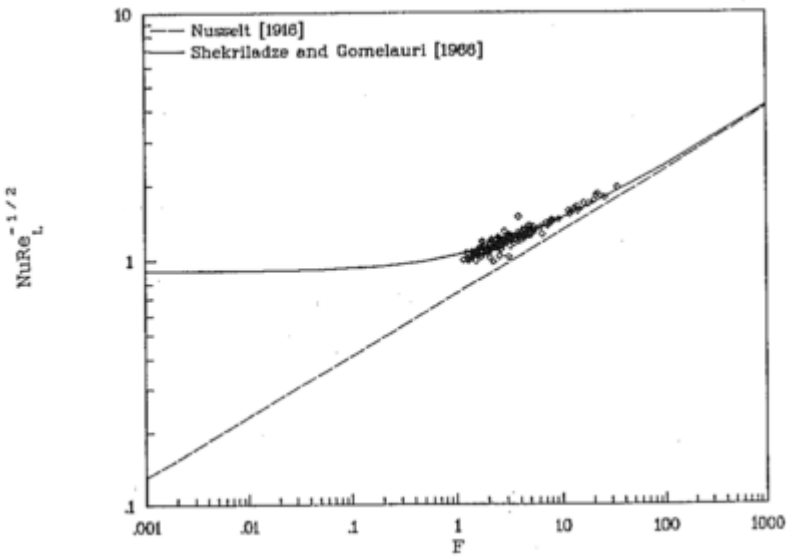

Figure 1.20. Data of Lee (1982) and Lee and Rose (1984) for refrigerant-113.

The data of Rahbar and Rose (1984) and Rahbar (1989) for refrigerant-113 in figure 1.21 demonstrate a sharp upturn in $\mathrm{Nu}\,\tilde{\mathrm{Re}}^{-\frac{1}{2}}$ as F decreases at high velocity $(\mathrm{F}<1)$, similar to that seen in the data of Honda et al. (1982) in figure 1.19.

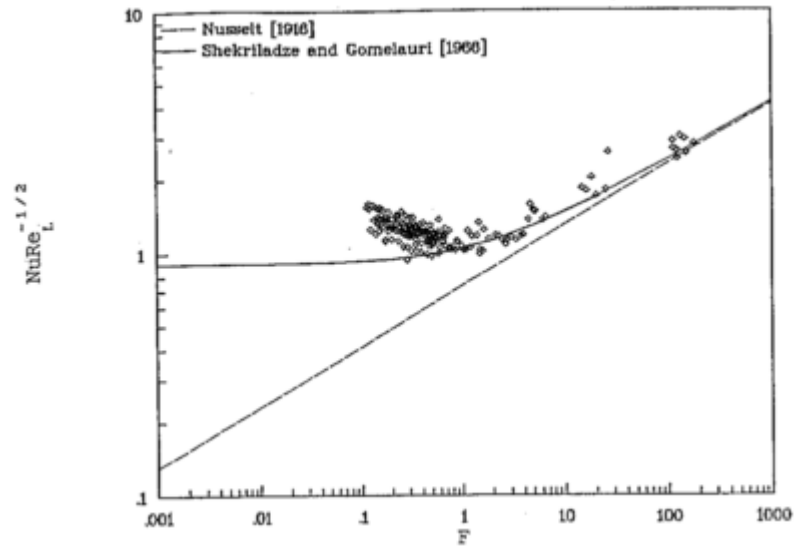

Figure 1.21. Data of Rahbar and Rose (1984) and Rahbar (1989) for refrigerant-113.

It can be observed in Figure 1.22 that most of the experimental data of Rahbar and Rose (1984) and Rahbar (1989) for ethylene glycol fall below the theoretical curve of Shekriladze and Gomelauri (equation (1.41)). High values of $\mathrm{Nu}\tilde{\mathrm{Re}}^{-\frac{1}{2}}$ were noticed for high condensation rates due to the temperature dependence in the viscosity of the condensate in the two-phase Reynolds number. At high pressures, an increase in $\mathrm{Nu}\tilde{\mathrm{Re}}^{-\frac{1}{2}}$ as F decreases can be seen, which was thought to be due to the onset of the turbulence. At low pressures, a decrease in $\mathrm{Nu}\tilde{\mathrm{Re}}^{-\frac{1}{2}}$ can be observed. It was recommended that this could be the effect of the pressure variation around the tube at high velocity, and also inter-phase mass resistance may become quite significant at low pressure and high condensation rate.

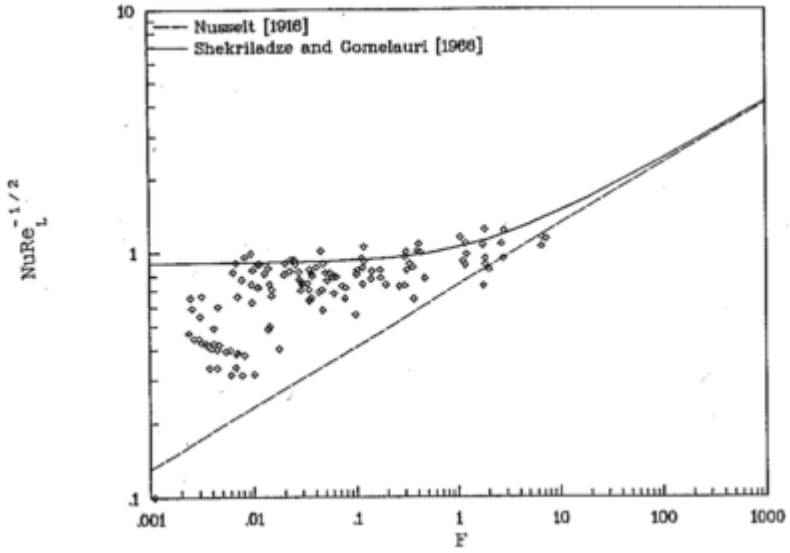

Figure 1.22. Data of Rahbar and Rose (1984) and Rahbar (1989) for ethylene-glycol.

The experimental data of Honda et al. (1986) for ethylene glycol shown in table 1.2 are plotted in Figure 1.23. A good agreement takes place between the data and the theories shown (equations (1.41) and (1.43)) for $\mathrm{F} > 1$. However, for $\mathrm{F} < 1$, it is observed that the experimental values of $\mathrm{Nu}\tilde{\mathrm{Re}}^{-\frac{1}{2}}$ increases more rapidly than indicated by the theories as F increases, which illustrates the role of turbulent mixing in the condensate film at high velocity. To determine the onset of turbulence, Honda performed a number of dye injection tests. The location, at which turbulence took place, was represented by the growth of the dye trace. This location was found to correspond to the upturn in $\mathrm{Nu}\tilde{\mathrm{Re}}^{-\frac{1}{2}}$.

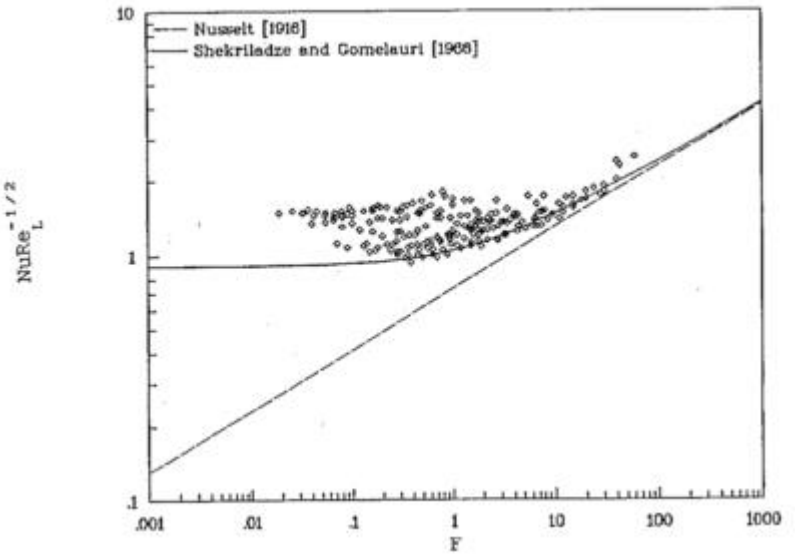

Figure 1.23. Data of Honda et al. (1986) for ethylene-glycol.

Figure 1.24 shows the data of Memory and Rose (1986) and Memory (1989) for ethylene-glycol, compared with equations (1.41) and (1.43). It is observed in this figure that there is a decline in the data of $\mathrm{Nu}\tilde{\mathrm{R}}\mathrm{e}^{-\frac{1}{2}}$ at low F (high vapour velocities and low pressure), which was attributed to the effects mentioned above (Rahbar and Rose (1984) and Rahbar (1989) for ethylene glycol).

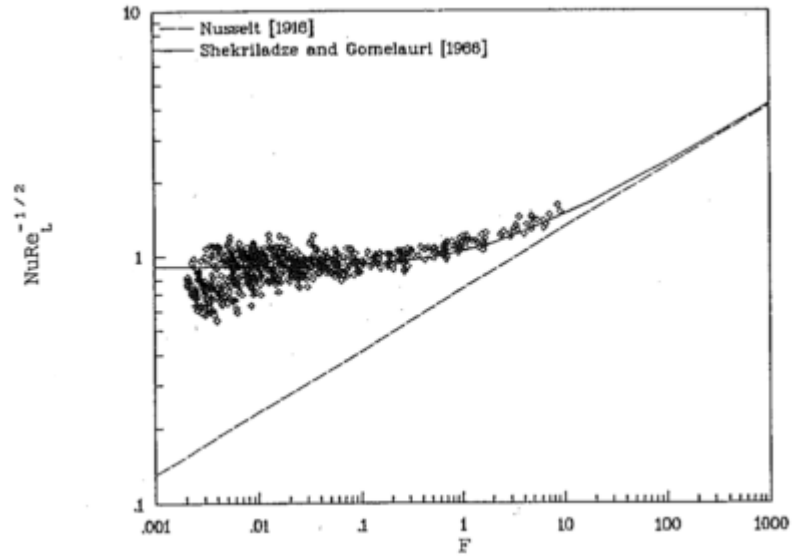

Figure 1.24. Data of Memory and Rose (1986) and Memory (1989) for ethylene-glycol.

The effect of the pressure variation around the tube at high vapour velocity, which results in a drop in the local saturation temperature at the condensate surface, was estimated by the following expression:

$$\Delta P_1 = a_1 \left(\frac{\rho_v U_\infty^{\ 2}}{2} \right) \tag{1.63}$$

Where a_1 is a constant. The pressure drop across the vapour condensate boundary, caused by the inter-phase mass transfer resistance, was approximated by the following equation:

$$\Delta P_2 = a_2 \frac{q(\gamma+1)\sqrt{R_v T_{sat}(P_\infty - \Delta P_1)}}{4h_{fg}(\gamma-1)} \tag{1.64}$$

Where a_2 is a constant, and γ is the ratio of specific heat capacity at constant pressure to that at constant volume. The data used in figure 1.25 same as that in figure 1.24 but corrected using $a_1 = 0.7$ and $a_2 = 0.8$, in equations (1.63) and (1.64) used to correct the temperature drop across the condensate film by evaluating the saturation pressure of the vapour at $(P_\infty - \Delta P_1 - \Delta P_2)$ .This correction had the effect of bringing the data for low values of F in line with theory, while having a negligible effect on the high F data.

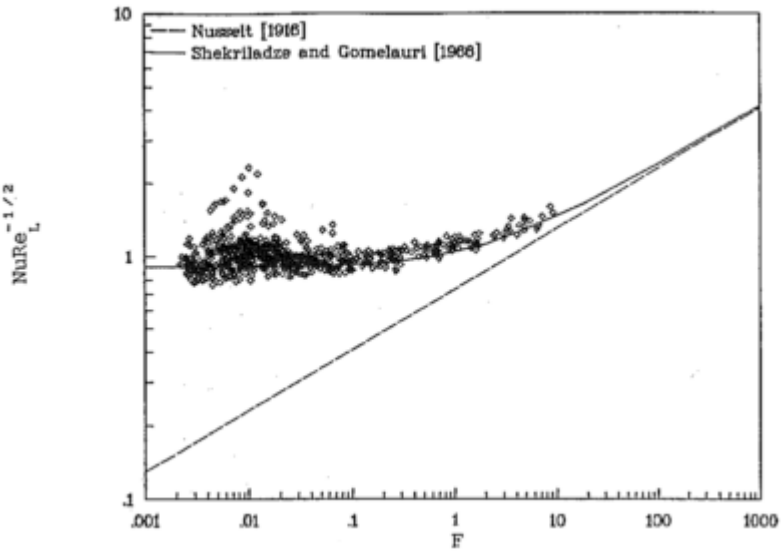

Figure 1.25. Data of Memory and Rose (1986) and Memory (1989) for ethylene-glycol.

Table 1.4 illustrates the key to curves in figure 1.26 (including their references), where the measurements for the condensation of different vapours under certain conditions were compared with equation (1.50).

Table 1.4. Symbols used in figure 1.26, and its corresponding experimental database.

Symbol	References	Type of the Fluid vapour	Pressure / (kPa)	G	Value of F for point with lowest G
×	Gogonin and Dorokhov (1972)	Refrigerant -21	520	0.2-1.5	248
◊	Nicol and Wallace (1974 and 1976)	Steam	17-30	2.8-5.7	0.15
□	Nobbs (1975) and Nobbs and Mayhew (1976)	Steam	105	2.7-5.4	0.88
○	Fujii, Honda and Oda (1979 and (1980)	Steam	3-6	1.0-3.6	19.9
△	Lee (1982)	Steam	4-101	0.5-7.2	1.28
+	Lee (1982)	Refrigerant -113	40-105	0.7-2.9	8.45

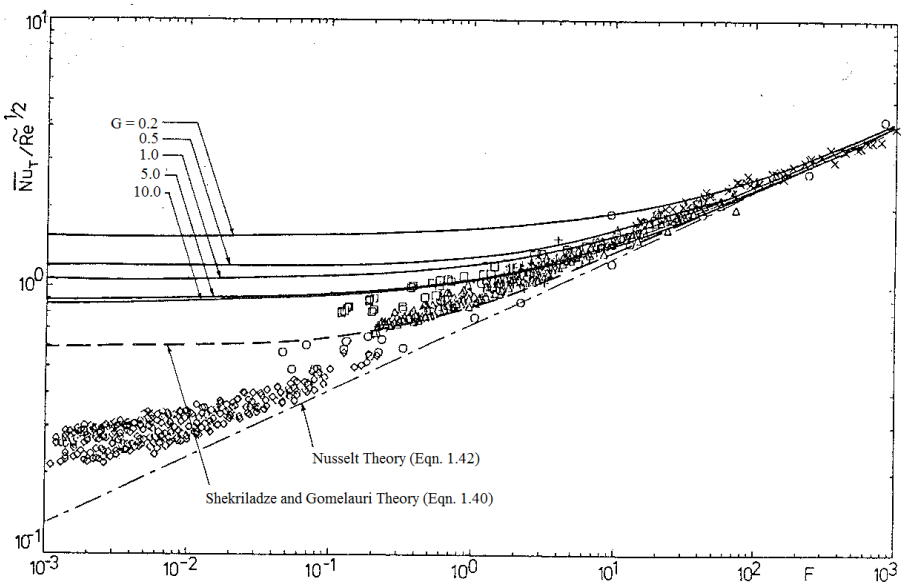

Figure 1.26. Comparison of experiment and theory (Uniform wall temperature) (after (Lee and Rose (1982))).

It is observed from figure 1.26 that the data of Gogonin and Dorokhov (1972) are in a good agreement with equation (1.50), since their velocities are low for different values of G .Equation (1.50) over-predicts the high velocity data of Nicol and Wallace (1974 and 1976). The data of Nobbs (1975) and Nobbs and Mayhew (1976) offer the highest Nusselt numbers and are in a good agreement with equation (1.50), while the data of Fujii, Honda and Oda (1979 and (1980) and Lee (1982) give the lowest Nusselt numbers. Figures 1.27 and 1.28 represent the comparison of equation (1.58) with the experimental data that are given by the researchers are based shown in the following table for the steam and refrigerant fluids.

Table 1.5. Approximate ranges of the parameters of experimental investigations.

References	Fluid	$\tilde{\mathrm{Re}}\times 10^4$	F	G	P	θ
Fujii (1972)	Steam	9.63-103	0.091-15	0.5-1.2	0.039-0.090	0.173-20.6
Fujii (1979)	Steam	2.89-377	0.036-840	1.0-3.6	0.017-0.05	0.138-3607
Nobbs (1975) and Nobbs and Mayhew (1976)	Steam	0.29-52.5	0.12-3310	1.8-6.2	0.024-0.072	0.449-13000
Lee (1982) and Lee and Rose (1984)	Steam	1.25-56.3	0.20-138	0.5-7.2	0.016-0.110	1.10-26.2
Nicol and Wallace (1974 and 1976) and Wallace (1975)	Steam	36.8-549	0.001-0.25	3.1-6.5	0.008-0.026	0.008-1.52
Gogonin and Dorokhov (1971)	R-21	0.91-4.89	14-1922	0.2-1.4	0.440-3.400	3.90-103
Gogonin and Dorokhov (1976)	R-21	0.57-48.1	0.028-94	0.2-2.5	0.240-3.600	0.012-7.85
Lee (1982) and Lee and Rose (1984)	R-113	1.37-7.87	1.2-36	0.7-2.9	0.180-0.540	0.766-14.8
Honda (1982)	R-113	0.37-31.8	0.083-1002	0.5-2.3	0.229-1.068	0.026-296

It is observed in table 1.5 that the values of P for the steam are lower compared to that of the refrigerants. For the fluids that have low values of P, an increase in the heat transfer rate for the forward half of the tube due to the pressure term that has been taken into account is insignificant, and avoids the heat transfer rate in the rear half. Therefore this would results the Nusselt numbers in equation (1.57) to be smaller than in equation (1.53). High values of P results the Nusselt numbers in equation (1.57) to be slightly higher than in equation (1.53), where the heat transfer rate in the rear half is not rejected. There is a good agreement between equation (1.57) and the experimental data for figures 1.27 (a)-(c), except figure 1.27 (d), where equation (1.57) under-estimates the experimental data of Wallace (1974), which was thought due to the high velocity data of Wallace (1974). According to figures 1.28, there is a good agreement between the calculated $\mathrm{Nu}\tilde{\mathrm{Re}}^{-\frac{1}{2}}$ and the observed $\mathrm{Nu}\tilde{\mathrm{Re}}^{-\frac{1}{2}}$ for both of R-113 and R-21.

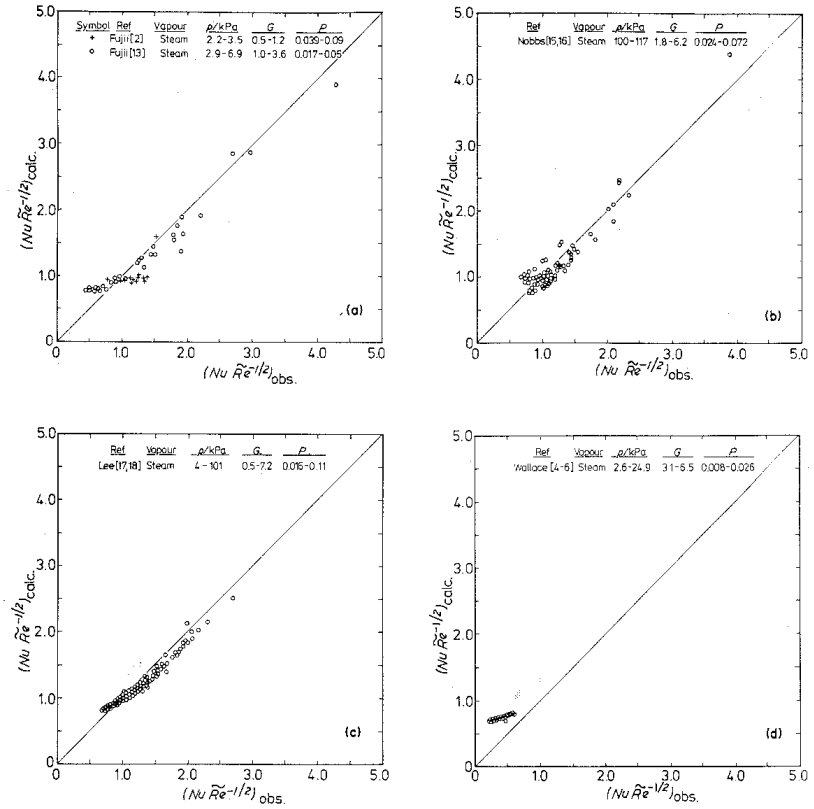

Figure 1.27. (a)-(d). Comparison of equation (1.57) with the experimental data for steam (Rose (1984)).

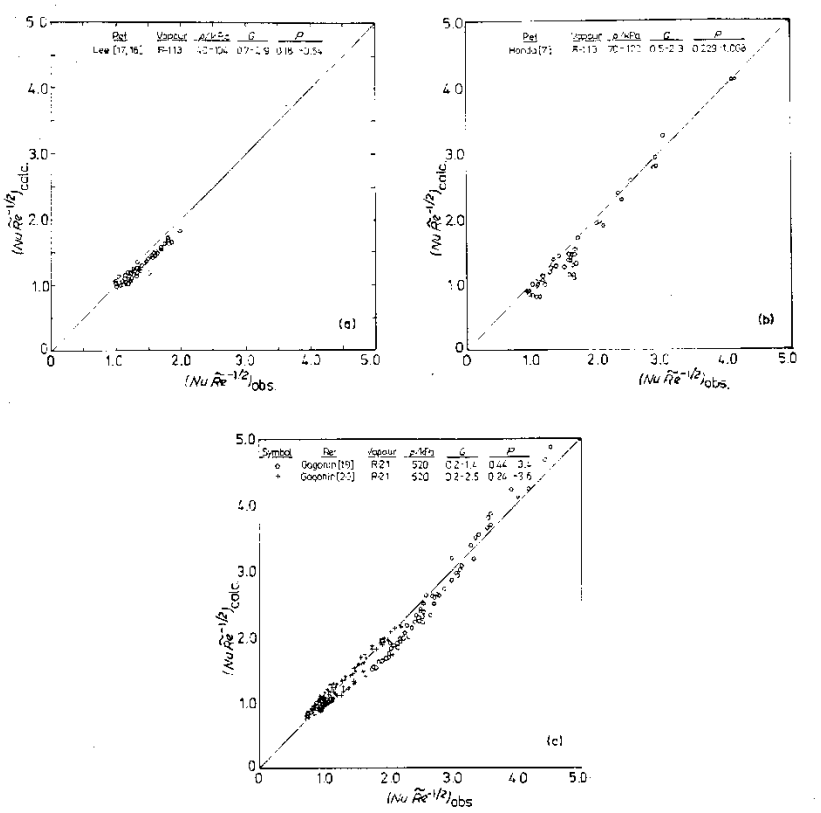

Figure 1.28. Comparison of equation (1.57) with the experimental data for R-113 and R-21 (Rose (1984)).

1.6. Condensation heat transfer on a bank of plain tubes.

The mechanisms involved in condensation on tube banks differs considerally from the case of a single tube due to the variation of vapour velocity and condensate inundation as the vapour mass flow rate is decreased by condensation. For a single tube, increasing the up-stream vapour velocity results the heat transfer-rate to the tube's surface to be increased due to the generation of the vapour shear stress at the surface of the condensate film, from which the thickness of the film condensate will be decreased. The effect of inundation is influenced by the condensate flow pattern which is governed by the tube surface geometry, the condensation rate and the surface tension of the fluid. Models including the combined effects of the inundation and vapour shear all involve some empiricism.

Many experimental measurements have been obtained to examine the above effects. Figure 1.29 illustrates some of the schematics of the test section geometries used in the studies. The test sections can be divided into two types; those where the whole test bank is active (with the exception of dummy half tubes on the walls of the triangular test banks) and those where a single active tube is positioned in a bank of dummy tubes. The velocity of the vapour that is passing through the bank of tubes can be characterised by one of the following cases:

1. Vapour approach velocity U_{min} i.e. that which would occur in the absence of the tubes (based on the local mass flow rate and the maximum cross-sectional area).
2. Maximum velocity U_{max} based on the minimum cross-sectional area between the tubes.
3. Mean-void velocity $U_{mean-void}$, defined by Nobbs (1975) as:

$$U_{mean-void} = \frac{U_{min}}{\varepsilon} \tag{1.65}$$

Where is ε the void fraction, (total volume of the test section not occupied by the tubes divided by the total volume) relating to the row considered. For the first row, in the absence of preceding dummy tubes, the void fraction is determined by the following equation:

$$\varepsilon = 1 - \frac{\pi d^2}{8 P_t P_l} \tag{1.66}$$

and, for rows in the core of the bundle it is obtained from:

$$\varepsilon = 1 - \frac{\pi d^2}{4 P_t P_l} \tag{1.67}$$

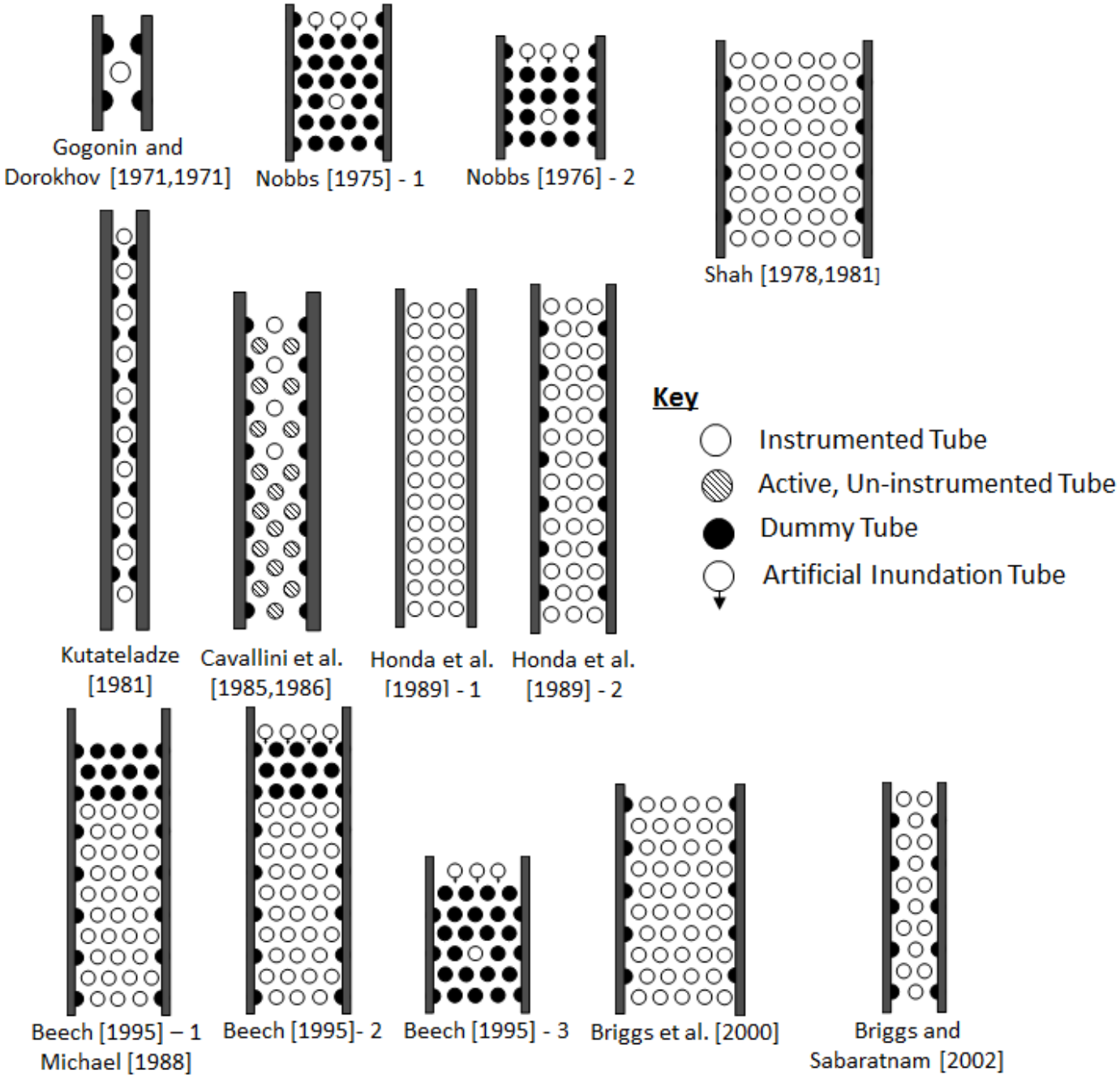

Figure 1.29. Schematics of test banks (Briggs (2008)).

Where P_t and P_l represent the horizontal and vertical tube pitches as shown for each of the inline and staggered tube bundles in figures 1.30.

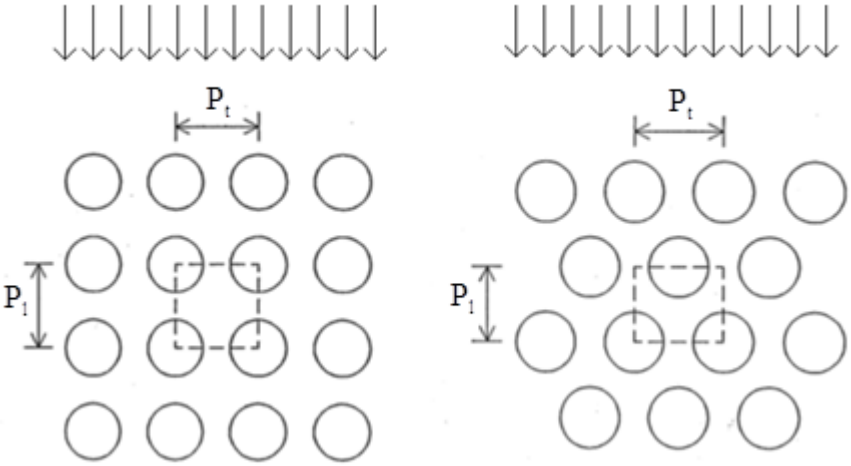

Figure 1.30. Calculation of mean flow widths.

Investigations based on the test section geometries shown in Figure 1.29 are discussed below.

1.6.1. Measurements with steam.

Table 1.6 summarizes the experimental data-base for condensation on banks of plain tubes for steam data.

Short and Brown (1951) performed experiments with steam and Refrigerant-11 condensing on a vertical column of twenty horizontal brass tubes, with a tube outside diameter of 15.88 mm, and tube length of 1334 mm. The vertical tube pitch P_v was 38.1 mm. The heat flux was obtained from the rise of the temperature of the coolant water. The temperature of the vapour was obtained from the pressure of the vapour (which was measured by a U-tube manometer filled with mercury).

Fuks (1957) conducted experiments with steam on a staggered bank of 11 rows. Each row had either 6 or 7 tubes, with a tube outside diameter of 19mm, and tube length of 522mm. The horizontal and vertical tube pitches were 28.03mm and 24.23mm. These tubes were positioned in a rectangular duct. Condensing tubes were placed in rows one, two, three, five, seven and eleven and were instrumented to obtain the wall temperature and the rise of the temperature of the coolant water. Condensate inundation was simulated through a tube

having 1.25mm diameter holes at 50mm spaces along of this tube, located in the first row. Fuks (1957) obtained a model that predicts the heat-transfer coefficient within the tube's bundle based on his experimental data, which will be discussed later.

Table 1.6. Condensation of the steam on banks of tubes-Experimental data base.

Reference	Bank layout	Outside diameter / mm	Length / mm	U_{min} / ms^{-1}	T_v / °C	ΔT / K
Short and Brown (1951)	Vertical-column	15.88	1334	Not available	Not available	Not available
Fuks (1957)	Staggered	19.0	522	0.9-1.4 (based on mean-void velocity)	Not available	Not available
Grant and Osment (1968)	Staggered	19.05	2130	Not available	Not available	Not available
Nobbs (1975)	Staggered	19.05	500	0.31-9.20	100-104	7.96-38.0
Nobbs and Mayhew(1976)	In-line	19.05	500	0.41-8.29	99.8-103	6.18-41.7
Michael (1988)	Staggered	14.0	252	5.97-21.63	100-102	4.9-18.5
Beech (1995)-1	Staggered	14.0	180	6.08 - 18.31	102-103	5.56-41.25
Beech (1995)-2	Staggered	14.0	252	17.34 - 19.62	101-103	9.64-23.71
Beech (1995)-3	Staggered	14.0	252	4.18-10.19	102-103	11.69-22.72
Briggs and Sabaratnam (2003)	Staggered	19.1	272	4.40-10.62	99.8-101.1	13.76-70.15

Grant and Osment (1968) performed experiments with steam flowing vertically downwards over a staggered tube bank of 14 rows that consists of 139 tubes, with a tube outside diameter of 19.05mm, and a tube length of 2.13m. The horizontal and vertical tube pitches were 28.58mm and 24.75mm. Grant and Osment (1968) obtained a model that predicts the heat-transfer coefficient within the tube's bundle based on his experimental data, which will be discussed later.

Nobbs (1975) and Nobbs and Mayhew (1976) carried out experiments where vertically downward flowing steam condensed on a single tube situated in the fifth row of a dummy in-line bank that consisted of 6 rows of 3 tubes each, and a staggered bank which consists of 7 rows of 3 and 4 tubes (illustrated in figure 1.29). The horizontal and vertical pitches were 23.8mm and 20.6mm respectively. Dummy half tubes were attached to the duct walls for rows having only three tubes in the staggered bank. Simulated inundation was supplied by three inundation tubes situated in the first row of the in-line bank and the second

row of the staggered bank. Each tube had a series of holes along the forward stagnation line. The temperature of the inundating condensate was measured by a thermocouple situated at the entrance of the inundation tubes.

Michael (1988) studied the effect of high vapour velocity on condensation of steam on a triangular bank of 10 rows. Each row had either 3 or 4 tubes, with tube outside diameter of 14 mm and tube length of 180 mm. The horizontal and vertical tube pitches were 20 mm and 17.32 mm respectively. Four thermocouples were inserted in instrumented tubes, evenly distributed around their circumference, mid-way along the tube length to measure the tube wall temperature. These instrumented tubes were located in rows one, two, four, six, eight and ten. The experimental data of Michael (1988) and Michael et al. (1992) are compared with the Nusselt (1916) and Shekriladze and Gomelauri (1966) models in figure 1.31. It can be observed in figure 1.31 that most of the data fall above the Shekriladze and Gomelauri model (1966) line.

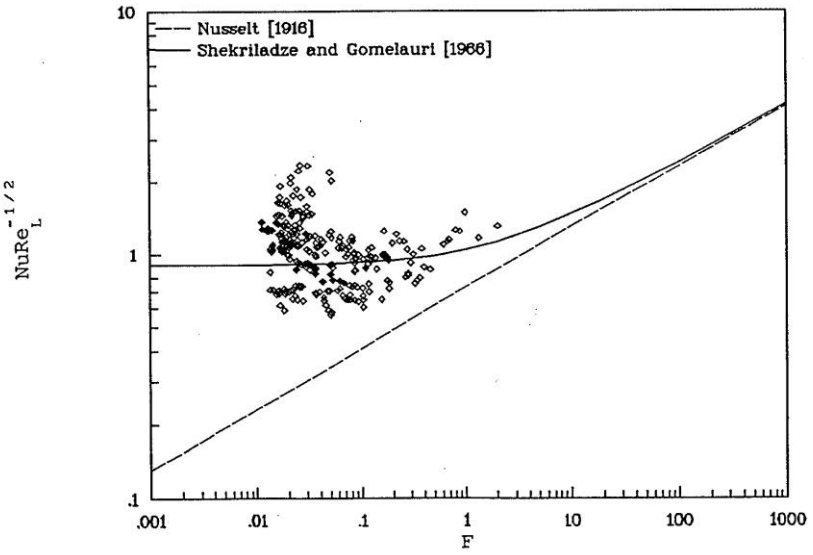

Figure 1.31. Data of Michael (1988) and Michael (1991) for steam.

Beech et al. (1995) performed experiments with three different test banks at near atmospheric pressure for condensation of steam on staggered banks of 4 tubes per row (as shown in figure 1.29), having a horizontal and vertical tube pitches of 20mm and 17.3mm. It can be observed in figure 1.29 that there are 13 rows in a first test bank, where 10 instrumented rows of the tubes (same as the test bank of Michael (1988)) are active rows. The second test bank consists of 14 rows, where the steam condensing on the 10 instrumented

rows of tubes. The simulated inundation was supplied by the four inundation tubes located in the first row of this bank. In both these test banks, the wall temperatures of the instrumented tubes were measured by groups of four thermocouples, which were distributed evenly around the circumference. A third test bank was made of 7 rows, where steam condensed on a single tube located in the fourth row of a dummy staggered bank. The simulated inundation was supplied by three inundation tubes positioned in the first row of this bank. Six thermocouples were embedded in this single instrumented tube, distributed around its circumference to measure its wall temperature. The experimental database by Beech (1995) is summarized in table 1.6. Figure 1.32 illustrates the experimental data of Beech (1995), Nobbs (1975) and Michael (1988) which were compared with the Nusselt (1916) and Shekriladze & Gomelauri (1966) models. The data are for steam velocities based on the mean void area. It can be seen that the data of Beech (1995) lie between the limiting values of $\mathrm{Nu}\tilde{\mathrm{Re}}^{-\frac{1}{2}}$ for the Nusselt (1916) and Shekriladze and Gomelauri (1966) models.

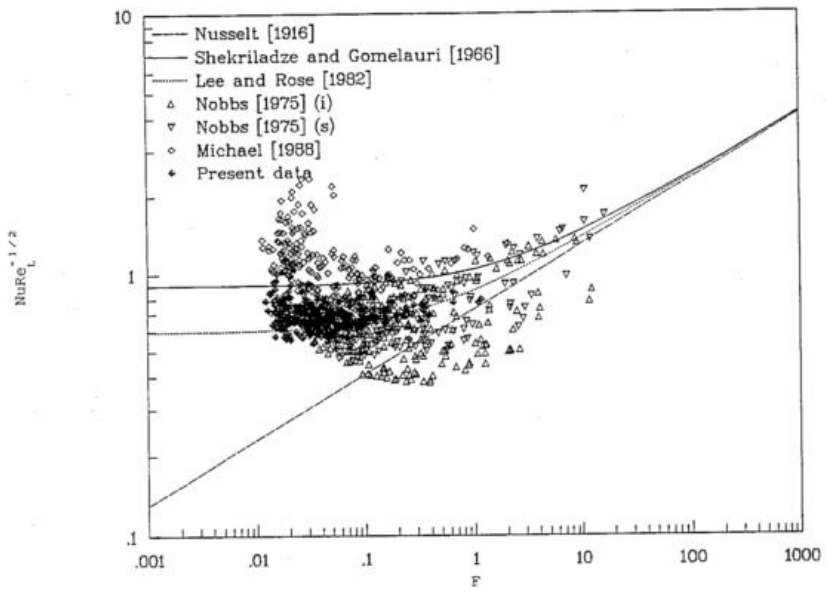

Figure 1.32. Comparison of the data of Beech (1995), and those of Nobbs (1975), Michael (1988) with Nusselt (1916) and Shekriladze & Gomelauri (1966) models.

Figure 1.33 represents the experimental data of Beech (1995) for a single condensing tube within a dummy bundle compared with the Shekriladze and Gomelauri (1966) and Lee and Rose Models (1982). It can be seen in figure 1.33 that all the data fall below the Shekriladze and Gomelauri (1966) model line, while most of these data fall above the Lee and Rose model (1982) line.

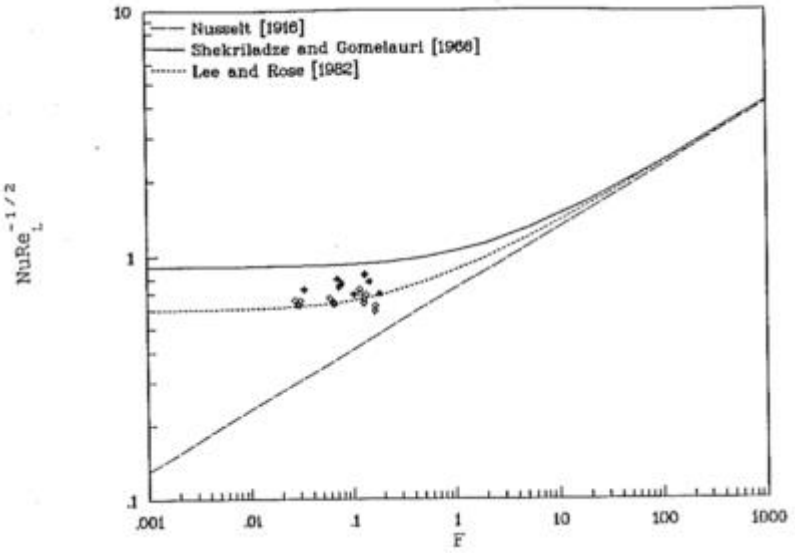

Figure 1.33. Comparison of the data of Beech (1995) for single condensing tube within dummy bundle with the Nusslet (1916) and Shekriladze and Gomelauri (1966) models.

Briggs and Sabaratnam (2003) studied condensation of steam on a staggered bank of two rows with a tube outside diameter of 19.1mm, and a tube length of 272mm. The horizontal and vertical tube pitches were 26.2mm and 22.7mm respectively. One tube row had two half-tubes mounted on the duct walls. Four thermocouples were fitted at the mid-point of the instrumented tubes to measure the tube wall temperature. The ranges of the experimental parameters of Briggs and Sabaratnam (2003) are shown in table 1.6.

Figure 1.34 illustrates the data of Briggs and Sabaratnam (2003) for each row, which were compared with the Nusselt (1916) and Shekriladze & Gomelauri (1966) models. The vapour velocity in figure 1.34 is based on the arithmetic mean of the upstream and downstream vapour mass flow rates for the given row and the maximum test section area. It can be seen that there is agreement between the data of Briggs and Sabaratnam (2003) and the Shekriladze and Gomelauri (1966) model, which suggests that decrease in the vapour velocity is the main reason for the decrease in the heat-transfer coefficient down the bank.

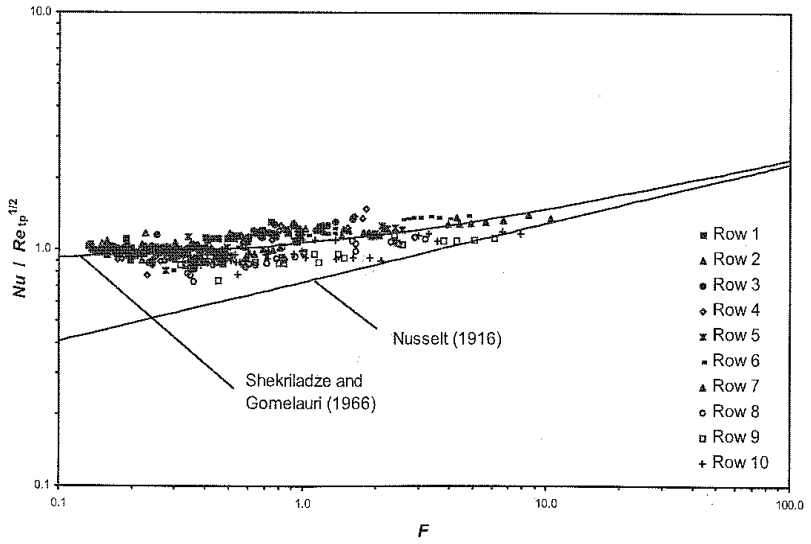

Figure 1.34. Comparison of data of Briggs and Sabaratnam (2003) with the Nusslet (1916) and Shekriladze and Gomelauri (1966) Models.

1.6.2 . Measurements with other Fluids.

Table 1.7 summarizes some the experimental data-base for the condensation on banks of plain tubes for steam data.

Table 1.7. Condensation of the non-steam vapours on bank of tubes-Experimental data base.

Reference	Fluid	Bank layout	Outside diameter / mm	Length / mm	U_{min} / ms^{-1}	T_{sat} / ^oC	ΔT/K
Young and Wholenberg (1942)	R-12	Vertical-column	19.05	609.6	Not available	29-52	Not available
Short and Brown (1951)	R-11	Vertical-column	15.88	1334	Not available	Not available	Not available
Gogonin and Dorokhov (1971)	R-21	Staggered	17	522	0.001-0.21	60	2.62-21.1
Gogonin and Dorokhov (1976)	R-21	Staggered	17	522	0.001-2.04	60	3.13-31.6
Shah (1978)	Iso-propanol	Staggered	12.7	180	0.35-4.30	85.9-96.6	21.2-29.6
Shah (1981)	Methanol	Staggered	12.7	180	0.40-0.62	67.4-68.6	5.1-18.3
Kutateladze (1981)	R-21	Staggered	16	585	0.22-1.68	60	1.90-30.4
Cavallini (1985)	R-11	Staggered	10	250	0.51-4.25	23.5-45.3	7.75-24.2
Cavallini (1988)	R-113	Staggered	10	250	0.92-5.13	47.0-50.8	5.1-27.1
Honda (1989)	R-113	In-line	15.9	100	0.77-6.76	49.8-51.9	2.77-29.8
		Staggered			0.70-7.05	48.5-51.1	3.80-27.9
Briggs (1995)	R-113	Staggered	18.7	272	0.13-0.44	46.2-47.6	18.75-28.45

Young and Wholenberg (1942) carried out experiments with flowing refrigerant-12 vertically downwards on a vertical column of horizontal tubes with a tube outside diameter of 19.05mm and tube length of 609.6mm. The tubes were placed within a circular duct, with a diameter of 254mm. The temperatures of the tube's wall were measured by three thermocouples, which were inserted at 90° from the vertical. The temperature of the vapour varied from $29^\circ C$ to $52^\circ C$.

Gogonin and Dorokhov (1971 and 1976) studied condensation of R-21 on a single tube located in the fourth row of a staggered bank of five rows of un-cooled tubes with a tube outside diameter of 17 mm, tube length of 522 mm and a transverse tube pitch of 24.3 mm. Figure 1.35 shows the data of Gogonin and Dorokhov for a vapour velocity of about 0.2m/s (based on the maximum area of the test section). The data agreed with the Nusselt Theory (1916) to within 10%. The other data for a vapour velocity of about 2.04m/s agreed with the Shekrialdze and Gomelauri Model (1966) to within 15%.

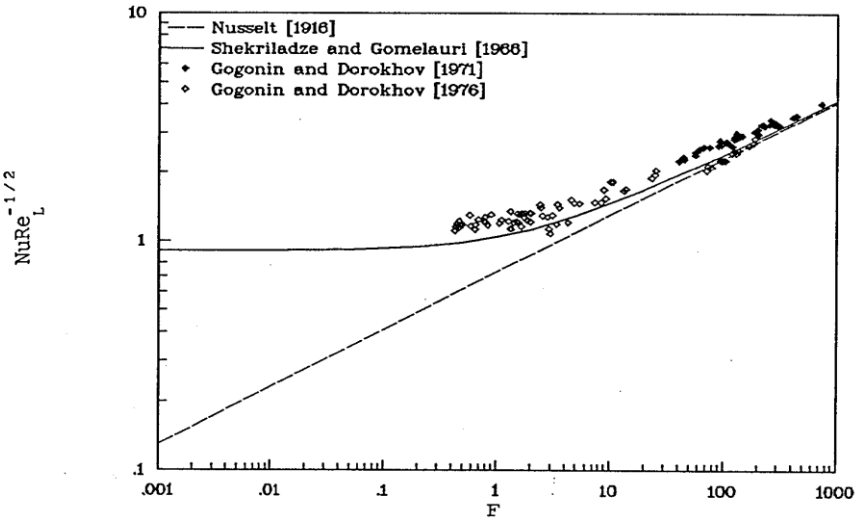

Figure 1.35. Data of Gogonin and Dorokhov (1971 and 1976) for R-21.

Shah (1978 and 1981) observed condensation of pure iso-propanol and methanol on a staggered bank of five rows of 54 stainless steel tubes with tube outside diameter of 12.7mm and tube length of 180mm. The horizontal and vertical tube pitches were 24.5mm and 21.2mm respectively. The temperature of the vapour was measured at inlet and outlet of the test section. Figure 1.36 represents a typical dataset of Shah (1978) for iso-propanol, illustrating the variation of the vapour-side heat transfer coefficient through the bundle. It was

observed that the heat-transfer coefficients for rows having only five condensing tubes were higher than those with six as shown in figure 1.36.

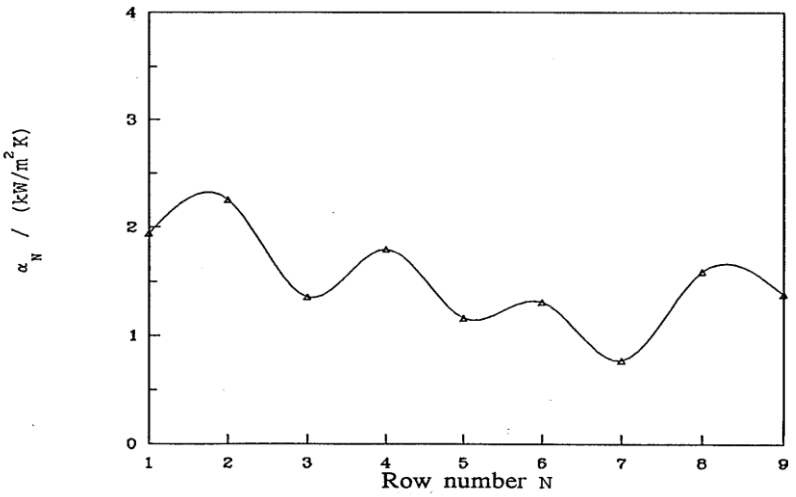

Figure 1.36. Data of Shah (1978, 1981) for iso-propanol and methanol.

Kutateladze (1981) carried out experiments, with near stationary and slowly moving (vertical downwards), R-21 vapour condensing on a vertical column of ten nickel tubes. The ranges of the experimental parameters of Kutateladze (1981) are shown in table 1.7. Figure 1.37 shows the data of Kutateladze (1981) for R-21. It can be seen that for a stationary vapour, the experimental data for the first row of the bank were 5% higher than that predicted by Nusselt (1916), while for the lower tubes of the bank, the heat transfer coefficient at the N^{th} row is almost unchanged, which becomes independent of the temperature difference across the film, due to the change in the condensate drainage mode. For the low moving vapour velocities, it was recommended for each tube within the bank to be correlated using a single tube model, from which equation (1.46) was suggested as illustrated in figure 1.37, since the inundation rates that occur through the bank is very low.

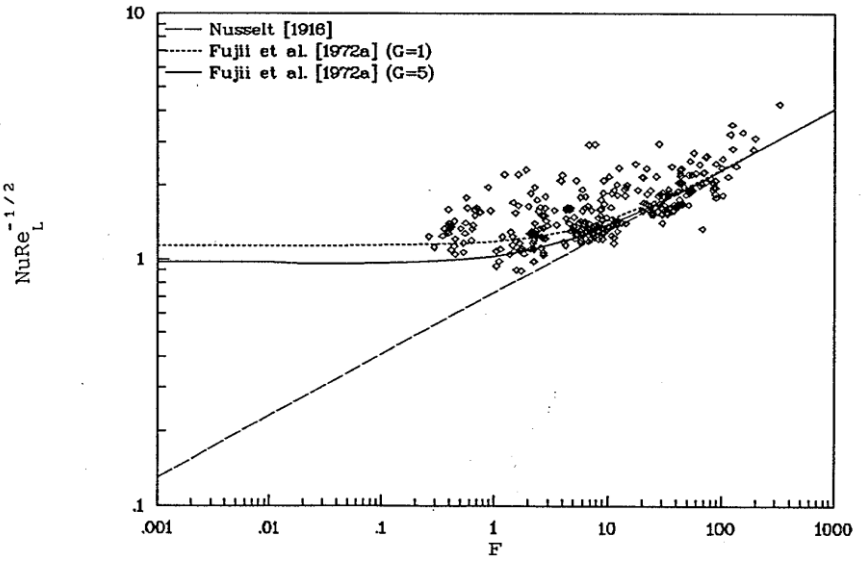

Figure 1.37. Data of Kutateladze (1981) for R-21.

Cavallini (1985 and 1988) observed condensation of R-11 and R-113 respectively on a staggered bank of 38 tubes. The horizontal and vertical tube pitches were 13.3mm and 11.5mm respectively. Eight thermocouples were fitted in longitudinal grooves to measure the tube wall temperature. The range of the experimental data of Cavallini et al. (1985) and (1988) are shown in table 1.7. Cavallini et al. (1986) obtained an empirical model that evaluates the heat-transfer coefficient within the tube's bundle based on the experimental data of R-11 which will be discussed later.

Honda et al. (1989a) observed condensation of R-113 on in-line and staggered banks with tube outside diameter of 15.9mm, tube length of 100mm and horizontal and vertical tube pitches of 22mm and 19.05mm. The temperatures of the flowing upstream and downstream vapour were measured using two sheathed thermocouples that were inserted to the duct wall 70mm above the top row and 70mm below the last row of the test-section. The ranges of the experimental parameters covered in his experiments are demonstrated in the table 1.7.

Briggs et al. (1995) carried out experiments, with R-113 condensing on a triangular bank which consisted of 10 rows of 4 and 5 tubes, with the tube outside diameter of 18.7mm and tube length of 272 mm. The horizontal and vertical tube pitches were 26.2mm and 22.7mm respectively (the same as Briggs and Sabaratnam (2003) for flowing steam). Four thermocouples were embedded to the instrumented tubes to measure their wall temperatures.

1.7. Condensation heat transfer on a bank of plain tubes-theoretical studies.

1.7.1. Free-Convection Condensation.

Nusselt (1916) extended his single-tube theory for quiescent vapour to a vertical column of horizontal tubes in order to investigate the effect of the condensate falling successively for one tube to the next. The assumptions that were made in addition to those for a single-tube were:

1. The laminar condensate film falls from one tube to the next as a continuous sheet as shown in Figure 1.38, which is uniform along the length of the tube.
2. The wall temperature and hence the vapour-side temperature difference is the same for all tubes in the vertical column.

Figure 1.38. Nusselt (1916) idealised model.

Based on these assumptions, the following equation for the mean heat-transfer coefficient $\overline{\alpha}_N$ for a column of N tubes was derived:

$$\frac{\overline{\alpha}_N}{\alpha_1} = N^{-\frac{1}{4}} \tag{1.68}$$

Where α_1 is the heat-transfer coefficient for the top tube in the bank, obtained using Nusselt single tube model (eqn. (1.15)). The following equation is an alternative form of single tube model of Nusselt (1916):

$$\frac{\alpha_1}{k}\left(\frac{\nu^2}{g}\right)^{\frac{1}{3}} = 1.5\left(\frac{4\Gamma_1}{\mu}\right)^{-\frac{1}{3}} \tag{1.69}$$

With Γ_1 represents the mass flow rate of the condensate per unit length drained from the top tube (or tube row). It can be seen in equation (1.69) that the heat-transfer coefficient is dependent on the mass flow rate of the condensate drained from the preceding tube.

Figure 1.39 illustrates the experimental data of Young and Wholenberg (1942) for refrigerant-12, including the Nusselt (1916) model for the single tube, which is given by the equation (1.69). It can be observed in this figure that the measured heat-transfer coefficients for the first tube fall below Nusselt's model for single tube. The measured heat-transfer coefficients for the following rows were beyond Nusselt's line for top tube.

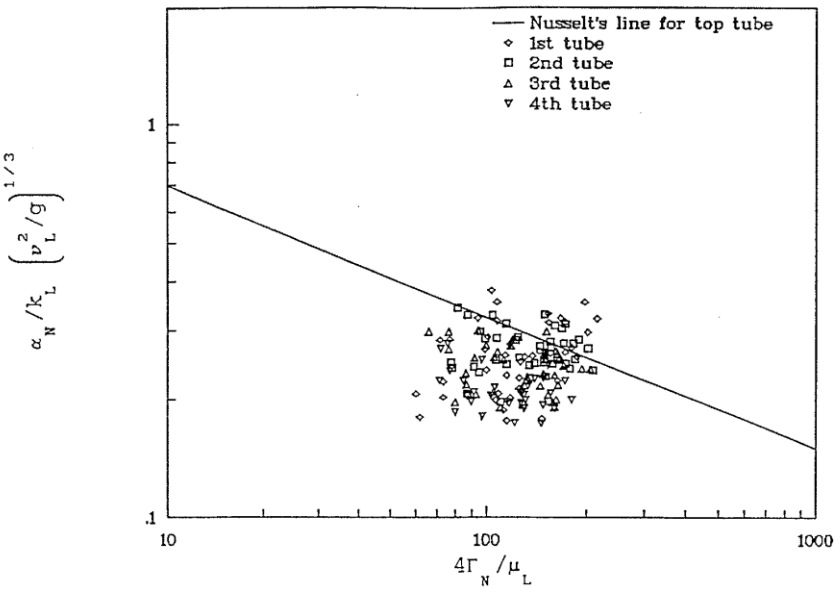

Figure 1.39. Data of Young and Wholenberg (1942) for refrigerant-12.

Figure 1.40 demonstrates the experimental data of Short and Brown (1951) for refrigerant-11 and steam, from which they are distributed about the Nusselt's model for single tube. The results for both fluids recommended that the average heat-transfer coefficient for a column of twenty tubes was approximately equal to the predicted value by the Nusselt (1916) model for the top tube of the bank.

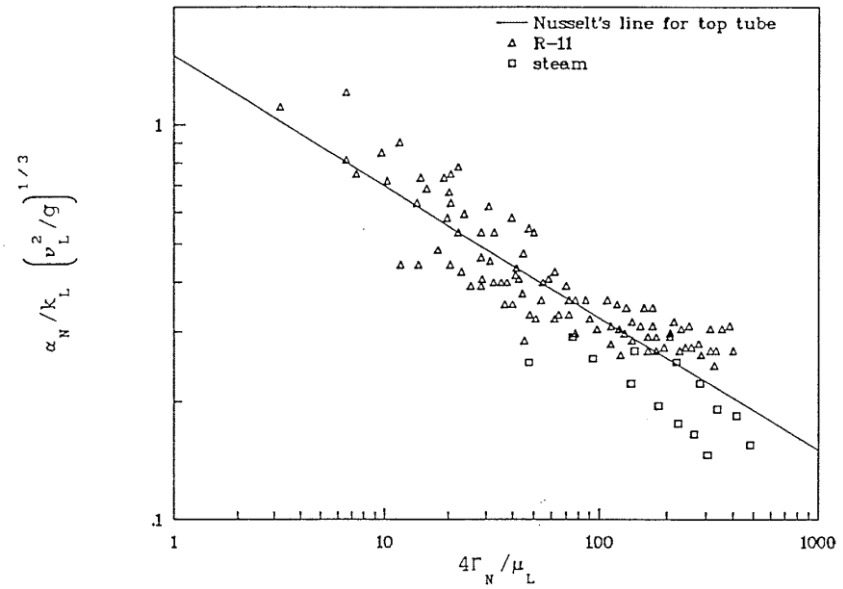

Figure 1.40. Data of Short and Brown (1951) for refrigerant-11 and steam.

Kern (1958) suggested the effects of ripples (shown in figure 1.41) formed by droplets from the upper tubes would increase heat-transfer coefficients above those predicted by Nusselt's (1916) equation (1.68) and therefore, proposed the following semi-empirical equation:

$$\frac{\overline{\alpha}_N}{\alpha_1} = N^{-\frac{1}{6}} \tag{1.70}$$

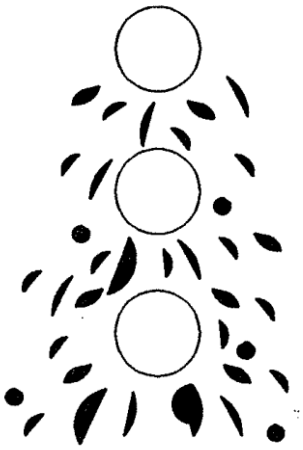

Figure 1.41. Ripples, splashing and turbulence (Kern (1958)).

Fuks (1957) obtained a model that predicts the heat-transfer coefficient within the tube's bundle based on his experimental data from the seventh and eleventh row of his test bank as follows:

$$\frac{\alpha_N}{\alpha_1} = \left(\frac{\Gamma_N}{\gamma_N}\right)^{-0.07} \tag{1.71}$$

Where Γ_N is the mass flow rate of the condensate per unit length drained from the Nth tube and γ_N is the condensation rate per unit length on the Nth tube.

Chen (1961) proposed that the mean temperature of the condensate leaving the first tube was slightly lower than the saturation temperature of the vapour, where the additional condensation occurs on the liquid sheet between the tubes. He assumed that the film temperature would reach the saturation temperature by the time it reached the second tube. By this assumption, condensation on the second tube would not start until a thermal boundary layer penetrated the film of the fluid that had fallen from the upper tube. The Chen expression is as follows:

$$\frac{\overline{\alpha}_N}{\alpha_1} = \left(1 + 0.2H(N-1)\right)\left(\frac{1 + H(0.68 + 0.02J)}{1 + J(0.95 - 0.15H)}\right)^{\frac{1}{4}} \tag{1.72}$$

It can be seen that for the top tube of a bank, heat-transfer coefficient from equation (1.73) would reduce into equation (1.20).

The following expression shows a correlation obtained by a Grant and Osment (1968) based on the experimental data from their test bank (figure 1.42) (mentioned above in the experimental studies section):

$$\frac{\alpha_N}{\alpha_1} = \left(\frac{\Gamma_N}{\gamma_N}\right)^{-0.223} \tag{1.73}$$

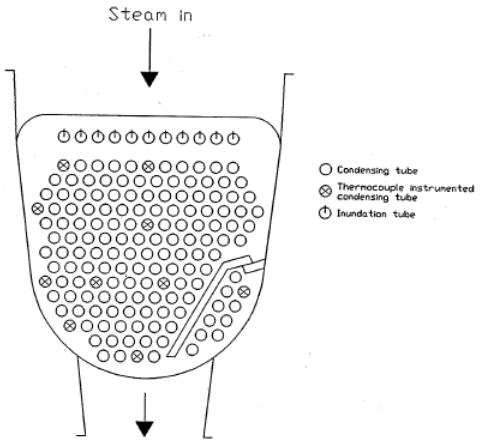

Figure 1.42. Schematic view of test section used by Grant and Osment (1968).

Figure 1.43 demonstrates the experimental data of Nobbs (1975) and Nobbs and Mayhew (1976) (based on the experimental parameters given in table 1.7), which were plotted as $\frac{\alpha_N}{\alpha_{Nu}}$ against $\left(\frac{\Gamma_N}{\gamma_N}\right)$, along with Nusselt theoretical equation (1916) and the empirical correlations of Fuks (1957) and Grant and Osment (1968). It is observed that all the data illustrated in this figure are above the Nusselt line (1916) and most of these data lie between Fuks (1957) and Grant and Osment (1968) lines.

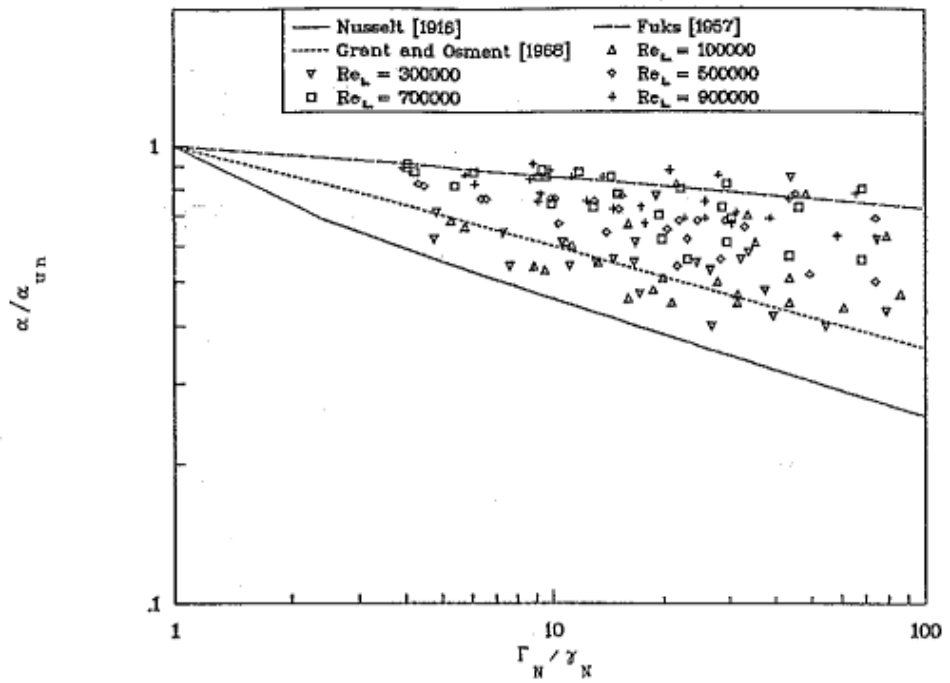

Figure 1.43. Data of Nobbs (1975) and Nobbs and Mayhew (1976) for steam.

Eissenberg (1972) considered the effects of side drainage, as shown in figure 1.44. He assumed that drops strike close to the midpoint of the upper half of the following tubes. For the bottom of the tube, he assumed Nusselt's (1916) model (equation (1.69)). Eissenberg's side drainage model mentioned that the inundation collected by the tubes in a row is the amount of condensate formed on all preceding rows. In his theoretical analysis, he made an assumption that inundation could only influence the condensate flow on the bottom portions of the tube, not the top. Using this assumption, he obtained a semi-empirical expression that predicts the smallest effect of inundation, as follows:

$$\frac{\overline{\alpha}_N}{\alpha_1} = 0.6 + 0.42N^{-\frac{1}{4}} \tag{1.74}$$

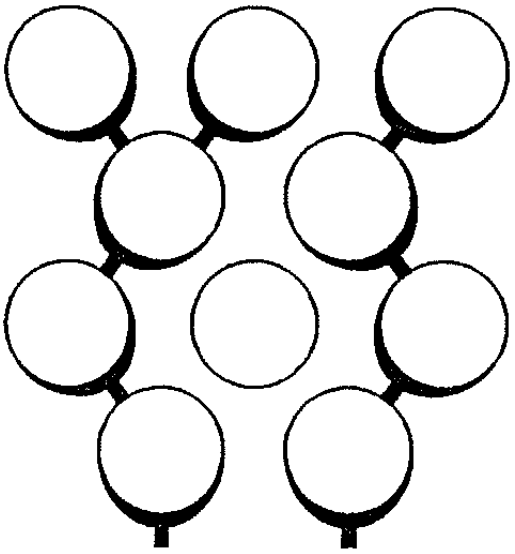

Figure 1.44. Side drainage model (Eissenberg (1972)).

Fujii and Oda (1981) and Fujii (1983) suggested two inundation models shown in figure 1.45, for condensation on a column of tubes. They adopted the assumptions of Nusselt for the condensate film and considered the effect of the amount of the condensate impinging on the lower tubes.

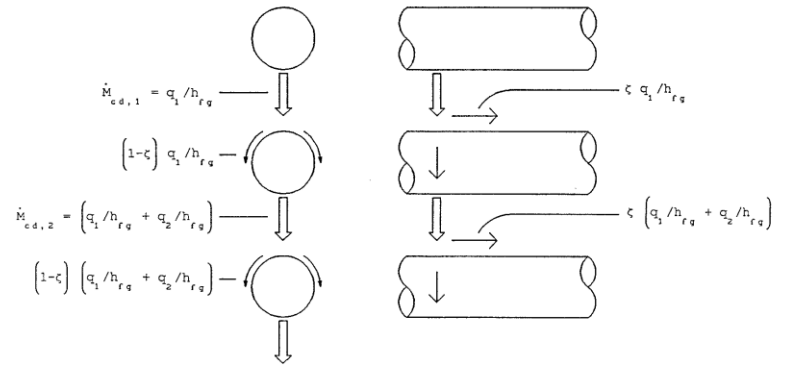

(a) Model I.

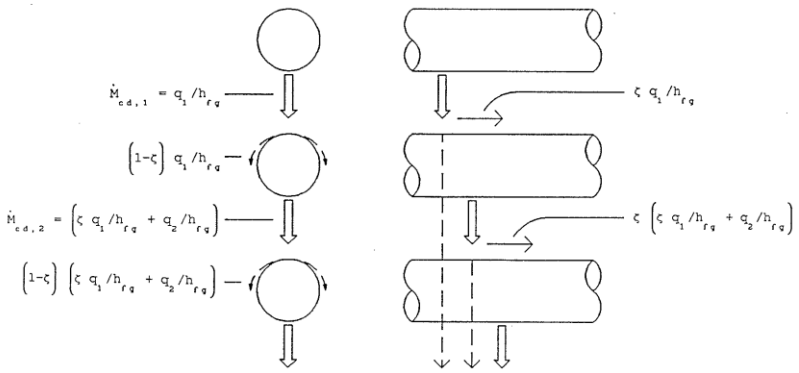

(b) Model II.

Figure 1.45. Physical model for inundation without vapour shear, after Fujii and Oda (1981) and Fujii (1983).

In the first model, they assumed that when the condensate approaches the (N+1) tube, a fraction ξ of the condensate spreads axially along the tube, while the rest 1- ξ, which is carried by the vapour, flows to the bottom of the tube without disturbing the thickness of the condensate film. This approach generated the following expression:

$$\left(\mathrm{Nu_N}\right)_{\mathrm{I}} = \left(\xi \sum_{i=1}^{N-1} \mathrm{Nu_i} \frac{\mathrm{H_i}}{\mathrm{H_N}}\right) \left\{ 1 + \left\{ \frac{\left(\frac{\mathrm{H_1}}{\mathrm{H_N}}\right)^{\frac{1}{3}} \mathrm{Nu_1}^{\frac{4}{3}}}{\left(\xi \sum_{i=1}^{N-1} \mathrm{Nu_i} \frac{\mathrm{H_i}}{\mathrm{H_N}}\right)^{\frac{4}{3}}} \right\}^{\frac{3}{4}} - 1 \right\} \tag{1.75}$$

In a second model, it was assumed that a fraction 1-ξ of condensate was assumed to avoid all the following tubes, which gave the following expression:

$$\left(Nu_N\right)_{II} = \sum_{i=1}^{N-1} \xi^{N-1} Nu_i \frac{H_i}{H_N} \left(\left\{ 1 + \frac{\left(\frac{H_1}{H_N}\right)^{1/3} Nu_1^{4/3}}{\left(\sum_{i=1}^{N-1} \xi^{N-1} Nu_i \frac{H_i}{H_N} \right)^{4/3}} \right\}^{3/4} - 1 \right) \qquad (1.76)$$

Numerical results for values of ξ in the range of 0.2-1.0 were given by Fujii (1983), as shown in figure 1.46. It was found that the Nusselt Numbers obtained for the second model were higher than those for the first at the same value of ξ because less condensate impinged on the lower tubes for the second model. Nusselt numbers for both models decrease with increasing ξ.

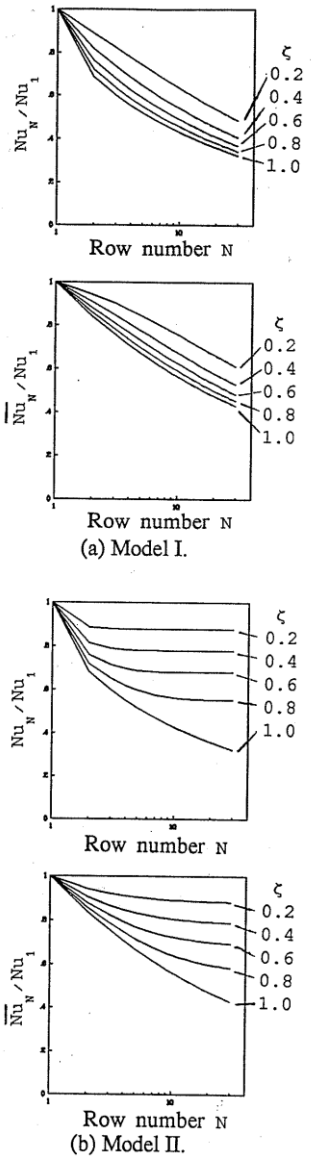

Figure 1.46. Theoretical results for inundation without vapour shear, after Fujii (1983).

Jacobs and Nadig (1984) investigated heat transfer from the vapour to the film condensate between two tubes. They considered the effects of condensation on the sub-cooled liquid between the tubes and their tube spacing (space between two successive rows), from which the temperature of the falling condensate film reaching the subsequent tube was estimated, from which their solution is given by the following expression:

$$\frac{\bar{\alpha}_N}{\bar{\alpha}_{Nu}} = \left(1 + 0.103H^{0.212}\sqrt{N-1}\right) \tag{1.77}$$

They assumed that the condensate is well mixed when it comes into contact with the following tube.

1.7.2. Forced-Convection Condensation

McNaught (1982) examined the relationship between vapour shear and gravity and recommended the following equation that combined their effects.

$$Nu = \left(Nu_{gr}^2 + Nu_{sh}^2\right)^{1/2} \tag{1.78}$$

A dimensionless parameter, J_v was recommended to specify the relative importance of vapour shear and gravity effects

$$J_v = \frac{xG}{\sqrt{dg\rho_v(\rho - \rho_v)}} \tag{1.79}$$

Where x is the vapour quality upstream of a given row. Based on the data of Nobbs (1975) and Nobbs-2 and Mayhew (1976), where $J_v < 1.5$, McNaught (1982) suggested the following expression for the gravity-controlled region:

$$Nu_{gr} = Nu_{Nu}\left(\frac{\Gamma}{\gamma}\right)^{-j} \tag{1.80}$$

Where $j = 0.22$ for in-line banks and 0.13 for staggered banks. The constants j and the critical J_v were obtained using only the data of Nobbs, which might not be applicable to other data for different geometries of tube bank and condensing fluids.

For the shear-controlled region were $J_v > 1.5$,an empirical equation based on the data of Nobbs, was proposed, as follows,

$$Nu_{sh} = 1.26 Nu_l \left(\frac{1}{X_{tt}} \right)^{0.78} \tag{1.81}$$

Where X_{tt} represents the Lockhart-Martinelli parameter for two phase flow, given by the following expression:

$$X_{tt} = \left(\frac{1-x}{x} \right)^{0.9} \left(\frac{\rho_v}{\rho} \right)^{0.5} \left(\frac{\mu}{\mu_v} \right)^{0.1} \tag{1.82}$$

Nu_l is the Nusselt Number obtained as if the liquid was flowing alone through the bank of tubes (ESDU (1973)) , is given as follows:

$$Nu_l = C_1 \left(Re_{l,max} \right)^{C_2} Pr^{0.34} \left(\frac{\mu c_p k_w}{\mu_w c_{pw} k} \right)^{0.26} (1-x)^{C_2} \tag{1.83}$$

Where $Re_{l,max}$ is the Reynolds number of the liquid flowing alone through the bank (through the minimum flow area between the tubes). The following table shows the empirical constants C_1 and C_2 in equation (1.83) corresponding to the range of $Re_{l,max}$.

Table 1.8. The range of $Re_{l,max}$ and the constants C_1 and C_2 in equation (1.83).

Range of $Re_{l,max}$	Constant C_1	Constant C_2
$Re_{l,max} \leq 300$	1.309	0.36
$300 \leq Re_{l,max} \leq 2 \times 10^5$	0.273	0.635
$Re_{l,max} \geq 2 \times 10^5$	0.124	0.7

Cavallini et al. (1986) inserted a correction to the Shekriladze and Gomelauri (1984) model to account for the effect of condensate inundation, based on experimental data of R-11 (table 1.7). This resulted in the heat-transfer coefficient for a given row to be given by the following equation:

$$\frac{\alpha_N}{\alpha_1} = \left(\frac{\Gamma_N}{\gamma_N} \right)^{-0.16} \tag{1.84}$$

Equation (1.84) correction was based on work by Cipollone et al. (1983), where α_1 is the heat transfer coefficient for the single non-inundated-tube of Shekriladze and Gomelauri (1966) Model in a bank of tubes. Figure 1.47 shows the comparison of the experimental results of Cavallini et al. (1985) for condensation of R-11 on a bank of plain tubes (given in table 1.7) with equation (1.84), using the mean velocity, $U_{mean-void}$.

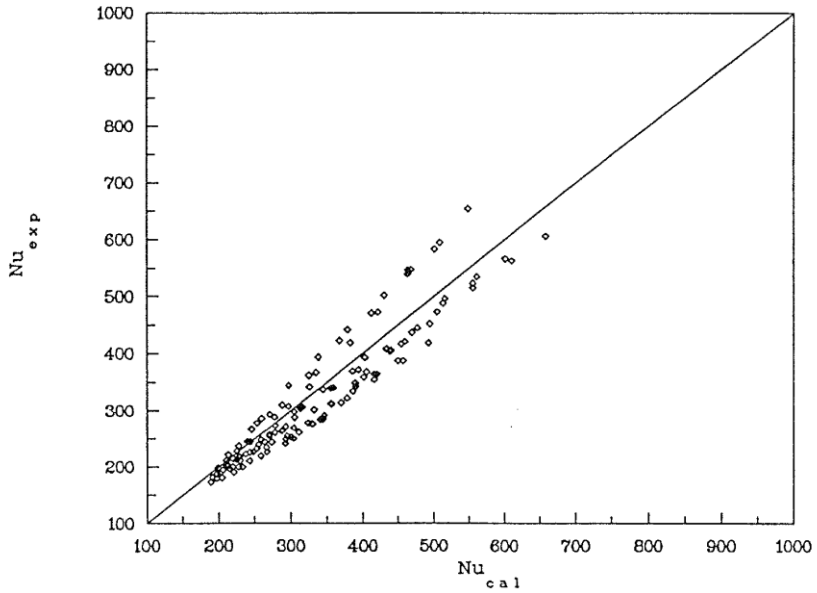

Figure 1.47. Experimental results of Cavallini et al. (1986) for condensation of R-11 on a bank of plain tubes.

Fujii and Oda (1986) studied the steam data of Nobbs and Mayhew (1976) and the refrigerant-21 data of Kutateladze et al. (1981). They proposed the following empirical equation for the heat-transfer coefficient:

$$\alpha_v = \left(\alpha_{gr}{}^4 + \alpha_{sh}{}^4\right)^{\frac{1}{4}} \tag{1.85}$$

Where

$$\alpha_{gr} = \alpha_{Nu} N^{-s} \tag{1.86}$$

α_{Nu} is calculated from equation (1.15)

s = 0.16 for in-line bundles

s = 0.08 for staggered bundles

and,

$$\alpha_{sh} = 0.9\left(\frac{k}{d}\right)\left(1+G^{-1}\right)\tilde{Re}_{\varepsilon}^{\frac{1}{2}}\, N^{-0.14} \qquad (1.87)$$

Honda (1989) regarded the flow of the condensate through the bundles, using gravity drained and uniformly dispersed flow models to determine the condensate inundation rate at low and high vapour velocities respectively. In the case of a gravity drainage (low vapour velocity (shown in Figure 1.48)), it was assumed that the condensate falls onto the tube directly below (i.e. in the next row for inline bundles and two rows down for staggered bundles), while with high vapour shear, the condensate is assumed to be uniformly distributed (shown in Figure 1.49) across the test section normal to the flow and hence only a fraction of the condensate impinges on the tubes below.

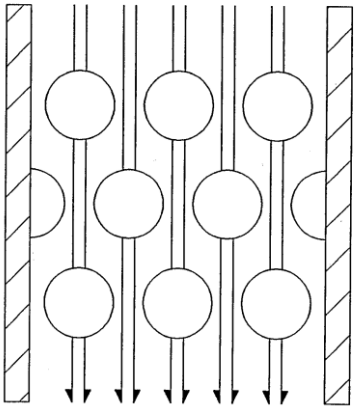

Figure 1.48. Gravity drained model.

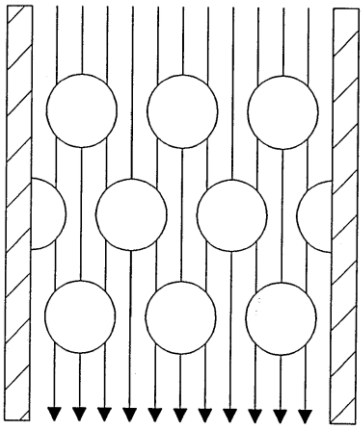

Figure 1.49. Uniform dispersed model.

For in-line bundles, the heat-transfer coefficient was determined using the following equation

$$Nu = \left(Nu_{gr}^4 + Nu_{sh}^4\right)^{\frac{1}{4}} \tag{1.88}$$

and for the staggered bundles,

$$Nu = \left(Nu_{gr}^4 + Nu_{gr}{}^2 Nu_{sh}{}^2 + Nu_{sh}^4\right)^{\frac{1}{4}} \tag{1.89}$$

Where Nu_{gr} is the Nusselt model for the gravity-controlled regime given by the following expression:

$$Nu_{gr} = d\left(\frac{g}{\nu^2}\right)^{\frac{1}{3}}\left(2.1Re_{f,gr}^{-1.2} + 2.7\times10^{-5}Re_{f,gr}^{0.8}\right)^{\frac{1}{4}} \tag{1.90}$$

$Re_{f,gr}$ is the film Reynolds number determined under the assumption of gravity-controlled flow. Equation (1.91) was based on the low vapour velocity data of Kutateladze et al. (1985) and Kutateladze and Gogonin (1979), for R-21 and R-12. Nu_{sh} is the shear-controlled flow, which is given by the following expression:

$$Nu_{sh} = a_1\left(1 + a_2A_1\right)^{\frac{1}{2}}A_2\tilde{R}e_{max}^{(1-(m/2))}Re_{f,u}^{-n} \tag{1.91}$$

Where

$$A_1 = Re_{v,max}^{m}\left(\frac{q}{\rho_v U_{max} h_{fg}}\right) \tag{1.92}$$

$$A_2 = \left(\frac{\rho_v}{\rho}\right)^{1/2}\left(\frac{\nu_v}{\nu}\right)^{m/2}Pr^{0.4} \tag{1.93}$$

$$Re_{v,max} = \frac{\rho_v U_{max} d}{\mu_v} \tag{1.94}$$

Where the empirical constants a_1, a_2, m and n within equations (1.91-1.94) were obtained by Honda et al. (1986) (based on their own data for R-113), which are given in table 1.9.

Table 1.9. Values of empirical constants in equations (1.91-1.93).

Bundles	a_1	a_2	m	n
In-line	0.053	1.83	0.4	0.2
Staggered	$0.165(P_t / P_l)^{0.7}$	18.0	0.2	0.2

Honda et al. (1989) also developed equation (1.85) of Fujii and Oda (1986) to give a better satisfaction with the refrigerant data by replacing the proportionality constant of 0.9 with $1.23\sqrt{\frac{d}{P_l}}$ in equation (1.87).

1.8. Key Findings.

1.8.1. Summary of Models.

The following tables summarise the theoretical and semi-empirical models described in this section. These are followed by a summary of the key findings from this section. These models will be compared with existing experimental data in chapter 3.

Table 1.10. Free-convection models for tube columns.

Reference	Methodology and Assumptions
Nusselt (1916)	Modified his analytical model for free convection on a single tube to account for inundation, using a simple row number correction with the following assumptions: 1. The condensate film falls from one tube to the next as a continuous sheet. 2. The wall-to-vapour temperature difference is the same for all tubes in a vertical column.
Fuks (1957)	An empirical correlation based his own data accounting for the effect of condensate inundation by considering the drained mass flow rate from the tubes. The heat-transfer coefficient for the first condensing tube row was estimated using the Nusselt (1916) solution for a horizontal tube.
Kern (1958)	A modification to the analytical model of the Nusselt (1916) for the tube bundle that accounts for the effect of the ripples being formed on the condensate film due to the droplets from the upper tubes.
Chen (1961)	A modification to the Chen (1961) model for single tube including condensate on the sub-cooled condensate as it falls between tubes. Assumes the film temperature reaches saturation by the time it reaches the next tube.
Grant and Osment (1968)	A similar approach to Fuks (1957) but based on the authors own data for steam condensing on a staggered tube bank.
Eissenberg (1972)	Accounted for the effects of side drainage by assuming drops strike close to the midpoint of the upper half of the following tubes.
Fujii and Oda (1981)	Assumed that a portion ξ of the falling condensate spreads axially along the next tube, while the remaining $1 - \xi$ flows directly to the bottom of the tube without disturbing the condensate film.
Fujii (1983)	Assumed that a portion ξ of the condensate spreads axially along the tube, while the remaining $1 - \xi$ was carried away by the vapour and did not impinge on any lower tubes.
Jacobs and Nadig (1984)	Accounts for condensation on the sub-cooled liquid between the tubes including the effect of tube spacing.

Table 1.11. Forced-convection models for single tubes.

Reference	Methodology and Assumptions
Shekriladze and Gomelauri (1966)	Used assumptions of Nusselt model for free convection on a single tube but added asymptotic, infinite condensation rate approximation for the shear stress at the liquid-vapour interface.
Fujii (1972)	Used an approximate-integral method for the vapour and conensate boundary layers.
Rose (1984)	Modified the approaches of Sheariladze and Gomelauri (1966) and Fujii (1972) to include the effect of of the pressure variation around the tube.
Honda (1986)	Semi-empirical model based on authors experimental data for R-113.

Table 1.12. Forced-convection models for tube banks.

Reference	Methodology and Assumptions
McNaught (1982)	Semi-empirical correlation based on steam data of Nobbs (1975) and Nobbs and Mayhew (1976).
Cavallini (1986)	A modification to the Shekriladze and Gomelauri (1966) model by including the effect of the condensate inundation semi-empiracally.
Fujii and Oda (1986)	Semi-empirical correlation based on the data of steam data of Nobbs and Mayhew (1976) and the R-21 data of Kutateladze et al. (1981).
Honda (1989)	Semi-empirical correlation consisting of a gravity controlled region, based on the low vapour velocity data of Kutateladze et al. (1985) and Kutateladze and Gogonin (1979), for R-21 and R-12 and a shear controlled region, based on the author's own data for R-113.

1.8.2. Free Convection Single Tube Models.

In a case of a free-convection condensation on a horizontal tube, there is good agreement between the Nusselt (1916) theory and experimental data. Later researches have included many of the effects originally neglected in the Nusselt theory and found their influence to be in most cases negligible. It can be concluded that provided the conditions of the original Nusselt (1916) model are prevalent (in particular low to zero vapour velocity and no condensate inundation) then the model is satisfactory.

1.8.3. Forced Convection Single Tube Models.

For the case of a Forced-Convection Condensation on the single tube**,** the Shekriladze and Gomelauri (1966) Model, which considers the shear stress at the liquid-vapour interface using an asymptotic infinite suction approximation, gives a good agreement for low to moderate vapour velocities. At high vapour velocities, agreement is less satisfactory, possibly due to boundary layer separation and / or turbulence in the condensate film. Later adaptions of this model (eg Fujii et al. (1972b), Rose (1984)) have shed more light on these effects but have not really improved the accuracy.

1.8.4. Free Convection Tube Column Models.

Generally these models attempt to include the effect of condensate inundation from higher tubes onto lower ones, with subsequent thickening and disturbing of the film. These mainly consist of semi-empirically correlating experimental data using the inundation mass flow rate. They are unrealistic since all real condensers will involve more complex flow through tube banks rather than simple columns and will also be affected by vapour shear, particularly near the entrance where vapour velocities can be high. In addition, validation of these models has been somewhat limited and a more comprehensive investigation of their efficacy will be presented in Section 3 of this work.

1.8.5. Forced Convection Tube Bank Models.

These models attempt to include the effects of both vapour shear and condensate inundation (and their variation down the bank as vapour is condensed). As with the tube column models above, validation is limited, with many researchers using limited

experimental data sets to both formulate and then validate their correlations. This can lead to models which may work well over a limited range of conditions (e.g. a particular tube bank geometry or condensing fluid) but are unproven over a wider range of conditions. As with the tube column models, a more comprehensive evaluation will be presented in Section 3.

1.9. Aims of the Present Project.

The aims of the present work can be conveniently split into three sections:

- Compile a comprehension and systematic database of experimental data from the available literature, and use this data base to evaluate existing models for condensation on banks of tubes.

- Use the data base above to develop a single empirical model for condensation on banks of tubes using the existing experimental data.

- Validate and where necessary modify and improve the new model such that it can be used with confidence over the widest possible range of parameters encountered in practical condensers.

1.10. A thesis structure/outline.

The thesis consists of five chapters. Chapter 1 reviews the background information for condensation on single tubes and banks of tubes, including existing theories and experimental investigations. Chapter 2 describes the collection, organization and processing of the available experimental data, to form a consistent and extensive data base. In Chapter 3 this data base is used to evaluate theoretical and empirical models available in the literature. Chapter 4 describes the development and validation of a new, simple semi-empirical model. Finally chapter 5 will summarise the findings and make recommendations for future work in the field.

2. Data Collection, Organization and Processing.

2.1. Introduction.

In the previous section it was pointed out that most semi-empirical models for tube columns and tube banks available in the literature have been developed using somewhat limited data sets. Furthermore, no comprehensive evaluation of existing models is available in the literature. This casts doubt on the reliability of these models, since they may give satisfactory results when compared to the data used in their development, but nothing is known about their reliability over a wider range of operational parameters. One of the aims of this project, therefore, is to bring together a comprehensive data base of experimental results from the literature for condensation on banks of tubes, and use it to test the validity of existing models and to develop new models where appropriate.

2.2. Data organisation.

For a full comparison with theoretical models, certain fundamental data items are needed from a given data set. Table 2.1 shows a typical data set as compiled in the present project. It comprises two parts-

1) Fundamental information regarding the test fluid and tube bank geometry
2) "Row-by-row" results showing how the important parameters vary down the bank.

Where possible all data were obtained directly from the original research work, either by extracting the data from published papers or PhD thesis, or by contacting the researchers directly. Where gaps appeared in the data sets (i.e. all boxes in table 2.1 could not be filled in directly from the researchers own data) then calculations were carried out to evaluate the missing data. A typical example might be where condensation inundation mass flow rates were not given and these had to be calculated from the heat flux to upstream rows, or only upstream vapour velocity was quoted, and this had to be corrected for lower rows, again using the heat flux. Details of the calculations performed are given in the next sub-section.

Table 2.1. Typical data set for condensation on a bank of tubes.

Data Set Identifier	Beech-1				
Test Fluid	Steam				
Outer Diameter / m	0.014				
Inner Diameter / m	0.0099				
Length / m	0.252				
Width / m	0.08				
Horizontal Pitch / m	0.02				
Vertical Pitch / m	0.0173				
Number of odd tubes	4				
Number of even tubes	3				
Row Number N	U_{min} / ms^{-1}	T_{sat} / °C	ΔT / K	q / kWm^{-2}	m_c / kg/m s
1	374.88	6.28	278.30	363.32	0.00
2	374.88	5.85	289.60	363.00	0.00
3	374.88	5.51	274.20	363.02	0.01
4	374.88	5.09	313.70	360.02	0.00
5	374.88	4.73	253.50	364.11	0.01
6	374.88	4.33	283.50	360.00	0.01
7	374.88	4.00	260.20	360.92	0.02
8	374.88	3.60	265.30	360.79	0.01
9	374.88	3.29	236.90	364.02	0.02
10	374.88	2.92	268.00	353.75	0.02
1	374.85	6.08	411.70	357.26	0.00
2	374.85	5.45	439.80	357.30	0.00
etc.					

2.3. Data processing.

The existing experimental data came from direct from the authors through their thesis and papers, and the data that are needed to be filled in table 2.1 for rows 2 to 10 are the up-stream velocity, heat flux, mass condensate and heat-transfer coefficient. The equations that are required to fill the gaps within table 2.2 are explained in the following sub-sections. All thermo-physical and transport properties were evaluated using the equations given in Appendix A.

2.3.1. Condensate mass flow-rate.

The condensate mass flow rate on the outside of an active tube in a row of a bank was determined from the following equation,

$$m_{condensate} = \frac{Q_N}{h_{fgN}} \tag{2.1}$$

Where

h_{fgN} = specific enthalpy at Nth row of evaporation estimated at T_v.

Q_n = heat-transfer rate to the tubes in N_{th} row.

2.3.2. Condensate inundation rate.

The condensate inundation rate on (N+1)th row was obtained from the following equation,

$$m_{N+1} = m_N + m_{condensate} \tag{2.2}$$

Where

m_N = mass flow rate of the condensate drained from the Nth row.

m_{N+1} = mass flow rate of the condensate drained from the (N+1) th row.

2.3.3. Heat-transfer coefficient.

The heat-transfer coefficient on the outside of the active tubes in a row of a bank was calculated from the following equation,

$$\alpha = \frac{q_N}{\Delta T} \tag{2.3}$$

Where

ΔT = Vapour-side temperature difference

q_N = heat flux to the tubes in N_{th} row, which can be obtained from the following equation.

$$q_N = \frac{Q_N}{n\pi ld} \tag{2.4}$$

Where n = number of tubes in a row.

d = diameter of the tubes.

l = length of a tube.

2.3.4. Vapour velocity.

The vapour mass flow rate and hence the vapour velocity at approach to any row was calculated from the upstream values and the heat transfer to that given row

$$m_{v,(N+1)} = m_{v,(N)} + m_{condensate} \tag{2.5}$$

Where

$m_{v,(N)}$ = vapour mass flow rate to Nth row.

$m_{v,(N+1)}$ = vapour mass flow rate to (N+1)th row.

Therefore, the vapour velocity in the test-section at approach to the $(N+1)_{th}$ row would be:

$$U_{\infty(N+1)} = \frac{m_{v(N+1)}}{A_{ts}\rho_v} \tag{2.6}$$

Where

$U_{\infty,(N+1)}$ = vapour velocity to $(N+1)_{th}$ row.

A_{ts} = Area of a test-section normal to the flow.

ρ_v = Density of the vapour evaluated at T_v, assuming the negligible pressure drop.

2.3.5. Calculation of the mean and the absolute percentage errors between the model and the experimental values.

In statistics, the mean percentage deviation E_1 is the calculated mean of the percentage errors between the predicted values of the model and the actual experimental values, which is given by the following equation:

$$E_1 = \left(\frac{100}{N}\right)\sum_{i=1}^{N}\left(1-\left(\frac{Nu_{cal}}{Nu_{exp}}\right)\right) \tag{2.7}$$

Where N = The number of the experimental data.

Nu_{cal} = The calculated Nusselt Number.

Nu_{exp} = The measured Nusselt Number.

The advantage of using the mean percentage deviation E_1 (equation 2.7) is to determine whether the model over-predicts or under-predicts most of the data. In other words, if the value of E_1 is positive, this indicates that the model under-estimates most of the data, while if the value of E_1 is negative, this shows that the model over-estimates most of the data. If the value of E_1 is nearly zero, this demonstrates that the percentage deviations of the model under-predicts the data is nearly same as the percentage deviations of the model over-predicts the data.

The disadvantage of the mean percentage deviation E_1 is it does not indicates how better results of the model. Therefore, another type of the percentage deviation is required, which is absolute percentage deviation E_2, also known as mean absolute percentage deviation is the obtained average absolute of the percentage errors between the calculated values of the model and the actual experimental values, and is defined by the following equation:

$$E_2 = \left(\frac{100}{N}\right)\sum_{i=1}^{N}\left|1-\left(\frac{Nu_{cal}}{Nu_{exp}}\right)\right| \qquad (2.8)$$

From equation (2.8), as the value of the mean absolute percentage deviation E_2 is smaller, it demonstrates that results of the model is better.

2.4. Summary.

The full data base for condensation on banks of tubes is given in Appendices B and C. The ranges and scope of the data base is summarised in Table 2.2.

Table 2.2. Condensation of vapours on banks of tubes – Range and scope of experimental data base.

Number of data points	Approximately 4200
Number of tube bank geometries	13
Number of test fluids	7
Range of tube length / m	0.1-0.585
Range of tube outside diameter / m	0.01-0.0191
Range of horizontal pitch / m	0.0133-0.027
Range of vertical pitch / m	0.0115-0.0238
Range of U_{min} / ms^{-1}	0.001-21.63
Range of T_{sat} / $^{\circ}C$	23.5-104
Range of ΔT / $^{\circ}C$	4.9-31.6
Range of q / kWm^{-2}	3.00-694.90

3. Comparison of the Experimental Database with Some of the Existing Theories for a Bank of tubes.

In this section, the experimental database described and summarised in section 2, and presented in full in Appendices B and C, will be compared in detail with the theoretical and semi-empirical models described in Section 1. Tables 3.1 and 3.2 summarize the experimental data-base and give the symbols used in the figures throughout this section.

Table 3.1. Condensation of the steam vapours on the banks of plain tubes – Experimental data base.

Reference	Bank layout	Tube outside diameter / mm	Vapour velocity $U_{\infty,1}$ / ms^{-1}	Symbols used in Figures
Beech (1995)-1	Staggered	14.0	6.08 - 18.31	
Beech (1995)-2	Staggered	14.0	17.34 - 19.62	
Beech (1995)-3	Staggered	14.0	4.18-10.19	
Michael (1988)	Staggered	14.0	5.97-21.63	
Nobbs-1 (1975)	Staggered	19.05	0.31-9.20	
Nobbs-2(1976)	In-line	19.05	0.41-8.29	
Briggs and Sabaratnam (2003)	Staggered	19.1	4.40-10.62	

Table 3.2. Condensation of the non-steam vapours on the banks of plain tubes –Experimental data base.

Reference	Fluid	Bank layout	Tube outside diameter / mm	Vapour velocity $U_{\infty,1}$ / ms^{-1}	Symbols used in Figures
Cavallini-1(1985)	Refrigerant-11	Staggered	10.0	0.51-4.25	
Cavallini-2 (1988)	Refrigerant-113	Staggered	10.0	0.92-5.13	
Honda-1 (1988)	Refrigerant-113	Staggered	15.9	0.61-5.37	
Honda-2 (1988)	Refrigerant-113	In-line	15.9	0.56-5.60	
Gogonin-1 (1971)	Refrigerant-21	Staggered	17.0	0.001-0.21	
Gogonin-2 (1976)	Refrigerant-21	Staggered	17.0	0.001-2.04	
Shah-1 (1978)	Iso-propanol	Staggered	12.7	0.35-4.30	
Shah-2 (1981)	Methanol	Staggered	12.7	0.40-0.62	
Kutateladze (1981)	Refrigerant-21	Staggered	16.0	0.22-1.68	
Briggs (2000)	Refrigerant-113	Staggered	18.7	0.13-0.44	

The method of comparison chosen was to plot the percentage difference between the calculated Nusselt number (from the relevant model) and the experimental value, against the

dimensionless number F. As discussed in section 1, F represents the relative importance of gravity and vapour shear on the condensation process, with large values of F representing gravity dominated flows and small values for flows dominated by vapour shear. This method was chosen for two reasons; firstly vapour shear is one of the most (but by no means the only) important flow parameter in condensation in tube banks, and secondly, it was thought desirable to use the same method of comparison for all models, even those which did not include vapour shear in their formulation. Indeed in these "free-convection" models it is informative to see if the models deviate from experimental data only where high vapour shear is experienced, or if in fact they are inaccurate under low vapour shear regimes as well.

3.1. Free-convection Models.

3.1.1. Nusselt (1916) Model.

Nusselt (1916) modified his model for free convection on a single tube using the simple assumptions that the laminar condensate film falls from one tube to the next as a continuous sheet and the wall-to-vapour temperature difference is the same for all tubes in a vertical column to calculate the mean heat-transfer coefficient of a vertical column of the horizontal tubes accounting for inundation.

Table 3.3. Summary of the mean deviation E_1 and the standard mean deviation E_2 for Nusselt (1916), Fuks (1957), Kern (1958) and Chen (1961) models.

	Steam Data		Non-Steam Data		Non-Steam Data	
	E_1	E_2	E_1	E_2	E_1	E_2
Nusselt (1916)	49.43	55.37	48.55	50.19	48.85	51.97
Fuks (1957)	36.53	43.67	26.08	36.79	29.67	39.15
Kern (1958)	45.36	51.78	39.62	42.83	41.59	45.91
Chen (1961)	38.96	55.54	41.07	44.42	40.35	48.25

Figures 3.1 and 3.2 compare the Nusselt model with the data for steam and non-steam respectively. It can be seen in these figures, that the agreement is very poor for both steam and non-steam fluids at low F, for high vapour velocities, due to the existing shear stress on a condensate film, leading the decrease of the condensate film's thickness, where the model under-estimated most of the experimental heat transfer data. At high F (low vapour velocity), some of the data were under-predicted by the model, which shows the effect the condensate inundation on the heat-transfer is insignificant compared to the effect of the low vapour velocity. Some of the experimental data for both of the steam and non-steam fluids were

over-predicted by the model; where it represents the effect of the condensate inundation dominates the effect of the shear stress on the surface of the condensate on the heat transfer. For steam, the model under-predicts the entire data of Nobbs-1(1975), Nobbs-2 (1976) and Briggs and Sabaratnam (2003).

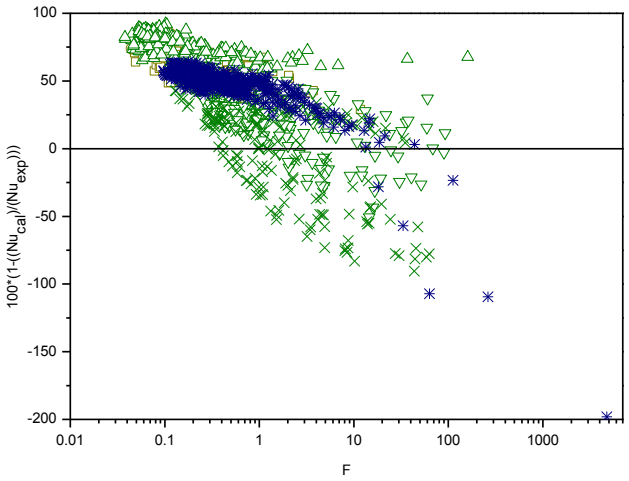

Figure 3.1. Comparison of Nusselt model (1916) to the experimental data of steam.

For the non-steam fluids, the model under-predicts most of its data, excluding that of Cavallini-1 (1985), Cavallini-2 (1988), Honda-1 (1988) and Honda-2 (1988). Overall the agreement is not good, since the Nusselt (1916) model does not consider the effect of shear stress on a condensate film due to the flowing vapour velocity. Simple row number in Nusselt (1916) Model is not a realistic way of accounting the effect of the inundation.

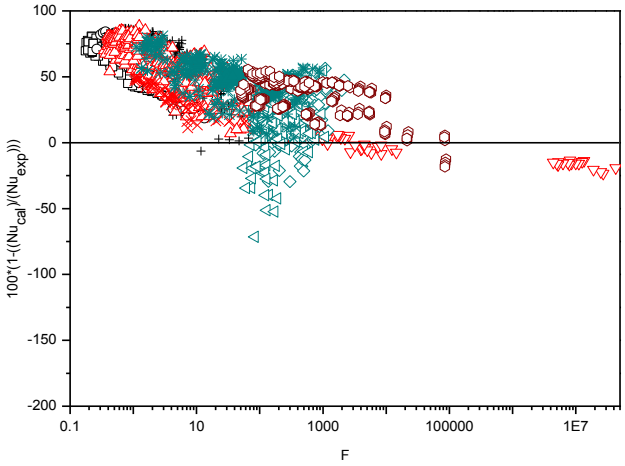

Figure 3.2. Comparison of Nusselt model (1916) to the experimental data of non-steam fluids.

3.1.2. Fuks (1957) Model.

Fuks (1957) obtained a model, in which the heat-transfer coefficient was estimated for the first condensing tube row, using Nusselt's analytical solution for a horizontal tube. It accounts for the effect of the condensate inundation by considering the drained mass flow rate from the tubes into the account, allowing an estimation of the heat-transfer coefficients through the bundle. The Fuks (1957) model was based on the experimental data obtained by Fuks from the seventh and eleventh row of a staggered bank of 11 rows with a steam. Figures 3.3 and 3.4 compare the Fuks (1957) model with the data for steam and non-steam respectively. For steam, the model underestimates most of the data, except those of Nobbs-2 (1976).

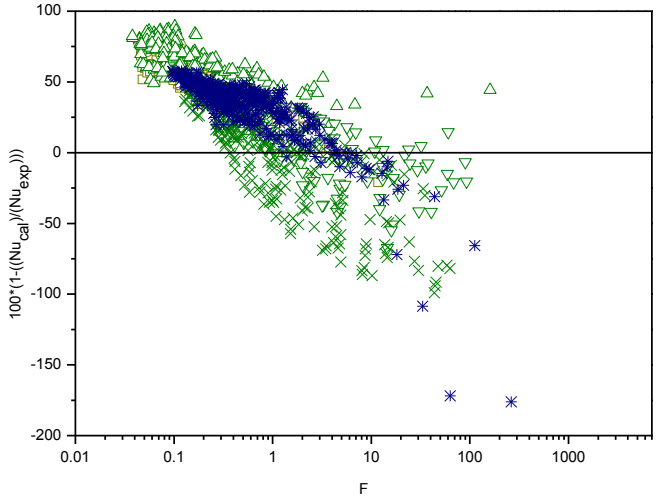

Figure 3.3. Comparison of Fuks (1957) to the experimental data of steam.

For the non-steam data, the correlation under-estimates much of the data: the exception being that of Shah-1 (1978) and Shah-2 (1981). The agreement between the model and the experimental data is again particularly poorly predicted, where the model does not account the effect of the shear stress.

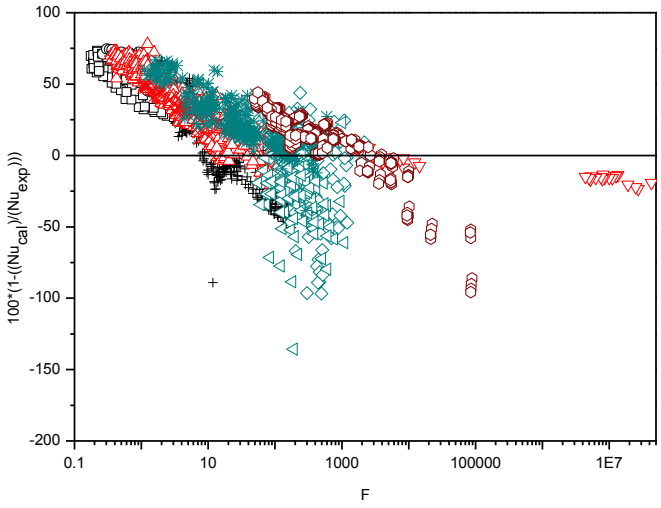

Figure 3.4. Comparison of Fuks (1957) to the experimental data of non-steam fluids.

3.1.3. Kern (1958) Model.

Kern (1958) modified the Nusselt model to account for the effect of ripples being formed on the condensate film due to the droplets from the upper tubes. This modification shifts the data in figures 3.1 and 3.2 slightly downwards by changing the exponent in Nusselt model from $-1/4$ to $-1/6$, as shown in figures 3.5 and 3.6, from which it improved its performance as illustrated in table 3.1. For the steam data, the correlation under-predicts most of its data, the exceptions being the data of Beech-3 (1995), Nobbs-1 (1975) and Nobbs (1976). For non-steam, the model under-estimates the majority of the data, the exception being that of Shah (1981). The theoretical output data of Gogonin (1971) and Gogonin (1976) from this model have not changed from that of the Nusselt (1916) model for the bank of tubes, since their tube-bundles consist of only 1-active tube (as demonstrated in figure 1.29). This correction did not give a good agreement, since again this model does not account the effects of the shear stress on a condensate film due to the flowing vapour velocity and the inundation due to the drained liquid from the tubes.

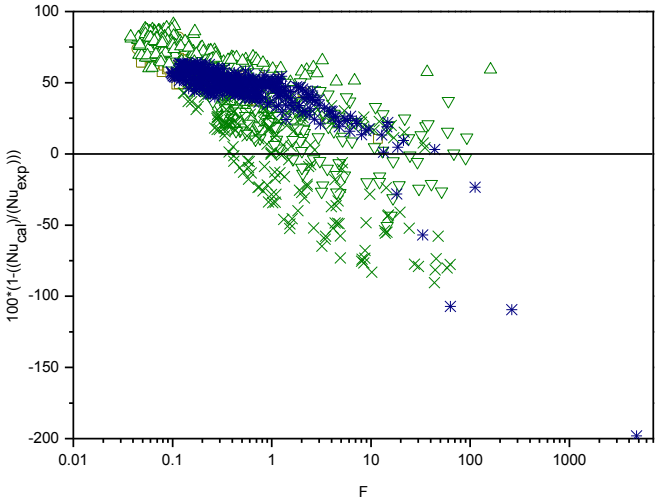

Figure 3.5. Comparison of Kern model (1958) to the experimental data of steam.

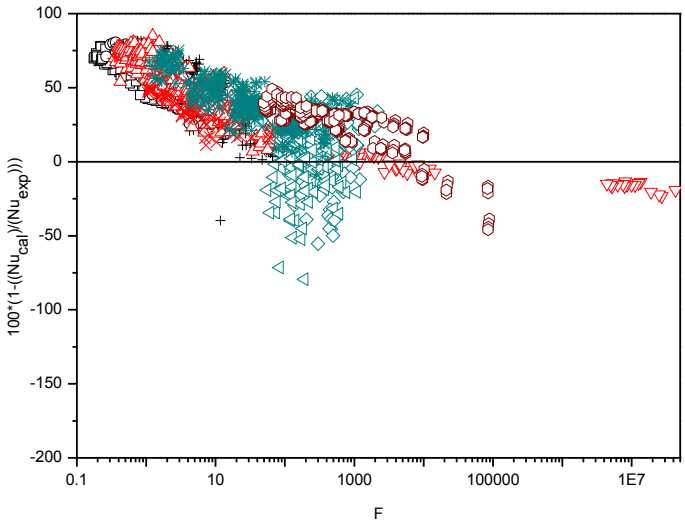

Figure 3.6. Comparison of Kern model (1958) to the experimental data of non-steam fluids.

3.1.4. Chen (1961) Model.

Chen (1961) recommended in his model for the bank of tubes that the mean temperature of the film condensate leaving the first tube was slightly lower than the saturation temperature of the vapour, where the additional condensation took place on the liquid sheet between the tubes. Figures 3.7 and 3.8 illustrate an obvious disagreement between the Chen (1961) model, and the experimental data of steam and non-steam fluids. The model under-predicts most of the data for steam, apart from that of Nobbs-1(1975) and Nobbs-2 (1976). The model underestimates the entire data of Cavallini-1(1985), Cavallini-2 (1988), Honda-2 (1988) and Kutateladze (1981) while it under-predicts the majority of the data of the other investigators for non-steam fluids. The reasons for this disagreement are same as that for the Nusselt model.

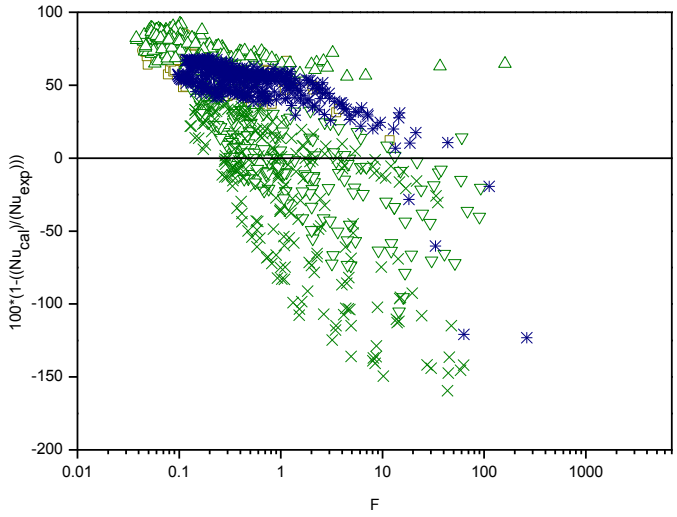

Figure 3.7. Comparison of Chen (1961) to the experimental data of steam.

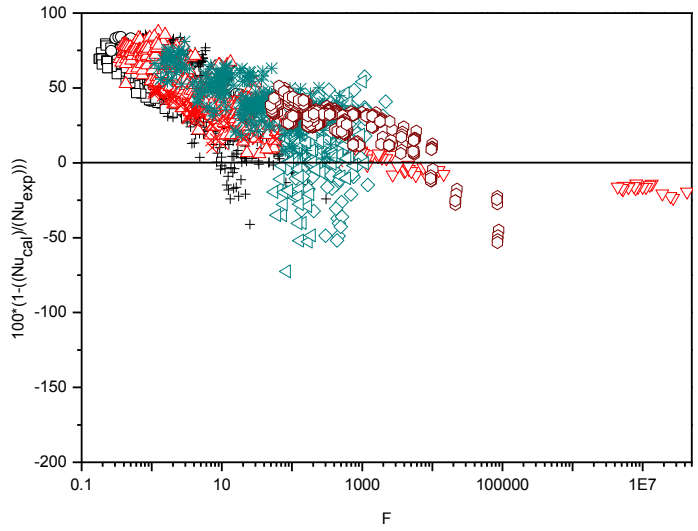

Figure 3.8. Comparison of Chen (1961) to the experimental data of non-steam fluids.

Table 3.4. Summary of the mean deviation E_1 and the standard mean deviation E_2 for Grant and Osment (1968), Eissenberg (1972) and Jacobs and Nadig (1984) models.

	Steam Data		Non-Steam Data		Non-Steam Data	
	E_1	E_2	E_1	E_2	E_1	E_2
Grant and Osment (1968)	55.35	59.64	37.72	40.99	43.78	47.40
Eissenberg (1972)	30.72	48.79	28.07	36.05	28.98	40.43
Jacobs and Nadig (1984)	28.98	40.89	5.81	34.88	13.81	36.96

3.1.5. Grant and Osment (1968) Model.

Changing the exponent in Fuks model from -0.07 into -0.332 as proposed by Grant and Osment (1968), where their correlation was based on the experimental data of their

staggered bank of 14 rows that consists of 139 tubes, shifts the experimental data for each of the steam and non-steam fluids in figures 5.3 and 5.4 upwards (as illustrated in figures 3.9 and 3.10), from which the agreement between the model and the experimental data becomes poor compared to that of Fuks (1957) model according to table 3.4. For steam, the model under-estimates the entire data by the investigators, except that of Nobbs-1 (1975), Nobbs-2 (1976) and Briggs (2000) where the model under-predicts most of their data.

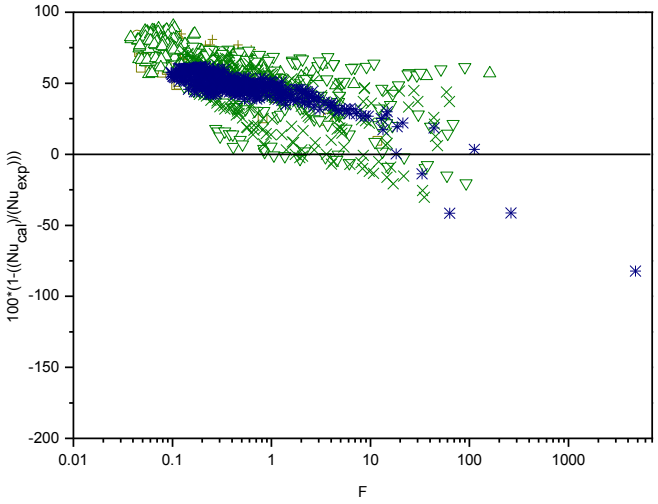

Figure 3.9. Comparison of Grant and Osment (1968) to the experimental data of steam.

The Grant and Osment (1968) model under-estimates most of the experimental data of the non-steam fluids, excluding that of Shah-2(1981). The calculated heat-transfer coefficient of Gogonin (1971) and Gogonin (1976) from this model have not been changed from that of Fuks (1957) model, since there is one active tube and no artificial inundation in his tube-bundles. Again the main reason for this model that does not give a good agreement with the experimental data is same as that of Fuks model.

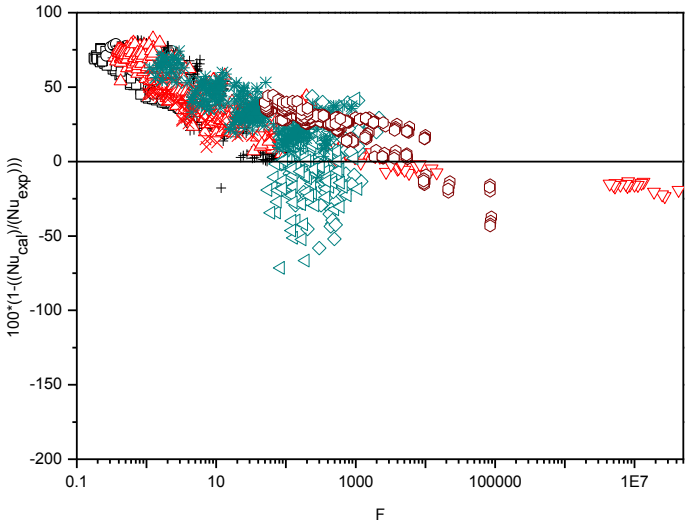

Figure 3.10. Comparison of Grant and Osment (1968) to the experimental data of non-steam fluids.

3.1.6. Eissenberg (1972) Model.

Eissenberg (1972) developed a Nusselt type model for the bank of tubes empirically to account for the effects of side drainage, where he proposed that the drops do not strike only the tops of lower tubes, but strike anywhere on the upper half. He made an unrealistic assumption that the inundation could only influence the condensate flow on the bottom parts of the tube, not on the top. This assumption shifts the data in figures 3.1 and 3.2 downwards, which provided poor satisfaction between the model and the data of steam and non-steam fluids respectively, as demonstrated in table 3.4. Their results are shown in figures 3.11 and 3.12. For steam, the model underestimates most of the data, with the exclusion of Nobbs-2 (1976), as illustrated in table 3.6.

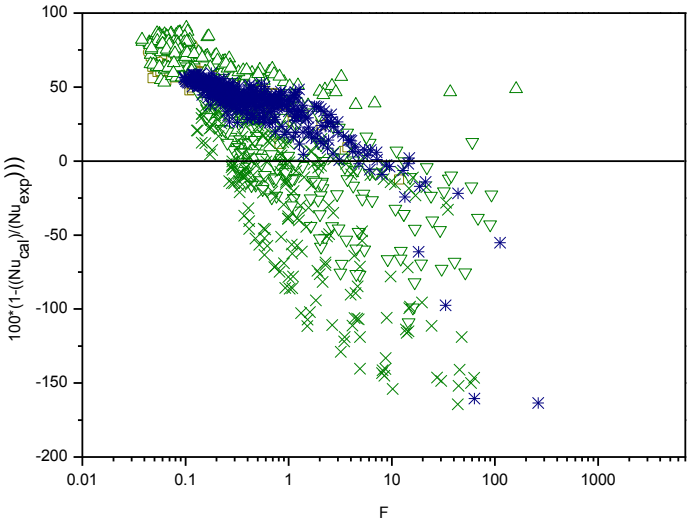

Figure 3.11. Comparison of Eissenberg (1972) model to the experimental data of steam.

For the non-steam data, model under-estimates the majority of the data, again the exception being that of Shah-1 (1978) and Shah-2 (1981). Overall the agreement is not good, since this model depends on the Nth row of the bank, which is not a realistic way of accounting the effect of the inundation, and does not account the effect of the shear stress on a condensate film due to the flowing vapour velocity.

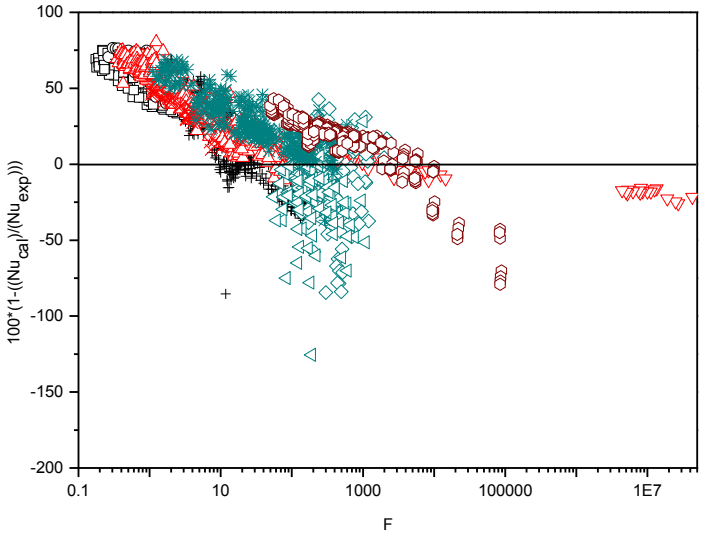

Figure 3.12. Comparison of Eissenberg (1972) model to the experimental data of non-steam fluids.

3.1.7. Fujii and Oda (1981) Model.

Fujii and Oda (1981) supposed that when the film condensate falls on the (N+1) tube, only a portion ξ of the condensate spreads axially along the tube, while the remains $1 - \xi$ (which is carried by the vapour) flows to the bottom of the bank without disturbing the condensate film. Table 3.5 represents the comparisons between the Fujii and Oda model (1981) and the experimental data of steam and non-steam fluids for the values of ξ takes place between 0.1 and 1 at interval of 0.1.

Table 3.5. Summary of the mean deviation E_1 and the standard mean deviation E_2 for Fujii and Oda model (1981) at different values of ξ.

	Steam Data		Non-Steam Data		All Data	
ξ	E_1	E_2	E_1	E_2	E_1	E_2
0.1	40.96	47.87	28.58	36.52	32.84	40.42
0.2	43.00	49.67	33.98	39.33	37.08	42.89
0.3	44.46	50.99	37.55	41.65	39.92	44.86
0.4	45.59	52.01	40.19	43.52	42.05	46.44
0.5	46.51	52.85	42.27	45.06	43.73	47.74
0.6	47.28	53.55	43.98	46.38	45.12	48.85
0.7	47.94	54.15	45.42	47.54	46.29	49.81
0.8	48.51	54.67	46.66	48.57	47.30	50.67
0.9	49.01	55.14	47.75	49.50	48.18	51.44
1	49.90	56.00	48.71	50.34	49.12	52.28

For the steam, this model under-estimates most of its experimental data for all values of ξ given in table 3.5, and is the most successful at $\xi = 0.1$, when compared to the other values of ξ. For the non-steam fluids, the model under-predicts most of the experimental data for all values of ξ, apart from that of Shah-1 (1978) for Isopropanol (where this model over-estimates his data for $\xi = 0.1$ and 0.2) and Shah-2 (1981) for methanol (from this model this model over-estimates his data for $\xi = 0.7$, 0.8, 0.9 and 1.0). In general, the model is the most successful at $\xi = 0.1$ for non-steam fluids (as given in table 3.5). Figures 3.13 and 3.14 compare the Fujii and Oda model (1981) with the data of steam and non-steam respectively at $\xi = 0.1$ (since it is the most successful value of ξ for the all data as shown in table in 3.11).

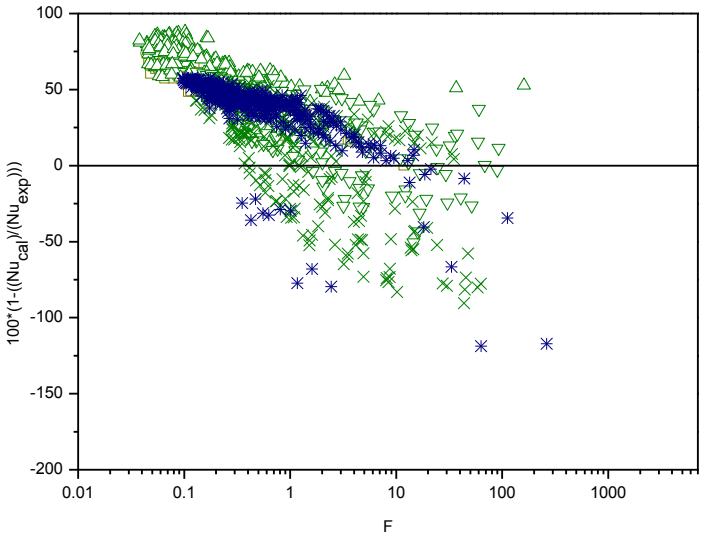

Figure 3.13. Comparison of Fujii and Oda model (1981) (based on $\xi = 0.1$) to the experimental data of steam.

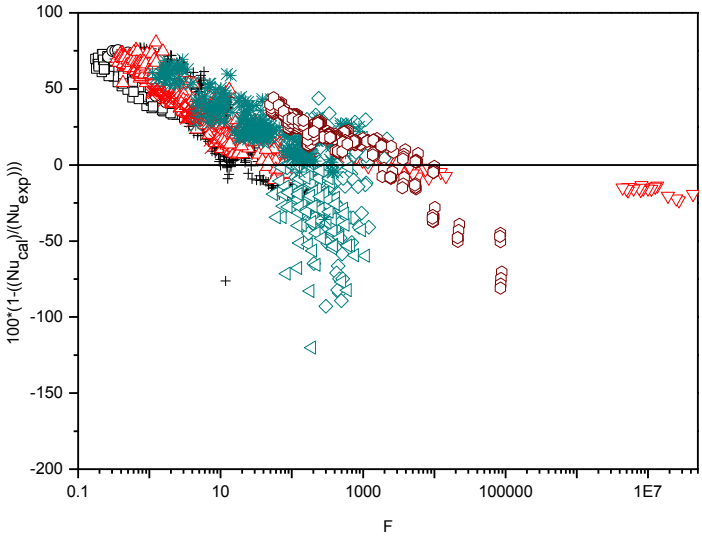

Figure 3.14. Comparison of Fujii and Oda model (1981) (based on $\xi = 0.1$) to the experimental data of non-steam fluids.

Figures 3.15 and 3.16 compare the Fujii and Oda model (1981) with the data of steam and non-steam respectively at $\xi = 0.5$, where it shifts the majority of the steam data in figure 3.13 (at $\xi = 0.1$) upwards, except that of Beech-3 (1995), Nobbs-1(1975) and Nobbs-2 (1976), where their data have not been shifted, since there is one active single-tube in their tube bundles. The values of the percentage deviations for the non-steam fluids in figure 3.14 have been shifted upwards using $\xi = 0.5$, as illustrated in figure 3.16, apart from that of Shah-1 (1978) and Shah-2 (1981), where their values of the percentage deviations were moved

downwards, and that of Gogonin-1 (1971) and Gogonin-2 (1976) have not been effected, since there is one active single-tube in his tube bundle and no artificial tubes, as shown in table 3.5. Practically, the value of ξ cannot be obtained from the given operating conditions, which makes it to be unreliable.

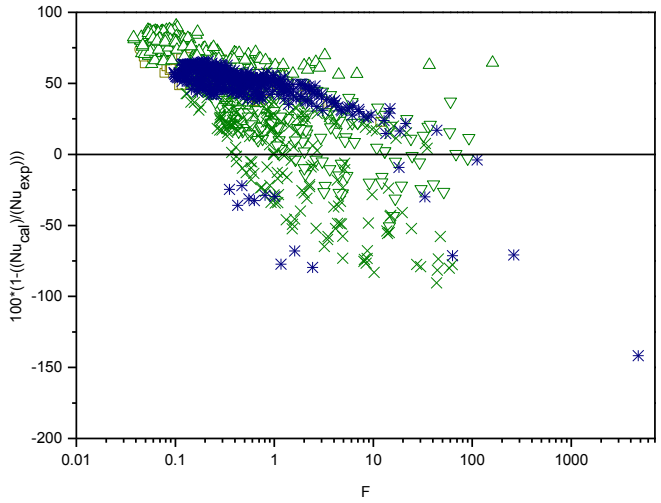

Figure 3.15. Comparison of Fujii and Oda model (1981) (based on ξ = 0.5) to the experimental data of steam.

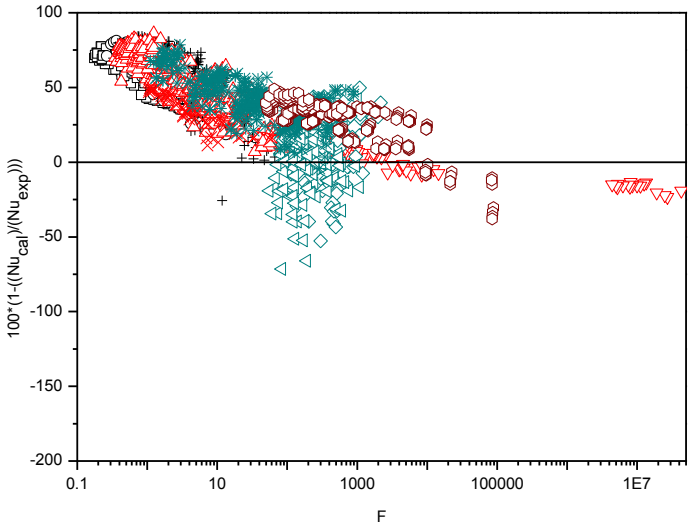

Figure 3.16. Comparison of Fujii and Oda model (1981) (based on ξ = 0.5) to the experimental data of non-steam fluids.

3.1.8. Fujii (1983) Model.

Fujii (1983) altered the assumption that was suggested in Fujii and Oda (1981) model, assuming instead that a fraction 1 - ξ of a condensate drained from the tube avoided all the following tubes. Table 3.6 demonstrates the comparisons between the Fujii model (1983) and the experimental data of steam and non-steam fluids for the values of ξ lie between 0.1 and 1 at interval of 0.1.

Table 3.6. Summary of the mean deviation E_1 and the standard mean deviation E_2 for Fujii (1983) model at different values of ξ.

	Steam Data		Non-Steam Data		All Data	
ξ	E_1	E_2	E_1	E_2	E_1	E_2
0.1	37.83	45.83	17.89	34.32	24.75	38.27
0.2	38.49	46.42	19.08	34.68	25.75	38.72
0.3	39.40	47.20	20.71	35.10	27.13	39.26
0.4	40.60	48.17	22.88	35.62	28.97	39.93
0.5	42.05	49.33	25.72	36.41	31.34	40.85
0.6	43.67	50.64	29.34	37.81	34.27	42.22
0.7	45.34	51.99	33.84	39.91	37.80	44.06
0.8	46.94	53.30	39.14	42.63	41.82	46.30
0.9	48.41	54.52	44.50	46.61	45.84	49.33
1	49.73	55.63	49.06	50.68	49.29	52.38

For the steam, the model under-estimates the majority of its experimental data for all values of ξ as given in table 3.12, where it is the most successful at ξ = 0.1, when compared to the other values of ξ, where it shifts the steam data in figure 3.13 downwards as demonstrated in figure 3.17. For the non-steam data, the model under-predicts most of its experimental data for all values of ξ, except that of Shah-1 (1978), which over-estimates his data for ξ = 0.1, 0.2, 0.3, 0.4 and 0.5, Shah-2 (1981) that under-estimates his data for ξ = 0.9 and 1.0 and Briggs (2000), which over-predicts the model for ξ = 0.1 and 0.2. In overall, the model is the most successful for the non-steam fluids at ξ = 0.1, (based on table 3.6), as illustrated in figure 3.18.

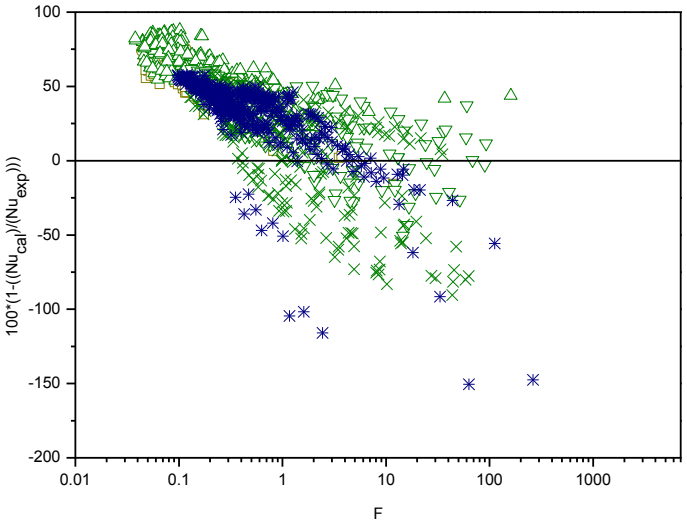

Figure 3.17. Comparison of Fujii (1983) model (based on $\xi = 0.1$) to the experimental data of steam.

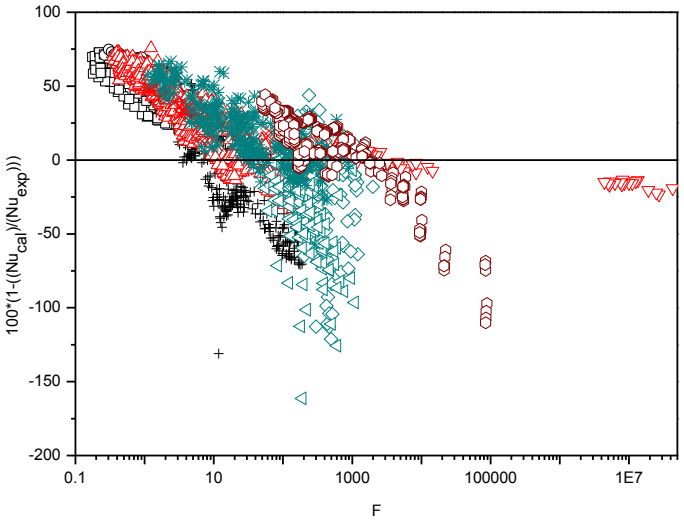

Figure 3.18. Comparison of Fujii (1983) model (based on $\xi = 0.1$) to the experimental data of non-steam fluids.

Figures 3.19 and 3.20 compare the Fujii (1983) model with the data of steam and non-steam respectively at $\xi = 0.5$, where it moves most of their percentage deviation values in figure 3.17 (at $\xi = 0.1$) upwards, again the exception being that of Beech-3 (1995), Nobbs-1(1975) and Nobbs-2 (1976). For the non-steam fluids, the percentage deviation values in figure 3.18 have been shifted upwards using $\xi = 0.5$, as shown in figure 3.20, again excluding that of Shah-1 (1978) and Shah-2 (1981) as shown in table 3.6 ,where again their percentage deviation values were shifted downwards, and again the percentage deviation values of Gogonin-1 (1971) and Gogonin-2 (1976) have not been moved, since there is one active

single-tube in his tube bundle and no artificial tubes, as shown in table 3.6. The main reason for not relying in this model is same as that of Fujii and Oda (1981).

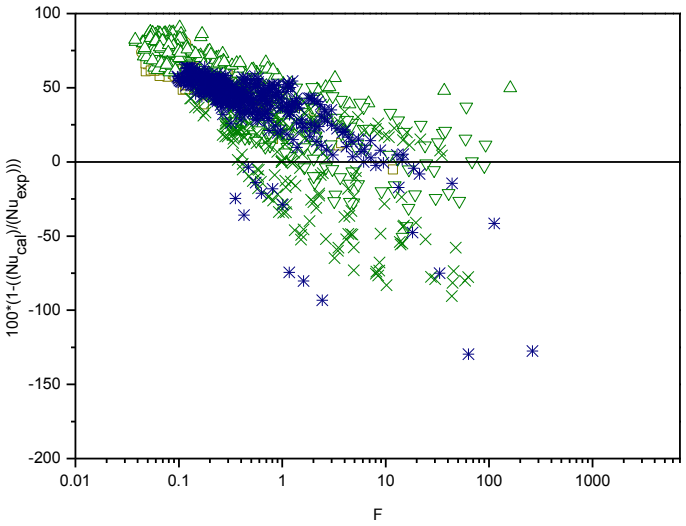

Figure 3.19. Comparison of Fujii model (1983) (based on $\xi = 0.5$) to the experimental data of steam.

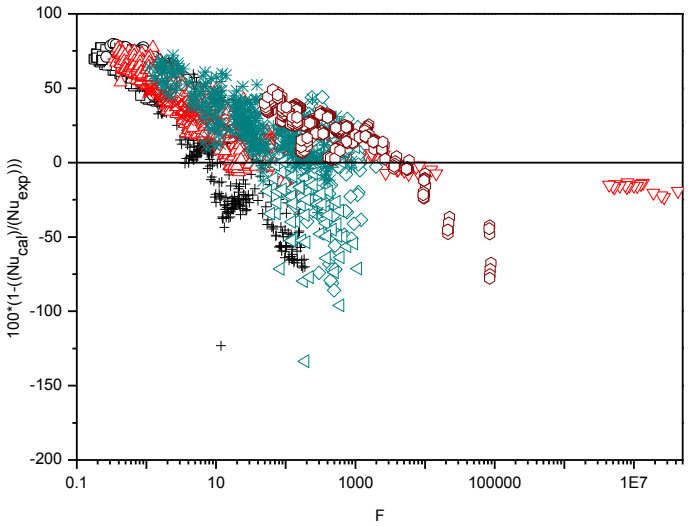

Figure 3.20. Comparison of Fujii model (1983) (based on $\xi = 0.5$) to the experimental data of non-steam fluids.

3.1.9. Jacobs and Nadig (1984) Model.

Jacobs and Nadig (1984) studied the heat transfer from the vapour to the film condensate between two tubes. They have taken the effects of the condensation on the sub-cooled liquid between the tubes and its tube spacing (space between two successive rows) into account, where the temperature of the condensate film leaving the first tube was slightly lower than the saturation temperature of the vapour. There is poor agreement between Jacobs and Nadig (1984) model and the experimental data for each of the steam and non-steam fluids as shown in figures 3.21 and 3.22. For steam, the model under-estimates the entire data of Beech-2 (1995), Beech-3 (1995) and Michael (1988), while it under-predicts majority of data by other investigators. The model under-estimates most of the experimental data of the non-steam fluids, except that of Shah-1(1978), Shah-2 (1981) and Briggs (2000). The reasons for this disagreement are it does not consider the effects of the shear stress on a condensate film due to the flowing vapour velocity and the inundation.

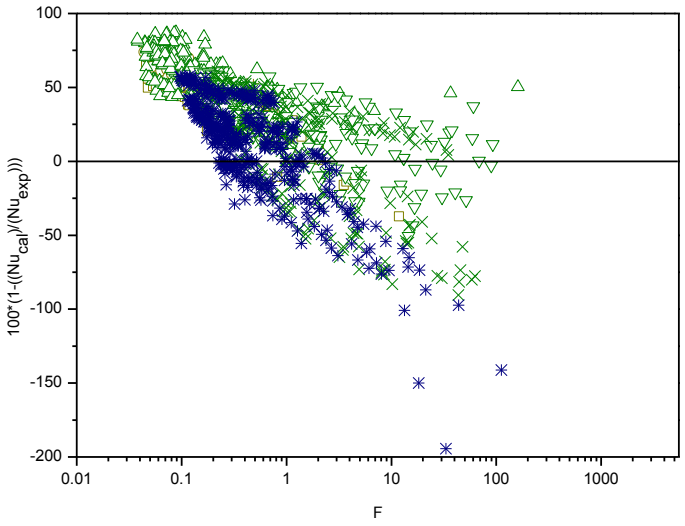

Figure 3.21. Comparison of Jacobs and Nadig (1984) model to the experimental data of steam.

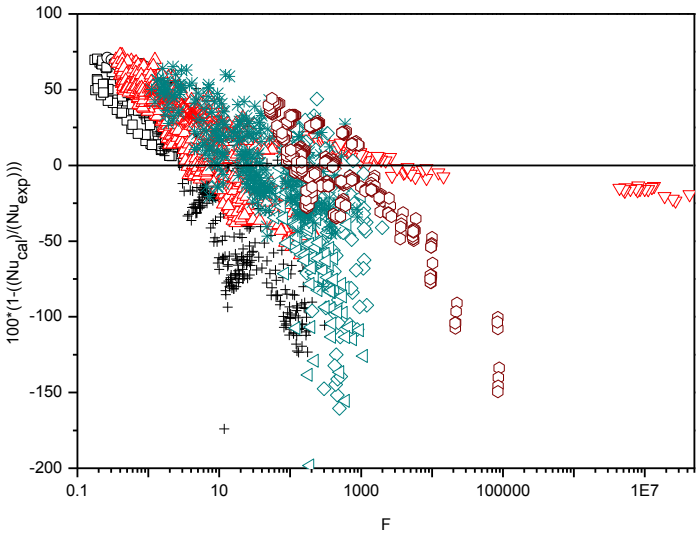

Figure 3.22. Comparison of Jacobs and Nadig (1984) model to the experimental data of non-steam fluids.

3.2. Single –Tube Forced-Convection Models.

3.2.1. Shekriladze and Gomelauri (1966) Model.

Shekriladze and Gomelauri (1966) model is the model where the assumptions of Nusselt Model for a free convection on a single tube was used, but added asymptotic, infinite condensation rate approximation for the shear stress at the liquid-vapour interface. This model does not consider the effect of condensate inundation. Rose modified Shekriladze and Gomelauri (1966) model that gives values of $\mathrm{Nu}\tilde{\mathrm{R}}\mathrm{e}^{-\frac{1}{2}}$ to within 0.4% of the numerically obtained values for all the ranges F.

Table 3.7. Summary of the mean deviation E_1 and the standard mean deviation E_2 for single-tube forced-convection models.

	Steam Data		Non-Steam Data		All Data	
	E_1	E_2	E_1	E_2	E_1	E_2
Shekriladze and Gomelauri (1966)	-31.27	38.22	-3.99	22.42	-12.96	27.62
Fujii (1972)	-41.76	45.11	-24.97	29.04	-30.49	34.32
Rose (1984)	-11.63	24.18	-35.86	40.33	-27.67	34.88
Honda (1986)	-40.44	43.89	-107.25	110.01	-85.29	88.28

Figures 3.23 and 3.24 represent the comparison between the new version of Shekriladze and Gomelauri (1966) model been represented by Rose (1984) and the experimental data of steam and non-steam fluids. The vapour velocity used is based on the

vapour mass flow rate just upstream of the tubes of the bank and the mean void area of the test-section (the total volume of the test section not occupied by the tubes divided by its height in the direction of the flow).

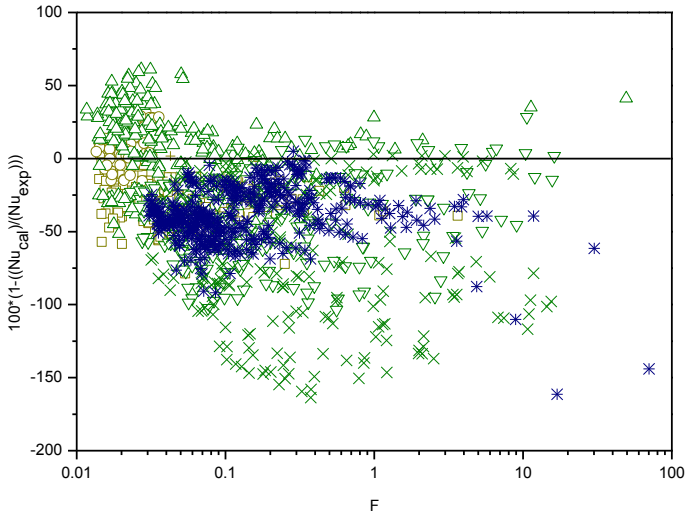

Figure 3.23. Comparison of Shekriladze and Gomelauri (1966) model (based on the mean void vapour velocity) to the experimental data of steam.

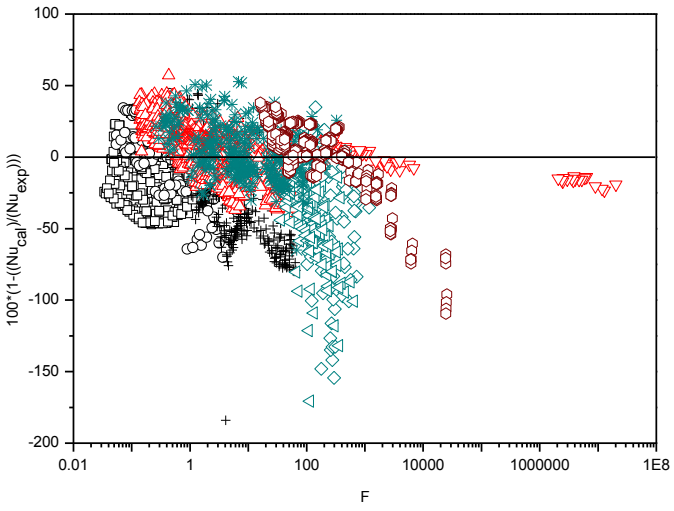

Figure 3.24. Comparison of Shekriladze and Gomelauri (1966) model (based on the mean void vapour velocity) to the experimental data of non-steam fluids.

For steam, at high vapour velocity (which takes place in a range of $F < 1$), the model over-predicts most of its experimental data, not including that of Beech (1995)-2 and Michael

(1988). The trend of the data of Michael (1988) for steam at high velocity (which occurs in a range of $F < 0.1$), was proposed to be a transition that occurs within the condensate film from the laminar to the turbulent flow. For the non-steam fluids, most of its experimental data were under-estimated by the model in a range of $F < 1000$, excluding that of Cavallini-1(1985), Honda-1 (1988), Shah-1 (1978) and Shah-2(1981).

3.2.2. Fujii (1972) Model

The integral approach of Fujii et al. (1972) accounts the vapour shear stress on a surface of a film condensate more accurately by solving simultaneously the liquid and vapour boundary layer equations with the boundary conditions matched at the interface, where he assumed that there is no vapour boundary layer separation. The addition of the effect that accounts the vapour shear stress on a surface of a film condensate more accurately based on the integral approach of Fujii et al. (1972) to the new version of the Fujii (1972) model demonstrated by Rose (1984) shifts the percentage deviation values in figures 3.23 and 3.24 downwards, as illustrated in figures 3.25 and 3.26. The model over-predicts most of the data for steam and non-steam fluids. Again, this model does not account for the effect of the condensate inundation.

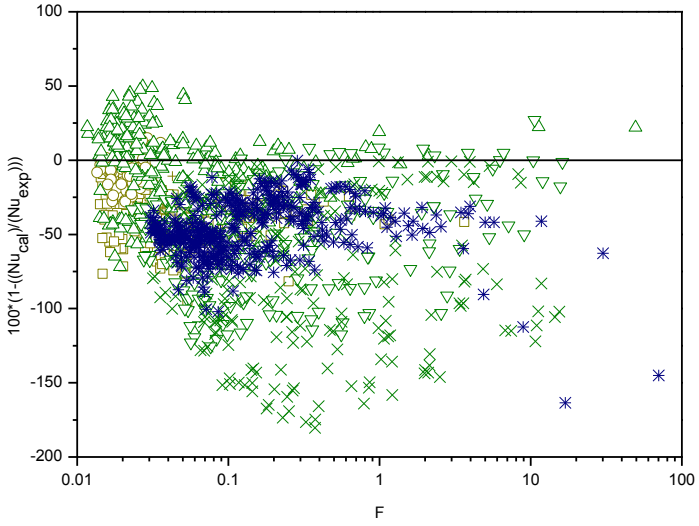

Figure 3.25. Comparison of Fujii (1972) model (based on the mean void vapour velocity) to the experimental data of steam.

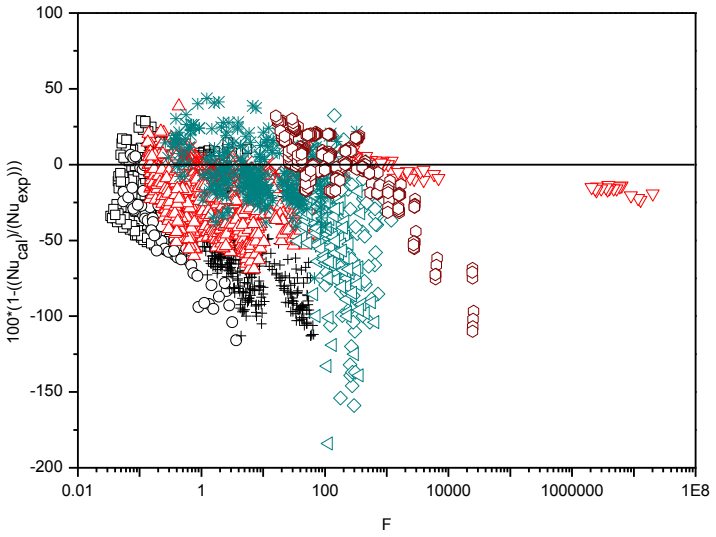

Figure 3.26. Comparison of Fujii (1972) model (based on the mean void vapour velocity) to the experimental data of non-steam fluids.

3.2.3. Rose (1984) Model.

Rose (1984) included the effect of the variation of the pressure gradient around the tube to the new version of the Fujii (1972) model, which was represented by Rose (1984). The inclusion of the effect of the variation of the pressure gradient around the tube shifts all the percentage deviation values of the steam data demonstrated in figure 3.25 upwards, since its experimental values of P are low, as illustrated in figure 3.27. Therefore, the model over-estimated the majority of the data apart from that of Beech (1995)-2, Beech (1995)-3 and Michael (1988).

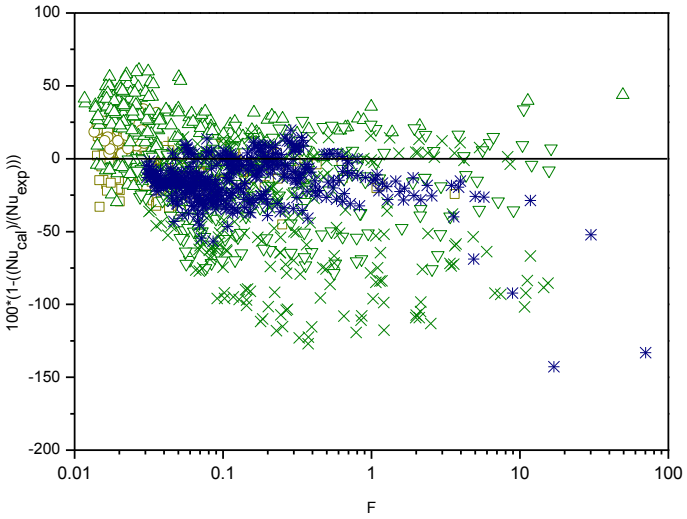

Figure 3.27. Comparison of Rose (1984) model (based on the mean void vapour velocity) to the experimental data of steam.

For non-steam fluids, the experimental values of P used by the investigators such as Cavallini-2 (1988), Honda-1 (1988), Honda-2 (1988) and Briggs (2000) were high, caused their percentage deviation values in figure 3.26 to move downwards, while the rest of the percentage deviation values by the other investigators were shifted upwards, since their experimental values of P were low, as illustrated in figure 3.28. Therefore, that leads the model to over-predict the majority of the non-steam data, apart from that of Cavallini-1(1985), Gogonin-1 (1971) and Gogonin-2 (1976).

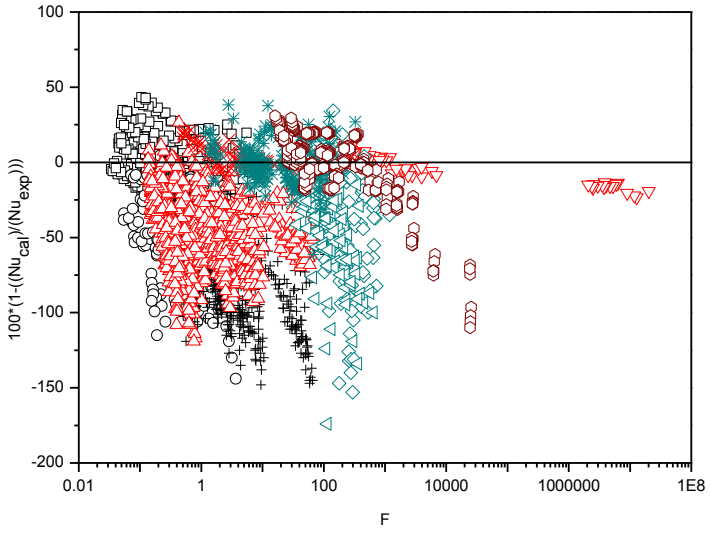

Figure 3.28. Comparison of Rose (1984) model (based on the mean void vapour velocity) to the experimental data of non-steam fluids.

3.2.4. Honda (1986) Model.

The Honda (1986) model was based on the experimental data of Honda et al. (1986) for a flowing refrigerant-113 over a single tube. He made a number of dye injection tests to find out the onset of turbulence where he correlated his experimental data. Figure 3.29 represents the comparison between the Honda model (1986) and the experimental data of steam, where the model over-estimates the majority of the data (based on table 3.21).For non-steam fluids, much of its experimental data were over-predicted by their correlations (demonstrated in figure 3.30), except that for Gogonin-1 (1971), as given in table 3.22.

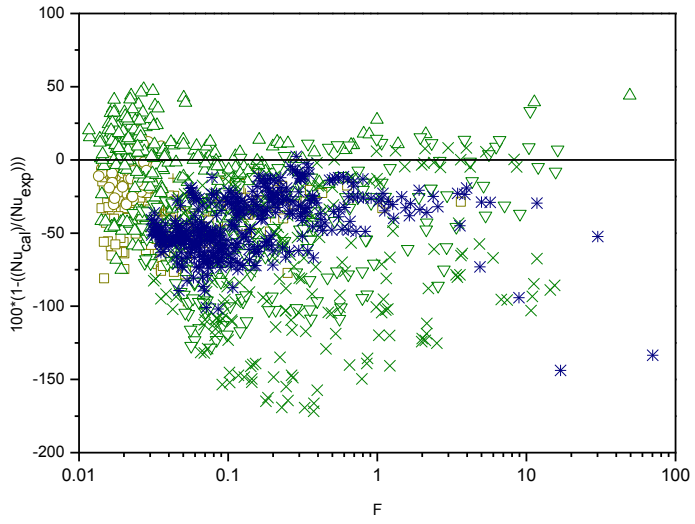

Figure 3.29. Comparison of Honda (1986) model for single tube (based on the mean void vapour velocity) to the experimental data of steam.

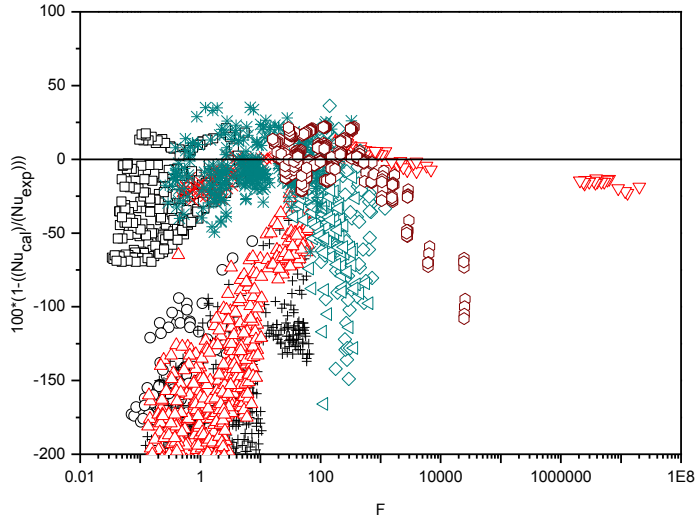

Figure 3.30. Comparison of Honda (1986) model for single tube (based on the mean void vapour velocity) to the experimental data of non-steam fluids.

3.3. Forced-Convection Models (Bank-Tube Empirical Models).

3.3.1. McNaught (1982) Model.

McNaught (1982) correlated the steam data of Nobbs-1 (1975) and Nobbs-2 and Mayhew (1976) in the region where the gravity effect is significant compared to that of the vapour shear, the heat transfer coefficients were determined, using Nusselt's analytical solution for a horizontal tube, coupled with a factor, which accounts the effect of the condensate inundation. In a shear controlled region, a two-phase forced convection approach was used to predict its heat transfer coefficients. The values of exponent in equation (5.18) are 0.22 and 0.13 for the in-line bundles and for staggered bundles. In the shear contolled

region, McNaught (1982) recommended the Lockart Martinelli parameter (equation (3.23)) and the ESDU (1973) equation for calculating the liquid phase forced convection coefficient, where it requires the presence of a vapour and liquid phase. Using this approach, the combined heat transfer coefficient for both of the gravity controlled and shear controlled cannot be determined for the first condensing row, since its upstream vapour quality is 1.

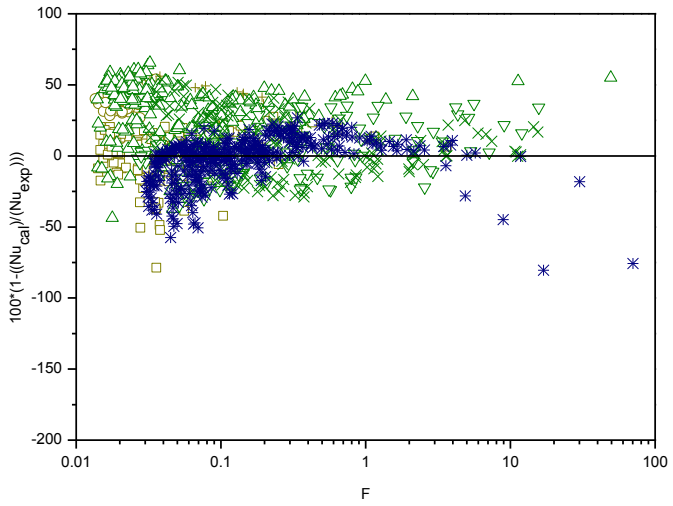

Figure 3.31. Comparison of McNaught (1982) model to the experimental data of steam.

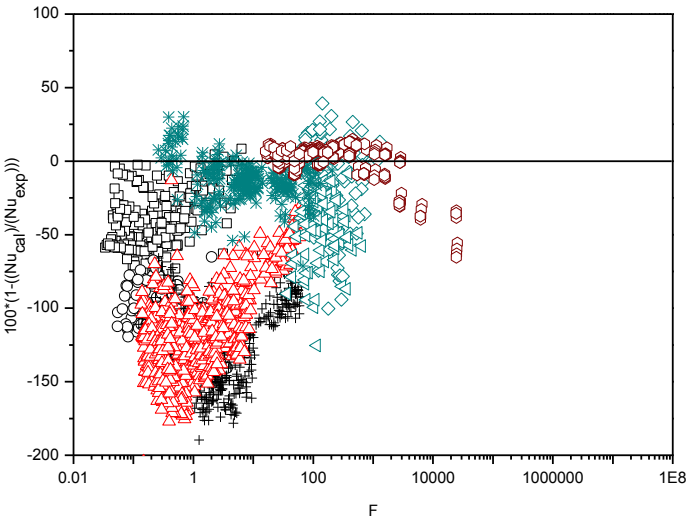

Figure 3.32. Comparison of McNaught (1982) model to the experimental data of non-steam fluids.

It can be observed in figures 3.31 and 3.32 that the agreement between the McNaught (1982) model and the experimental data for each of steam and non-steam fluids are not good. For steam, the correlation under-estimates most of its experimental data, apart from that of Nobbs-2 (1976). It should be noticed that the model was based on only the data of Nobbs-1 (1975), which gives good agreement compared to some other steam data of the other investigators as shown in table 3.24. For non-steam fluids, the model over-predicts the majority of its data, excluding that of Briggs. The significant over-prediction of the data of Cavallini-2 (1988), Honda-1 (1988) and Honda-2 (1988) is perhaps more serious, which is by as much as 100%, as illustrated in figure 3.32.

Table 3.8. Summary of the mean deviation E_1 and the standard mean deviation E_2 for the bank-tube forced-convection models.

	Steam Data		Non-Steam Data		All Data	
	E_1	E_2	E_1	E_2	E_1	E_2
McNaught (1982)	10.76	20.27	-78.34	80.07	-48.79	60.24
Cavallini (1986)	-4.34	18.43	16.88	22.69	9.90	21.29
Fujii and Oda (1986)	-22.58	32.13	-1.50	15.62	-8.78	21.33
Fujii and Oda (after the correction by Honda (1989))	-50.35	53.93	-13.25	19.38	-26.07	31.31
Honda (1989)	-15.52	36.95	19.20	24.73	7.79	28.75

3.3.2. Cavallini (1986) Model (Empirical correction to Shekriladze and Gomelauri (1966) Model).

Cavallini (1986) suggested an equation, where the predicted heat-transfer coefficient for the first row of the condensing bundles was determined using the Shekriladze and Gomelauri (1966) model, where there was no inundation. For the following rows, a modification to Shekriladze and Gomelauri (1966) model was considered by including the effect of the condensate inundation. This modification was based on work by Cipollone (1983) for condensation at low vapour velocity of R-11 on staggered tube banks. This correction shifts the percentage deviation values of steam and non-steam fluids data in figures 3.23 and 3.24 upwards, as shown in figures 3.33 and 3.34. The model over-estimates only that of Beech (1995)-2, Beech-3 (1995)-3 and Michael (1988) for the steam (shown in figure 3.33). For the non-steam fluids, the model over-predicts that of Shah-1 (1978) and Shah-2 (1981), as demonstrated in figure 3.34. The percentage deviation values of the data of Gogonin-1 (1971) and Gogonin-2 (1976) for this model have not been changed from that of

Shekriladze and Gomelauri (1966) model, since that there were not any inundations in their tube bundles. The model gave better results than that of the Shekriladze and Gomelauri (1966) model, since it considers the effect of the inundation.

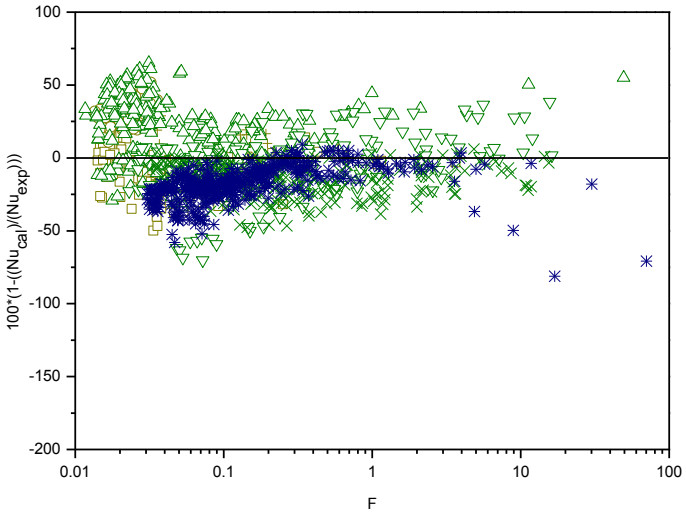

Figure 3.33. Comparison of Cavallini (1986) model (based on the mean void vapour velocity) to the experimental data of steam.

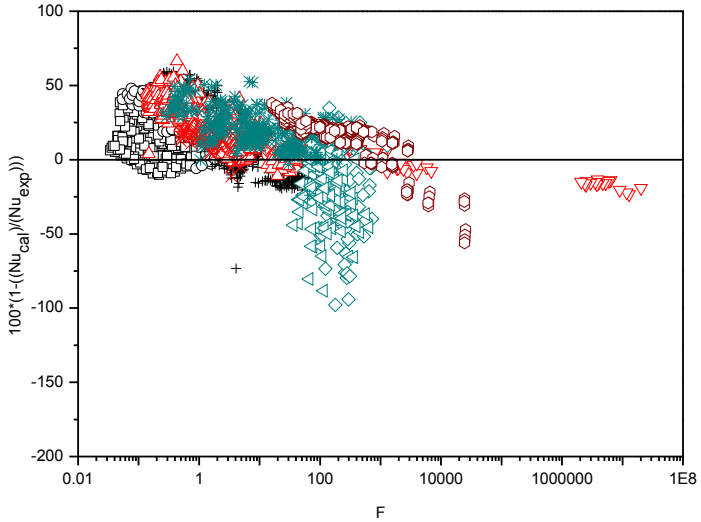

Figure 3.34. Comparison of Cavallini (1986) model (based on the mean void vapour velocity) to the experimental data of non-steam fluids.

3.3.3. Fujii and Oda (1986) Model.

Fujii and Oda (1986) used the experimental data of Nobbs and Mayhew (1976) for steam and Kutateladze (1981) for Refrigerant-21 in the region where the gravity effect dominates the shear effect, where the heat transfer coefficient were obtained, coupled with the row number. In a case of the shear effect is significant compared to that of the gravity effect, allowing an evaluation of the heat-transfer coefficients through the bundle using Fujii (1972) model for single tube at $F \to 0$, combined with the row number. In the gravity controlled region model, the values of exponent are 0.16 and 0.08 for the in-line bundles and for staggered bundles.

Figures 3.35 and 3.36 compare the Fujii and Oda (1986) model with the data of steam and non-steam fluids respectively. For steam, based on the table 3.24, the correlation under-estimates most of the data of Beech (1995)-2 and Michael (1988), while with the non-steam fluids, it over-predicts that of Honda-1 (1988), Honda-2 (1988), Shah-1 (1978) and Shah-2 (1981).

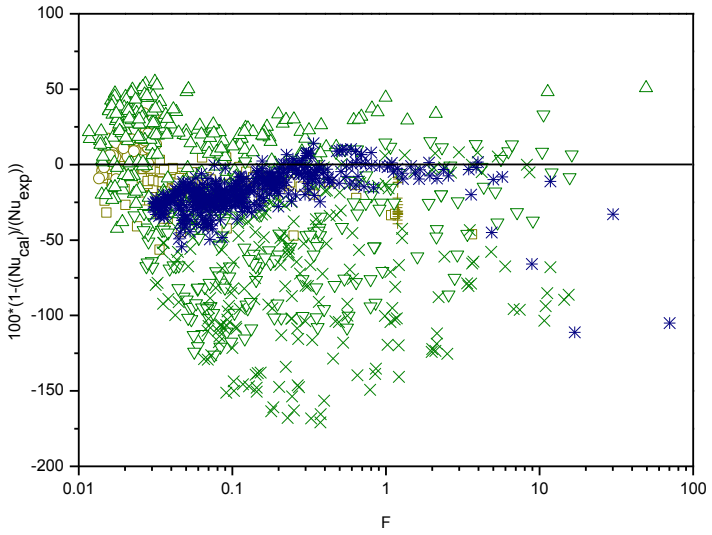

Figure 3.35. Comparison of Fujii and Oda (1986) model to the experimental data of steam.

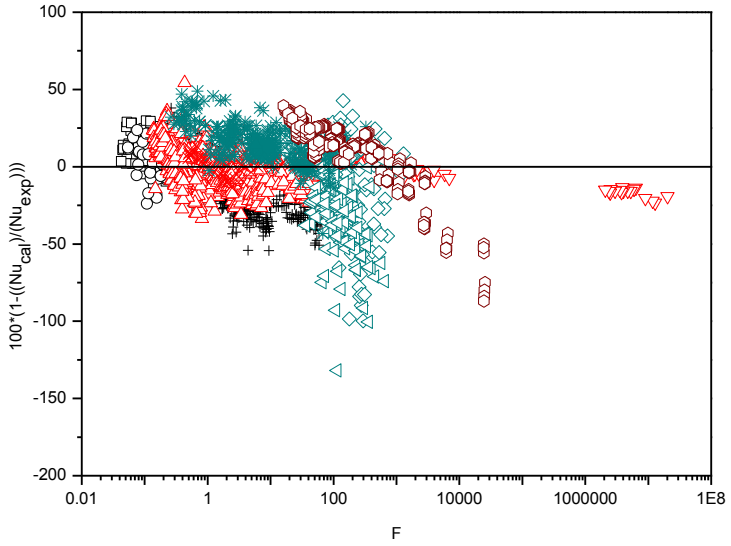

Figure 3.36. Comparison of Fujii and Oda (1986) model to the experimental data of non-steam fluids.

Replacing the proportionality constant of 0.9 as recommended by Honda (1989) in the model of Fujii and Oda (1986) with $1.23\sqrt{d/P_v}$ caused the experimental data of steam and non-steam fluids in figures 3.35 and 3.36 to shift downwards, as demonstrated in figures 3.37 and 3.38, from which it caused most the steam and non-steam data to be over-estimated by the model (in the presence of the correction by Honda (1989)), excluding that of Gogonin-1(1971) and Briggs (2000). Row number in Fujii and Oda (1986) model is not a practical way of accounting for the effect of the inundation.

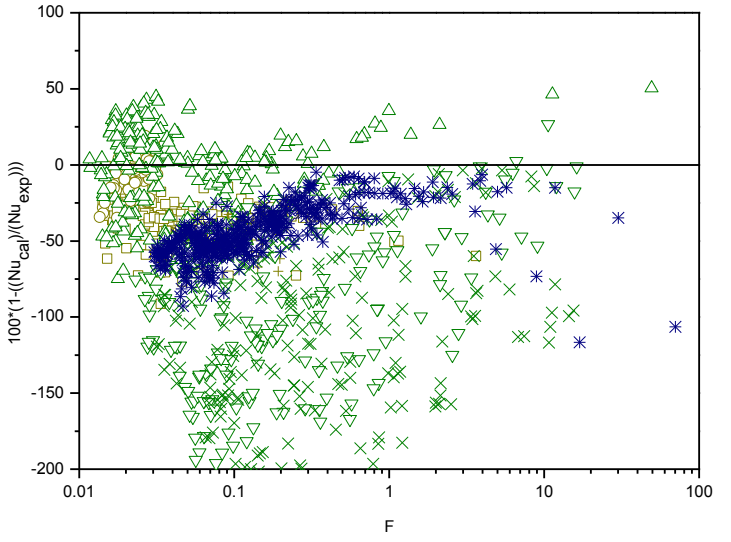

Figure 3.37. Comparison of Fujii and Oda (1986) model (after the correction by Honda (1989)) to the experimental data of steam.

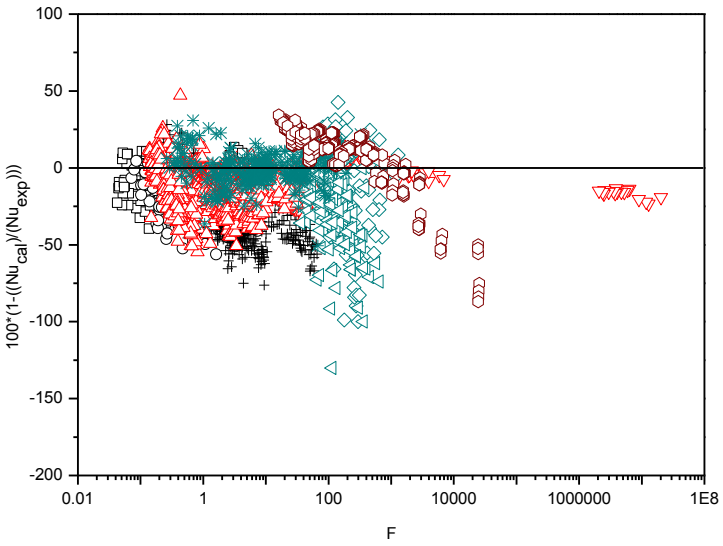

Figure 3.38. Comparison of Fujii and Oda (1986) model (after the correction by Honda (1989)) to the experimental data of the non-steam fluids.

3.3.4. Honda (1989) Model.

Honda (1989) proposed correlations for both the gravity controlled and shear controlled regions. Gravity controlled region model was based on the low vapour velocity data of Kutateladze et al. (1985) and Kutateladze and Gogonin (1979), for R-21 and R-12, while the shear controlled region model is based on the experimental data of Honda (1989). Figures 3.39 and 3.40 compare the Honda (1989) model with the data of steam and non-steam fluids respectively.

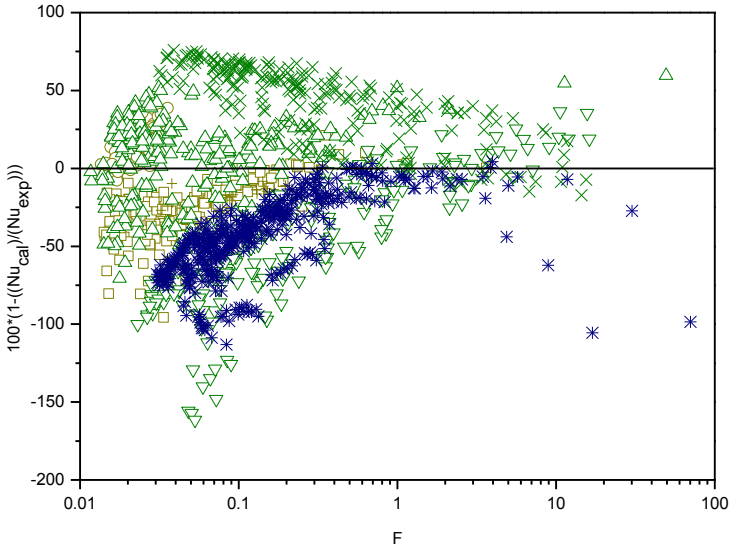

Figure 3.39. Comparison of Honda (1989) model to the experimental data of steam.

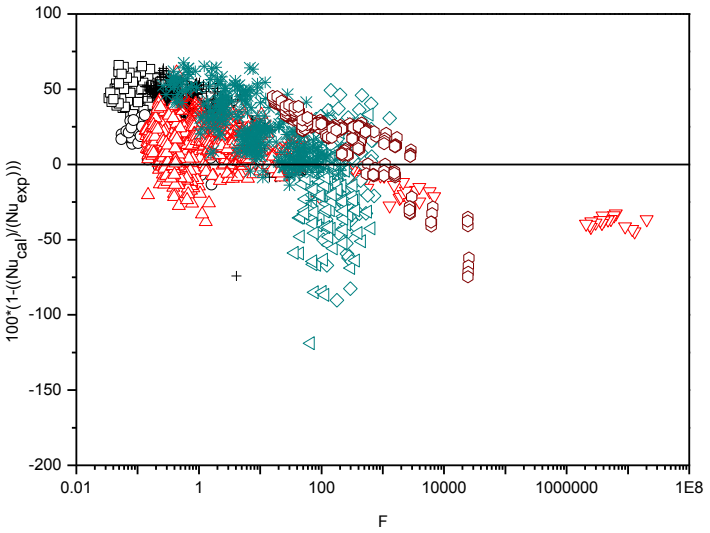

Figure 3.40. Comparison of Honda (1989) model to the experimental data of non-steam fluids.

The model over-estimates much of its steam data, not including that of Beech-2 (1995), Michael (1988) and Nobbs-2(1976) as demonstrated in figure 3.39. For non-steam fluids, the model over-predicts only the data of Gogonin-1 (1971), Shah-1 (1978) and Shah-2 (1981), as shown in figure 3.40.

3.4. Summary.

Tables 3.3-3.6 represent the summary of the mean deviation E_1 and the standard mean deviation E_2 of the experimental data for the free-convection models. The poor results of the free convection models are expected, since that these models do not consider the effects of shear stress on the surface of the film condensate. The model of Jacobs and Nadig (1984) is the most successful when compared to the full data, and is particular effective for the non-steam data.

Table 3.7 demonstrates the summary of the mean deviation E_1 and the standard mean deviation E_2 of the experimental data for the single tube forced-convection models. In all cases the local vapour velocity at a given tube row was corrected based on condensation on preceding rows and was evaluated using the mean-void area of the tube bank since this tended to give the best results for all the models. None of these models takes into account the effect of condensate inundation. It can be seen in table 3.33 that the Rose (1984) model is the

most successful for the steam data while that of Shekriladze and Gomelauri (1966) model is best for both the non-steam data and for the whole data taken together. Both these models are purely theoretical with no empirical "correction". The single-tube model of Honda (1986) provides the worst results among all the single tube-models. While this model is empirically based, it used only data for R-113; demonstrating the danger in trying to extend the applicability of an empirical model beyond the range of the parameters of the data on which it is based.

Table 3.8 illustrates the above point further. All of the tube bank models investigated had some empirical input, and all perform poorly when compared to the extensive and wide ranging data based compiled in the present study. The McNaught (1982) model gives good agreement with the data for steam, since it was based on the steam data of Nobbs-1 (1975), while the results of this model with the non-steam fluids and the data based as a whole is poor. The addition of Cavallini's correction for condensate inundation to the Shekriladze and Gomelauri (1966) model improves its performance considerably (compare the values in table 3.8 for Cavallini to those in table 3.7 for Sheriladze and Gomelauri) and in fact this model is probably the pick of those evaluated when compared to the whole data base. This is despite the empirical correction for inundation being based on data for refrigerants only, and probably reflects the original effectiveness of the Shekriladze and Gomelauri (1966) model in accounting for vapour shear effects.

4. Development of an Empirical Model for Condensation on a bank of Plain Tubes.

4.1. Introduction.

The aim of this section is to develop a simple and reliable empirical model to predict the heat-transfer coefficient on a given row of tubes within a tube bundle, which includes the effects of the inundation and vapour velocity. Data from previous investigations covering a wide range of the tube geometries, fluid properties and operating conditions will be used in the analysis. A number of models were developed and evaluated against this data base and these models have also been described; the most successful is described in full in the conclusions section.

4.2. Assumptions.

The basic assumptions that were made for the development of the empirical models are as follows:

1. Condensing vapour is saturated (no superheating).
2. The vapour contained no non-condensing gas.
3. The vapour velocity is assumed to vary down the bank due to condensation but the vapour velocity in a horizontal plane across the bank is assumed uniform and constant.
4. The heat flux to all tubes in a row is uniform and equal.
5. The wall temperature of all tubes in a given row is uniform and equal.
6. The vapour velocity upstream of a given row is based on the mass flow rate of the vapour alone (volume occupied by condensate is assumed negligible).
7. The air concentration within the flowing fluid vapour throughout the bank is negligible.
8. The condensate properties are evaluated at the following temperature:

$$T^* = \frac{1}{3}T_V + \frac{2}{3}T_W \qquad (4.1)$$

The exception to this is h_{fg}, which is evaluated at the vapour temperature T_V.

4.3. Development of the Empirical Models.

An important step in the analysis of the existing steam and non-steam data is to identify which of the experimental data correspond to the gravity and shear controlled regions. A parameter which can be used to measure the relative importance of vapour shear and gravity effects, taken from McNaught (1982), is defined below:

$$J_v = \frac{xG}{\sqrt{dg\rho_v(\rho - \rho_v)}} \tag{4.2}$$

Before attempting to develop models for the gravity and shear controlled regions, it is suggested that the gravity controlled region takes place in the range of $J_v < J_{v(critical)}$, while the shear controlled region occurs in the range of $J_v > J_{v(critical)}$, where $J_{v(critical)}$ corresponds to a transition between the gravity and shear controlled regions.

4.3.1. Gravity Controlled Region.

The gravity controlled region ($J_v < J_{v(critical)}$) model, based on all the existing data is given by the following equation:

$$\frac{Nu}{Nu^*} = B_{gr}^a F^b Pr^c H^d G^e P^f \tag{4.3}$$

Where

$$B_{gr} = \frac{\Gamma_{N-gr}}{\gamma_{N-gr}} \tag{4.4}$$

$$F = \frac{\mu h_{fg} gd}{k\overline{\Delta T}U_\infty^{\,2}} \tag{4.5}$$

$$Pr = \frac{c_P \mu}{k} \tag{4.6}$$

$$H = \frac{c_P \overline{\Delta T}}{h_{fg}} \tag{4.7}$$

$$G = \frac{k\overline{\Delta T}}{\mu h_{fg}}\left[\frac{\mu\rho}{\rho_v \mu_v}\right]^{\frac{1}{2}} \tag{4.8}$$

$$P = \frac{\rho_v h_{fg} \mu}{\rho k \overline{\Delta T}} \tag{4.9}$$

Nu is the predicted Nusselt number and Nu^* is the Nusselt number determined by one of the existing models, where the type of the models that were tested are single-tube forced convection models.

In equation (4.3), B_{gr} is defined as the ratio of the the mass flow rate of the condensate per unit length drained from the Nth tube (or tube row) Γ_{N-gr} to the condensation rate per unit length on the tube γ_{N-gr} . It was assumed that the condensate falls onto the tube directly below (i.e. in the next row for inline bundles and two rows down the bank for staggered bundles).

Dimensionless variable F in equation (4.3) is based on the maximum cross-sectional area of the test section (Free-stream velocity)).

Dimensionless variable Pr is the condensate Prandtl number measures the size of the ratio of the momentum diffusity to the thermal diffusity.

H defines as the ratio of the heat due to the sub-cooling takes place within the condensate film to the heat due to the condensation a saturated vapour temperature.

Dimensionless variable G measures the vapour shear stress on a surface of a film condensate more precisely using the integral approach of Fujii et al. (1972), where it was assumed that the separation of the vapour boundary layer does not occurs.

P measures the variation of the pressure gradient within the condensate film around the tube, which was suggested by Rose (1984).

Taking K_{gr} as the ratio of the predicted Nusselt number Nu to the Nusselt number been obtained by the selected model for a single non-inundated tube Nu^* as shown in equation (4.3), is given in the following equation.

$$K_{gr} = B_{gr}^{a} F^{b} Pr^{c} H^{d} G^{e} P^{f} \tag{4.10}$$

Taking the natural logarithm of equation (4.10) gives the following:

$$\ln(K_{gr}) = a\ln(B_{gr}) + b\ln(F) + c\ln(Pr) + d\ln(H) + e\ln(G) + f\ln(P) \tag{4.11}$$

The unknown constant parameters in equation (4.11) will be determined from the following equation, which represents the sum of squares of residuals between the natural logarithmic of K_{gr} and that of the experimental K_{exp}.

$$R = \sum_{1}^{N} \left(\left(\ln(K_{exp}) \right) - \left(\ln(K_{gr}) \right) \right)^2 \tag{4.12}$$

$$R = \sum_{1}^{N} \left(\left(\ln(K_{exp}) \right) - \left(a\ln(B_{gr}) + b\ln(F) + c\ln(Pr) + d\ln(H) + e\ln(G) + f\ln(P) \right) \right)^2 \tag{4.13}$$

The following equations represent the first partial derivatives of residual R with respect to the unknown constant parameters shown in equation (4.13).

$$\frac{\partial R}{\partial a} = 2\sum_{1}^{N} \left(\ln(K_{exp}) - a\ln(B_{gr}) - b\ln(F) - c\ln(Pr) - d\ln(H) - e\ln(G) - f\ln(P) \right)\left(-\ln(B_{gr}) \right) \tag{4.14}$$

$$\frac{\partial R}{\partial b} = 2\sum_{1}^{N} \left(\ln(K_{exp}) - a\ln(B_{gr}) - b\ln(F) - c\ln(Pr) - d\ln(H) - e\ln(G) - f\ln(P) \right)\left(-\ln(F) \right) \tag{4.15}$$

$$\frac{\partial R}{\partial c} = 2\sum_{1}^{N} \left(\ln(K_{exp}) - a\ln(B_{gr}) - b\ln(F) - c\ln(Pr) - d\ln(H) - e\ln(G) - f\ln(P) \right)\left(-\ln(Pr) \right) \tag{4.16}$$

$$\frac{\partial R}{\partial d} = 2\sum_{1}^{N} \left(\ln(K_{exp}) - a\ln(B_{gr}) - b\ln(F) - c\ln(Pr) - d\ln(H) - e\ln(G) - f\ln(P) \right)\left(-\ln(H) \right) \tag{4.17}$$

$$\frac{\partial R}{\partial e} = 2\sum_{1}^{N} \left(\ln(K_{exp}) - a\ln(B_{gr}) - b\ln(F) - c\ln(Pr) - d\ln(H) - e\ln(G) - f\ln(P) \right)\left(-\ln(G) \right) \tag{4.18}$$

$$\frac{\partial R}{\partial f} = 2\sum_{1}^{N} \left(\ln(K_{exp}) - a\ln(B_{gr}) - b\ln(F) - c\ln(Pr) - d\ln(H) - e\ln(G) - f\ln(P) \right)\left(-\ln(P) \right) \tag{4.19}$$

Minimum of the squares of the residual R takes place under the following conditions

$$\frac{\partial R}{\partial a} = \frac{\partial R}{\partial b} = \frac{\partial R}{\partial c} = \frac{\partial R}{\partial d} = \frac{\partial R}{\partial e} = \frac{\partial R}{\partial f} = 0 \tag{4.20}$$

Using the conditions given in equation (4.20) gives the following matrix equation:

$$\begin{pmatrix} \sum_1^N (\ln(B_{gr}))^2 & \sum_1^N \ln(B_{gr})\ln(F) & \sum_1^N \ln(B_{gr})\ln(Pr) & \sum_1^N \ln(B_{gr})\ln(H) & \sum_1^N \ln(B_{gr})\ln(G) & \sum_1^N \ln(B_{gr})\ln(P) \\ \sum_1^N \ln(F)\ln(B_{gr}) & \sum_1^N (\ln(F))^2 & \sum_1^N \ln(F)\ln(Pr) & \sum_1^N \ln(F)\ln(H) & \sum_1^N \ln(F)\ln(G) & \sum_1^N \ln(F)\ln(P) \\ \sum_1^N \ln(Pr)\ln(B_{gr}) & \sum_1^N \ln(Pr)\ln(F) & \sum_1^N (\ln(Pr))^2 & \sum_1^N \ln(Pr)\ln(H) & \sum_1^N \ln(Pr)\ln(G) & \sum_1^N \ln(Pr)\ln(P) \\ \sum_1^N \ln(H)\ln(B_{gr}) & \sum_1^N \ln(H)\ln(F) & \sum_1^N \ln(H)\ln(Pr) & \sum_1^N (\ln(H))^2 & \sum_1^N \ln(H)\ln(G) & \sum_1^N \ln(H)\ln(P) \\ \sum_1^N \ln(G)\ln(B_{gr}) & \sum_1^N \ln(G)\ln(F) & \sum_1^N \ln(G)\ln(Pr) & \sum_1^N \ln(G)\ln(H) & \sum_1^N (\ln(G))^2 & \sum_1^N \ln(G)\ln(P) \\ \sum_1^N \ln(P)\ln(B_{gr}) & \sum_1^N \ln(P)\ln(F) & \sum_1^N \ln(P)\ln(Pr) & \sum_1^N \ln(P)\ln(H) & \sum_1^N \ln(P)\ln(G) & \sum_1^N (\ln(P))^2 \end{pmatrix} \begin{pmatrix} a \\ b \\ c \\ d \\ e \\ f \end{pmatrix} = \begin{pmatrix} \sum_1^N \ln(B_{gr})\ln(K_{exp}) \\ \sum_1^N \ln(F)\ln(K_{exp}) \\ \sum_1^N \ln(Pr)\ln(K_{exp}) \\ \sum_1^N \ln(H)\ln(K_{exp}) \\ \sum_1^N \ln(G)\ln(K_{exp}) \\ \sum_1^N \ln(P)\ln(K_{exp}) \end{pmatrix} \tag{4.21}$$

The unknown constant parameters in equation (4.21) can be determined from the following matrix equation:

$$\begin{pmatrix} a \\ b \\ c \\ d \\ e \\ f \end{pmatrix} = \begin{pmatrix} \sum_1^N (\ln(B_{gr}))^2 & \sum_1^N \ln(B_{gr})\ln(F) & \sum_1^N \ln(B_{gr})\ln(Pr) & \sum_1^N \ln(B_{gr})\ln(H) & \sum_1^N \ln(B_{gr})\ln(G) & \sum_1^N \ln(B_{gr})\ln(P) \\ \sum_1^N \ln(F)\ln(B_{gr}) & \sum_1^N (\ln(F))^2 & \sum_1^N \ln(F)\ln(Pr) & \sum_1^N \ln(F)\ln(H) & \sum_1^N \ln(F)\ln(G) & \sum_1^N \ln(F)\ln(P) \\ \sum_1^N \ln(Pr)\ln(B_{gr}) & \sum_1^N \ln(Pr)\ln(F) & \sum_1^N (\ln(Pr))^2 & \sum_1^N \ln(Pr)\ln(H) & \sum_1^N \ln(Pr)\ln(G) & \sum_1^N \ln(Pr)\ln(P) \\ \sum_1^N \ln(H)\ln(B_{gr}) & \sum_1^N \ln(H)\ln(F) & \sum_1^N \ln(H)\ln(Pr) & \sum_1^N (\ln(H))^2 & \sum_1^N \ln(H)\ln(G) & \sum_1^N \ln(H)\ln(P) \\ \sum_1^N \ln(G)\ln(B_{gr}) & \sum_1^N \ln(G)\ln(F) & \sum_1^N \ln(G)\ln(Pr) & \sum_1^N \ln(G)\ln(H) & \sum_1^N (\ln(G))^2 & \sum_1^N \ln(G)\ln(P) \\ \sum_1^N \ln(P)\ln(B_{gr}) & \sum_1^N \ln(P)\ln(F) & \sum_1^N \ln(P)\ln(Pr) & \sum_1^N \ln(P)\ln(H) & \sum_1^N \ln(P)\ln(G) & \sum_1^N (\ln(P))^2 \end{pmatrix}^{-1} \begin{pmatrix} \sum_1^N \ln(B_{gr})\ln(K_{exp}) \\ \sum_1^N \ln(F)\ln(K_{exp}) \\ \sum_1^N \ln(Pr)\ln(K_{exp}) \\ \sum_1^N \ln(H)\ln(K_{exp}) \\ \sum_1^N \ln(G)\ln(K_{exp}) \\ \sum_1^N \ln(P^*)\ln(K_{exp}) \end{pmatrix} \tag{4.22}$$

4.3.2. Shear Controlled Region.

The Nusselt shear controlled region ($J_v > J_{v(critical)}$) model, based on the existing data is given by the following equation,

$$\frac{Nu}{Nu^*} = B_{sh}^a F^b Pr^c H^d G^e P^f \tag{4.23}$$

Where

$$B_{sh} = \frac{\Gamma_{N-sh}}{\gamma_{N-sh}} \tag{4.24}$$

In equation (4.23), B_{sh} is defined as the ratio of the mass flow rate of the condensate per unit length drained from the Nth tube (or tube row) Γ_{N-sh} to the condensation rate per unit length on the Nth tube γ_{N-sh} in the shear controlled region, where the condensate was suggested to be uniformly distributed across the test section normal to the flow and hence only a fraction of the condensate impinges on the tubes below.

Taking K_{sh} as the ratio of the predicted Nusselt number Nu to the Nusselt number obtained by the chosen model for a single non-inundated tube Nu^{*} as shown in equation (4.23), from which is given in the following equation.

$$K_{sh} = B_{sh}^{a} F^{b} Pr^{c} H^{d} G^{e} P^{f} \tag{4.25}$$

Taking the natural logarithm of K_{sh} in equation (4.25) gives the following equation:

$$\ln(K_{sh}) = a\ln(B_{sh}) + b\ln(F) + c\ln(Pr) + d\ln(H) + e\ln(G) + f\ln(P) \tag{4.26}$$

The unknown constant parameters in equation (4.26) will be determined from the following equation, which represents the sum of squares of residuals between the natural logarithmic of K_{sh} and that of the experimental K_{exp}.

$$R = \sum_{1}^{N} \left(\left(\ln(K_{exp}) \right) - \left(\ln(K_{gr}) \right) \right)^{2} \tag{4.27}$$

$$R = \sum_{1}^{N} \left(\left(\ln(K_{exp}) \right) - \left(a\ln(B_{sh}) + b\ln(F) + c\ln(Pr) + d\ln(H) + e\ln(G) + f\ln(P) \right) \right)^{2} \tag{4.28}$$

Equation (4.28) was derived partially with respect to each of the unknown constant parameters, using the conditions demonstrated in equation (4.20) that provides the minimum residual in equation (4.28) to give the following matrix equation:

$$\begin{pmatrix} \sum_{1}^{N} (\ln(B_{sh}))^{2} & \sum_{1}^{N} \ln(B_{sh})\ln(F) & \sum_{1}^{N} \ln(B_{sh})\ln(Pr) & \sum_{1}^{N} \ln(B_{sh})\ln(H) & \sum_{1}^{N} \ln(B_{sh})\ln(G) & \sum_{1}^{N} \ln(B_{sh})\ln(P) \\ \sum_{1}^{N} \ln(F)\ln(B_{sh}) & \sum_{1}^{N} (\ln(F))^{2} & \sum_{1}^{N} \ln(F)\ln(Pr) & \sum_{1}^{N} \ln(F)\ln(H) & \sum_{1}^{N} \ln(F)\ln(G) & \sum_{1}^{N} \ln(F)\ln(P) \\ \sum_{1}^{N} \ln(Pr)\ln(B_{sh}) & \sum_{1}^{N} \ln(Pr)\ln(F) & \sum_{1}^{N} (\ln(Pr))^{2} & \sum_{1}^{N} \ln(Pr)\ln(H) & \sum_{1}^{N} \ln(Pr)\ln(G) & \sum_{1}^{N} \ln(Pr)\ln(P) \\ \sum_{1}^{N} \ln(H)\ln(B_{sh}) & \sum_{1}^{N} \ln(H)\ln(F) & \sum_{1}^{N} \ln(H)\ln(Pr) & \sum_{1}^{N} (\ln(H))^{2} & \sum_{1}^{N} \ln(H)\ln(G) & \sum_{1}^{N} \ln(H)\ln(P) \\ \sum_{1}^{N} \ln(G)\ln(B_{sh}) & \sum_{1}^{N} \ln(G)\ln(F) & \sum_{1}^{N} \ln(G)\ln(Pr) & \sum_{1}^{N} \ln(G)\ln(H) & \sum_{1}^{N} (\ln(G))^{2} & \sum_{1}^{N} \ln(G)\ln(P) \\ \sum_{1}^{N} \ln(P)\ln(B_{sh}) & \sum_{1}^{N} \ln(P)\ln(F) & \sum_{1}^{N} \ln(P)\ln(Pr) & \sum_{1}^{N} \ln(P)\ln(H) & \sum_{1}^{N} \ln(P)\ln(G) & \sum_{1}^{N} (\ln(P))^{2} \end{pmatrix} \begin{pmatrix} a \\ b \\ c \\ d \\ e \\ f \end{pmatrix} = \begin{pmatrix} \sum_{1}^{N} \ln(B_{sh})\ln(K_{exp}) \\ \sum_{1}^{N} \ln(F)\ln(K_{exp}) \\ \sum_{1}^{N} \ln(Pr)\ln(K_{exp}) \\ \sum_{1}^{N} \ln(H)\ln(K_{exp}) \\ \sum_{1}^{N} \ln(G)\ln(K_{exp}) \\ \sum_{1}^{N} \ln(P)\ln(K_{exp}) \end{pmatrix} \tag{4.29}$$

The unknown constant parameters in equation (4.25) can be determined from the following matrix equation:

$$\begin{pmatrix} a \\ b \\ c \\ d \\ e \\ f \end{pmatrix} = \begin{pmatrix} \sum_1^N (\ln(B_{sh}))^2 & \sum_1^N \ln(B_{sh})\ln(F) & \sum_1^N \ln(B_{sh})\ln(Pr) & \sum_1^N \ln(B_{sh})\ln(H) & \sum_1^N \ln(B_{sh})\ln(G) & \sum_1^N \ln(B_{sh})\ln(P) \\ \sum_1^N \ln(F)\ln(B_{sh}) & \sum_1^N (\ln(F))^2 & \sum_1^N \ln(F)\ln(Pr) & \sum_1^N \ln(F)\ln(H) & \sum_1^N \ln(F)\ln(G) & \sum_1^N \ln(F)\ln(P) \\ \sum_1^N \ln(Pr)\ln(B_{sh}) & \sum_1^N \ln(Pr)\ln(F) & \sum_1^N (\ln(Pr))^2 & \sum_1^N \ln(Pr)\ln(H) & \sum_1^N \ln(Pr)\ln(G) & \sum_1^N \ln(Pr)\ln(P) \\ \sum_1^N \ln(H)\ln(B_{sh}) & \sum_1^N \ln(H)\ln(F) & \sum_1^N \ln(H)\ln(Pr) & \sum_1^N (\ln(H))^2 & \sum_1^N \ln(H)\ln(G) & \sum_1^N \ln(H)\ln(P) \\ \sum_1^N \ln(G)\ln(B_{sh}) & \sum_1^N \ln(G)\ln(F) & \sum_1^N \ln(G)\ln(Pr) & \sum_1^N \ln(G)\ln(H) & \sum_1^N (\ln(G))^2 & \sum_1^N \ln(G)\ln(P) \\ \sum_1^N \ln(P)\ln(B_{sh}) & \sum_1^N \ln(P)\ln(F) & \sum_1^N \ln(P)\ln(Pr) & \sum_1^N \ln(P)\ln(H) & \sum_1^N \ln(P)\ln(G) & \sum_1^N (\ln(P))^2 \end{pmatrix}^{-1} \begin{pmatrix} \sum_1^N \ln(B_{sh})\ln(K_{exp}) \\ \sum_1^N \ln(F)\ln(K_{exp}) \\ \sum_1^N \ln(Pr)\ln(K_{exp}) \\ \sum_1^N \ln(H)\ln(K_{exp}) \\ \sum_1^N \ln(G)\ln(K_{exp}) \\ \sum_1^N \ln(P^*)\ln(K_{exp}) \end{pmatrix} \quad (4.30)$$

4.4. Selecting independent variables in the given developed empirical models.

4.4.1. Procedure of selecting independent variables.

The steps that are required for some of these independent dimensionless variables to be chosen in the gravity (4.3) and shear (4.23) controlled region models for the selected Nu^* of the single non-inundated tube model are given below:

- Select a value for $J_{v\,(critical)}$.

- Using the experimental data in the range $J_v < J_{v\,(critical),}$ obtain the values of the unknown constant parameters in equation (4.22) and (4.30).

- Determine the residuals R in equation (4.13) and (4.28) for the data in a range of $J_v < J_{v\,(critical)}$ using the values of the unknown constant parameters calculated from equations (4.22) and (4.30) from the previous step.

- Repeat the process starting from equation (4.10) to equation (4.22) for the gravity region model and from equation (4.23) to equation (4.30) for the shear region model by eliminating a dimensionless number whose output power is closest to 0. Calculate the new values of the unknown constant parameters in equations (4.23) and (4.30) and then determine its new Residual R from equations (4.13) and (4.28). Carry on this process in a loop until all the dimensionless parameters are eliminated one by one at the selected values of $J_{v\,(critical)}$.

The selection of the dimensionless variables within the gravity and shear controlled region models for each of the new developed model are discussed below.

4.4.2. Present Model I.

In this model, the outputs of the process of selecting the independent variables at different selected values of $J_{v\,(critical)}$ for both of the gravity and shear models, using Nu* as Shekriladze and Gomelauri (1966) model are tabulated in tables 4.1-4.4, where the graphs of the residual R (equation 4.13) against the number of the dimensionless variables for the experimental values of $J_v < J_{v\,(critical)}$ (gravity controlled region) and the Residual R (4.28) against the number of Dimensionless groups for the experimental values of $J_v > J_{v\,(critical)}$ (shear controlled region) were plotted in figures 4.1 and 4.2.

The number of the dimensionless variables from equation (4.3) (Gravity controlled region model) that are required, which would cause a sharp increase in the residual R (as illustrated in figures 4.1) by eliminating one more dimensionless variable from the required number of the dimensionless variables for the ranges of $0.1 \leq J_{v\,(critical)} \leq 0.4$ and $0.7 \leq J_{v\,(critical)} \leq 1.0$ is 5, while for $0.5 \leq J_{v\,(critical)} \leq 0.6$, the number of the dimensionless variables from equation (4.3) that are required which would cause a sharp increase in the value of R by eliminating one more dimensionless variable is 4.

Going through the same process as that of the gravity controlled region, that the required number of the dimensionless variables in equation (4.23) (Shear Controlled Region) that are required to give a sharp increase in the residuals R by eliminating one more dimensionless variable from the required number of the dimensionless variables (as shown in figure in 4.2) for $J_{v\,(critical)} = 0.1$ and 0.2 is 4 , while for $J_{v(critical)} = 0.3$ and 0.4, the number of the dimensionless variables from equation (4.23) that are required to give a sharp increase in the value of R as demonstrated in figure 4.2 by eliminating one more dimensionless variable is 3, and 5 dimensionless variables are required for $J_{v\,(critical)} \geq 0.5$.

Table 4.5 represents the required number of the dimensionless variables for each of gravity and shear region models within each of new developed models (corresponding to their minimum residuals R), mean deviation E_1 and the standard mean deviation E_2 of all data (steam and non-steam fluids), equivalents to each $J_{v(critical)}$. From the table, it shows that the minimum standard mean deviation E_2 for the first new developed model takes place at

$J_{v(critical)}$ of 0.6, from which the expressions of its gravity and shear region models are illustrated below:

For $J_v < 0.6$

$$K_{gr} = B_{gr}^{-0.157} H^{-0.088} G^{0.307} P^{0.155} \tag{4.31}$$

For $J_v > 0.6$

$$K_{sh} = F^{-0.201} Pr^{0.408} H^{0.254} G^{-0.889} P^{-0.430} \tag{4.32}$$

The Nusselt models for the gravity and shear controlled regions for the first new developed models are given below:

For $J_v < 0.6$

$$Nu = \left(\frac{0.9 + 0.728F^{\frac{1}{2}}}{\left(1 + 3.44F^{\frac{1}{2}} + F\right)^{\frac{1}{4}}} \right) \left(\frac{\Gamma_{N-gr}}{\gamma_{N-gr}} \right)^{-0.157} H^{-0.088} G^{0.307} P^{0.155} \tilde{Re}^{\frac{1}{2}} \tag{4.33}$$

For $J_v > 0.6$

$$Nu = \left(\frac{0.9 + 0.728F^{\frac{1}{2}}}{\left(1 + 3.44F^{\frac{1}{2}} + F\right)^{\frac{1}{4}}} \right) F^{-0.201} Pr^{0.408} H^{0.254} G^{-0.889} P^{-0.430} \tilde{Re}^{\frac{1}{2}} \tag{4.34}$$

Figures 4.3 and 4.4 compare the gravity and shear controlled region models represented in equations (4.33) and (4.34) with the data of steam and non-steam fluids respectively. The symbols that have been used in figures 4.3 and 4.4 for steam and non-steam are shown in Tables 3.1 and 3.2. The models represented in equations (4.33) and (4.34) under-estimate most of the data for steam, the exception being that of Beech-1 (1995), Nobbs-2 (1976) and Briggs and Sabaratnam (2003). For the non-steam data, the correlations over-predict most of its data, apart from that of Cavallini-1 (1985), Gogonin-2 (1976), Kutateladze (1981) and Briggs (2000).

Table 4.1. The obtained unknown constant parameters from equation (4.2) within present model I for $J_v < J_{v(critical)}$, where $J_{v(critical)}$ = 0.1, 0.2, 0.3, 0.4 and 0.5 and their residuals R.

$J_{v(critical)}$	N	a	b	c	d	e	f	R
0.1	6	-0.165	-0.035	-0.176	-0.294	0.736	0.475	21.612
	5	-0.153		-0.196	-0.210	0.629	0.373	26.024
	4			-0.228	-0.138	0.429	0.305	45.465
	3			-0.055		0.134	0.099	48.331
	2					0.196	0.133	52.338
	1					-0.070		67.069
0.2	6	-0.161	-0.029	-0.128	-0.242	0.643	0.408	30.942
	5	-0.153		-0.177	-0.211	0.640	0.379	35.714
	4			-0.195	-0.130	0.441	0.298	67.124
	3			-0.032		0.132	0.088	71.151
	2					0.160	0.105	73.264
	1					-0.053		85.611
0.3	6	-0.159	-0.024	-0.117	-0.220	0.592	0.373	47.991
	5	-0.155		-0.172	-0.213	0.623	0.371	52.561
	4			-0.195	-0.134	0.443	0.293	94.393
	3			-0.025		0.102	0.068	99.820
	2					0.126	0.081	101.580
	1					-0.038		111.327
0.4	6	-0.159	-0.019	-0.111	-0.199	0.570	0.345	58.979
	5	-0.156		-0.158	-0.199	0.604	0.350	62.272
	4			-0.183	-0.120	0.421	0.266	110.047
	3			-0.031		0.107	0.061	114.777
	2					0.139	0.079	117.802
	1					-0.019		128.350
0.5	6	-0.152	-0.018	-0.090	-0.177	0.527	0.313	74.009
	5	-0.150		-0.138	-0.182	0.570	0.325	77.527
	4	-0.154			-0.083	0.317	0.159	81.648
	3	-0.085				0.050	0.006	101.543
	2	-0.087				0.038		101.602
	1	-0.077						105.586

Table 4.2. The obtained unknown constant parameters from equation (4.2) within present model I for $J_v < J_{v(critical)}$, where $J_{v(critical)}$ = 0.6, 0.7, 0.8, 0.9 and 1.0 and their residuals R.

$J_{v(critical)}$	N	a	b	c	d	e	f	R
0.6	6	-0.154	-0.021	-0.084	-0.180	0.514	0.309	86.469
	5	-0.152		-0.141	-0.189	0.569	0.327	91.733
	4	-0.157			-0.088	0.307	0.155	96.215
	3	-0.084				0.021	-0.009	119.648
	2	-0.082				0.037		119.779
	1	-0.073						123.878
0.7	6	-0.153	-0.023	-0.077	-0.176	0.495	0.298	94.531
	5	-0.151		-0.142	-0.189	0.560	0.322	101.542
	4	-0.156			-0.088	0.295	0.147	106.177
	3	-0.082				0.005	-0.018	130.936
	2	-0.082				0.000		130.946
	1	-0.069						136.116
0.8	6	-0.152	-0.026	-0.072	-0.175	0.478	0.289	103.954
	5	-0.149		-0.146	-0.193	0.555	0.319	113.546
	4	-0.154			-0.088	0.277	0.137	118.556
	3	-0.079				-0.012	-0.027	144.038
	2	-0.078				0.000		144.103
	1	-0.065						150.439
0.9	6	-0.150	-0.029	-0.071	-0.177	0.464	0.284	111.728
	5	-0.147		-0.155	-0.199	0.553	0.320	124.274
	4			-0.205	-0.141	0.408	0.255	179.840
	3			-0.025		0.021	0.005	188.063
	2			-0.026		0.010		188.126
	1			-0.027				188.484
1.0	6	-0.147	-0.032	-0.072	-0.179	0.450	0.280	120.435
	5	-0.144		-0.165	-0.206	0.551	0.323	136.065
	4			-0.214	-0.149	0.409	0.259	191.221
	3			-0.023		-0.003	-0.006	200.489
	2			-0.023			-0.005	200.492
	1			-0.022				200.908

Table 4.3. The obtained unknown constant parameters from equation (4.22) within present model I for $J_v > J_{v(critical)}$, where $J_{v(critical)}$ = 0.1, 0.2, 0.3, 0.4 and 0.5 and their residuals R.

$J_{v(critical)}$	N	a	b	c	d	e	f	R
0.1	6	-0.142	-0.101	0.179	-0.034	-0.078	0.012	144.572
	5	-0.141	-0.102	0.186	-0.028	-0.099		144.609
	4	-0.126	-0.110	0.224		-0.092		149.388
	3	-0.134	-0.092	0.250				178.338
	2	-0.051		0.118				278.613
	1			0.079				284.408
0.2	6	-0.130	-0.132	0.247	0.034	-0.301	-0.105	114.713
	5	-0.135	-0.126	0.209		-0.202	-0.048	115.462
	4	-0.124	-0.131	0.216		-0.115		119.002
	3	-0.121	-0.105	0.246				152.592
	2	-0.027		0.107				260.239
	1			0.087				261.632
0.3	6	-0.109	-0.168	0.334	0.121	-0.547	-0.238	81.213
	5		-0.162	0.294	0.156	-0.608	-0.276	96.199
	4		-0.121	0.107		-0.148	-0.018	107.864
	3		-0.123	0.112		-0.116		108.283
	2		-0.111			-0.201		161.778
	1					-0.093		263.168
0.4	6	-0.104	-0.170	0.337	0.127	-0.574	-0.253	70.785
	5		-0.164	0.298	0.159	-0.625	-0.286	83.209
	4		-0.117	0.111		-0.163	-0.030	92.715
	3		-0.122	0.120		-0.109		93.795
	2		-0.106	0.165				113.244
	1			0.106				205.966
0.5	6	-0.104	-0.183	0.377	0.166	-0.707	-0.324	54.711
	5		-0.184	0.358	0.214	-0.797	-0.378	65.645
	4			-0.140	-0.198	0.332	0.220	127.957
	3				-0.092	0.058	0.046	140.430
	2				-0.078	-0.033		141.285
	1				-0.087			143.557

.

Table 4.4. The obtained unknown constant parameters from equation (4.22) within present model I for $J_v > J_{v(critical)}$, where $J_{v(critical)}$ = 0.6, 0.7, 0.8, 0.9 and 1.0 and their residuals R.

$J_{v(critical)}$	N	a	b	c	d	e	f	R
0.6	6	-0.089	-0.198	0.417	0.207	-0.800	-0.378	40.984
	5		-0.201	0.408	0.254	-0.889	-0.430	47.983
	4			-0.147	-0.219	0.407	0.254	108.477
	3				-0.107	0.121	0.073	121.961
	2				-0.084	-0.028		123.864
	1				-0.092			125.144
0.7	6	-0.085	-0.199	0.416	0.205	-0.796	-0.379	35.144
	5		-0.203	0.412	0.254	-0.891	-0.434	40.870
	4			-0.158	-0.244	0.476	0.286	90.548
	3				-0.121	0.168	0.094	105.811
	2				-0.092	-0.024		108.538
	1				-0.099			109.302
0.8	6	-0.086	-0.195	0.399	0.188	-0.757	-0.361	30.373
	5		-0.198	0.393	0.234	-0.851	-0.416	35.700
	4			-0.168	-0.264	0.521	0.308	74.579
	3				-0.131	0.196	0.109	91.253
	2				-0.096	-0.027		94.476
	1				-0.106			95.263
0.9	6	-0.084	-0.196	0.398	0.182	-0.745	-0.361	26.363
	5		-0.203	0.398	0.232	-0.852	-0.425	30.973
	4			-0.178	-0.289	0.580	0.332	64.783
	3				-0.141	0.231	0.125	82.898
	2				-0.101	-0.026		86.770
	1				-0.111			87.322
1.0	6	-0.083	-0.197	0.393	0.169	-0.714	-0.353	22.182
	5		-0.209	0.405	0.228	-0.856	-0.436	26.126
	4			-0.191	-0.321	0.670	0.369	56.157
	3				-0.152	0.294	0.159	75.338
	2					-0.341	-0.091	102.243
	1					-0.206		105.913

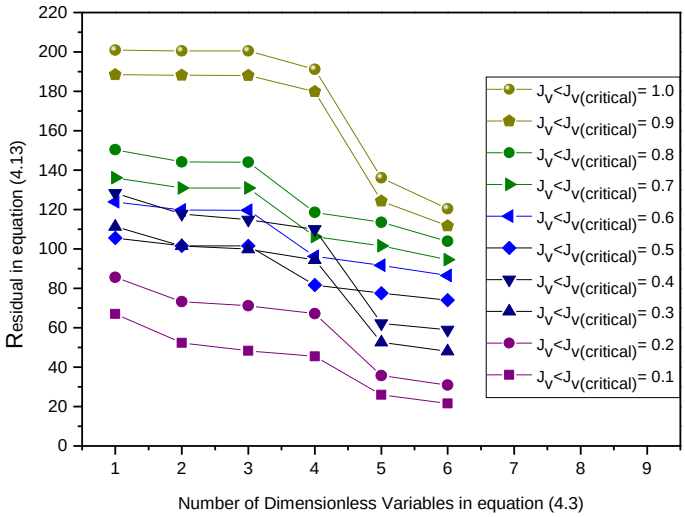

Figure 4.1. Residual R against the number of the dimensionless variables for the experimental values of $J_v < J_{v(critical)}$ for both of steam and non-steam fluids, where Nu* is taken as Shekriladze and Gomelauri (1966) model.

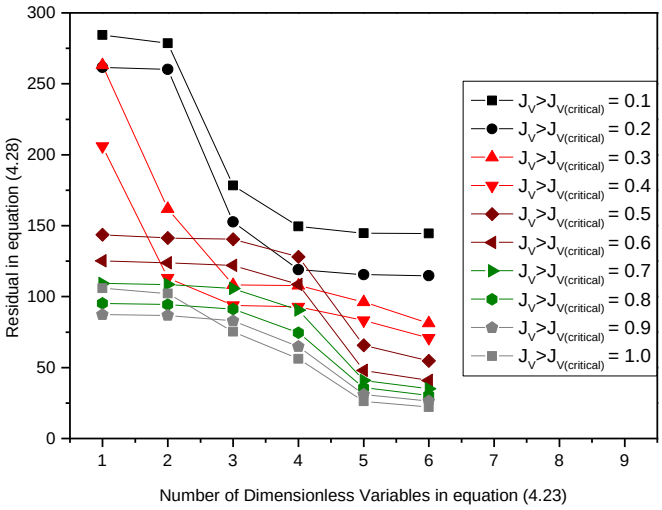

Figure 4.2. Residual R against the number of the dimensionless variables for the experimental values of $J_v > J_{v(critical)}$ for both of steam and non-steam fluids, where Nu* is taken as Shekriladze and Gomelauri (1966) model.

Table 4.5. Comparison of the present model I with all experimental data for the selected values of $J_{v(critical)}$.

$J_{v(critical)}$	Required dimensionless numbers in the gravity model	Required dimensionless numbers in the shear model	E_1	E_2
0.1	5	4	-0.967	15.544
0.2	5	4	-1.187	14.293
0.3	5	3	-2.017	15.075
0.4	5	3	-1.786	14.739
0.5	4	5	-1.568	13.818
0.6	4	5	-1.598	13.761
0.7	4	5	-1.651	13.859
0.8	4	5	-1.743	14.101
0.9	5	5	-1.577	14.307
1	5	5	-1.668	14.628

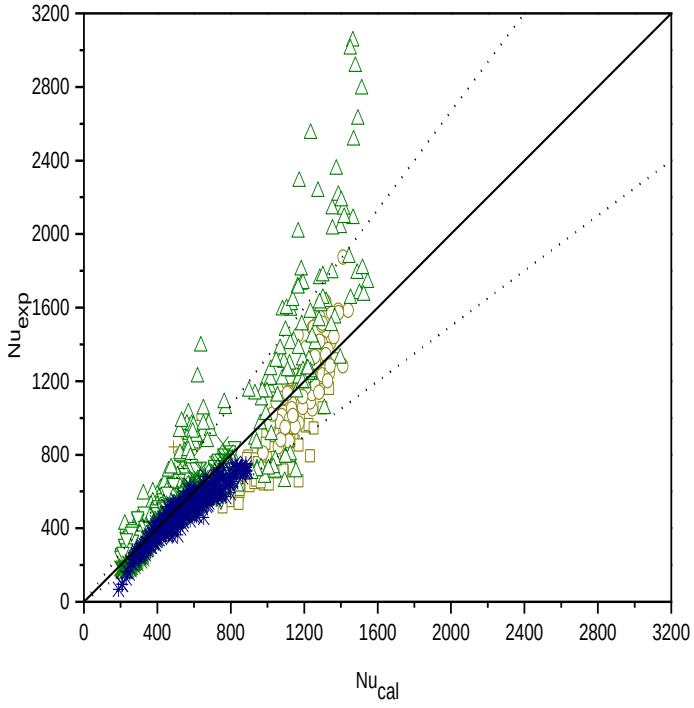

Figure 4.3. Comparison of present model I to the experimental data of steam, taking Nu* as Shekriladze and Gomelauri (1966) model.

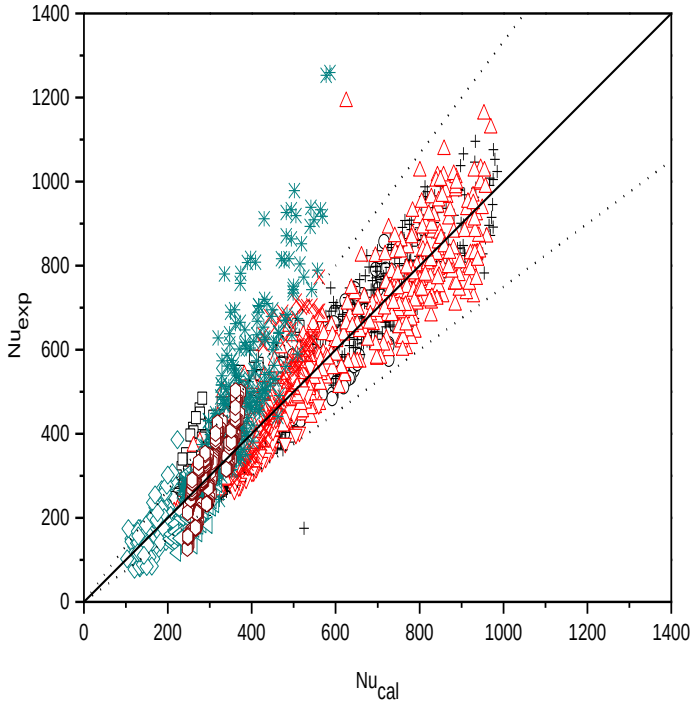

Figure 4.4. Comparison of present model I to the experimental data of non-steam, taking Nu* as Shekriladze and Gomelauri (1966) model.

4.4.3. Present Model II.

In this model, Fujii (1972) model for the single tube was selected for Nu^*, from which the outputs of the process of selecting the independent variables at certain values of $J_{v(critical)}$ for both of the gravity and shear models are demonstrated in tables 4.6-4.9 and figures 4.5 and 4.6.

Going through the same process as in section 4.3.2, the required number of the dimensionless groups within the gravity controlled region model (equation 4.3) for $J_{v\,(critical)} = 0.1$ and 0.2 is 5, while for $J_{v\,(critical)} \geq 0.3$ the number of the dimensionless variables that are required would be 4. For the shear controlled region model, 3 dimensionless numbers are required for $J_{v\,(critical)} = 0.1$ and 0.2, while 5 dimensionless numbers are needed for $J_{v\,(critical)} \geq 0.3$.

From table 4.10, $J_{v(critical)} = 0.6$ would be chosen, since it provide the minimum standard mean deviation E_2 for this developed model, where the expressions of the gravity and shear region models are given below:

For $J_v < 0.6$

$$K_{gr} = B_{gr}^{-0.158} H^{-0.064} G^{0.293} P^{0.141} \tag{4.35}$$

For $J_v > 0.6$

$$K_{sh} = F^{-0.141} Pr^{0.276} H^{0.205} G^{-0.593} P^{-0.331} \tag{4.36}$$

Therefore, the Nusselt models for the gravity and shear controlled regions (equations (4.35) and (4.36)) are given by the following equations:

For $J_v < 0.6$

$$Nu = \left(\frac{0.9\left(1 + G^{-1}\right)^{\frac{1}{3}} + 0.728F^{\frac{1}{2}}}{\left(1 + 3.44F^{\frac{1}{2}} + F\right)^{\frac{1}{4}}} \right) \left(\frac{\Gamma_{N-gr}}{\gamma_{N-gr}} \right)^{-0.158} H^{-0.064} G^{0.293} P^{0.141} \tilde{Re}^{\frac{1}{2}} \tag{4.37}$$

For $J_v > 0.6$

$$Nu = \left(\frac{0.9\left(1 + G^{-1}\right)^{\frac{1}{3}} + 0.728F^{\frac{1}{2}}}{\left(1 + 3.44F^{\frac{1}{2}} + F\right)^{\frac{1}{4}}} \right) F^{-0.141} Pr^{0.276} H^{0.205} G^{-0.593} P^{-0.331} \tilde{Re}^{\frac{1}{2}} \tag{4.38}$$

Present models II (equation 4.37 and 4.38) are plotted in figures 4.7 and 4.8, where it under-predict most of the data for steam, the exception again being that of Beech-1 (1995), Nobbs-2 (1976) and Briggs and Sabaratnam (2003). For the non-steam data, the models over-estimate most of its data, again the exception of Cavallini-1 (1985), Gogonin-2 (1976), Kutateladze (1981) and Briggs (2000).

Table 4.6. The obtained unknown constant parameters from equation (4.2) within present model II for $J_v < J_{v(critical)}$, where $J_{v(critical)}$ = 0.1, 0.2, 0.3, 0.4 and 0.5 and their residuals R.

$J_{v(critical)}$	N	a	b	c	d	e	f	R
0.1	6	-0.165	-0.035	-0.176	-0.294	0.736	0.475	21.612
	5	-0.153		-0.196	-0.210	0.629	0.373	26.024
	4			-0.228	-0.138	0.429	0.305	45.465
	3			-0.055		0.134	0.099	48.331
	2					0.196	0.133	52.338
	1					-0.070		67.069
0.2	6	-0.162	-0.023	-0.128	-0.215	0.617	0.385	32.781
	5	-0.156		-0.167	-0.192	0.615	0.362	37.376
	4			-0.184	-0.109	0.412	0.279	68.775
	3			-0.048		0.153	0.104	72.687
	2					0.195	0.129	74.237
	1					-0.067		85.920
0.3	6	-0.161	-0.017	-0.116	-0.188	0.562	0.343	51.852
	5	-0.157		-0.154	-0.183	0.583	0.342	55.977
	4	-0.160			-0.071	0.306	0.158	61.130
	3	-0.102				0.092	0.036	77.989
	2	-0.111				0.026		77.729
	1	-0.103						78.732
0.4	6	-0.160	-0.011	-0.112	-0.166	0.539	0.314	64.426
	5	-0.159		-0.138	-0.166	0.558	0.317	67.086
	4	-0.161			-0.066	0.304	0.150	71.731
	3	-0.107				0.099	0.033	89.074
	2	-0.115				0.039		88.407
	1	-0.105						91.173
0.5	6	-0.153	-0.009	-0.094	-0.144	0.498	0.282	81.320
	5	-0.152		-0.118	-0.146	0.519	0.288	83.926
	4	-0.156			-0.062	0.304	0.146	87.971
	3	-0.104				0.104	0.033	106.576
	2	-0.113				0.044		105.577
	1	-0.101						109.472

Table 4.7. The obtained unknown constant parameters from equation (4.2) within present model II for $J_v < J_{v(critical)}$, where $J_{v(critical)}$ = 0.6, 0.7, 0.8, 0.9 and 1.0 and their residuals R.

$J_{v(critical)}$	N	a	b	c	d	e	f	R
0.6	6	-0.156	-0.011	-0.090	-0.145	0.485	0.276	95.910
	5	-0.155		-0.119	-0.149	0.513	0.285	99.928
	4	-0.158			-0.064	0.293	0.141	104.307
	3	-0.105				0.083	0.021	126.076
	2	-0.110				0.044		124.742
	1	-0.100						128.696
0.7	6	-0.155	-0.012	-0.084	-0.140	0.467	0.264	106.321
	5	-0.153		-0.117	-0.147	0.500	0.276	111.714
	4	-0.157			-0.063	0.281	0.132	116.262
	3	-0.105				0.073	0.014	138.966
	2	-0.108				0.047		137.716
	1	-0.098						142.080
0.8	6	-0.154	-0.014	-0.080	-0.138	0.450	0.254	118.165
	5	-0.152		-0.120	-0.148	0.492	0.270	125.678
	4	-0.156			-0.062	0.263	0.121	130.564
	3	-0.104				0.061	0.006	153.756
	2	-0.105				0.050		153.057
	1	-0.095						157.689
0.9	6	-0.152	-0.016	-0.081	-0.139	0.437	0.248	128.363
	5	-0.150		-0.128	-0.152	0.487	0.268	138.506
	4	-0.154			-0.060	0.242	0.109	144.033
	3	-0.103				0.044	-0.003	167.758
	2	-0.102				0.049		168.193
	1	-0.093						172.276
1.0	6	-0.149	-0.018	-0.083	-0.140	0.423	0.243	139.593
	5	-0.147		-0.136	-0.156	0.481	0.267	152.327
	4	-0.151			-0.058	0.218	0.096	158.745
	3	-0.102				0.025	-0.012	182.779
	2	-0.098				0.048		184.896
	1	-0.090						188.021

Table 4.8. The obtained unknown constant parameters from equation (4.22) within present model II for $J_v > J_{v(critical)}$, where $J_{v(critical)}$ = 0.1, 0.2, 0.3, 0.4 and 0.5 and their residuals R.

$J_{v(critical)}$	N	a	b	c	d	e	f	R
0.1	6	-0.142	-0.101	0.179	-0.034	-0.078	0.012	144.572
	5	-0.141	-0.102	0.186	-0.028		0.000	144.609
	4	-0.126	-0.110	0.224	0.000			149.388
	3	-0.134	-0.092	0.250				178.338
	2	-0.051		0.118				278.613
	1	0.000						284.408
0.2	6	-0.123	-0.085	0.153	0.036	-0.171	-0.083	235.683
	5	-0.128	-0.078	0.112		-0.064	-0.022	236.469
	4	-0.123	-0.080	0.115		-0.025		238.988
	3	-0.122	-0.075	0.122				251.812
	2	-0.055		0.023				350.650
	1	-0.034						360.875
0.3	6	-0.103	-0.115	0.225	0.107	-0.365	-0.192	201.305
	5		-0.110	0.187	0.140	-0.422	-0.227	216.167
	4			-0.090	-0.072	0.164	0.081	297.477
	3			-0.013		-0.062	-0.053	314.866
	2					-0.037	-0.044	309.602
	1						-0.025	323.188
0.4	6	-0.099	-0.116	0.225	0.107	-0.367	-0.197	189.470
	5		-0.111	0.188	0.137	-0.415	-0.227	201.945
	4			-0.098	-0.089	0.200	0.098	264.925
	3			-0.005		-0.083	-0.067	286.647
	2					-0.072	-0.063	284.887
	1					0.031		311.980
0.5	6	-0.099	-0.127	0.256	0.133	-0.457	-0.248	172.007
	5		-0.128	0.238	0.179	-0.542	-0.299	182.994
	4			-0.108	-0.107	0.242	0.117	239.421
	3			-0.003		-0.104	-0.079	264.985
	2					-0.099	-0.078	264.321
	1					0.026		292.813

Table 4.9. The obtained unknown constant parameters from equation (4.22) within present model II for $J_v > J_{v(critical)}$, where $J_{v(critical)}$ = 0.6, 0.7, 0.8, 0.9 and 1.0 and their residuals R.

$J_{v(critical)}$	N	a	b	c	d	e	f	R
0.6	6	-0.087	-0.138	0.285	0.159	-0.506	-0.280	156.362
	5		-0.141	0.276	0.205	-0.593	-0.331	163.233
	4			-0.114	-0.126	0.316	0.149	218.482
	3				-0.040	0.095	0.009	231.181
	2				-0.037	0.077		231.571
	1					0.022		272.992
0.7	6	-0.087	-0.136	0.274	0.144	-0.464	-0.264	148.049
	5		-0.140	0.271	0.194	-0.561	-0.320	153.900
	4			-0.124	-0.150	0.384	0.178	198.790
	3				-0.054	0.143	0.028	213.338
	2				-0.046	0.086		214.679
	1					0.014		255.024
0.8	6	-0.088	-0.132	0.257	0.123	-0.411	-0.240	140.752
	5		-0.135	0.251	0.171	-0.508	-0.296	146.222
	4			-0.132	-0.170	0.430	0.199	181.172
	3				-0.065	0.173	0.041	196.968
	2				-0.051	0.088		199.092
	1					0.004		233.831
0.9	6	-0.086	-0.134	0.257	0.116	-0.392	-0.237	134.359
	5		-0.140	0.257	0.167	-0.503	-0.303	138.913
	4			-0.143	-0.193	0.489	0.221	169.560
	3				-0.075	0.210	0.056	186.957
	2				-0.057	0.095		189.542
	1					-0.002		217.752
1.0	6	-0.086	-0.134	0.249	0.100	-0.349	-0.223	127.566
	5		-0.146	0.261	0.161	-0.496	-0.310	131.338
	4			-0.155	-0.223	0.570	0.253	158.670
	3				-0.086	0.265	0.082	177.263
	2				-0.061	0.099		181.383
	1					-0.007		202.353

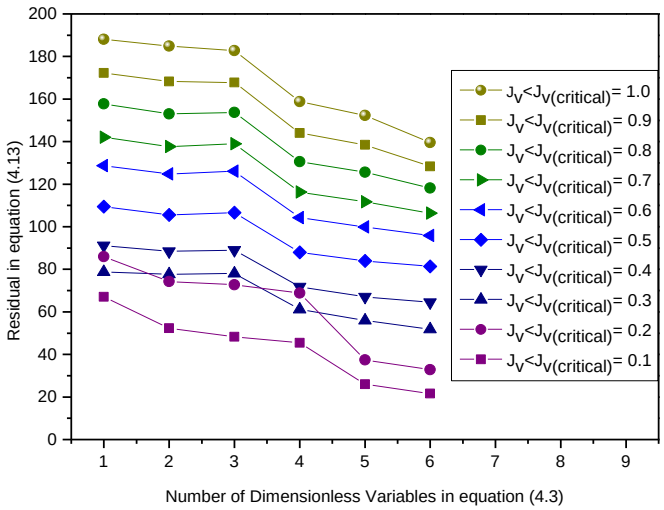

Figure 4.5. Residual R against the number of the dimensionless variables for the experimental values of $J_v < J_{v(critical)}$ for both of steam and non-steam fluids, where Nu* is taken as Fujii (1972) model.

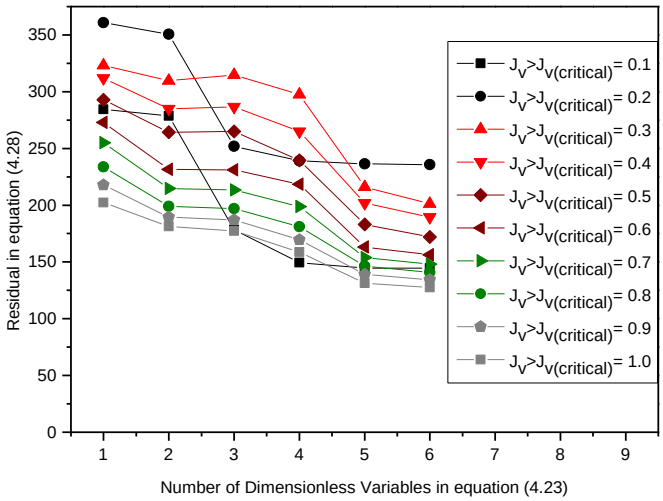

Figure 4.6. Residual R against the number of the dimensionless variables for the experimental values of $J_v > J_{v(critical)}$ for both of steam and non-steam fluids, where Nu* is taken as Fujii (1972) model.

Table 4.10. Comparison of the present model II with all experimental data for the selected values of $J_{v(critical)}$.

$J_{v(critical)}$	Required dimensionless numbers in the gravity model	Required dimensionless numbers in the shear model	E_1	E_2
0.1	5	3	-1.452	14.889
0.2	5	3	-1.599	14.098
0.3	4	5	-1.579	14.158
0.4	4	5	-1.560	13.975
0.5	4	5	-1.488	13.749
0.6	4	5	-1.490	13.633
0.7	4	5	-1.509	13.668
0.8	4	5	-1.589	13.869
0.9	4	5	-1.652	14.057
1	4	5	-1.716	14.268

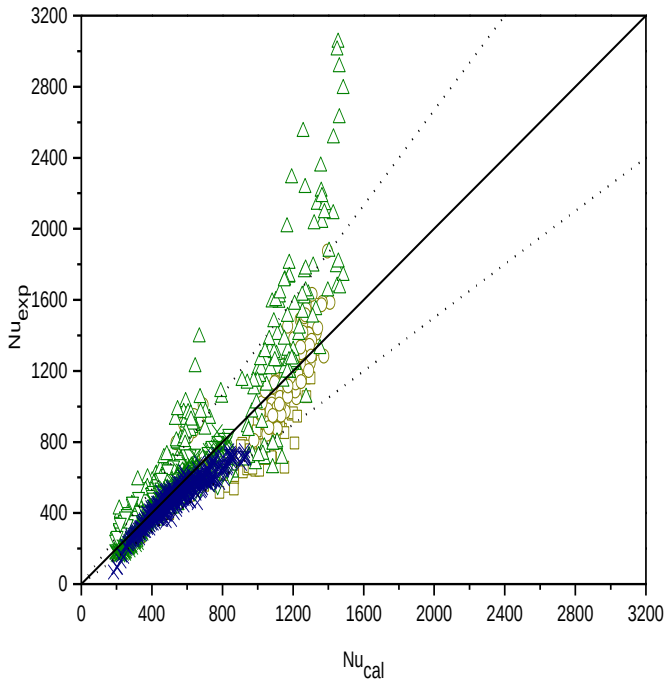

Figure 4.7. Comparison of present model II to the experimental data of steam, taking Nu* as Fujii (1972) model.

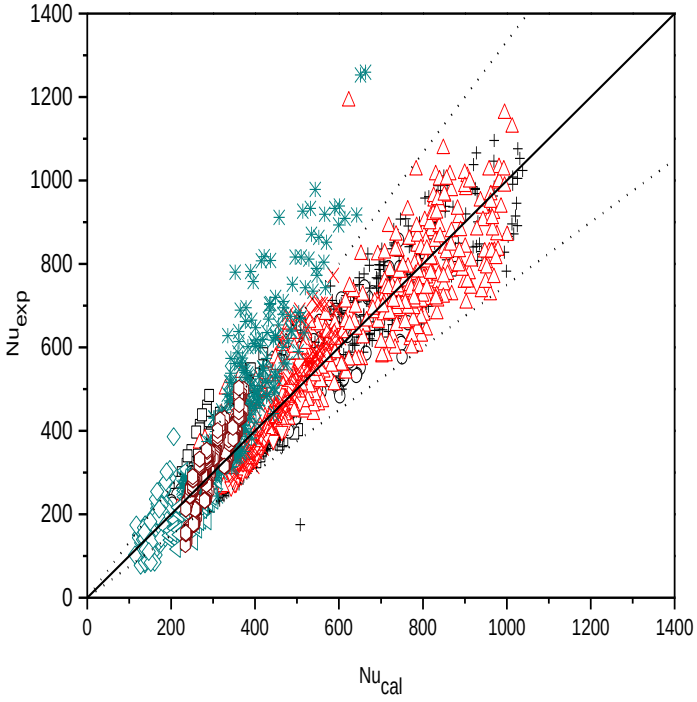

Figure 4.8. Comparison of present model II to the experimental data of non-steam, taking Nu* as Fujii (1972) model.

4.4.4. Present Model III.

The outputs of the process of selecting the independent variables at certain values of $J_{v(critical)}$ for both of the gravity and shear models, where Rose (1984) model for the single tube was selected for Nu^{*} are shown in tables 4.11-4.14 and figures 4.9 and 4.10.

From table 4.15, the numbers of the dimensionless groups that are needed within the gravity controlled region model (equation 4.3) for $J_{v\,(critical)} \leq 0.4$ is 5, while for $J_{v\,(critical)} \geq 0.4$ the number of the dimensionless variables that are required would be 4. In the shear controlled region model, 3 dimensionless numbers are needed for $J_{v\,(critical)} = 0.1$, while for the range of $0.2 \leq J_{v\,(critical)} \leq 0.7$, it required 4 dimensionless numbers and 5 dimensionless numbers are needed for the $J_{v\,(critical)}$ values of 0.8, 0.9 and 1.0. The expressions of the gravity and shear models for $J_{v(critical)} = 0.6$ (since its offers a minimum standard mean deviation for this model) are shown below:

For $J_v < 0.6$

$$K_{gr} = B_{gr}^{-0.167} H^{-0.091} G^{0.353} P^{0.130} \qquad (4.39)$$

For $J_v > 0.6$

$$K_{sh} = B_{sh}^{-0.088} F^{-0.095} Pr^{0.135} P^{-0.098} \tag{4.40}$$

Therefore, the Nusselt models for the gravity and shear controlled regions are given as follows:

For $J_v < 0.6$

$$Nu = \left(\frac{0.64(1+1.81P)^{0.209}\left(1+G^{-1}\right)^{\frac{1}{3}} + 0.728F^{\frac{1}{2}}}{\left(1+3.51F^{0.53}+F\right)^{\frac{1}{4}}} \right) \left(\frac{\Gamma_{N-gr}}{\gamma_{N-gr}} \right)^{-0.167} H^{-0.091} G^{0.353} P^{0.130} \tilde{Re}^{\frac{1}{2}} \tag{4.41}$$

For $J_v > 0.6$

$$Nu = \left(\frac{0.64(1+1.81P)^{0.209}\left(1+G^{-1}\right)^{\frac{1}{3}} + 0.728F^{\frac{1}{2}}}{\left(1+3.51F^{0.53}+F\right)^{\frac{1}{4}}} \right) \left(\frac{\Gamma_{N-sh}}{\gamma_{N-sh}} \right)^{-0.088} F^{-0.095} Pr^{0.135} P^{-0.098} \tilde{Re}^{\frac{1}{2}} \tag{4.42}$$

Equations (4.41) and (4.42) were plotted in figures 4.11 and 4.12, from which the distribution of the steam and non-steam data are similar to figures 4.7 and 4.8.

Table 4.11. The obtained unknown constant parameters from equation (4.2) within present model III for $J_v < J_{v(critical)}$, where $J_{v(critical)}$ = 0.1, 0.2, 0.3, 0.4 and 0.5 and their residuals R.

$J_{v(critical)}$	N	a	b	c	d	e	f	R
0.1	6	-0.167	-0.040	-0.188	-0.322	0.812	0.497	21.268
	5	-0.152		-0.211	-0.226	0.689	0.379	27.065
	4			-0.243	-0.154	0.489	0.312	46.447
	3			-0.050		0.159	0.081	50.035
	2					0.215	0.111	53.249
	1					-0.008		63.565
0.2	6	-0.164	-0.034	-0.134	-0.264	0.709	0.416	30.883
	5	-0.156		-0.192	-0.228	0.706	0.381	37.491
	4			-0.209	-0.146	0.503	0.299	69.995
	3			-0.027		0.157	0.065	75.033
	2					0.181	0.079	76.587
	1					0.021		83.586
0.3	6	-0.166	-0.028	-0.117	-0.234	0.650	0.367	47.886
	5	-0.160		-0.181	-0.225	0.685	0.365	53.976
	4			-0.205	-0.144	0.499	0.284	98.748
	3			-0.023		0.134	0.043	104.973
	2					0.134	0.043	106.660
	1					0.044		110.984
0.4	6	-0.167	-0.022	-0.111	-0.210	0.626	0.334	60.989
	5	-0.163		-0.165	-0.210	0.666	0.341	65.458
	4			-0.192	-0.127	0.474	0.253	117.753
	3			-0.031		0.141	0.036	123.079
	2					0.173	0.053	126.000
	1					0.068		130.696
0.5	6	-0.160	-0.021	-0.091	-0.186	0.581	0.298	77.725
	5	-0.158		-0.145	-0.192	0.629	0.312	82.175
	4	-0.162			-0.088	0.364	0.137	86.736
	3	-0.090				0.081	-0.024	108.906
	2	-0.084				0.127		109.815
	1					0.083		149.132

Table 4.12. The obtained unknown constant parameters from equation (4.2) within present model III for $J_v < J_{v(critical)}$, where $J_{v(critical)}$ = 0.6, 0.7, 0.8, 0.9 and 1.0 and their residuals R.

$J_{v(critical)}$	N	a	b	c	d	e	f	R
0.6	6	-0.164	-0.023	-0.086	-0.186	0.566	0.289	90.355
	5	-0.162		-0.147	-0.196	0.625	0.308	96.271
	4	-0.167			-0.091	0.353	0.130	101.085
	3	-0.091				0.055	-0.040	126.468
	2	-0.081				0.131		129.178
	1					0.091		169.225
0.7	6	-0.164	-0.024	-0.080	-0.181	0.546	0.274	100.506
	5	-0.162		-0.146	-0.194	0.612	0.298	107.643
	4	-0.167			-0.090	0.339	0.119	112.534
	3	-0.091				0.042	-0.050	138.539
	2	-0.095					-0.069	139.300
	1	-0.049						201.834
0.8	6	-0.164	-0.025	-0.078	-0.179	0.527	0.262	112.443
	5	-0.161		-0.150	-0.196	0.602	0.291	121.478
	4	-0.166			-0.089	0.317	0.105	126.716
	3	-0.091				0.027	-0.060	152.580
	2	-0.093					-0.072	152.911
	1	-0.047						226.076
0.9	6	-0.162	-0.027	-0.079	-0.179	0.512	0.254	121.760
	5	-0.159		-0.158	-0.200	0.595	0.288	132.896
	4	-0.164			-0.087	0.291	0.090	138.838
	3	-0.090				0.005	-0.072	164.444
	2	-0.090					-0.074	164.458
	1	-0.044						245.399
1.0	6	-0.159	-0.029	-0.084	-0.180	0.496	0.247	131.426
	5	-0.156		-0.169	-0.205	0.588	0.286	144.433
	4			-0.222	-0.143	0.434	0.216	208.973
	3			-0.038		0.038	-0.038	217.555
	2					0.083	-0.017	224.209
	1					0.116		224.965

Table 4.13. The obtained unknown constant parameters from equation (4.22) within present model III for $J_v > J_{v(critical)}$, where $J_{v(critical)}$ = 0.1, 0.2, 0.3, 0.4 and 0.5 and their residuals R.

$J_{v(critical)}$	N	a	b	c	d	e	f	R
0.1	6	-0.132	-0.046	0.052	-0.058	0.116	0.006	149.192
	5	-0.131	-0.046	0.056	-0.055	0.106		149.201
	4	-0.113		-0.016	-0.075	0.126		168.589
	3	-0.120			-0.072	0.131		169.030
	2	-0.003				0.139		218.325
	1					0.140		218.371
0.2	6	-0.117	-0.066	0.091	-0.018	-0.015	-0.071	121.989
	5	-0.117	-0.066	0.086	-0.022		-0.062	122.004
	4	-0.108	-0.071	0.119			-0.070	124.000
	3	-0.096	-0.106	0.096				172.400
	2		-0.092	0.015				187.268
	1		-0.087					188.652
0.3	6	-0.097	-0.092	0.150	0.038	-0.163	-0.158	91.285
	5	-0.102	-0.083	0.108		-0.053	-0.096	91.947
	4	-0.096	-0.084	0.115			-0.072	92.851
	3	-0.094	-0.120	0.089				133.512
	2	-0.014	-0.099					145.186
	1		-0.101					146.177
0.4	6	-0.094	-0.093	0.146	0.030	-0.140	-0.154	78.900
	5	-0.097	-0.084	0.113		-0.052	-0.105	79.238
	4	-0.092	-0.085	0.120			-0.081	80.012
	3	-0.092	-0.120	0.085				123.332
	2	-0.014	-0.099					133.305
	1		-0.101					134.294
0.5	6	-0.097	-0.101	0.166	0.041	-0.179	-0.182	62.299
	5	-0.101	-0.089	0.123		-0.063	-0.119	62.702
	4	-0.094	-0.091	0.131			-0.090	63.667
	3	-0.095	-0.120	0.083				108.341
	2	-0.0182	-0.0997					117.032
	1		-0.102					118.522

Table 4.14. The obtained unknown constant parameters from equation (4.22) within present model III for $J_v > J_{v(critical)}$, where $J_{v(critical)}$ = 0.6, 0.7, 0.8, 0.9 and 1.0 and their residuals R.

$J_{v(critical)}$	N	a	b	c	d	e	f	R
0.6	6	-0.086	-0.110	0.186	0.055	-0.194	-0.199	47.988
	5	-0.092	-0.093	0.130		-0.039	-0.116	48.552
	4	-0.088	-0.095	0.135			-0.098	48.880
	3		-0.080	0.065			-0.098	115.491
	2		-0.069				-0.069	70.724
	1		-0.102					101.748
0.7	6	-0.088	-0.106	0.169	0.029	-0.120	-0.168	40.394
	5	-0.091	-0.097	0.140		-0.039	-0.125	40.515
	4	-0.087	-0.098	0.146			-0.108	40.806
	3		-0.084	0.078			-0.108	47.487
	2		-0.069				-0.069	64.358
	1		-0.098					93.733
0.8	6	-0.090	-0.101	0.151	0.004	-0.055	-0.140	34.494
	5	-0.090	-0.100	0.147		-0.043	-0.134	34.496
	4	-0.086	-0.101	0.153			-0.114	34.815
	3		-0.088	0.089			-0.117	40.731
	2			0.041			-0.117	80.562
	1						-0.091	85.001
0.9	6	-0.088	-0.104	0.150	-0.005	-0.029	-0.135	29.388
	5	-0.088	-0.105	0.155		-0.044	-0.143	29.391
	4	-0.084	-0.106	0.162			-0.123	29.680
	3		-0.096	0.103			-0.129	34.738
	2			0.035			-0.109	75.356
	1						-0.085	78.127
1.0	6	-0.088	-0.103	0.141	-0.025	0.024	-0.117	24.214
	5	-0.087	-0.106	0.149	-0.017		-0.130	24.219
	4	-0.083	-0.111	0.171			-0.131	24.528
	3		-0.104	0.119			-0.142	28.808
	2			0.025			-0.098	68.902
	1						-0.079	70.150

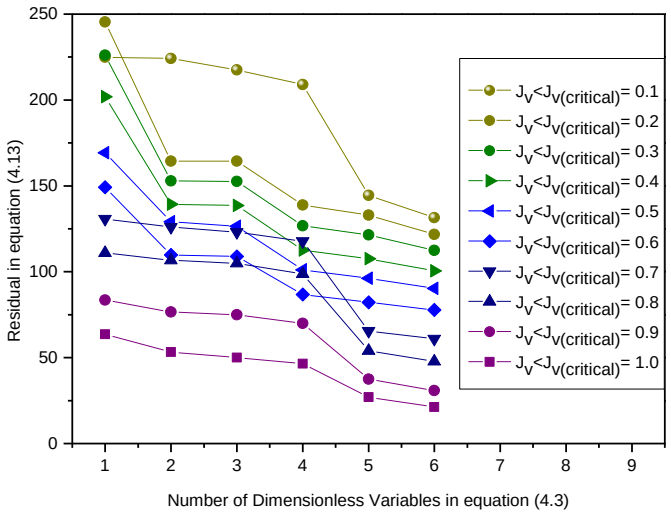

Figure 4.9. Residual R against the number of the dimensionless variables for the experimental values of $J_v < J_{v(critical)}$ for both of steam and non-steam fluids, where Nu* is taken as Rose (1984) model.

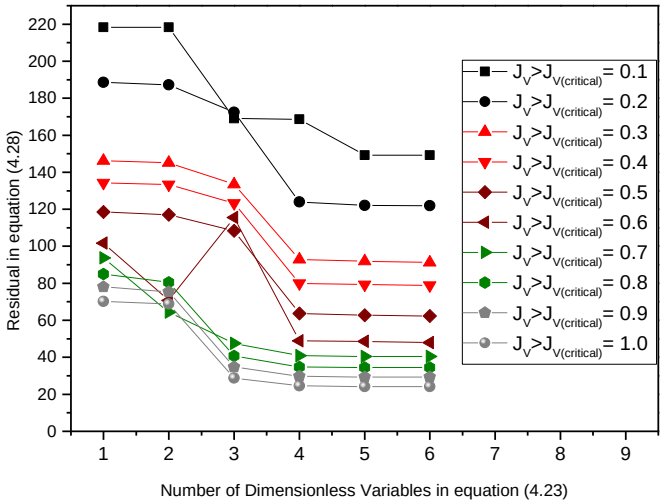

Figure 4.10. Residual R against the number of the dimensionless variables for the experimental values of $J_v > J_{v(critical)}$ for both of steam and non-steam fluids, where Nu* is taken as Rose (1984) model.

Table 4.15. Comparison of the present model III with all experimental data for the selected values of $J_{v(critical)}$.

$J_{v(critical)}$	Required dimensionless numbers in the gravity model	Required dimensionless numbers in the shear model	E_1	E_2
0.1	5	3	-2.222	16.726
0.2	5	4	-1.318	14.617
0.3	5	4	-1.482	14.125
0.4	5	4	-1.447	13.989
0.5	4	4	-1.633	13.936
0.6	4	4	-1.725	13.931
0.7	4	4	-1.735	14.027
0.8	4	5	-1.812	14.324
0.9	4	5	-2.053	15.135
1	4	5	-1.689	14.747

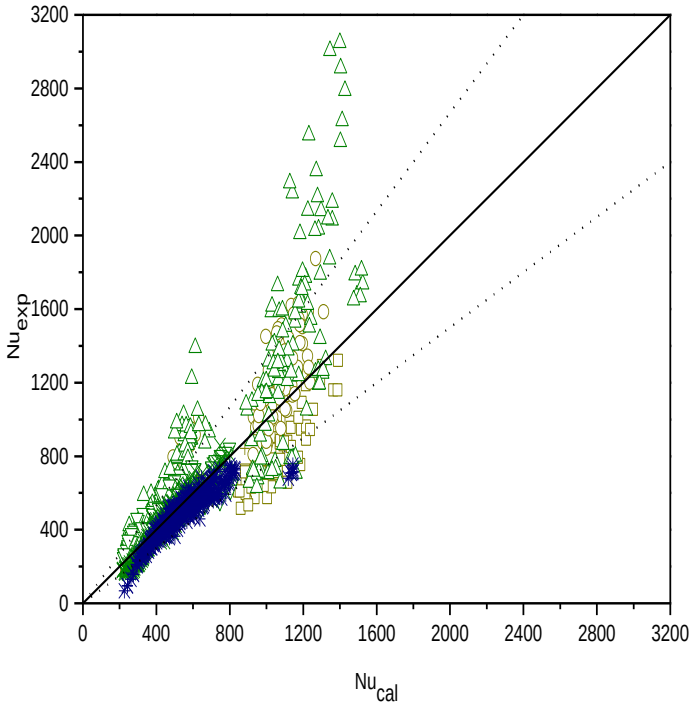

Figure 4.11. Comparison of present model III to the experimental data of steam, taking Nu* as Rose (1984) model.

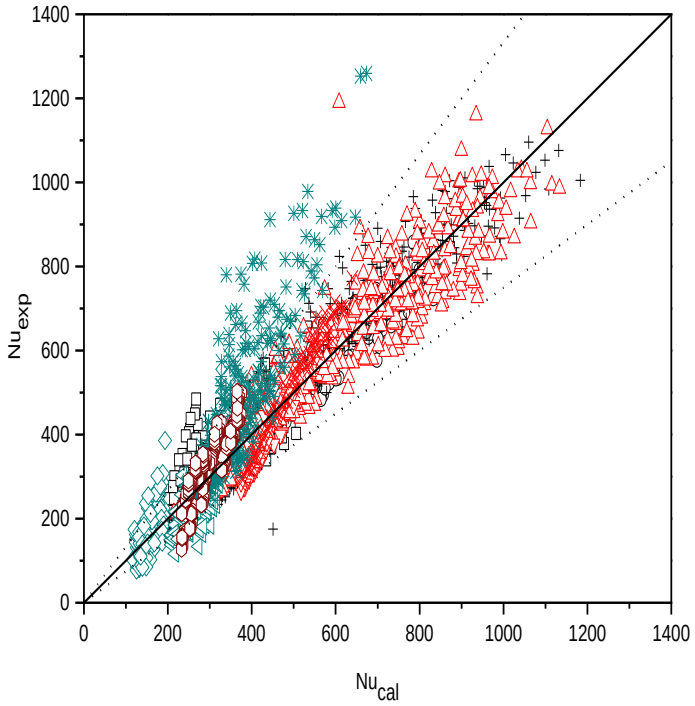

Figure 4.12. Comparison of present model III to the experimental data of non-steam, taking Nu* as Rose (1984) model.

4.4.5. Present Model IV.

In this model, Honda (1986) model for the single tube was nominated for Nu^{*}, where the outputs of the process of choosing the independent variables at certain values of $J_{v(critical)}$ for both of the gravity and shear models are demonstrated in tables 4.16-4.19 and figures 4.13 and 4.14.

The expressions that represent gravity and shear region models are given below, based on table 4.20, where the $J_{v(critical)}$ value of 0.4 was selected, which offers the minimum standard deviation E_2.

For $J_v < 0.4$

$$K_{gr} = B_{gr}^{-0.164} H^{-0.076} G^{0.305} P^{0.142} \tag{4.43}$$

For $J_v > 0.4$

$$K_{sh} = B_{sh}^{-0.102} F^{0.045} Pr^{-0.159} G^{-0.209} P^{-0.232} \tag{4.44}$$

The expressions for Nusselt models within the gravity and shear controlled regions would be as follows:

For $J_v < 0.4$

$$Nu = Nu_{Honda}\left(\frac{\Gamma_{N-gr}}{\gamma_{N-gr}}\right)^{-0.164} H^{-0.076} G^{0.305} P^{0.142} \quad (4.45)$$

For $J_v > 0.4$

$$Nu = Nu_{Honda}\left(\frac{\Gamma_{N-sh}}{\gamma_{N-sh}}\right)^{-0.102} F^{0.045} Pr^{-0.159} G^{-0.209} P^{-0.232} \quad (4.46)$$

Where Nu_{-Honda} represents the Nusselt number been obtained from the Honda (1986) model for the non-inundated forced convection single tube. Figures 4.15 and 4.16 represent the comparison of the models in equations (4.45) and (4.46) with its experimental data for steam and non-steam fluids, where the distribution of the steam data is similar to that within figures 4.13 and 4.14. Again the distribution of the non-steam data is similar to that in figure 4.12, the exceptions for the data of Cavallini-2 (1988), where the models under-predicts its data and that of Gogonin-2 (1976), from which the models over-estimate its data.

Table 4.16. The obtained unknown constant parameters from equation (4.2) within present model IV for $J_v < J_{v(critical)}$, where $J_{v(critical)}$ = 0.1, 0.2, 0.3, 0.4 and 0.5 and their residuals R.

$J_{v(critical)}$	N	a	b	c	d	e	f	R
0.1	6	-0.166	-0.033	-0.167	-0.292	0.744	0.466	22.476
	5	-0.154		-0.185	-0.212	0.642	0.369	26.472
	4			-0.218	-0.140	0.439	0.300	46.406
	3			-0.043		0.141	0.091	49.342
	2					0.189	0.118	51.751
	1					-0.046		63.268
0.2	6	-0.163	-0.022	-0.116	-0.222	0.622	0.376	33.832
	5	-0.157		-0.153	-0.200	0.620	0.354	36.530
	4	-0.159			-0.087	0.360	0.177	39.844
	3	-0.088				0.104	0.033	53.197
	2	-0.096				0.044		54.209
	1	-0.082						56.695
0.3	6	-0.162	-0.012	-0.112	-0.191	0.557	0.327	53.940
	5	-0.159		-0.140	-0.188	0.572	0.326	55.137
	4	-0.161			-0.085	0.320	0.158	58.606
	3	-0.092				0.062	0.011	75.373
	2	-0.095				0.042		75.524
	1	-0.083						78.831
0.4	6	-0.162	-0.003	-0.114	-0.165	0.525	0.290	68.840
	5	-0.162		-0.122	-0.165	0.531	0.291	68.936
	4	-0.164			-0.076	0.305	0.142	71.801
	3	-0.101				0.068	0.007	86.652
	2	-0.103				0.056		86.713
	1	-0.088						94.145
0.5	6	-0.156	0.002	-0.108	-0.140	0.476	0.250	86.582
	5	-0.157		-0.102	-0.139	0.471	0.248	86.632
	4	-0.160			-0.066	0.285	0.125	88.877
	3	-0.105				0.072	0.004	101.534
	2	-0.106				0.064		101.556
	1	-0.089						112.934

Table 4.17. The obtained unknown constant parameters from equation (4.2) within present model IV for $J_v < J_{v(critical)}$, where $J_{v(critical)}$ = 0.6, 0.7, 0.8, 0.9 and 1.0 and their residuals R.

$J_{v(critical)}$	N	a	b	c	d	e	f	R
0.6	6	-0.161	0.004	-0.114	-0.138	0.457	0.235	102.764
	5	-0.162		-0.102	-0.136	0.446	0.231	102.989
	4	-0.165			-0.063	0.257	0.107	105.319
	3	-0.113				0.051	-0.010	117.372
	2	-0.110				0.070		117.547
	1	-0.093						132.262
0.7	6	-0.162	0.007	-0.118	-0.131	0.435	0.215	116.518
	5	-0.163		-0.099	-0.127	0.416	0.208	117.138
	4	-0.166			-0.056	0.230	0.087	119.402
	3	-0.120				0.046	-0.018	129.400
	2	-0.115				0.080		130.005
	1	-0.097						150.405
0.8	6	-0.162	0.008	-0.125	-0.127	0.414	0.199	131.672
	5	-0.163		-0.102	-0.122	0.390	0.189	132.582
	4	-0.167			-0.049	0.197	0.063	135.006
	3	-0.125				0.037	-0.028	142.884
	2	-0.118				0.089		144.379
	1	-0.100						171.412
0.9	6	-0.161	0.009	-0.133	-0.126	0.396	0.186	144.001
	5	-0.162		-0.108	-0.120	0.369	0.175	145.120
	4	-0.165			-0.042	0.162	0.040	147.893
	3	-0.156			-0.027	0.089		148.962
	2	-0.120				0.095		156.861
	1	-0.102						188.955
1.0	6	-0.159	0.010	-0.146	-0.126	0.376	0.174	157.834
	5	-0.160		-0.117	-0.117	0.345	0.160	159.375
	4	-0.163			-0.034	0.120	0.014	162.609
	3	-0.134				0.008	-0.049	166.624
	2	-0.135					-0.053	166.657
	1	-0.104						208.828

Table 4.18. The obtained unknown constant parameters from equation (4.22) within present model IV for $J_v > J_{v(critical)}$, where $J_{v(critical)}$ = 0.1, 0.2, 0.3, 0.4 and 0.5 and their residuals R.

$J_{v(critical)}$	N	a	b	c	d	e	f	R
0.1	6	-0.130	0.075	-0.193	-0.050	0.044	-0.077	171.450
	5	-0.129	0.074	-0.180	-0.037		-0.102	171.611
	4	-0.113	0.066	-0.126			-0.116	178.337
	3	-0.154		-0.055			-0.092	222.047
	2	-0.203					-0.101	228.880
	1	-0.218						417.222
0.2	6	-0.119	0.064	-0.184	-0.031	-0.064	-0.141	137.667
	5	-0.115	0.058	-0.149		-0.154	-0.193	138.285
	4	-0.151		-0.094		-0.140	-0.163	164.745
	3	-0.226				-0.096	-0.157	181.481
	2	-0.207					-0.112	185.300
	1	-0.242						372.611
0.3	6	-0.102	0.045	-0.150	0.009	-0.209	-0.226	103.137
	5	-0.103	0.047	-0.160		-0.182	-0.211	103.175
	4	-0.135		-0.117		-0.164	-0.183	117.583
	3	-0.227				-0.101	-0.174	139.863
	2	-0.206					-0.126	143.395
	1	-0.263						331.005
0.4	6	-0.103	0.045	-0.161	-0.001	-0.206	-0.230	86.017
	5	-0.102	0.045	-0.159		-0.209	-0.232	86.018
	4	-0.135		-0.117		-0.185	-0.204	97.824
	3	-0.223				-0.116	-0.195	118.271
	2	-0.198					-0.140	122.435
	1	-0.274						309.672
0.5	6	-0.110	0.037	-0.145	0.009	-0.272	-0.271	64.716
	5	-0.111	0.040	-0.154		-0.246	-0.256	64.737
	4	-0.140		-0.116		-0.220	-0.232	73.178
	3	-0.224				-0.153	-0.226	91.370
	2	-0.190					-0.155	97.619
	1	-0.287						280.435

Table 4.19. The obtained unknown constant parameters from equation (4.22) within present model IV for $J_v > J_{v(critical)}$, where $J_{v(critical)}$ = 0.6, 0.7, 0.8, 0.9 and 1.0 and their residuals R.

$J_{v(critical)}$	N	a	b	c	d	e	f	R
0.6	6	-0.109	0.031	-0.136	0.017	-0.306	-0.293	50.395
	5	-0.111	0.036	-0.153		-0.258	-0.267	50.448
	4	-0.138		-0.116		-0.233	-0.247	57.050
	3	-0.220				-0.163	-0.242	73.633
	2	-0.182					-0.166	79.848
	1	-0.300						253.227
0.7	6	-0.117	0.034	-0.154	-0.004	-0.280	-0.282	40.930
	5	-0.117	0.033	-0.150		-0.290	-0.288	40.932
	4	-0.143		-0.113		-0.265	-0.271	46.208
	3	-0.220				-0.194	-0.267	60.504
	2	-0.175					-0.176	68.315
	1						-0.247	148.162
0.8	6	-0.119	0.035	-0.162	-0.008	-0.295	-0.290	33.450
	5	-0.118	0.033	-0.154		-0.316	-0.302	33.457
	4	-0.142		-0.115		-0.290	-0.289	38.089
	3	-0.220				-0.208	-0.280	51.912
	2	-0.173					-0.180	60.166
	1						-0.259	122.571
0.9	6	-0.116	0.030	-0.155	-0.002	-0.323	-0.310	28.331
	5	-0.116	0.030	-0.153		-0.328	-0.312	28.331
	4	-0.135		-0.117		-0.308	-0.307	31.808
	3	-0.215				-0.217	-0.292	45.319
	2					0.084	-0.221	98.591
	1						-0.272	100.292
1.0	6	-0.114	0.025	-0.148	0.002	-0.345	-0.327	23.820
	5	-0.114	0.026	-0.150		-0.339	-0.324	23.821
	4	-0.114		-0.150		-0.339	-0.324	27.524
	3			-0.182		-0.290	-0.329	36.314
	2					0.021	-0.267	83.650
	1						-0.280	83.732

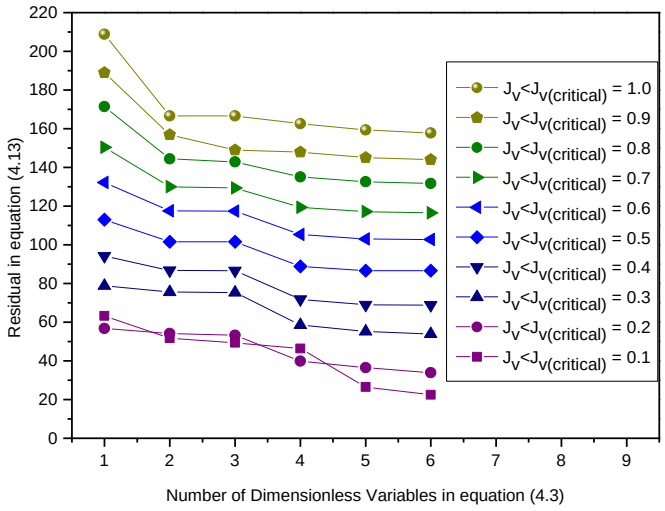

Figure 4.13. Residual R against the number of the dimensionless variables for the experimental values of $J_v < J_{v(critical)}$ for both of steam and non-steam fluids, where Nu* is taken as Honda (1984) model.

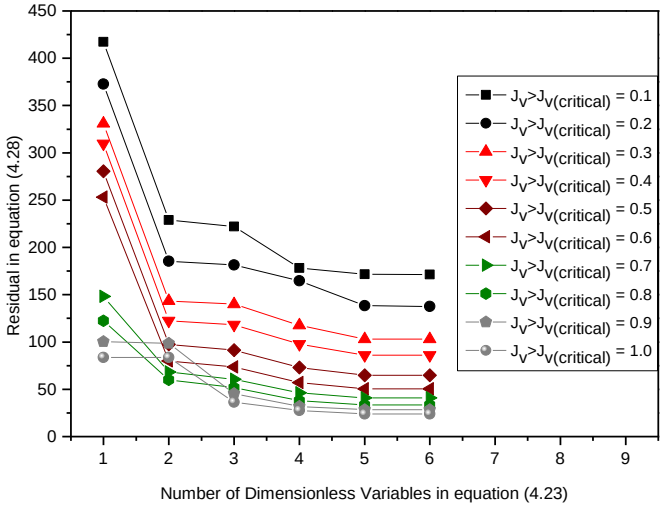

Figure 4.14. Residual R against the number of the dimensionless variables for the experimental values of $J_v > J_{v(critical)}$ for both of steam and non-steam fluids, where Nu* is taken as Honda (1984) model.

Table 4.20. Comparison of the Present Model IV with all experimental data for the selected values of $J_{v(critical)}$.

$J_{v(critical)}$	Required dimensionless numbers in the gravity model	Required dimensionless numbers in the shear model	E_1	E_2
0.1	5	4	-1.442	16.278
0.2	4	5	-1.796	15.451
0.3	4	5	-1.806	14.913
0.4	4	5	-1.720	14.763
0.5	4	4	-2.224	15.273
0.6	4	4	-2.200	15.330
0.7	4	4	-2.132	15.502
0.8	4	4	-2.202	15.905
0.9	3	4	-1.925	16.367
1	2	3	-1.323	17.334

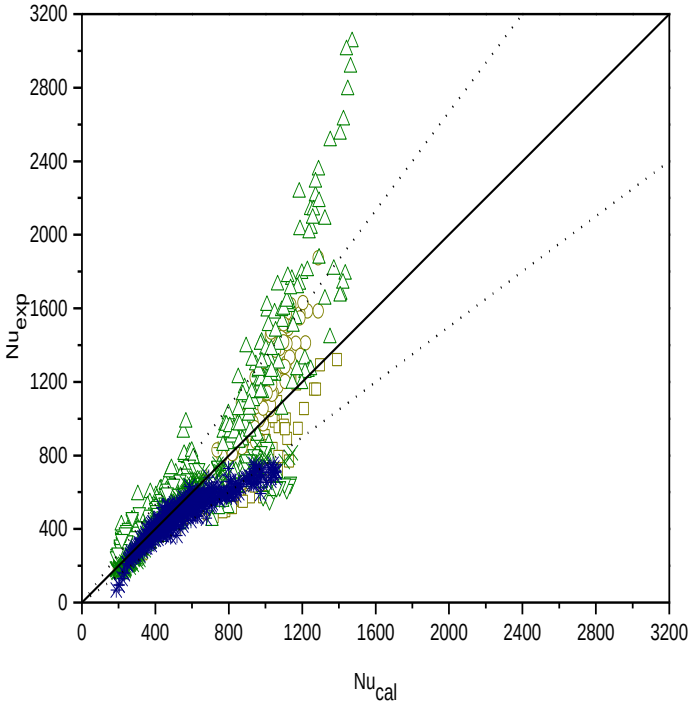

Figure 4.15. Comparison of present model IV to the experimental data of steam, taking Nu* as Honda (1984) model.

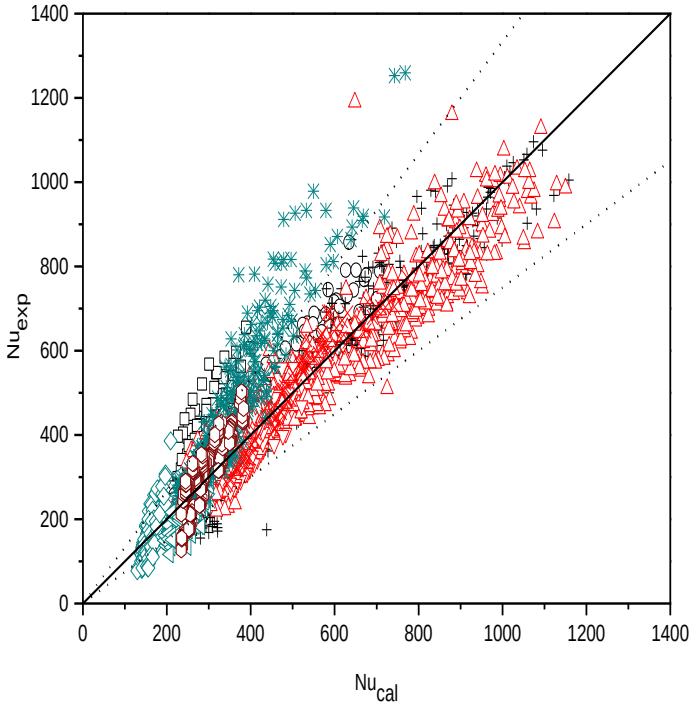

Figure 4.16. Comparison of present model IV to the experimental data of non-steam, taking Nu* as Honda (1984) model.

4.5. Selected present Models and their modification.

Among the four selected present models, and based on table 4.21, present model II is the most successful model, since it offers the minimum mean absolute percentage deviation E_2 for all data.

Table 4.21. Summary of the mean deviation E_1 and the standard mean deviation E_2 for present models.

	Steam Data		Non-Steam Data		All Data	
	E_1	E_2	E_1	E_2	E_1	E_2
Model I	-3.382	15.041	-0.724	13.135	-1.598	13.761
Model II	-3.463	15.018	-0.524	12.955	-1.490	13.633
Model III	-0.724	13.135	-0.848	12.516	-1.725	13.931
Model IV	-4.989	17.545	-0.119	13.401	-1.720	14.763

It can be seen that the present models II predict 60% of the data of Michael (1988) to within 25%. Beech (1995) measured the wall temperatures of the instrumented tubes by the four thermocouples, which were distributed around their circumference. Michael (1988) measured the wall temperatures of the instrumented tubes by the four thermocouples, which were located in rows one, two, four, six, eight and ten mid-way along the tube length, while

the heat-transfer coefficient for the non-instrumented tube rows were obtained by subtracting the coolant and the tube's thermal resistances from the overall thermal resistance. The present models II predict 72% of the data of Kutateladze (1981) to within 25% even though the reasons for this are not comprehensible. Due to the significant scatter of their data (as shown in figures 4.5 and 4.6), the process of obtaining the models for the gravity and shear regions at $J_{v(critical)} = 0.6$ was repeated, excluding the data of Michael (1988) and Kutateladze (1981), where the outputs for the gravity and shear regions are tabulated in tables (4.22) and (4.23).

Table 4.22. The obtained unknown constant parameters from equation (4.2) within the modified present model II for $J_v < J_{v(critical)}$, where $J_{v(critical)} = 0.6$ and their residuals R.

	a	b	c	d	e	f	R
6	-0.159	-0.010	-0.023	-0.084	0.419	0.217	46.405
5	-0.158		-0.050	-0.089	0.449	0.228	47.309
4	-0.159			-0.053	0.359	0.168	47.839
3	-0.115				0.191	0.073	55.840
2	-0.130				0.051		63.067
1	-0.117						70.112

Table 4.23. The obtained unknown constant parameters from equation (4.22) within the modified present model II for $J_v > J_{v(critical)}$, where $J_{v(critical)} = 0.6$ and their residuals R.

	a	B	C	d	e	f	R
6	-0.082	-0.135	0.292	0.169	-0.459	-0.250	29.457
5		-0.137	0.285	0.213	-0.539	-0.296	35.106
4			-0.093	-0.108	0.348	0.173	63.082
3				-0.035	0.174	0.066	68.214
2					0.008	-0.007	71.255
1					0.018		71.291

Figures 4.17 and 4.18 represent the residual R against the number of the dimensionless variables for the gravity and shear regions at $J_{v(critical)} = 0.6$. It is shown from these graphs that the required number of the dimensionless variables for the gravity and shear regions are 4 and 5, which correspond to the following equations:

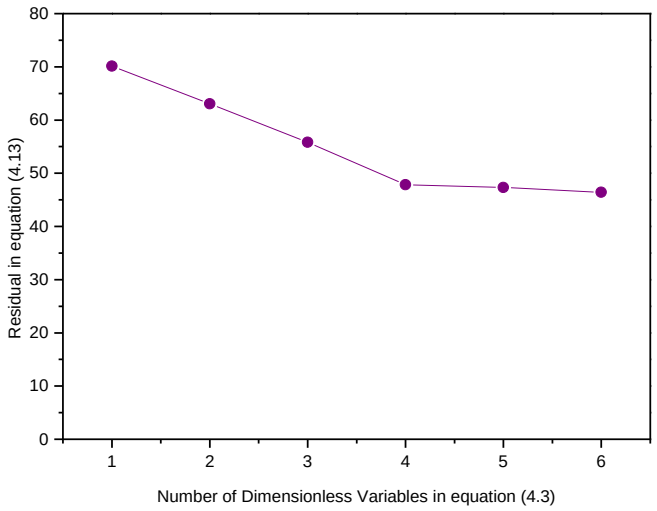

Figure 4.17. Residual R against the number of the dimensionless numbers for the experimental values of $J_v > 0.6$ for both of steam and non-steam fluids (excluding the data of Michael (1988) and Kutateladze (1981)).

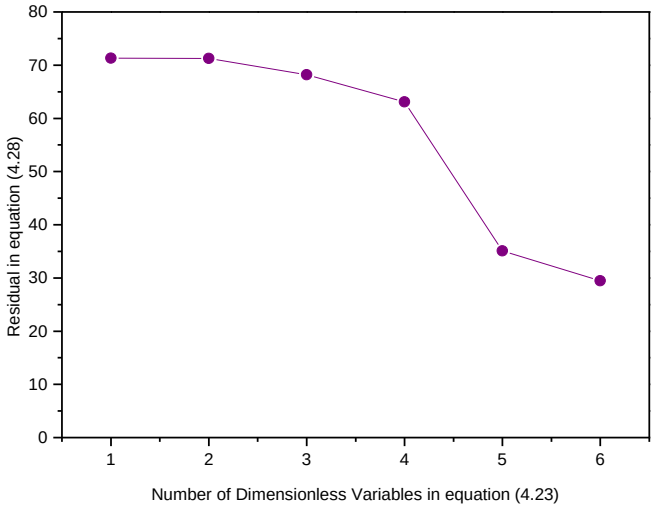

Figure 4.18. Residual R against the number of the dimensionless numbers for the experimental values of $J_v > 0.6$ for both of steam and non-steam fluids (excluding the data of Michael (1988) and Kutateladze (1981)).

For $J_v < 0.6$

$$K_{gr} = B_{gr}^{-0.159} H^{-0.053} G^{0.359} P^{0.168} \qquad (4.47)$$

For $J_v > 0.6$

$$K_{sh} = F^{-0.137} Pr^{0.285} H^{0.213} G^{-0.539} P^{-0.296} \tag{4.48}$$

Therefore, the Nusselt models for the gravity and shear controlled region for $J_{v(critical)} = 0.6$ are given by the following equations:

For $J_v < 0.6$

$$Nu = \left(\frac{0.9\left(1 + G^{-1}\right)^{\frac{1}{3}} + 0.728F^{\frac{1}{2}}}{\left(1 + 3.44F^{\frac{1}{2}} + F\right)^{\frac{1}{4}}} \right) \left(\frac{\Gamma_{N-gr}}{\gamma_{N-gr}} \right)^{-0.159} H^{-0.053} G^{0.359} P^{0.168} \tilde{Re}^{\frac{1}{2}} \tag{4.49}$$

For $J_v > 0.6$

$$Nu = \left(\frac{0.9\left(1 + G^{-1}\right)^{\frac{1}{3}} + 0.728F^{\frac{1}{2}}}{\left(1 + 3.44F^{\frac{1}{2}} + F\right)^{\frac{1}{4}}} \right) F^{-0.137} Pr^{0.285} H^{0.213} G^{-0.539} P^{-0.296} \tilde{Re}^{\frac{1}{2}} \tag{4.50}$$

Equations (4.49) and (4.50) shift most of the data of steam and non-steam fluids in figures 4.5 and 4.6 to the left slightly, as represented in figures 4.19 and 4.20, excluding that of Cavallini (1985), Cavallini (1988) and Shah-1 (1988). The model again under-predicts most of the data for steam and the exception again being those of Beech-1 (1995), Nobbs-2 (1976) and Briggs and Sabaratnam (2003). For the non-steam data, these models over-estimate most of its data, the exception again being those of Cavallini (1985), Gogonin-2 (1976) and Briggs (2000), in addition to Gogonin-1 (1971). Table 4.24 represents the summary of the mean deviation E_1 and the standard mean deviation E_2 for modified model II.

Table 4.24. Summary of the mean deviation E_1 and the standard mean deviation E_2 for modified model II.

	Steam Data		Non-Steam Data		All Data	
	E_1	E_2	E_1	E_2	E_1	E_2
Modified model II	-1.703	11.797	-0.920	11.685	-1.164	11.720

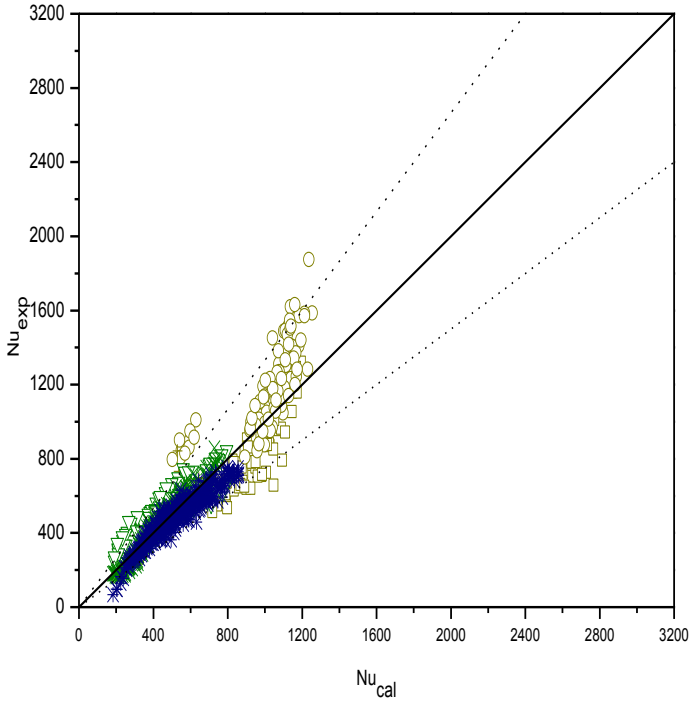

Figure 4.19. Comparison of modified present model II to the experimental data of steam.

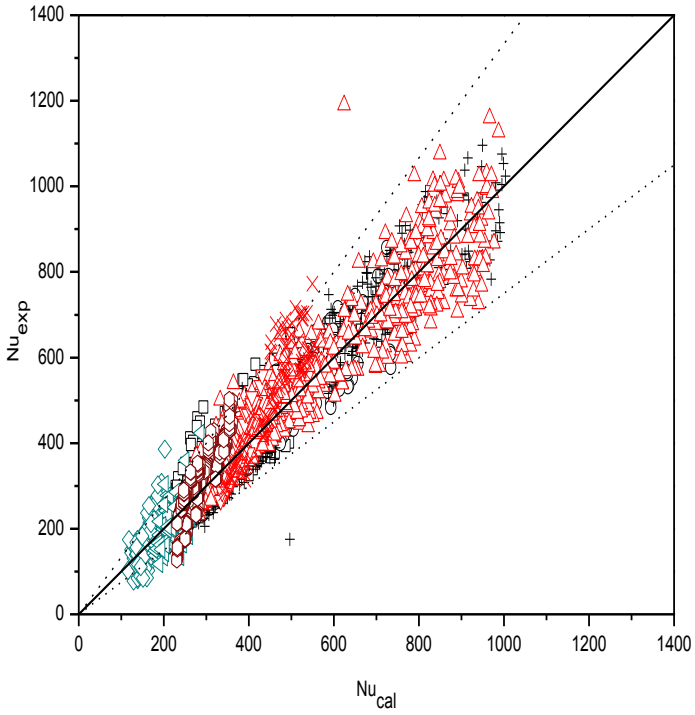

Figure 4.20. Comparison of modified present model II to the experimental data of non-steam.

4.6. Parametric studies.

Figures 4.21 and 4.22 show the variations of vapour-side heat transfer coefficient with row for the experimental data of Beech-1 (1995) and Beech-2 (1995) and the modified present model II (equations 4.49 and 4.50) with and without the artificial inundation tubes.

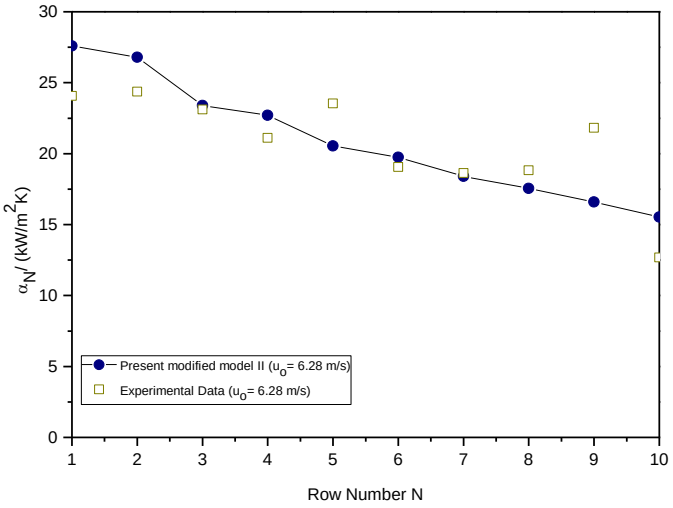

Figure 4.21. Variation of the heat transfer coefficient with the number of vertical tube row for the experimental data of Beech-1 (1995) and the modified present model II in the absence of the artificial inundation tubes.

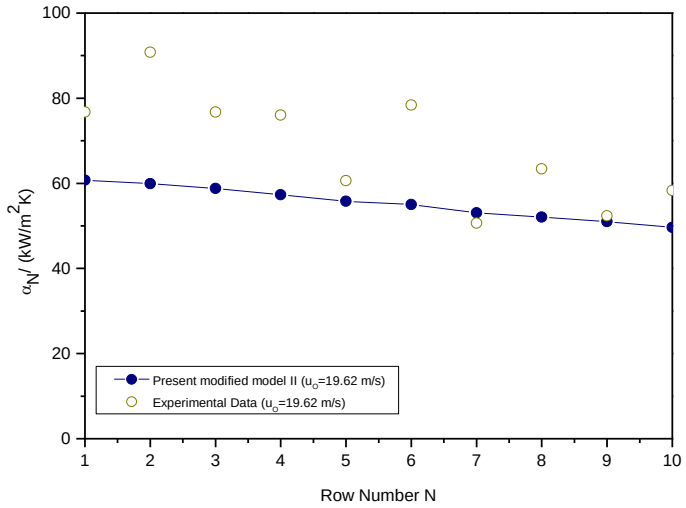

Figure 4.22. Variation of the heat transfer coefficient with the number of vertical tube row for the experimental data of Beech-1 (1995) and the modified present model II in the absence of the artificial inundation tubes.

It can be observed from figure 4.21 (absence of artificial inundation tubes), that the determined heat-transfer coefficient for the four-condensing tube rows decreasing with the row is due to the decreasing in the velocity, leads to the decrease in the vapour shear and the increasing in the condensate inundation. For the three-condensing tube rows, it was noticed there was a rise in the value of the heat-transfer coefficient from row 7 to 9, which suggested that high turbulence has taken place within the condensate film due to the inundation. It is seen from figure 4.21 that there is a good satisfaction between the modified present models II and the experimental data of Beech-1 (1995).

In the presence of the artificial inundation, the heat-transfer coefficients for the three-condensing tubes rows are low compared to that of the four-condensing rows, due to the effect of the inundation of the artificial inundation tubes (demonstrated in figure 4.22) on the three-condensing tubes rows, which leads their condensate film thickness to be greater compared to that of the four condensing tubes rows, where their thermal resistances has increased, which results in the lower rates of the heat transfer relative to that of the four condensing tubes rows. The heat transfer coefficients in this figure are greater compared to that in figure 4.21. This indicates that the effect of the flowing steam velocity overcomes the effect of the inundation on the heat transfer, since the inlet velocity of the flowing steam in this bank (uo=19.62 m/s) is higher comparative to that given in figure 4.21 (uo= 6.28 m/s).

The modified present models II under-predict the experimental data of Beech-2 (1995) for steam as illustrated in figure 4.22, which indicates that these models do not consider the effect of the turbulence within the condensate film, since the film Reynolds number of the experimental data of Beech-2 (1995) given in figure 4.22 are higher compared to that of Beech-1 shown in figure 4.21.

It is observed that there is a good agreement between the experimental data of Cavallini-1(1985) for R-11 and the modified present models with vertical columns at given different inlet velocities, as demonstrated in figure 4.23, while these models under-estimate the experimental data of Cavallini-2 (1988) for R-113 at given different velocities as shown in figure 4.24, which again that these models do not account the effect of the film Reynolds number. It suggests that the turbulence flow has taken place within the condensate film, since its film Reynolds number are higher compared to that in figure 4.23.

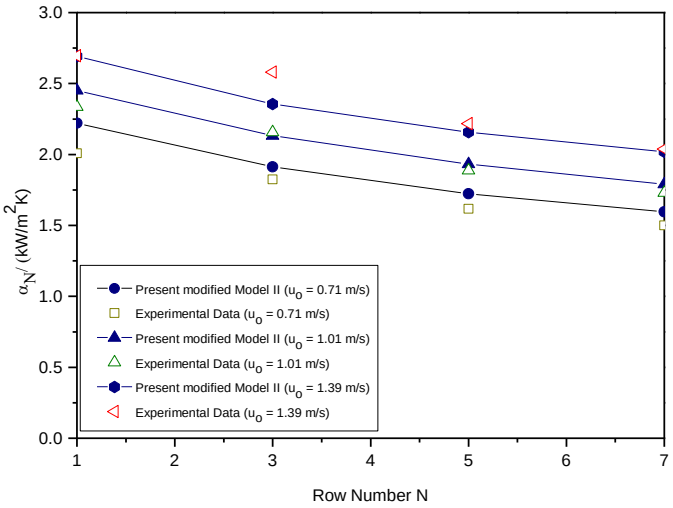

Figure 4.23. Variation of the heat-transfer coefficient with the number of vertical tube row for the experimental data of Cavallini-1 (1985) and the modified present model II for R-11.

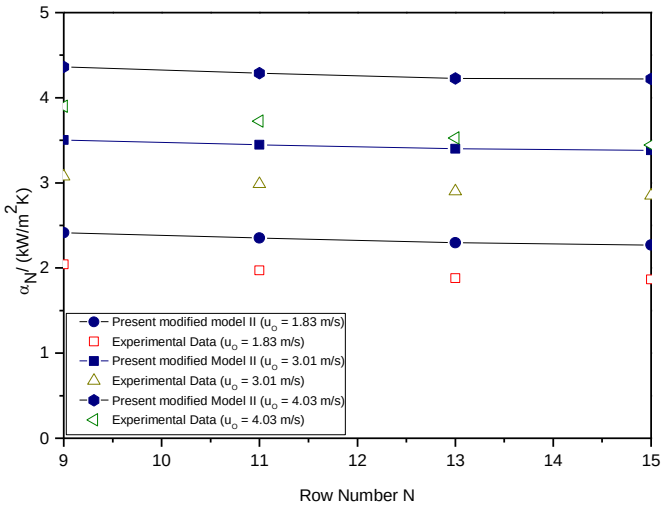

Figure 4.24. Variation of the heat-transfer coefficient with the number of vertical tube row for the experimental data of Cavallini-2 (1988) and the modified present model II for R-113.

Figures 4.25 and 4.26 demonstrate the variations of the vapour-side heat transfer coefficient with row, include the experimental data of Honda-1 (1989) for the in-line tube bundle and Honda-2 (1989) for the staggered tube bundle and the modified present model II (equations 4.49 and 4.50).

In Figures 4.25 and 4.26, the heat-transfer coefficients decrease due to the decrease in the vapour velocity and the increase of the condensate inundation with row. It was suggested by Honda [14] that the upturn in the value of the heat-transfer coefficient for both tube bundles, which are illustrated in figures 4.25 and 4.26, was due to the flow oscillation, which

is due to the contraction at about 120 mm downstream of the last tube rows. It is seen in both of Figures 4.25 and 4.26 that the heat-transfer coefficient for the second row is higher than that of the first row for both of Honda-1 (1989) and Honda-2 (1989), i.e in-line and staggered tube bundles respectively. The heat-transfer coefficient decrease with increasing row number and shows an upturn at the last four rows for the in-line and staggered tube bundles. The modified present model II over-predicts the experimental data of the in-line tube bundle from row 8 to 12, which also over-estimates the experimental data of the staggered tube bundle from row 4 to 14.

The experimental heat-transfer coefficient decreases with increasing row number and shows an upturn at the last four rows for the in-line and staggered tube bundles. Overall, it is seen in figures 4.25 and 4.26 that the agreement between the present combined models and the experimental data of Honda (1989) for both of in-line and staggered banks is good.

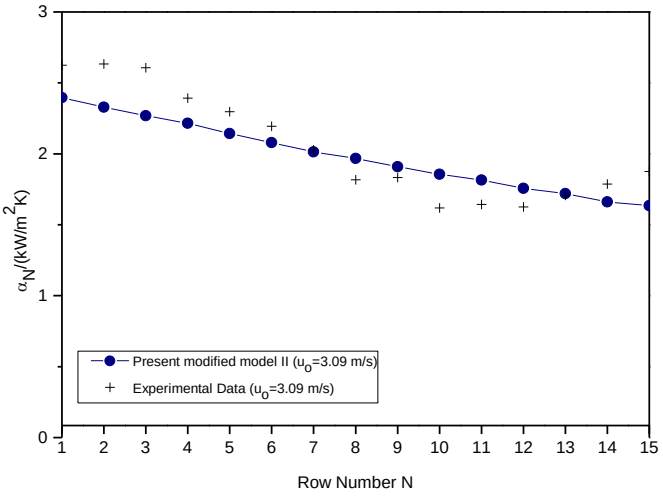

Figure 4.25. Variation of the heat transfer coefficient with the number of vertical tube row for the experimental data of Honda (1989) and the modified present model II for tube in-line bundle.

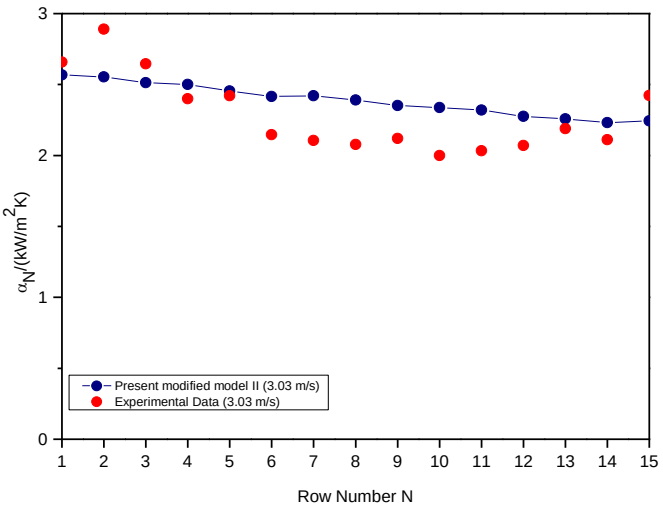

Figure 4.26. Variation of the heat transfer coefficient with the number of vertical tube row for the experimental data of Honda (1989) and the modified present model II for tube staggered bundle.

4.7. Summary.

An empirically based model has been developed for condensation of downward flowing pure vapour on a bank of horizontal plain tubes. Basic assumptions, listed at the start of this section, were made. These were broadly based on the assumptions of Nusselt (1916) for single tubes and low vapour velocity, but adapted for the more complex situation encountered in tube banks. The dimensionless parameter J_v (see equation 4.2) was used to distinguish between conditions where gravity drained flow dominated the condensation process and those where vapour shear dominated. A number of dimensionless groups were then defined to account for the main physical effects occurring during condensation on banks, and these where combined into a general function for the condensate Nusselt number, involving a number of unknown empirical constants. These constants were evaluated using the extensive experimental data base described in detail in sections 1 and 2. An iterative scheme was then used to simplify the resulting equation by eliminating the less important of the dimensionless groups and unknown constants (i.e. those having little or no effect on the accuracy of the final equation).

The most successful model, the above named model II, is given by equations 4.49 and 4.50, for gravity and shear dominated flows respectively. This model represents the majority of the experimental data to within 12.2%, as illustrated in table 4.24 and figures 4.19 and 4.20. In a parametric study, this model predicted the correct dependence of heat-transfer coefficient on row number and vapour velocity.

5. Conclusions and Recommendations for Future Work.

5.1. Summary of the current literature.

A review of the current research on condensation on single tubes and banks of tubes was carried out and the following conclusions drawn.

1. For free-convection condensation on horizontal tubes there is good agreement between the Nusselt (1916) theory and experimental data. Later researches have included many of the effects originally neglected in the Nusselt theory and found their influence to be in most cases negligible.

2. For forced-convection condensation on the single tube**,** the Shekriladze and Gomelauri (1966) model, which considers the shear stress at the liquid-vapour interface using an asymptotic infinite suction approximation, gives a good agreement for low to moderate vapour velocities. At high vapour velocities, boundary layer separation and / or turbulence in the condensate film cause complications and later models have so far failed to correct for these factors.

3. Modelling condensing tube banks as single tube columns using semi-empirical correlations, with inundation mass flow rate as a correlating factor, have proved unrealistic, since all real condensers will involve more complex flow through tube banks rather than simple columns and will also be affected by vapour shear. In addition, validation of these models has been somewhat limited.

4. More complex, and potentially more realistic models, attempt to include the effects of both vapour shear and condensate inundation (and their variation down the bank as vapour is condensed). As with the tube column models above, validation is limited, with many researchers using limited experimental data sets to both formulate and then validate their correlations.

5.2. Compilation of an experimental data base.

In light of the limited attempts to validate existing models described above, an extensive experimental data base has been compiled from the literature and other sources. The accuracy and reliability of the data has been assessed as well as possible and the data has been systematically compiled to allow validation of the existing models for condensation on banks of tubes and develop new, more reliable ones. The data base contains results for 13 different tube bank geometries and 7 different condensing fluids, and covers a wide range of the important parameters, including vapour velocity, heat flux and condensate inundation mass flux.

5.3. Validation of existing models.

Models based on either single tubes (with or without the effects of vapour shear) or tube columns (including condensate inundation but not the effects of vapour shear) proved inadequate in predicting the complex heat transfer behaviour in banks of tubes.

All the tube bank models investigated had some empirical input, and all performed poorly when compared to the present data based described above. The McNaught (1982) model gave good agreement with the data for steam, since it was based on the steam data of Nobbs (1975) but was less reliable when compared to data for, for instance, refrigerants, with very different thermophysical properties to steam. The model of Cavallini (1986) model, which contained an empirical correction to the purely theoretical, single tube model of Shekriladze and Gomelauri (1966) to account for condensate inundation, was the best of those evaluated when compared to the whole data base. This is despite the empirical correction for inundation being based on data for refrigerants only, and probably reflects the original effectiveness of the Shekriladze and Gomelauri (1966) model in accounting for vapour shear effects.

5.4. Development of a new model for condensation on banks of tubes.

A new, empirically based, model has been developed for condensation of downward flowing pure vapour on a bank of horizontal plain tubes. Basic assumptions based on the work of Nusselt (1916) for single tubes and low vapour velocity were adapted for the more

complex situation encountered in tube banks. A dimensionless parameter J_v was used to distinguish between conditions where gravity drained flow dominated the condensation process and those where vapour shear dominated.

The result was the following model, nominally named model II in the previous sections.

For $J_v < 0.6$

$$Nu = \left(\frac{0.9\left(1 + G^{-1}\right)^{\frac{1}{3}} + 0.728F^{\frac{1}{2}}}{\left(1 + 3.44F^{\frac{1}{2}} + F\right)^{\frac{1}{4}}} \right) \left(\frac{\Gamma_{N-gr}}{\gamma_{N-gr}} \right)^{-0.159} H^{-0.053} G^{0.359} P^{0.168} \tilde{Re}^{\frac{1}{2}} \qquad (5.1)$$

For $J_v > 0.6$

$$Nu = \left(\frac{0.9\left(1 + G^{-1}\right)^{\frac{1}{3}} + 0.728F^{\frac{1}{2}}}{\left(1 + 3.44F^{\frac{1}{2}} + F\right)^{\frac{1}{4}}} \right) F^{-0.137} Pr^{0.285} H^{0.213} G^{-0.539} P^{-0.296} \tilde{Re}^{\frac{1}{2}} \qquad (5.2)$$

This model represents the majority of the experimental data to within 12.2%, as illustrated in table 4.24 and figures 4.19 and 4.20. In a parametric study, this model predicted the correct dependence of heat-transfer coefficient on row number and vapour velocity.

5.5. Future work.

The available experimental data for condensation on pure vapours on banks of tubes is extensive and covers most of the range of the important parameters encountered in practical condensers. The above new model gives reasonable overall agreement with this data as well as correctly predicting the trends within the data. Any attempts to increase the accuracy of future empirical correlations would inevitably increase the complexity of the model by including further dimensionless groups and hence more unknown constants to find.

While this may increase overall accuracy it will do nothing to increase design capability and so is not recommended as a fruitful area for future research.

The following areas are therefore suggested for future work.

1. Targeted experimental investigations on specific aspects of the condensation process thought to be inadequately modelled in the present and earlier work. These should include the onset of turbulence in the condensate layer, separation of the vapour boundary layer and subsequent reduction in shear stress on the condensate film and distribution of condensate inundation within the bank and its subsequent impingement on lower tubes. This may necessitate experiments on single tubes and banks at vapour velocities hitherto not investigated.

2. Targeted computational studies of the vapour-liquid interaction during condensation. This can be problematic due to the very thin films (or order of tens of microns) encountered in condensation compared to the length scales encountered in the vapour (of order centimetres). One approach might be to model the vapour velocity through the bank using computational methods and use this to calculate a vapour shear distribution on the condensate film, which can then be used to model the film itself by analytical methods.

The present study has concentrated on the relatively tractable problem of pure vapours condensing on plain tubes. Other areas of condensation on banks still need much investigation.

1. The effects of none-condensing gas in the vapour, of particular concern in low pressure steam condensers, will lower the saturation temperature at the vapour-liquid interface where vapour is removed by condensation, and thus dramatically lower the effective temperature difference across the condensate film. The build-up of these gases at the bottom of the condenser where much of the steam has condensed becomes the major contributor to the vapour-side thermal resistance.

2. The use of low, integral fins in refrigerant condensers is now the industry standard. While much work has been done to model the enhancing effects of these fins on

single tube, including the vital effect of surface tension drained condensate flow, the interaction of these fins with condensate inundation in banks is still the subject of much uncertainty.

3. Condensation of mixtures of fluids where both fluids are condensing can lead to condensate film instabilities, or Marangoni flow, which can significantly enhance the heat transfer even when one of the fluids is present only in very small quantities (1 or 2%) and could be a practical method of enhancing condenser performance. The variation of mixture concentration down a bank of tubes as the two fluids condense at different rates leads to complex variations in behaviour from row to row.

6. References.

Beech, P.M., (1995). Filmwise condensation of high velocity downward flowing steam on a bundle of horizontal tubes, Ph.D. These, University of London , UK.

Belghazi. M., Bontemps. A, Signe. J.C and Marvillet C. (2001)., "Condensation heat transfer of a pure fluid and binary mixture outside a bundle of smooth horizontal tubes. Comparison of experimental results and a classical model", International Journal of Refrigeration, 24, 841-855 (2001).

Berman,L.D. and Tumanov.Y.A.,(1962), Issledovanie Teplootdachi pri Kondesatsii Dvijushtshegosa para na Gorizontalinoi Trube, Teploenergetika, 9, 77-83.

Briggs.A and Sabaratnam.S, (1984), "Condensation of Steam on Integral-fin tubes in a bank", *ASME J. Heat Transfer* ,106 , 524-530.

Briggs, A., Bui, H.H. and Rose,J.W. (1999)., Condensation of refrigerant on banks of smooth and finned tubes, Proceedings of 20th IIR Int. Cong. of Refrigeration, Sydney, Australia, Vol.2, Paper No.518, pp. 2620-2626.

Briggs.A and Sabaratnam.S (2003), 'Condensation of Steam on Integral-fin tubes in a bank", ASME Summer Heat Transfer Conference, Las Vegas, Nevada, USA.

Briggs A.,Theroetical and Experimental studies in shell-side condensation, 6th International Conference on Heat Transfer, Fluid Mechanics and Thermodynamics, Queen Mary, University of London, UK (2008).

Bromley, L.A., (1952), Heat Transfer in Condensation :Effect of Heat Capacity of Condensate, Ind. Eng.Chem., 44, 2966-2969.

Cavallini, A., Frizzerin, S. and Rossetto, L., (1985). R-11 vapor condensation on a horizontal tube bundle, Rept. No. 121, Inst. di Fisica Tecnica, Universita di Padova .

Cavallini, A., Frizzerin, S. and Rossetto (1986), Condensation of R-11 vapor flowing downward outside a horizontal tube bundle, Proceedings of 8th Int. Heat Transfer Conference, San Francisco, USA, 4, pp. 1707-1712.

Cavallini, A., Frizzerin, S. and Rossetto, (1988) L., R-113 vapor condensation on a horizontal tube bundle, Rept. No. 133, Inst. di Fisica Tecnica, Universita di Padova.

Chen. M. M., (1961)., "An Analytical Study of Laminar Film Condensation," part 1, "Flat Plates," and part 2, "Single and Multiple Horizontal Tubes," Trans. ASME, Ser.C, 83, 48-60.

Cipollone, E., Cumo, M., Naviglio, A., and Spezia, U., Condensazione su File di Tubi Orizzontali per " Downflow" del Vapore a Bassa Velocita (Condensation on Lines of Horizontal Tubes for Downflow of Vapour at Low Veliocity), Atti 38^0 Congr. Naz. ATI, Bari, Vol.1, 1983, pp.57-99.

Denny ,V.E. and South ,V., (1972), Effects of Forced Flow, Non-Condensables and Variable Properties on Film Condensation of Pure and Binary Vapours at the Forward Stagnation Point of a Horizontal Cylinder, Int. J. Heat Mass Transf., 15, 2133-2142.

Eissenberg, D.M. (1972), "An Investigation of the Variables Affecting Steam Condensation on the Outside of a Horizontal Tube Bundle," Ph.D Thesis, University of Tennessee, Knoxville, TN.

ESDU (1973), Convective heat transfer during cross-flow of fluids over plain tube banks, Data ITEM No. 73031, Engineering Sciences Data Unit, London.

Faghri, A., and Zhang, Y., 2006, *Transport Phenomena in Multiphase Systems*, Elsevier, Burlington, MA.

Fujii,T., Uehara, H., Hirata, and Kurata, C., (1972a), "Laminar Filmwise Condensation of Flowing Vapour on a Horizontal Cylinder," *Int. J. Heat Mass Transfer*, 15, 235-246.

Fujii, T., Uehara, H. and Oda, K. (1972b), "Filmwise condensation on a surface with unifrom heat flux and body forced convection", Heat Transfer Japanese Research, 1, 76-83.

Fujii, T., Nozu, S. and Honda, H., (1978), Expressions of Thermodynamic and Transport Properties of Refrigerants R-11, R-12, R-22 and R-113, University of Kyushu, Res. Inst. Ind. Sci. Report 67, 43-59.

Fujii, T., Honda, H., and Oda, K. (1979), "Condensation of Steam on a Horizontal Tube,"Condensation Heat Transfer, ASME, New York, 35-43.

Fujii, T. and Oda, K. (1981), “On the inundation in condensation of quiescent vapour”. Proc. 19th Jap. Heat Transfer Symp., p.343.

Fujii, T. (1983), “Condensation in tube banks”. IChemE.Symp.Ser., No.75, pp 3-22.

Fujii, T. and Oda, K. (1986), “Correlation equations of heat transfer for condensate inundation on horizontal tube bundles”. Trans. Jpn. Soc .Mech. Engrs., 52-474, B , pp.822-826 (in Japanese).

Fuks, S.N. (1957), “Heat transfer condensation of steam flowing in a horizontal tube bundle”. Teploenergetika, 4[1], pp.35-39; English translation NEL 1041.

Gogonin, I.I and Dorokhov, A.R. (1971), Heat transfer from condensing Freon-21 vapour moving over a horizontal tube, *Heat Transfer-Soviet Research*, 3, 157-161.

Gogonin, I.I and Dorokhov, A.R. (1976), Experimental investigation of heat transfer with condensation of the moving vapour of Freon-21 on horizontal cylinders, *J. Appl. Mech. Tech. Phys.*, 17, 252-257.

Goto, M., Hotta, H. and Tezuka,S., (1979), Film Condensation of Refrigerant Vapours on a Horizontal Tube, 15th Int. Cong. Refrigeration, B1,1-8.

Grant ,I.D.R and Osment ,P.D.J. (1968), “ The effect of condensate drainage on condenser performance”. NEL Report No.350. National Engineering Laboratory, East Kilbride, Glasgow, 22 pp.

Honda, H., Nozu, S., Bunken, U. and Fujii, T. (1986), “Effect of vapour velocity on film condensation of R-113 on horizontal tubes in a crossflow”.Int J. Heat Mass Transfer, Vol. 29, No.3, pp.429- 438.

Honda, H., Fujii, T., Uchima, B., Nozu, S. and Nakata, S. (1989), Condensation of downward flowing R-113 vapour on bundles of horizontal smooth tubes, Heat Transfer-Japanese Research,18, 31-52.

Jacobs, H.R. and Nadig,R. (1984), “Condensation on a film flowing over single and multiple isothermal horizontal tubes.”, Proc. ASME 38, 115-121.

Jakob ,M. (1949), “Heat Transfer”, Vol.1, J. Wiley and Sons Inc. , New York, USA, pp.667-673.

Kern. D.Q (1958),"Mathematical development of tube loading in horizontal condensers". J.Am. IChemE, Vol.4,No.2, pp.157-160.

Kutateladze and S.S., Gogonin, I.I. (1979), "Heat transfer in film condensation of slowly moving vapour, *Int. J. Heat Mass Transfer*, 22, 1593-1599.

Kutateladze, S.S., Gogonin, I.I., Dorokhov, A.R., and Sosunov, V.I. (1981), Heat transfer in vapour condensation on a horizontal tube bundle, *Heat Transfer-Soviet Research*, 13, 32-50.

Kutateladze, S.S., Gogonin, I.I and Sosunov, V.I. (1985), "The influence of condensate flow rate on heat transfer in film condensation of stationary vapour on horizontal tube banks, *Int. J. Heat Mass Transfer*, 28, 1011-1018.

Lee, W.C., (1982),Filmwise Condensation on a Horizontal Tube in the Presence of Forced Convection and Non-Condensing Gas, Ph.D. Thesis,Univ. of London.

Lee, W.C. and Rose, J. W., (1982), Film Condensation on a Horizontal Tube-Effect of Vapour Velocity, Proc. 7th Int. Heat Transf. Conf., 5, 101-106.

Lee W.C and Rose J.W (1984),"Forced Convection Film Condensation On a horizontal tube with and without non-condensing gases", *Int. J .Heat Mass Transfer*, 27, No. 4, 519-528.

Maekawa,T. and Rose, J.W., (2015), In Preparation.

McNaught, J.M. (1982), Two-phase forced-convection heat transfer during condensation on horizontal tube banks, Proceedings of 7th Int Heat Transfer Conference, Munich, Germany, 5, 125-131 (1982).

Memory.S.B and Rose J.W (1986)., Film Condensation of Ethylene Glycol on a Horizontal Tube at High Vapour Velocity, 8th Int. Heat Transf. Conf., 4,1607-1612.

Memory.S.B., (1989), Forced Convection Film Condensation on a Horizontal Tube at High Vapour Velocity, Ph.D Thesis, Univ of London.

Memory.S.B and Rose J.W (1991).,"Free convection laminar film condensation on a horizontal tube with variable wall temperature", *Int. J. Heat Mass Transfer*, 34, No.11, 2775-2778 .

Michael, A.G. (1988), "Condensation of steam at high velocity on a horizontal tube at high vapour velocity". Ph.d Thesis, Queen Mary Col., Univ of London.

Michael, A.G., Lee, W.C. and Rose, J.W (1992), Forced convection condensation of steam on a small bank of horizontal tubes, Trans ASME J Heat Transfer, Vol. 114, pp. 708-713.

Nicol, A.A. and Wallace, D.J. (1974).,"The influence of vapour shear force on condensation on a cylinder", ICHemE ,Symp. Ser., No.38, pp 1-19.

Nicol, A.A. and Wallace, D.J. (1976)., "Condensation with appreciable vapour velocity and variable wall temperature", Symp, on Steam Turbine Condensers, NEL Report No.619, pp 27-38.

Nobbs, D.W., (1975), "The Effect OF Downward Vapour Velocity and Inundation on Condensation Rates on Horizontal Tubes and Tube Banks," PhD Thesis, University of Bristol, United Kingdom.

Nobbs, D.W. and Mayhew, Y.R., (1976), Effect of Downward Vapour Velocity and Inundation on Condensation Rates on Horizontal Tube Banks, N.E.L. Report No 619,39-53.

Nusselt, W (1916), Die Oberflachenkondensation des Wasserdamfes, Z. Ver.Dt.Ing.60, 569-575.

Prandtl, L. (1935), "The Mechanics of Viscous Fluids," Aerodynamic Theory, W.F.Durand, ed., III, 34-208.

Rohsenow. W.M. (1956), "Heat Transfer and Temperature Distribution in laminar-film condensation," Trans. ASME, 78, 1645-1648.

Rahbar, S. and Rose, J.W., (1984), "New Measurements for Forced-Convection Film Condensation in the presence of a non-condensing gas".1st U.K. Nat .Conf. on Heat Transf.,Vol.1, pp 619-632.

Rose J.W. (1984), "Effect of Pressure Gradient in Forced convection Film condensation on a horizontal tube", *Int. J. Heat Mass Transfer*, 27, 39-47.

Rose, J.W. (1989), "Use of 'Wilson Plots' for condensation on tubes". Queen Mary Col., Univ of London.

Schlichting.H, (1968)., "Boundary Layer Theory", 6th Edition, McGraw-Hill.

Shah, A.K. (1978), Multicomponent condensation on a horizontal tube bank, M.Sc. Thesis, University of Manchester, UK.

Shah, A.K. (1981), Condensation of vapours on a horizontal tube bank, Ph.D.Thesis, University of Manchester, UK.

Shekriladze, I.G. and Gomelauri, V.I., (1966), Theoretical study of laminar film condensation of flowing vapour, *Int. J .Heat Mass Transfer*, 9, 581-591.

Shekriladze, I.G. and Zohrzohliani, G.I., (1973), Analysis of the Process of Film Condensation of Moving Vapour on a Horizontal Cylinder, Inzhenerno-Fizicheskii Zhurnal,25, 14-19.

Short, B.E. and Brown, H.E. (1951), "Condensation of vapours on vertical banks of horizontal tubes" .Proc. IMechE, General Discussion Heat Transfer, pp 27-31.

Sugawara.S, Michiyoshi.I and Minamiyama.T, (1995). "The condensation of Vapour flowing Normal to a horizontal pipe", Proccedings of the 6th Japan National Congress for App. Mech.

Vargaftik, N.B., 1975, Handbook of Physical Properties of Liquids and Gases, Hemisphere, New York, NY.

Wallace, D.J. (1975).,"A study of the influence of vapour velocity upon the condensation on a horizontal tube", PhD Thesis, Univ of Strathclyde , Glasgow.

Young, F.L. and Wholenberg, W.J. , (1942)," Condensation of saturated Freon-12 vapour on bank of horizontal tubes". Trans. ASME, Vol.64, pp 787-794.

Appendix A. Thermophysical properties of test fluids.

A.1. Properties of R-113.

Saturation pressure (Fujii et al. (1978))

$$P_{sat} = 3.413 \times 10^{6} \times 10^{A} \tag{A.1-1}$$

Where

$$A = -A_1 \left\{ 2.8 + 0.1\left(1 + 185 \times A_1^{\,5.8}\right)^{0.2} \right\} \tag{A.1-2}$$

and

$$A_1 = \frac{\left(487.25 - T_v\right)}{T_v} \tag{A.1-3}$$

Saturation temperature (Fujii et al. (1978))

The saturation temperature, T_v, was found from the determined pressure using a Newton-Raphson iteration to find the relevant roots of Equations (A.1-1) to (A.1-3).

Specific volume of saturated liquid (Fujii et al. (1978))

$$v = \left\{ 0.617 + 0.00064\left(T - 273.15\right)^{1.1} \right\} \times 10^{-3} \tag{A.1-4}$$

Specific volume of saturated vapour (Fujii et al. (1978))

$$v_v = \frac{8314 Z T_v}{187.39 P_{sat}} \tag{A.1-5}$$

Where

$$Z = \frac{1}{1 + 0.636\left(\dfrac{P}{3413000}\right)^{0.816}} \tag{A.1-6}$$

Specific isobaric heat capacity of saturated liquid (Fujii et al. (1978))

$$c_p = 929 + 1.03\left(T - 273.15\right) \tag{A.1-7}$$

Specific enthalpy of evaporation (Fujii et al. (1978))

$$h_{fg} = \left\{ 1.611 - 0.0031\left(T - 273.15\right) \right\} \times 10^{5} \tag{A.1-8}$$

Thermal conductivity of saturated liquid (Fujii et al. (1978))

$$k = 0.0802 - 0.000203(T - 273.15) \quad \text{(A.1-9)}$$

Dynamic viscosity of saturated liquid (Fujii et al. (1978))

$$\mu = 1.34 \times 10^{-5`} \times 10^{B} \quad \text{(A.1-10)}$$

Where

$$B = \frac{503}{(T - 2.15)} \quad \text{(A.1-11)}$$

Dynamic viscosity of saturated vapour (Fujii et al. (1978))

$$\mu_v = 0.00001(0.92 + 0.0003(T_v - 273)) \quad \text{(A.1-12)}$$

A.2. Properties of Water.

Saturation pressure (Beech (1995))

$$P_{sat} = 10^6 \times \exp^{A} \tag{A.2-1}$$

Where

$$A = A_1 + \frac{A_2}{T_f} + A_3 \ln(T_f) + A_4 T_f + A_5 T_f^{\,2} + A_6 T_f^{\,3} + A_7 T_f^{\,4} + A_8 T_f^{\,5} + A_9 T_f^{\,6} + A_{10} T_f^{\,7} + A_{11} T_f^{\,8} \tag{A.2-2}$$

$$T_f = \frac{T_v}{1000} \tag{A.2-3}$$

and

$$\begin{aligned} A_1 &= 15.49217901 \\ A_2 &= -5.6783717693 \\ A_3 &= 1.4597584637 \\ A_4 &= 13.877000608 \\ A_5 &= -80.887673591 \\ A_6 &= 123.56883468 \\ A_7 &= -188.31212064 \\ A_8 &= 660.91763485 \\ A_9 &= -1382.4740091 \\ A_{10} &= 1300.1040184 \\ A_{11} &= -449.39571976 \end{aligned}$$

Saturation temperature (Beech (1995))

The saturation temperature, T_v, was found from the determined pressure using a Newton-Raphson iteration to find the relevant root of Equations (A.2-1) to (A.2-3).

Specific volume of saturated liquid (Beech (1995))

$$v = 0.0012674 - T\left(2.02915 \times 10^{-6} - 3.8333 \times 10^{-9} T\right) \tag{A.2-4}$$

Specific volume of saturated vapour (Beech (1995))

$$v_v = \frac{\left\{1 + \left(1 + 2T_c T_d\right)^{\frac{1}{2}}\right\}}{T_d} \tag{A.2-5}$$

Where

$$T_a = \frac{1500}{T_v} \tag{A.2-6}$$

$$T_b = 2.5\ln\left(1-\exp\left(-T_a\right)\right) \tag{A.2-7}$$

$$T_c = \frac{0.0015}{1+0.0001T} - 0.000942\left(\frac{1}{T_a}\right)^{\frac{1}{2}}\exp\left(T_a + T_b\right) - 0.0004882T_a \tag{A.2-8}$$

$$T_d = \frac{P_{sat}}{230.755T_v} \tag{A.2-9}$$

Specific isobaric heat capacity of saturated liquid (Beech (1995))

$$c_p = 10768.539 - T\left\{57.216 - T\left(0.16359 - 1.536\times10^{-4}T\right)\right\} \tag{A.2-10}$$

Specific enthalpy of evaporation (Beech (1995))

$$h_{fg} = 3468920 - T\left(5707.4 - T\left(11.5562 - 0.0133103T\right)\right) \tag{A.2-11}$$

Thermal conductivity of saturated liquid (Beech (1995))

$$k = -0.92407 + T_g\left[2.8395 - T_g\left\{1.8007 - T_g\left(0.52577 - T_g\,0.07344\right)\right\}\right] \tag{A.2-12}$$

Where

$$T_g = \frac{T}{273.15} \tag{A.2-13}$$

Dynamic viscosity of saturated liquid (Beech (1995))

$$\mu = 0.00002414\times10^{A} \tag{A.2-14}$$

Where

$$A = \frac{247.8}{T-140.0} \tag{A.2-15}$$

Dynamic viscosity of saturated vapour (Beech (1995))

$$\mu_v = -\left(4.478415\times10^{-6}\right) + \left(T_v\left(5.0216\times10^{-8} - \left(T_v\left(1.579\times10^{-11}\right)\right)\right)\right) \tag{A.2-16}$$

A.3. Properties of R-11.

Saturation pressure (Fujii et al. (1978))

$$P_{sat} = \left(4.409 \times 10^{6}\right) \times 10^{-LM} \tag{A.3-1}$$

Where

$$L = 2.7 + 0.1\left(\frac{0.065}{M^{1.7}} + 8M^{5}\right)^{0.25} \tag{A.3-2}$$

$$M = \frac{1}{S} - 1 \tag{A.3-3}$$

$$S = \frac{T_v}{471.15} \tag{A.3-4}$$

Saturation temperature (Fujii et al. (1978))

The saturation temperature, T_v, was found from the determined pressure using a Newton-Raphson iteration to find the relevant root of Equations ((A.3-1)-(A.3-4)).

Specific volume of saturated liquid (Fujii et al. (1978))

$$v = 0.001\left(0.652 + 0.000752 {T_C}^{1.1}\right) \tag{A.3-5}$$

Where

$$T_C = T - 273.15 \tag{A.3-6}$$

Specific volume of saturated vapour (Fujii et al. (1978))

$$v_v = \frac{RT_v}{P_{sat}} \tag{A.3-7}$$

Where

$$R = 60.52 \tag{A.3-8}$$

Specific isobaric heat capacity of saturated liquid (Fujii et al. (1978))

$$c_p = 908.2 \tag{A.3-9}$$

Specific enthalpy of evaporation (Fujii et al. (1978))

$$h_{fg} = 100000\left(1.898 - \left(0.003943 T_C\right)\right) \tag{A.3-10}$$

Thermal conductivity of saturated liquid (Fujii et al. (1978))

$$k = 0.0943 - 0.000275T_C \tag{A.3-11}$$

Dynamic viscosity of saturated liquid (Fujii et al. (1978))

$$\mu = 2.29 \times 10^{-5} \times 10^{\left(\frac{385}{T+7.85}\right)} \tag{A.3-12}$$

Dynamic viscosity of saturated vapour (Fujii et al. (1978))

$$\mu_v = 1.1015 \times 10^{-5} \tag{A.3-13}$$

A.4. Properties of R-21.

Saturation pressure (Fujii et al. (1978))

$$P_{sat} = 68014.2 + T_C\left(3210.85 + T_C\left(40.7682 + 0.528584T_C\right)\right) \quad \text{(A.4-1)}$$

Where

$$T_C = T_v - 273.15 \quad \text{(A.4-2)}$$

Saturation temperature (Fujii et al. (1978))

The saturation temperature, T_v , was obtained from equation (A.4-2), where T_C was found the determined pressure using a Newton-Raphson iteration to find the relevant root of Equation (A.4-1).

Specific volume of saturated liquid (Fujii et al. (1978))

$$v = 0.663995\times10^{-3} + T_X\left(3.15831\times10^{-6} - T_X\left(4.72568\times10^{-8} - T_X\left(3.60577\times10^{-10}\right)\right)\right) \quad \text{(A.4-3)}$$

Where

$$T_X = T - 273.15 \quad \text{(A.4-4)}$$

Specific volume of saturated vapour (Fujii et al. (1978))

$$v_v = 0.260207 - T_C\left(7.40351\times10^{-3} - T_C\left(8.76279\times10^{-5} - T_C\left(3.97237\times10^{-7}\right)\right)\right) \quad \text{(A.4-5)}$$

Specific isobaric heat capacity of saturated liquid (Fujii et al. (1978))

$$c_p = 4186.8\left(0.19531 + 1.8896\times10^{-4}T\right) \quad \text{(A.4-6)}$$

Specific enthalpy of evaporation (Fujii et al. (1978))

$$h_{fg} = 243843 - T_C\left(519.532 + T_C\left(1.77353 - T_C\left(5.76085\times10^{-4}\right)\right)\right) \quad \text{(A.4-7)}$$

Thermal conductivity of saturated liquid (Fujii et al. (1978))

$$k = 0.00041868\left(502.47 - 0.815192T\right) \quad \text{(A.4-8)}$$

Dynamic viscosity of saturated liquid (Fujii et al. (1978))

$$\mu = 5.79764\times10^{-3} - T\left(4.40329\times10^{-5} - T\left(1.19167\times10^{-7} - T\left(1.11111\times10^{-10}\right)\right)\right) \quad \text{(A.4-9)}$$

Dynamic viscosity of saturated vapour (Fujii et al. (1978))

$$\mu_v = \frac{\left(-0.0208443 + T_v\left(\left(2.52333\times10^{-4}\right) - T_v\left(\left(7.29762\times10^{-7}\right) - T_v\left(8.33333\times10^{-10}\right)\right)\right)\right)}{1000} \quad \text{(A.4-10)}$$

A.5. Properties of Iso-propanol.

Saturation pressure (Shah (1978))

$$P_{sat} = 133.416L \tag{A.5-1}$$

Where

$$L = 10^{7.7563 - \frac{1366.14}{T_V - 75.18}} \tag{A.5-2}$$

Saturation temperature (Shah (1978))

$$T_v = 75.18 + \frac{1366.14}{7.7563 - \log\left(\frac{P_{sat}}{133.416}\right)} \tag{A.5-3}$$

Specific volume of saturated liquid (Shah (1978))

$$v = \left(\frac{508.15 - T}{508.15 - 293.15}\right)^{-\frac{0.25}{789.0}} \tag{A.5-4}$$

Specific volume of saturated vapour (Shah (1978))

$$v_v = \frac{1}{\left(\frac{60.09K}{8314.3T_v}\right)} \tag{A.5-5}$$

Where

$$K = 133.416A \tag{A.5-6}$$

$$A = 10^{7.7563 - \frac{1366.14}{T_v - 75.18}} \tag{A.5-7}$$

Specific isobaric heat capacity of saturated liquid (Shah (1978))

$$c_p = 16.642M \tag{A.5-8}$$

Where

$$M = -81.12 + 0.7954\,T \tag{A.5-9}$$

Specific enthalpy of evaporation (Shah (1978))

$$h_{fg} = \frac{N}{60.09} \tag{A.5-10}$$

Where

$$N = 40060695.8 + 84.443T - \left(219.719\times10^{-3}\right)T^2 - \left(70.003\times10^{-6}\right)T^3 + \left(12.1\times10^{-9}\right)T^4 \quad \text{(A.5-11)}$$

Thermal conductivity of saturated liquid (Shah (1978))

$$k = 0.157\left(1-\left(5.75\times10^{-3}\left(T-303.15\right)\right)\right) \quad \text{(A.5-12)}$$

Dynamic viscosity of saturated liquid (Shah (1978))

$$\mu = \left(0.329\times10^{-6}\right)\times10^{\frac{1131.8}{T}} \quad \text{(A.5-13)}$$

Dynamic viscosity of saturated vapour (Shah (1978))

$$\mu_v = \frac{1.09\times10^{-5}\times B}{0.8385} \quad \text{(A.5-14)}$$

Where

$$B = \left(1.058A^{0.645}\right) - \left(\frac{0.261}{\left(1.9A\right)^{0.9\left(\log_{10}\left(1.9A\right)\right)}}\right) \quad \text{(A.5-15)}$$

$$A = \frac{T_v}{273.15} \quad \text{(A.5-16}$$

A.6. Properties of Methanol.

Saturation pressure (Shah (1978))

$$P_{sat} = 109200 \tag{A.6-1}$$

Specific volume of saturated liquid (Shah (1981))

$$v = 0.0012674 - T\left(2.02915\times10^{-6} - T\left(\left(3.8333\times10^{-9}\right)\right)\right) \tag{A.6-2}$$

Specific volume of saturated vapour (Shah (1981))

$$v_v = 0.76 \tag{A.6-3}$$

Specific isobaric heat capacity of saturated liquid (Shah (1981))

$$c_p = \left(0.0316\left(\left(T - 273.15\right)^2\right)\right) + \left(4.5468\left(T - 273.15\right)\right) + 2411.7 \tag{A.6-4}$$

Specific enthalpy of evaporation (Shah (1981))

$$h_{fg} = 110500 \tag{A.6-5}$$

Thermal conductivity of saturated liquid (Shah (1981))

$$k = 0.0004187\left(687.314 - \left(0.680519T\right)\right) \tag{A.6-6}$$

Dynamic viscosity of saturated liquid (Shah (1981))

$$\mu = 10^{L} \tag{A.6-7}$$

Where

$$L = -8.857 + \left(\frac{3835}{T}\right) - \left(\frac{959300}{T^2}\right) + \left(\frac{93440000}{T^3}\right) \tag{A.6-8}$$

Dynamic viscosity of saturated vapour ((Faghri(2006)) and (Vargaftik (1975)))

$$\mu_v = 0.00001\left(0.8814 + 0.0033\left(T_v - 273\right)\right) \tag{A.6-9}$$

Appendix B. Experimental Data for steam condensing on a bank of Plain Tubes.

B.1. Nobbs (1975).

Outer Diameter / m	0.01905
Inner Diameter / m	0.0158
Length / m	0.5
Width / m	0.095
Horizontal Pitch / m	0.0238
Vertical Pitch / m	0.0206
Number of odd tubes	1
Number of even tubes	0

Row No.	T_V /K	U_V/ (ms^{-1})	q/ (kW/m^2)	T_W /K	M_C / kgs^{-1}
1	375.69	9.20	514.40	358.50	0.00
1	374.77	8.62	501.40	357.55	0.00
1	374.39	8.24	495.90	356.78	0.00
1	374.07	7.90	495.90	356.66	0.00
1	373.91	7.60	489.30	356.10	0.00
1	373.64	7.07	482.90	355.83	0.00
1	373.64	7.17	482.90	356.06	0.00
1	373.37	6.73	477.30	355.05	0.00
1	373.31	6.74	477.30	355.11	0.00
1	374.47	0.37	411.10	349.28	0.00
1	373.75	4.92	455.70	353.09	0.00
1	373.93	4.79	456.70	353.10	0.00
1	373.83	4.70	456.70	353.23	0.00
1	373.45	4.23	449.20	352.59	0.00
1	373.75	3.76	449.20	352.47	0.00
1	373.64	2.82	437.20	351.53	0.00
1	374.20	3.36	449.30	352.89	0.00
1	373.66	1.54	424.00	349.96	0.00
1	375.99	8.84	195.80	367.70	0.00
1	375.99	8.70	189.50	367.85	0.00
1	375.23	8.49	183.00	366.99	0.00
1	374.85	8.16	186.20	366.87	0.00
1	374.53	7.71	183.00	366.48	0.00
1	374.31	7.44	182.90	366.23	0.00
1	374.15	7.08	177.20	365.30	0.00
1	373.96	6.80	176.50	365.79	0.00
1	373.77	6.55	173.30	365.40	0.00
1	374.47	2.04	173.30	365.23	0.00
1	375.66	0.42	166.80	364.45	0.00
1	374.93	0.71	170.00	364.76	0.00
1	374.72	1.10	170.80	364.60	0.00
1	374.91	1.75	170.10	365.19	0.00

Row No.	T_V /K	U_V/ (ms^{-1})	q/ (kW/m^2)	T_W /K	M_C / kgs^{-1}
1	373.45	2.09	166.80	364.20	0.00
1	374.53	3.07	173.30	365.57	0.00
1	374.39	2.73	443.70	352.34	0.00
1	374.39	0.44	365.30	344.71	0.00
1	374.47	0.76	384.90	346.49	0.00
1	374.47	1.16	411.10	349.08	0.00
1	374.29	1.82	437.10	351.35	0.00
1	374.26	2.65	455.80	353.21	0.00
1	374.15	2.22	456.70	353.23	0.00
1	373.64	3.97	481.80	355.41	0.00
1	374.47	4.87	173.30	365.49	0.00
1	374.31	4.99	173.30	365.58	0.00
1	373.88	4.65	173.30	365.32	0.00
1	374.02	4.37	170.10	364.93	0.00
1	373.93	3.85	169.30	364.83	0.00
1	374.15	3.17	170.00	364.76	0.00
1	374.31	2.37	170.80	365.03	0.00
1	374.37	0.55	163.60	364.07	0.00
1	373.80	0.59	372.70	345.43	0.00
1	374.02	0.85	397.90	347.56	0.00
1	373.99	1.23	417.60	349.71	0.00
1	374.69	1.69	437.20	351.47	0.00
1	373.69	1.86	354.60	343.53	0.18
1	373.75	1.84	345.80	343.07	0.18
1	373.77	1.86	338.50	342.28	0.14
1	373.75	1.86	337.80	342.33	0.13
1	373.58	1.91	332.00	341.84	0.09
1	373.69	1.87	352.30	343.36	0.05
1	374.61	5.07	442.80	352.27	0.18
1	374.04	5.12	434.30	351.31	0.13
1	373.93	5.22	445.60	352.06	0.08
1	373.88	5.23	451.20	352.61	0.05

1	373.77	4.21	431.60	351.04	0.05
1	373.77	4.22	432.40	350.62	0.05
1	373.77	4.21	417.60	349.71	0.09
1	373.75	4.24	411.10	349.08	0.13
1	373.66	4.27	410.20	349.01	0.18
1	373.93	2.54	359.60	344.22	0.18
1	374.07	2.69	358.10	344.27	0.13
1	373.99	2.60	358.80	344.07	0.09
1	373.93	2.58	378.40	345.92	0.05
1	376.85	7.59	489.30	356.10	0.18
1	376.85	7.71	495.90	356.78	0.13
1	376.80	7.86	501.30	357.38	0.09
1	376.69	8.13	500.30	357.42	0.05
1	375.34	7.57	493.50	356.21	0.05
1	375.12	7.06	476.30	355.15	0.08
1	375.18	6.90	477.30	354.93	0.13
1	375.23	6.64	470.80	354.54	0.18
1	374.72	0.31	319.00	340.56	0.05
1	374.47	0.39	279.90	336.82	0.09
1	374.53	0.45	274.00	336.55	0.13
1	374.58	0.62	309.20	339.31	0.18
1	373.96	0.72	319.00	340.63	0.18
1	373.93	0.72	286.40	337.39	0.13
1	373.93	0.72	279.90	336.89	0.09
1	373.88	0.72	319.00	340.56	0.05
1	373.56	1.16	338.50	342.42	0.05
1	373.53	1.17	300.70	338.71	0.08
1	373.53	1.18	299.50	338.99	0.13
1	373.50	1.17	332.10	341.99	0.18
1	373.96	2.89	365.40	344.85	0.18
1	373.96	3.04	365.40	345.05	0.13
1	373.99	3.13	377.60	346.17	0.09
1	377.07	7.82	191.00	367.69	0.18
1	377.07	7.82	195.90	367.86	0.14
1	376.80	7.69	193.50	367.75	0.08
1	376.85	8.10	191.90	367.65	0.05
1	375.42	7.48	183.00	366.57	0.05
1	375.55	7.09	183.00	366.40	0.09
1	375.55	6.85	181.30	365.96	0.13
1	375.64	6.65	180.50	366.11	0.18
1	374.64	1.62	144.20	361.38	0.18
1	374.80	1.65	137.10	360.59	0.13
1	374.77	1.71	138.30	360.44	0.08
1	374.66	1.76	146.10	361.25	0.05

1	374.69	0.89	134.50	360.30	0.05
1	374.80	0.91	125.90	358.89	0.09
1	374.77	0.88	129.70	359.29	0.13
1	374.56	0.84	140.90	360.64	0.18
1	374.45	5.04	166.80	364.37	0.18
1	374.45	5.16	166.10	364.70	0.13
1	374.20	4.97	166.80	364.28	0.08
1	373.96	4.90	171.50	364.53	0.05
1	374.53	3.87	161.00	363.52	0.08
1	374.42	3.67	157.10	362.77	0.13
1	374.34	3.92	157.80	363.04	0.18
1	374.77	2.54	148.70	361.89	0.18
1	374.77	2.64	144.80	361.66	0.13
1	374.72	2.69	148.10	361.87	0.09
1	374.66	2.82	153.90	363.07	0.05
1	374.45	2.41	150.70	362.25	0.05
1	374.66	2.04	140.90	360.73	0.09
1	374.66	2.05	137.70	360.51	0.13
1	374.66	2.00	147.40	361.77	0.18
1	374.83	5.93	434.30	350.94	0.44
1	374.64	5.81	429.70	350.83	0.43
1	374.31	5.69	411.00	348.89	0.28
1	373.72	4.86	391.50	347.32	0.28
1	373.69	4.23	391.40	347.12	0.43
1	373.39	4.12	384.10	346.41	0.27
1	373.75	3.78	384.90	346.55	0.28
1	374.12	3.75	377.60	346.24	0.43
1	373.85	3.12	371.10	345.27	0.43
1	373.64	3.10	409.70	348.72	0.27
1	374.37	2.06	411.10	349.08	0.29
1	374.39	2.04	359.60	344.15	0.42
1	373.80	1.55	338.60	342.56	0.42
1	373.72	1.55	384.90	346.62	0.27
1	373.69	1.04	365.30	344.71	0.28
1	373.77	1.04	332.70	341.78	0.41
1	374.02	0.52	313.20	340.00	0.41
1	374.15	0.54	339.30	342.43	0.28
1	376.90	7.15	469.80	354.35	0.43
1	376.58	7.09	462.20	353.71	0.28
1	375.18	6.21	439.00	351.43	0.27
1	375.28	6.02	437.20	351.60	0.42
1	375.26	5.88	166.90	365.23	0.43
1	375.37	6.06	166.90	364.97	0.43
1	375.39	6.26	170.00	364.67	0.28

1	376.82	7.10	183.00	366.39	0.28
1	376.99	6.94	183.80	366.83	0.42
1	375.31	3.02	153.20	362.88	0.43
1	375.31	3.17	162.90	364.14	0.28
1	375.07	5.58	163.70	364.58	0.27
1	375.18	5.53	173.30	365.06	0.42
1	376.23	3.16	387.40	347.52	0.43
1	376.31	3.30	404.50	348.45	0.28
1	374.93	2.83	424.10	350.34	0.28
1	374.93	2.79	372.70	345.36	0.43
1	374.80	1.97	358.80	344.28	0.43
1	374.69	1.98	411.00	348.89	0.28
1	374.74	1.34	385.80	346.90	0.28
1	374.50	1.30	351.60	343.83	0.43

1	374.29	0.47	306.00	339.19	0.41
1	374.26	0.47	344.30	343.05	0.28
1	375.07	2.20	169.30	364.91	0.28
1	375.01	2.19	153.90	362.29	0.43
1	374.83	1.23	141.60	361.18	0.43
1	374.69	1.22	157.10	363.20	0.28
1	374.61	0.41	153.80	362.20	0.29
1	374.64	0.51	137.70	360.51	0.42
1	375.01	4.69	163.60	363.98	0.43
1	374.91	4.90	163.60	363.72	0.28
1	377.01	7.30	182.10	366.61	0.42
1	377.01	7.40	189.40	366.83	0.28
1	376.99	7.45	470.80	354.42	0.28
1	376.99	7.38	473.80	354.52	0.42

B.2. Nobbs (1975).

Outer Diameter / m	0.01905
Inner Diameter / m	0.0158
Length / m	0.5
Width / m	0.095
Horizontal Pitch / m	0.0238
Vertical Pitch / m	0.0238
Number of odd tubes	1
Number of even tubes	0

Row No.	T_V /K	U_V/ (ms^{-1})	q/ (kW/m^2)	T_W /K	M_C / kgs^{-1}
1	372.99	4.14	424.10	354.39	0.00
1	372.99	4.14	430.60	355.03	0.00
1	373.96	5.05	437.10	355.66	0.00
1	373.85	5.14	443.60	356.23	0.00
1	373.21	4.73	430.60	355.03	0.00
1	373.50	3.67	417.60	353.89	0.00
1	373.53	3.38	411.00	352.94	0.00
1	373.56	3.04	411.00	352.81	0.00
1	373.31	2.38	398.00	351.60	0.00
1	373.21	2.06	390.60	350.88	0.00
1	373.12	1.45	377.50	349.41	0.00
1	373.61	1.22	371.80	348.66	0.00
1	373.56	0.79	352.30	346.81	0.00
1	373.88	3.90	296.50	358.93	0.00
1	374.20	4.27	300.10	358.86	0.00
1	373.15	4.25	296.50	358.79	0.00
1	373.48	4.79	296.50	358.86	0.00
1	373.15	4.45	296.50	358.86	0.00
1	374.18	2.66	285.70	357.83	0.00
1	373.77	1.10	264.70	354.71	0.00
1	373.42	0.82	255.60	353.80	0.00
1	372.91	3.77	286.60	357.85	0.00
1	373.23	3.55	286.60	358.00	0.00
1	373.23	3.12	287.50	357.95	0.00
1	373.26	2.64	282.90	356.98	0.00
1	373.04	2.37	273.80	356.22	0.00
1	373.04	2.05	273.80	356.22	0.00
1	373.37	1.61	264.70	355.01	0.00
1	373.34	1.30	264.70	354.93	0.00
1	373.45	1.02	260.20	354.33	0.00
1	373.34	0.53	245.80	352.63	0.00
1	373.07	0.58	332.70	344.90	0.00
1	373.48	0.68	345.70	346.11	0.00
1	373.37	0.96	358.80	347.52	0.00
1	373.04	3.29	160.30	364.33	0.00
1	373.26	3.21	160.30	364.68	0.00

Row No.	T_V /K	U_V/ (ms^{-1})	q/ (kW/m^2)	T_W /K	M_C / kgs^{-1}
1	373.26	2.91	163.60	365.53	0.00
1	373.18	2.45	160.30	364.76	0.00
1	373.26	2.22	157.10	364.51	0.00
1	373.21	1.60	157.10	364.34	0.00
1	373.21	1.34	153.80	363.74	0.00
1	373.42	1.04	150.00	363.47	0.00
1	373.58	0.70	146.80	362.87	0.00
1	374.56	7.41	469.80	359.11	0.00
1	374.61	7.39	323.90	362.73	0.00
1	374.42	7.42	328.30	362.70	0.00
1	373.85	7.05	319.20	361.51	0.00
1	373.50	6.61	314.70	360.98	0.00
1	373.31	6.22	314.70	360.91	0.00
1	373.31	6.18	166.80	366.04	0.00
1	373.61	6.66	173.20	366.54	0.00
1	374.23	7.26	179.70	367.64	0.00
1	374.77	7.77	179.80	368.57	0.00
1	374.93	7.75	186.10	368.31	0.00
1	373.04	3.53	159.60	364.65	0.00
1	373.21	3.92	164.20	364.86	0.00
1	373.69	5.12	164.30	365.64	0.00
1	373.72	5.19	166.80	365.69	0.00
1	374.07	4.67	423.30	354.75	0.00
1	374.07	4.71	428.80	355.11	0.00
1	374.61	5.54	436.20	355.95	0.00
1	375.15	6.55	450.20	357.29	0.00
1	375.23	7.05	456.80	358.22	0.00
1	375.53	7.65	463.30	358.66	0.00
1	374.80	7.36	456.80	358.10	0.00
1	374.23	6.41	449.30	357.39	0.00
1	373.75	2.33	306.00	342.25	0.17
1	373.26	2.60	306.60	342.05	0.15
1	373.10	2.60	324.80	344.37	0.11
1	373.10	2.81	340.00	345.84	0.08
1	373.50	2.79	340.00	345.77	0.08
1	373.72	2.97	358.80	347.86	0.05

1	374.66	0.62	234.70	334.02	0.18
1	374.66	0.61	234.30	334.40	0.13
1	374.83	0.61	248.80	335.51	0.08
1	374.83	0.64	272.80	338.65	0.05
1	374.47	1.07	241.20	334.75	0.18
1	374.47	1.09	240.80	334.97	0.13
1	374.56	1.09	273.30	338.37	0.09
1	374.58	1.10	300.00	341.26	0.05
1	374.61	1.09	292.20	340.51	0.05
1	374.47	1.70	268.50	337.69	0.18
1	374.45	1.61	273.90	338.46	0.13
1	374.04	1.63	293.50	340.54	0.09
1	373.93	1.66	319.60	343.40	0.05
1	373.85	2.41	285.80	339.94	0.18
1	373.83	2.26	286.30	339.58	0.18
1	373.77	2.27	307.20	341.63	0.13
1	373.72	2.28	318.90	343.24	0.08
1	373.66	2.29	345.00	346.44	0.05
1	373.77	2.77	364.50	348.14	0.05
1	373.77	2.78	338.50	345.73	0.08
1	373.85	2.75	320.30	343.42	0.13
1	374.10	2.72	294.10	340.48	0.18
1	374.64	4.75	378.40	349.63	0.18
1	374.34	4.92	390.60	350.95	0.13
1	373.99	4.97	397.10	351.78	0.08
1	374.39	5.01	417.60	353.89	0.05
1	374.02	4.29	353.70	346.57	0.18
1	374.02	4.37	372.60	348.81	0.13
1	374.18	4.35	389.80	350.86	0.08
1	374.18	4.42	404.50	352.17	0.05
1	373.91	3.52	332.60	344.62	0.18
1	373.80	3.58	346.40	345.98	0.13
1	373.80	3.59	365.30	348.29	0.08
1	373.80	3.69	391.40	350.90	0.05
1	374.18	5.06	156.40	363.97	0.18
1	374.04	4.90	152.50	363.79	0.13
1	373.96	4.92	159.60	365.00	0.09
1	373.91	4.77	162.20	365.48	0.05
1	374.23	4.02	147.40	362.81	0.18
1	374.04	4.04	147.40	362.63	0.13
1	373.96	4.04	153.90	364.00	0.09
1	373.96	4.12	161.00	364.96	0.05
1	374.37	3.28	137.70	361.63	0.18
1	373.99	3.27	142.90	362.43	0.13
1	374.04	3.34	157.10	364.25	0.05
1	374.64	2.48	131.20	360.60	0.18
1	374.77	2.45	137.10	361.34	0.14
1	374.77	2.46	144.20	362.56	0.09
1	374.69	2.43	151.30	363.34	0.05
1	374.39	1.84	118.80	358.56	0.18
1	374.39	1.84	118.30	358.36	0.18
1	374.50	1.70	121.50	358.97	0.13
1	374.45	1.70	128.00	360.09	0.09
1	374.64	1.79	128.00	360.18	0.09
1	374.31	1.81	137.10	361.34	0.05
1	374.10	1.18	111.80	357.24	0.19
1	374.18	1.18	111.80	357.51	0.13
1	374.18	1.18	121.50	359.15	0.09
1	374.18	1.18	131.20	360.51	0.05
1	374.80	0.49	108.10	356.80	0.18
1	374.80	0.49	111.80	357.15	0.13
1	374.88	0.49	114.50	357.74	0.09
1	374.83	0.49	121.50	358.52	0.05
1	374.12	3.26	151.20	363.16	0.09
1	375.69	8.23	442.70	356.39	0.18
1	375.85	8.11	437.10	355.78	0.13
1	375.69	8.16	443.60	356.23	0.09
1	375.69	8.10	457.70	357.69	0.05
1	374.42	7.32	410.20	353.30	0.18
1	374.61	7.23	163.50	365.01	0.18
1	374.61	7.16	166.70	365.35	0.13
1	374.61	7.09	170.00	365.94	0.09
1	374.42	7.07	169.90	365.08	0.05
1	375.12	7.12	418.40	353.72	0.18
1	375.12	7.13	424.00	354.20	0.14
1	375.12	7.10	438.10	355.68	0.09
1	375.12	7.04	443.70	356.60	0.06
1	374.23	6.66	431.50	354.92	0.05
1	374.39	6.54	160.30	364.50	0.18
1	374.42	6.50	159.60	364.48	0.13
1	374.42	6.47	163.50	364.92	0.09
1	374.42	6.42	166.70	365.43	0.05
1	375.91	7.81	166.80	365.52	0.18
1	375.91	7.61	166.80	365.52	0.13
1	375.91	7.41	170.00	366.03	0.09
1	375.91	7.24	166.80	365.69	0.05
1	374.85	6.47	437.10	355.41	0.05
1	374.85	6.43	424.00	354.14	0.09
1	374.85	6.43	417.50	353.32	0.13
1	374.85	6.40	404.50	352.24	0.18
1	375.69	8.29	173.20	366.62	0.18
1	375.69	8.25	170.00	366.37	0.13
1	375.69	8.26	170.10	366.54	0.09
1	375.69	8.23	176.50	367.47	0.05

1	375.04	2.29	294.20	337.84	0.42
1	374.74	2.25	267.40	335.29	0.27
1	375.10	1.71	279.90	336.82	0.43
1	375.20	1.71	259.80	335.00	0.28
1	374.80	4.93	384.90	346.42	0.41
1	374.58	4.96	376.80	345.83	0.28
1	373.96	4.47	345.80	343.07	0.42
1	373.91	4.49	351.60	343.70	0.28
1	374.93	3.51	305.90	339.05	0.43
1	374.74	3.35	299.40	338.54	0.27
1	374.91	3.81	312.50	340.13	0.42
1	374.72	3.94	332.00	341.92	0.28
1	375.07	3.05	300.10	338.55	0.43
1	375.34	3.11	293.60	337.98	0.28
1	375.34	2.49	286.40	337.47	0.43
1	375.34	2.60	279.90	336.89	0.28
1	374.58	4.93	147.40	361.68	0.27
1	375.39	1.10	121.50	357.66	0.39
1	375.39	1.10	117.80	357.17	0.26
1	375.20	0.42	115.10	357.06	0.39
1	375.04	0.41	115.10	357.24	0.26
1	374.83	4.97	149.40	362.39	0.38
1	374.69	5.05	150.00	362.23	0.25
1	374.93	4.21	140.90	360.64	0.39
1	374.93	4.18	139.70	360.88	0.26
1	375.88	3.59	137.10	360.59	0.39
1	375.85	3.50	141.00	360.81	0.25
1	375.55	2.93	131.20	359.29	0.38
1	375.47	2.71	128.00	358.81	0.27
1	375.20	3.47	134.50	360.21	0.39
1	375.07	3.39	137.70	360.51	0.27
1	375.20	2.71	128.10	359.52	0.39
1	375.20	2.74	128.00	358.99	0.26
1	374.42	2.10	124.80	358.33	0.39
1	374.26	1.88	117.80	357.62	0.26
1	374.45	1.53	121.60	358.11	0.38
1	374.56	1.49	115.10	357.33	0.26
1	374.04	0.53	253.90	334.51	0.41
1	374.26	0.47	241.40	333.20	0.28
1	376.09	7.80	443.70	352.16	0.42
1	376.07	7.90	442.80	352.15	0.28
1	375.15	7.34	417.60	349.78	0.42
1	375.10	7.04	417.60	349.59	0.28
1	374.66	6.56	398.00	347.82	0.43
1	374.61	6.45	405.40	348.27	0.28
1	374.66	6.44	153.90	362.81	0.39
1	374.74	5.96	154.50	362.39	0.25
1	374.93	0.62	115.10	357.15	0.39
1	374.88	0.59	114.60	356.96	0.27
1	374.53	0.60	253.90	334.28	0.42
1	374.64	0.62	241.30	332.97	0.28
1	374.50	1.09	266.90	335.51	0.43
1	374.53	1.11	246.80	333.69	0.28
1	374.34	1.12	115.60	356.98	0.39
1	374.45	1.02	111.80	356.58	0.26
1	375.99	7.90	173.30	365.23	0.39
1	376.12	7.01	178.90	365.56	0.25
1	376.18	6.60	180.40	365.34	0.39
1	376.23	6.67	177.30	365.46	0.39

B.3. Michael (1988).

Outer Diameter / m	0.014
Inner Diameter / m	0.0099
Length / m	0.252
Width / m	0.08
Horizontal Pitch / m	0.02
Vertical Pitch / m	0.0173
Number of odd tubes	4
Number of even tubes	3

Run Number 1

Row No.	T_V /K	U_V/ (ms^{-1})	q/ (kW/m^2)	T_W /K	M_C / kgs^{-1}
1	374.77	20.50	494.50	369.05	0.00
2	374.66	19.80	549.90	370.94	0.00
3	374.53	19.24	480.60	367.02	0.01
4	374.39	18.57	527.50	369.76	0.01
5	374.29	18.02	454.10	365.33	0.01
6	374.18	17.36	515.10	368.12	0.01
7	374.07	16.81	472.60	366.16	0.02
8	373.96	16.13	451.40	366.74	0.02
9	373.85	15.64	464.10	365.44	0.03
10	373.77	14.94	498.40	367.27	0.02
1	373.75	20.86	507.10	367.49	0.00
2	373.64	20.12	535.10	369.84	0.00
3	373.45	19.60	484.20	370.12	0.01
4	373.34	18.88	532.60	368.36	0.01
5	373.23	18.30	466.60	368.72	0.01
6	373.12	17.59	502.10	366.67	0.01
7	373.02	17.04	467.90	368.68	0.02
8	372.94	16.32	475.10	365.18	0.02
9	372.80	15.80	451.50	367.39	0.03
10	372.75	15.09	511.80	366.19	0.02
1	373.18	21.63	536.90	366.78	0.00
2	373.07	20.82	565.20	368.88	0.00
3	372.88	20.25	520.90	367.71	0.01
4	372.77	19.47	555.80	367.39	0.01
5	372.67	18.85	490.90	366.08	0.01
6	372.53	18.12	536.50	365.73	0.01
7	372.45	17.50	495.60	365.74	0.02
8	372.31	16.75	500.10	364.43	0.02
9	372.18	16.21	483.30	364.56	0.03
10	372.10	15.44	533.00	364.29	0.02

Row No.	T_V /K	U_V/ (ms^{-1})	q/ (kW/m^2)	T_W /K	M_C / kgs^{-1}
1	373.15	21.32	529.00	366.58	0.00
2	373.04	20.52	556.60	368.66	0.00
3	372.85	19.96	512.00	367.20	0.01
4	372.77	19.18	539.30	367.29	0.01
5	372.67	18.58	500.60	365.77	0.01
6	372.56	17.82	528.10	365.93	0.01
7	372.45	17.22	488.30	365.25	0.02
8	372.34	16.47	488.10	364.04	0.02
9	372.21	15.94	475.80	364.10	0.03
10	372.15	15.16	524.80	364.41	0.02
1	374.91	20.20	678.00	366.40	0.00
2	374.80	19.22	684.60	368.31	0.00
3	374.64	18.52	651.80	367.10	0.01
4	374.58	17.54	668.60	366.07	0.01
5	374.50	16.80	633.40	363.90	0.02
6	374.39	15.87	663.00	364.43	0.01
7	374.34	15.11	621.30	364.09	0.03
8	374.23	14.19	614.40	362.85	0.02
9	374.15	13.50	612.10	363.29	0.04
10	374.10	12.55	653.30	363.02	0.03
1	375.10	21.15	682.10	367.31	0.00
2	374.99	20.17	694.90	369.27	0.00
3	374.85	19.46	661.40	368.31	0.01
4	374.72	18.51	676.70	367.82	0.01
5	374.64	17.77	661.20	366.92	0.02
6	374.53	16.80	677.60	365.62	0.01
7	374.45	16.05	629.50	365.80	0.03
8	374.31	15.13	650.00	363.90	0.02
9	374.23	14.40	615.50	364.55	0.04
10	374.18	13.45	660.70	364.34	0.03

Run Number 2

Row No.	T_V /K	U_V/ (ms^{-1})	q/ (kW/m^2)	T_W /K	M_C / kgs^{-1}
1	373.75	16.08	439.70	366.50	0.00
2	373.69	15.41	490.10	368.65	0.00
3	373.56	14.88	423.40	362.38	0.01
4	373.53	14.21	466.40	367.45	0.01
5	373.45	13.69	412.90	361.67	0.01
6	373.39	13.05	453.00	365.61	0.01
7	373.31	12.53	415.00	361.39	0.02
8	373.29	11.87	409.90	363.78	0.01
9	373.21	11.40	411.30	361.13	0.02
10	373.21	10.73	438.40	363.22	0.02
1	373.75	16.41	438.70	366.58	0.00
2	373.69	15.74	475.60	368.24	0.00
3	373.56	15.23	421.20	362.49	0.01
4	373.53	14.57	471.20	367.42	0.01
5	373.45	14.04	422.20	362.09	0.01
6	373.37	13.39	450.60	365.65	0.01
7	373.31	12.87	413.10	361.52	0.02
8	373.29	12.21	403.00	363.85	0.01
9	373.18	11.76	410.80	361.30	0.02
10	373.18	11.09	434.60	363.63	0.02
1	373.77	16.58	338.90	368.91	0.00
2	373.72	16.07	378.30	370.65	0.00
3	373.58	15.68	328.00	363.97	0.00
4	373.56	15.17	371.30	370.20	0.00
5	373.48	14.77	317.20	363.43	0.01
6	373.42	14.28	346.90	367.91	0.01
7	373.34	13.89	324.80	363.80	0.01
8	373.31	13.38	311.30	366.23	0.01
9	373.18	13.06	323.40	363.26	0.02
10	373.18	12.53	350.60	366.57	0.01
1	373.42	16.87	520.30	364.81	0.00
2	373.37	16.06	561.20	366.66	0.00
3	373.26	15.43	495.10	360.40	0.01
4	373.21	14.66	536.30	365.68	0.01
5	373.15	14.02	481.00	359.46	0.01

Row No.	T_V /K	U_V/ (ms^{-1})	q/ (kW/m^2)	T_W /K	M_C / kgs^{-1}
6	373.10	13.25	527.70	363.52	0.01
7	373.02	12.64	477.50	359.10	0.02
8	372.99	11.87	486.10	361.68	0.02
9	372.91	11.30	478.90	358.88	0.03
10	372.91	10.51	519.50	362.41	0.02
1	373.37	16.40	503.10	364.61	0.00
2	373.34	15.60	550.20	366.69	0.00
3	373.21	15.01	484.20	360.42	0.01
4	373.18	14.23	527.30	365.24	0.01
5	373.12	13.60	477.00	359.40	0.01
6	373.07	12.84	516.20	363.70	0.01
7	373.02	12.23	468.00	359.06	0.02
8	372.99	11.47	470.60	361.90	0.02
9	372.91	10.92	468.00	358.87	0.03
10	372.91	10.16	511.90	361.91	0.02
1	373.34	16.37	636.80	362.26	0.00
2	373.34	15.34	653.50	365.08	0.00
3	373.23	14.60	613.80	362.72	0.01
4	373.23	13.60	631.90	362.85	0.01
5	373.15	12.86	584.00	360.63	0.02
6	373.12	11.91	619.70	360.87	0.01
7	373.10	11.16	573.50	359.30	0.03
8	373.07	10.24	583.00	360.01	0.02
9	373.02	9.54	559.00	358.26	0.03
10	373.02	8.62	606.60	359.41	0.03
1	373.42	16.78	637.10	362.99	0.00
2	373.42	15.75	654.50	365.48	0.00
3	373.29	15.03	615.40	363.13	0.01
4	373.29	14.03	634.70	363.23	0.01
5	373.21	13.29	590.20	361.18	0.02
6	373.21	12.33	622.20	361.78	0.01
7	373.15	11.58	576.80	359.84	0.03
8	373.12	10.64	580.30	360.62	0.02
9	373.07	9.95	561.90	358.78	0.03
10	373.07	9.03	608.30	360.20	0.03

Run Number 3

Row No.	T_V /K	U_V/ (ms^{-1})	q/ (kW/m^2)	T_W /K	M_C / kgs^{-1}
1	373.34	10.40	423.90	362.32	0.00
2	373.31	9.72	467.60	364.10	0.00
3	373.29	9.16	404.40	359.06	0.01
4	373.29	8.51	440.80	363.43	0.00
5	373.26	7.97	396.60	357.59	0.01
6	373.23	7.33	427.10	362.06	0.01
7	373.23	6.81	393.10	357.50	0.02
8	373.21	6.18	379.50	359.90	0.01
9	373.18	5.72	385.10	356.85	0.02
10	373.21	5.09	411.80	359.38	0.02
1	373.48	10.29	420.40	362.35	0.00
2	373.48	9.61	475.80	364.38	0.00
3	373.42	9.05	401.90	359.01	0.01
4	373.39	8.40	449.40	363.65	0.01
5	373.37	7.86	395.80	358.57	0.01
6	373.37	7.22	426.20	362.39	0.01
7	373.34	6.71	391.30	357.82	0.02
8	373.31	6.08	384.20	359.88	0.01
9	373.29	5.62	384.20	357.15	0.02
10	373.29	5.00	407.30	359.45	0.02
1	373.15	9.57	319.60	364.06	0.00
2	373.10	9.05	346.60	365.39	0.00
3	373.07	8.64	308.90	360.64	0.00
4	373.07	8.14	343.00	365.37	0.00
5	373.04	7.72	300.80	359.01	0.01
6	373.04	7.23	320.40	363.60	0.01
7	373.02	6.84	306.30	359.96	0.01
8	373.02	6.34	291.20	361.46	0.01
9	372.96	6.00	297.60	359.19	0.02
10	372.99	5.50	321.30	362.66	0.01

Row No.	T_V /K	U_V/ (ms^{-1})	q/ (kW/m^2)	T_W /K	M_C / kgs^{-1}
1	373.31	9.17	383.90	361.19	0.00
2	373.31	8.55	414.10	363.46	0.00
3	373.29	8.05	374.90	358.03	0.01
4	373.29	7.44	396.40	362.24	0.00
5	373.26	6.97	360.70	355.69	0.01
6	373.26	6.38	392.20	361.17	0.01
7	373.23	5.91	362.10	356.25	0.02
8	373.23	5.32	340.20	358.12	0.01
9	373.21	4.91	353.10	355.59	0.02
10	373.23	4.33	386.30	359.40	0.02
1	373.23	9.54	467.50	359.71	0.00
2	373.23	8.78	515.40	362.19	0.00
3	373.18	8.17	446.90	356.47	0.01
4	373.18	7.44	481.70	360.78	0.01
5	373.15	6.85	403.50	353.55	0.01
6	373.15	6.20	462.60	359.50	0.01
7	373.15	5.63	428.10	354.92	0.02
8	373.15	4.93	428.80	357.30	0.02
9	373.12	4.41	412.30	353.64	0.02
10	373.15	3.74	458.00	357.19	0.02
1	373.37	12.47	483.00	361.77	0.00
2	373.34	11.70	531.40	363.72	0.00
3	373.29	11.07	462.50	358.02	0.01
4	373.29	10.32	496.40	362.63	0.01
5	373.23	9.73	446.30	356.72	0.01
6	373.23	9.00	489.10	361.36	0.01
7	373.21	8.42	444.60	356.64	0.02
8	373.21	7.69	455.20	359.39	0.02
9	373.15	7.15	436.90	355.96	0.03
10	373.18	6.43	482.40	359.07	0.02

Run Number 4

Row No.	T_V /K	U_V/ (ms^{-1})	q/ (kW/m^2)	T_W /K	M_C / kgs^{-1}
1	373.07	6.99	406.60	358.14	0.00
2	373.10	6.32	444.30	359.85	0.00
3	373.07	5.78	381.00	355.51	0.01
4	373.07	5.16	431.20	358.33	0.00
5	373.04	4.63	370.80	352.93	0.01
6	373.07	4.02	406.90	357.34	0.01
7	373.07	3.52	371.60	353.51	0.02
8	373.07	2.92	356.00	354.22	0.01
9	373.07	2.48	349.50	351.58	0.02
10	373.07	1.91	376.40	355.18	0.02
1	373.18	5.97	319.90	362.20	0.00
2	373.21	5.45	346.30	364.47	0.00
3	373.18	5.03	305.50	358.87	0.00
4	373.21	4.53	338.70	363.56	0.00
5	373.18	4.11	292.70	356.88	0.01
6	373.18	3.64	317.00	361.52	0.01
7	373.18	3.25	299.50	358.00	0.01
8	373.18	2.76	281.30	359.10	0.01
9	373.18	2.42	293.10	357.17	0.02
10	373.18	1.94	323.50	361.73	0.01
1	373.34	6.79	382.00	358.91	0.00
2	373.37	6.17	415.60	360.74	0.00
3	373.34	5.67	366.50	355.46	0.01
4	373.34	5.07	397.80	359.23	0.00
5	373.34	4.59	353.20	352.79	0.01
6	373.34	4.02	385.90	357.99	0.01
7	373.31	3.55	351.00	353.83	0.02
8	373.34	2.98	338.10	355.33	0.01
9	373.31	2.57	335.50	352.47	0.02
10	373.34	2.02	372.80	355.39	0.02

Row No.	T_V /K	U_V/ (ms^{-1})	q/ (kW/m^2)	T_W /K	M_C / kgs^{-1}
1	373.18	7.27	453.10	356.87	0.00
2	373.21	6.53	493.60	358.62	0.00
3	373.18	5.93	427.40	353.38	0.01
4	373.21	5.23	463.80	357.06	0.01
5	373.18	4.67	405.40	350.76	0.01
6	373.18	4.01	448.90	355.72	0.01
7	373.18	3.46	408.40	351.66	0.02
8	373.18	2.79	400.50	353.41	0.01
9	373.18	2.30	381.10	349.22	0.02
10	373.18	1.68	431.20	353.08	0.02
1	373.29	7.17	577.50	354.74	0.00
2	373.31	6.22	588.90	357.32	0.00
3	373.29	5.51	545.20	354.24	0.01
4	373.29	4.63	551.00	354.24	0.01
5	373.29	3.95	490.10	351.30	0.02
6	373.29	3.16	538.30	352.56	0.01
7	373.29	2.50	491.30	349.15	0.02
8	373.29	1.70	469.30	348.54	0.02
9	373.29	1.13	445.80	345.30	0.03
10	373.29	0.41	485.60	348.07	0.02
1	373.12	7.02	573.00	354.78	0.00
2	373.12	6.09	597.00	357.32	0.00
3	373.12	5.36	543.60	354.44	0.01
4	373.12	4.47	554.90	354.12	0.01
5	373.12	3.79	515.70	352.58	0.02
6	373.12	2.95	534.60	351.88	0.01
7	373.12	2.30	487.60	349.47	0.02
8	373.12	1.50	471.80	349.18	0.02
9	373.12	0.92	445.90	345.65	0.03
10	373.12	0.20	485.80	349.02	0.02

B.4. Beech-1 (1995).

Outer Diameter / m	0.014
Inner Diameter / m	0.0099
Length / m	0.252
Width / m	0.08
Horizontal Pitch / m	0.02
Vertical Pitch / m	0.0173
Number of odd tubes	4
Number of even tubes	3

Run Number 1

Row No.	T_V /K	U_V/ (ms^{-1})	q/ (kW/m^2)	T_W /K	M_C / kgs^{-1}
1	374.88	6.28	278.30	363.32	0.00
2	374.88	5.85	289.60	363.00	0.00
3	374.88	5.51	274.20	363.02	0.01
4	374.88	5.09	313.70	360.02	0.00
5	374.88	4.73	253.50	364.11	0.01
6	374.88	4.33	283.50	360.00	0.01
7	374.88	4.00	260.20	360.92	0.02
8	374.88	3.60	265.30	360.79	0.01
9	374.88	3.29	236.90	364.02	0.02
10	374.88	2.92	268.00	353.75	0.02
1	374.85	6.08	411.70	357.26	0.00
2	374.85	5.45	439.80	357.30	0.00
3	374.85	4.94	406.90	356.46	0.01
4	374.85	4.31	462.60	354.42	0.01
5	374.85	3.77	378.00	356.06	0.02

Row No.	T_V /K	U_V/ (ms^{-1})	q/ (kW/m^2)	T_W /K	M_C / kgs^{-1}
6	374.85	3.19	407.50	353.85	0.01
7	374.85	2.71	366.90	352.60	0.02
8	374.85	2.15	366.20	351.45	0.02
9	374.85	1.72	328.30	350.11	0.03
10	374.85	1.21	335.60	343.78	0.02
1	375.09	6.17	482.40	355.09	0.00
2	375.11	5.42	499.30	353.61	0.00
3	375.11	4.85	479.70	353.47	0.01
4	375.11	4.11	553.50	350.43	0.01
5	375.11	3.48	438.60	350.52	0.02
6	375.11	2.80	470.80	349.10	0.02
7	375.11	2.26	420.50	346.68	0.03
8	375.11	1.62	408.40	345.66	0.02
9	375.11	1.15	357.20	341.68	0.04
10	375.11	0.60	348.10	333.86	0.03

Run Number 2

Row No.	T_V /K	U_V/ (ms^{-1})	q/ (kW/m^2)	T_W /K	M_C / kgs^{-1}
1	375.59	8.52	334.10	363.12	0.00
2	375.59	8.01	334.30	364.01	0.00
3	375.59	7.63	319.00	363.63	0.01
4	375.56	7.16	378.40	360.88	0.00
5	375.56	6.73	303.00	361.89	0.01
6	375.56	6.27	331.10	363.98	0.01
7	375.56	5.89	306.80	361.17	0.02
8	375.56	5.43	308.60	361.18	0.02
9	375.54	5.08	286.20	361.74	0.02
10	375.56	4.65	313.50	359.62	0.02
1	375.54	8.83	428.10	360.24	0.00
2	375.54	8.18	463.50	360.90	0.00
3	375.54	7.66	423.70	359.90	0.01
4	375.54	7.02	486.70	357.02	0.01
5	375.54	6.46	397.70	357.36	0.02

Row No.	T_V /K	U_V/ (ms^{-1})	q/ (kW/m^2)	T_W /K	M_C / kgs^{-1}
6	375.54	5.86	418.90	356.63	0.01
7	375.54	5.39	389.20	356.21	0.02
8	375.54	4.80	396.50	355.99	0.02
9	375.54	4.35	361.80	356.64	0.03
10	375.54	3.80	403.40	354.05	0.03
1	375.38	9.09	438.50	359.79	0.00
2	375.36	8.43	477.20	360.47	0.00
3	375.36	7.89	443.80	359.68	0.01
4	375.36	7.21	494.40	357.53	0.01
5	375.36	6.65	409.90	359.09	0.02
6	375.36	6.02	438.40	356.25	0.01
7	375.32	5.53	405.10	355.10	0.03
8	375.36	4.90	408.00	356.05	0.02
9	375.32	4.45	376.10	357.32	0.03
10	375.32	3.88	411.20	353.24	0.03

1	375.11	8.13	510.30	357.02	0.00
2	375.11	7.34	530.10	356.17	0.00
3	375.11	6.73	501.60	354.95	0.01
4	375.14	5.96	573.20	352.32	0.01
5	375.14	5.30	461.40	353.28	0.02

6	375.14	4.59	502.30	350.54	0.02
7	375.14	4.01	458.70	349.55	0.03
8	375.14	3.31	457.10	348.28	0.02
9	375.14	2.79	410.60	349.75	0.04
10	375.14	2.16	422.80	343.69	0.03

Run Number 3

Row No.	T_V /K	U_V/ (ms^{-1})	q/ (kW/m^2)	T_W /K	M_C / kgs^{-1}
1	376.10	11.36	299.50	367.14	0.00
2	376.07	10.93	310.60	367.09	0.00
3	376.02	10.60	308.30	366.24	0.01
4	376.00	10.15	358.40	364.63	0.00
5	375.95	9.76	296.50	365.90	0.01
6	375.97	9.31	314.60	365.25	0.01
7	375.92	8.97	303.70	364.09	0.02
8	375.90	8.52	315.20	364.17	0.01
9	375.87	8.18	277.30	363.96	0.02
10	375.87	7.76	309.90	362.52	0.02
1	376.10	11.90	300.10	367.47	0.00
2	376.10	11.45	331.20	367.45	0.00
3	376.02	11.11	303.90	366.64	0.01
4	376.02	10.66	349.80	365.49	0.00
5	375.95	10.30	287.40	366.99	0.01
6	375.97	9.86	309.00	365.45	0.01
7	375.90	9.54	304.70	363.92	0.02
8	375.90	9.08	307.40	364.88	0.01
9	375.87	8.74	277.60	364.45	0.02
10	375.87	8.32	299.40	362.99	0.02
1	375.51	10.80	291.70	364.99	0.00
2	375.49	10.36	298.70	364.72	0.00
3	375.46	10.04	287.40	364.64	0.01
4	375.44	9.61	319.80	362.59	0.00
5	375.38	9.26	258.30	367.99	0.01
6	375.38	8.86	292.80	363.07	0.01
7	375.32	8.55	270.60	364.66	0.02
8	375.32	8.13	277.60	363.01	0.01
9	375.29	7.82	258.10	365.42	0.02
10	375.29	7.43	274.50	360.93	0.02

Row No.	T_V /K	U_V/ (ms^{-1})	q/ (kW/m^2)	T_W /K	M_C / kgs^{-1}
1	375.27	11.08	442.80	360.77	0.00
2	375.27	10.40	470.10	361.77	0.00
3	375.24	9.87	438.60	360.55	0.01
4	375.24	9.21	490.20	359.13	0.01
5	375.21	8.65	406.50	359.55	0.02
6	375.21	8.03	439.10	358.15	0.01
7	375.19	7.53	399.00	358.57	0.03
8	375.19	6.92	416.30	357.80	0.02
9	375.16	6.45	372.80	357.59	0.03
10	375.19	5.87	411.40	355.45	0.03
1	375.46	10.01	444.30	362.15	0.00
2	375.49	9.32	468.90	362.07	0.00
3	375.46	8.80	442.90	360.88	0.01
4	375.46	8.13	489.40	359.09	0.01
5	375.44	7.58	417.00	358.61	0.02
6	375.44	6.94	440.80	357.85	0.01
7	375.44	6.44	420.10	355.63	0.03
8	375.44	5.80	422.20	356.08	0.02
9	375.44	5.32	387.00	356.44	0.03
10	375.44	4.74	399.50	354.72	0.03
1	375.87	11.02	480.20	362.01	0.00
2	375.90	10.30	517.70	361.49	0.00
3	375.84	9.73	485.30	360.70	0.01
4	375.84	9.00	568.90	358.08	0.01
5	375.79	8.38	455.50	359.41	0.02
6	375.82	7.68	500.40	357.82	0.02
7	375.82	7.12	472.60	355.92	0.03
8	375.82	6.42	472.70	356.15	0.02
9	375.79	5.89	430.70	354.58	0.04
10	375.79	5.24	463.50	352.96	0.03

Run Number 4

Row No.	T_V /K	U_V/ (ms^{-1})	q/ (kW/m^2)	T_W /K	M_C / kgs^{-1}
1	375.87	13.42	309.80	367.55	0.00
2	375.84	12.97	328.70	367.17	0.00
3	375.77	12.63	326.10	366.49	0.01
4	375.77	12.14	373.90	365.34	0.00
5	375.69	11.74	306.70	366.84	0.01
6	375.69	11.28	330.30	365.73	0.01
7	375.62	10.94	330.80	364.16	0.02
8	375.62	10.44	328.80	365.08	0.02
9	375.56	10.08	296.30	364.06	0.03
10	375.56	9.64	313.40	363.23	0.02
1	375.54	14.34	348.20	367.93	0.00
2	375.54	13.81	341.40	368.47	0.00
3	375.44	13.47	329.00	367.32	0.01
4	375.41	12.98	372.90	366.90	0.01
5	375.36	12.58	320.00	365.59	0.01
6	375.32	12.10	345.90	366.11	0.01
7	375.24	11.74	326.80	364.53	0.02
8	375.24	11.24	333.00	365.59	0.02
9	375.19	10.88	302.10	364.95	0.03
10	375.16	10.43	323.10	363.80	0.02

Row No.	T_V /K	U_V/ (ms^{-1})	q/ (kW/m^2)	T_W /K	M_C / kgs^{-1}
1	375.90	14.71	461.80	365.19	0.00
2	375.92	14.01	481.70	365.81	0.00
3	375.82	13.52	453.00	363.84	0.01
4	375.79	12.84	519.40	362.94	0.01
5	375.74	12.28	439.40	361.68	0.02
6	375.72	11.63	466.70	362.34	0.01
7	375.67	11.12	450.60	358.19	0.03
8	375.67	10.44	453.90	361.18	0.02
9	375.62	9.95	421.40	360.21	0.04
10	375.62	9.31	429.00	359.26	0.03
1	375.74	13.98	519.40	361.47	0.00
2	375.77	13.19	561.10	362.29	0.00
3	375.69	12.59	538.10	360.91	0.01
4	375.72	11.77	631.00	358.89	0.01
5	375.64	11.09	501.20	360.22	0.02
6	375.64	10.33	551.20	358.41	0.02
7	375.62	9.72	522.20	358.17	0.03
8	375.62	8.93	530.90	356.83	0.03
9	375.59	8.33	477.40	356.39	0.04
10	375.59	7.61	515.30	353.40	0.03

Run Number 5

Row No.	T_V /K	U_V/ (ms^{-1})	q/ (kW/m^2)	T_W /K	M_C / kgs^{-1}
1	376.42	18.31	355.70	370.86	0.00
2	376.42	17.79	351.30	370.81	0.00
3	376.25	17.50	338.20	369.63	0.01
4	376.20	17.03	390.80	369.41	0.01
5	376.10	16.65	342.20	367.18	0.01
6	376.02	16.19	349.90	368.46	0.01
7	375.92	15.85	354.00	364.79	0.02
8	375.87	15.34	354.00	367.47	0.02
9	375.77	15.00	314.90	366.81	0.03
10	375.72	14.54	338.80	365.84	0.02
1	376.00	17.77	473.50	367.56	0.00
2	376.00	17.06	485.10	367.85	0.00
3	375.84	16.60	447.20	366.25	0.01
4	375.79	15.96	539.60	364.74	0.01
5	375.72	15.39	444.00	365.29	0.02

Row No.	T_V /K	U_V/ (ms^{-1})	q/ (kW/m^2)	T_W /K	M_C / kgs^{-1}
6	375.69	14.73	474.70	364.57	0.02
7	375.59	14.24	452.80	362.30	0.03
8	375.56	13.57	464.80	363.24	0.02
9	375.49	13.08	426.90	361.69	0.04
10	375.41	12.46	459.60	360.99	0.03
1	376.00	18.25	474.60	367.54	0.00
2	376.02	17.53	503.90	367.48	0.00
3	375.84	17.06	452.20	365.93	0.01
4	375.82	16.40	544.20	365.51	0.01
5	375.72	15.83	439.50	365.05	0.02
6	375.69	15.18	482.00	364.30	0.02
7	375.59	14.69	458.30	362.32	0.03
8	375.59	14.00	469.60	363.18	0.02
9	375.49	13.51	435.30	361.42	0.04
10	375.46	12.86	461.10	360.78	0.03

B.5. Beech-2 (1995).

Outer Diameter / m	0.014
Inner Diameter / m	0.0099
Length / m	0.252
Width / m	0.08
Horizontal Pitch / m	0.02
Vertical Pitch / m	0.0173
Number of odd tubes	4
Number of even tubes	3

Run Number 1

Row No.	T_V /K	U_V/ (ms^{-1})	q/ (kW/m^2)	T_W /K	M_C / kgs^{-1}
1	374.99	19.62	393.60	369.86	0.02
2	374.88	19.07	397.60	370.50	0.00
3	374.69	18.73	363.70	369.95	0.03
4	374.58	18.22	383.40	369.54	0.01
5	374.47	17.84	390.00	368.04	0.04
6	374.34	17.30	395.90	369.29	0.01
7	374.23	16.90	396.10	366.41	0.04
8	374.15	16.32	405.30	367.76	0.02
9	374.02	15.91	332.20	367.67	0.05
10	373.93	15.43	405.50	366.98	0.02
1	373.93	18.12	306.20	369.45	0.03
2	373.85	17.67	349.10	369.43	0.00
3	373.69	17.35	306.90	369.19	0.04
4	373.58	16.92	326.00	368.41	0.01
5	373.50	16.57	328.70	368.94	0.04
6	373.37	16.11	336.70	368.33	0.01
7	373.26	15.76	339.00	366.03	0.05
8	373.15	15.26	330.40	366.38	0.01
9	373.07	14.89	285.60	366.31	0.06
10	372.99	14.46	351.10	365.93	0.02
1	374.77	17.34	318.90	370.09	0.07
2	374.66	16.90	330.60	370.15	0.00
3	374.53	16.59	324.20	370.04	0.08
4	374.42	16.14	326.10	369.11	0.00
5	374.31	15.81	324.40	368.51	0.08
6	374.23	15.34	335.70	369.45	0.01
7	374.10	15.01	325.60	367.69	0.09
8	374.02	14.54	335.00	368.20	0.01
9	373.91	14.19	310.50	367.57	0.09
10	373.85	13.72	344.10	366.80	0.02
1	375.26	19.28	381.70	369.11	0.09
2	375.07	18.80	397.80	369.84	0.00
3	374.91	18.44	370.20	369.60	0.10
4	374.72	17.98	380.90	368.98	0.01
5	374.58	17.61	395.00	367.96	0.11
6	374.45	17.07	395.90	368.88	0.01
7	374.29	16.69	388.20	366.90	0.12
8	374.18	16.14	400.60	367.63	0.02
9	374.04	15.74	350.50	367.58	0.12
10	373.93	15.24	394.20	365.51	0.02
1	373.99	17.88	384.50	368.07	0.02
2	373.99	17.27	375.80	368.97	0.00
3	373.83	16.91	359.80	368.25	0.03
4	373.77	16.36	376.20	367.15	0.01
5	373.66	15.97	381.10	366.33	0.04
6	373.58	15.40	377.80	367.24	0.01
7	373.48	15.00	376.60	365.62	0.05
8	373.42	14.42	374.80	366.43	0.02
9	373.31	14.01	339.10	366.16	0.05
10	373.29	13.48	393.40	364.74	0.02
1	373.88	18.46	514.00	365.32	0.03
2	373.80	17.69	527.50	366.54	0.00
3	373.66	17.13	482.00	364.90	0.04
4	373.56	16.42	506.60	364.31	0.01
5	373.50	15.84	505.20	364.56	0.05
6	373.42	15.07	542.90	363.55	0.02
7	373.34	14.44	503.10	361.34	0.06
8	373.29	13.66	515.10	362.58	0.02
9	373.21	13.07	471.90	361.10	0.07
10	373.18	12.30	548.40	360.48	0.03
1	373.88	18.32	501.80	365.23	0.04
2	373.85	17.53	512.60	366.37	0.00
3	373.72	16.99	471.30	365.10	0.04
4	373.69	16.25	485.90	364.17	0.01
5	373.58	15.72	511.00	362.44	0.05
6	373.50	14.95	518.70	364.02	0.01
7	373.42	14.36	496.60	361.20	0.06
8	373.37	13.58	496.60	362.70	0.02
9	373.29	13.01	454.10	362.13	0.07
10	373.29	12.28	511.40	360.98	0.03

Run Number 2

Row No.	T_V /K	U_V/ (ms^{-1})	q/ (kW/m^2)	T_W /K	M_C / kgs^{-1}
1	373.91	18.51	512.20	365.64	0.04
2	373.80	17.75	531.60	366.54	0.00
3	373.69	17.17	478.80	365.32	0.05
4	373.56	16.48	503.30	364.61	0.01
5	373.50	15.91	507.70	364.57	0.06
6	373.37	15.15	542.60	364.18	0.02
7	373.29	14.54	495.60	361.61	0.07
8	373.21	13.77	510.70	362.82	0.02
9	373.12	13.17	463.50	361.22	0.08
10	373.07	12.43	550.80	361.03	0.03

Row No.	T_V /K	U_V/ (ms^{-1})	q/ (kW/m^2)	T_W /K	M_C / kgs^{-1}
1	374.58	17.60	543.60	364.71	0.08
2	374.47	16.81	560.70	365.06	0.00
3	374.37	16.21	510.60	364.89	0.09
4	374.31	15.43	514.80	363.78	0.01
5	374.23	14.87	549.50	362.21	0.10
6	374.18	14.02	560.10	363.49	0.02
7	374.10	13.40	524.70	362.02	0.11
8	374.07	12.58	530.80	362.06	0.02
9	374.02	11.97	502.70	360.92	0.12
10	373.99	11.19	556.60	360.05	0.03

B.6. Beech-3 (1995).

Outer Diameter / m	0.014
Inner Diameter / m	0.0099
Length / m	0.252
Width / m	0.08
Horizontal Pitch / m	0.02
Vertical Pitch / m	0.0173
Number of odd tubes	1
Number of even tubes	0

Row No.	T_V /K	U_V/ (ms^{-1})	q/ (kW/m^2)	T_W /K	M_C / kgs^{-1}
1	373.39	4.23	274.00	362.53	0.00
1	373.85	6.00	282.80	364.91	0.00
1	373.42	4.23	378.60	358.70	0.00
1	373.77	5.99	407.30	360.69	0.00
1	373.77	6.08	399.00	360.91	0.00
1	373.45	6.29	383.80	361.04	0.00
1	373.64	10.08	395.30	363.91	0.00
1	373.39	4.21	441.90	356.43	0.00
1	373.69	6.05	452.50	359.27	0.00
1	373.45	4.20	267.50	361.02	0.02
1	373.45	4.24	256.60	360.98	0.06
1	373.42	4.18	368.60	356.55	0.02

Row No.	T_V /K	U_V/ (ms^{-1})	q/ (kW/m^2)	T_W /K	M_C / kgs^{-1}
1	373.45	4.21	366.80	355.69	0.06
1	373.45	4.21	355.20	355.48	0.10
1	373.53	6.27	375.10	358.78	0.02
1	373.56	6.27	378.50	358.43	0.06
1	373.53	6.27	366.00	359.30	0.10
1	373.69	10.05	383.00	362.23	0.02
1	373.69	10.19	385.40	362.17	0.06
1	373.69	10.13	385.80	362.77	0.10
1	373.45	4.27	423.80	354.24	0.03
1	373.42	4.21	414.20	353.41	0.06
1	373.56	6.19	439.10	355.94	0.06
1	373.69	10.00	442.50	360.29	0.06

B.7. Briggs and Sabaratnam (2003).

Outer Diameter / m	0.0191m
Inner Diameter / m	0.0127m
Length / m	0.272m
Width / m	0.0524m
Horizontal Pitch / m	0.0262m
Vertical Pitch / m	0.0227m
Number of odd tubes	2
Number of even tubes	1

Run Number 1

Row No.	T_V /K	U_V/ (ms^{-1})	q/ (kW/m^2)	T_W /K	M_C / kgs^{-1}
1	373.02	10.39	502.15	353.53	0.00
2	373.02	9.53	492.79	354.37	0.00
3	373.02	9.11	492.11	352.05	0.01
4	373.02	8.28	493.14	349.30	0.00
5	373.03	7.86	479.87	349.86	0.01
6	373.03	7.04	498.79	346.54	0.01
7	373.03	6.62	473.15	347.84	0.02
8	373.03	5.81	467.88	346.20	0.01
9	373.03	5.42	416.61	345.43	0.03
10	373.04	4.71	419.74	343.19	0.01
1	373.04	10.40	480.09	354.25	0.00
2	373.04	9.58	468.78	354.79	0.00
3	373.05	9.18	473.06	353.11	0.01
4	373.05	8.38	473.91	350.46	0.00
5	373.05	7.98	462.61	350.48	0.01
6	373.05	7.19	480.55	348.22	0.01
7	373.06	6.78	455.83	350.04	0.02
8	373.06	6.01	451.58	346.72	0.01
9	373.07	5.62	405.45	347.08	0.03
10	373.08	4.94	406.60	346.32	0.01
1	373.05	10.39	457.15	354.73	0.00
2	373.05	9.61	446.42	355.43	0.00
3	373.05	9.23	452.66	353.94	0.01
4	373.06	8.46	454.37	351.47	0.00
5	373.06	8.07	445.01	351.77	0.01
6	373.07	7.32	463.68	349.27	0.01
7	373.07	6.92	437.53	350.71	0.02
8	373.08	6.18	432.72	348.10	0.01
9	373.08	5.81	393.09	348.30	0.03
10	373.09	5.14	392.93	347.66	0.01
1	373.00	10.46	435.51	355.49	0.00
2	373.00	9.72	423.61	356.31	0.00
3	373.00	9.36	431.31	355.00	0.01
4	373.00	8.63	432.00	352.03	0.00
5	373.00	8.26	422.52	352.71	0.01
6	373.00	7.54	442.08	351.36	0.01
7	373.00	7.17	417.96	352.05	0.02
8	373.00	6.46	406.57	351.24	0.01
9	373.00	6.11	377.13	350.67	0.02
10	373.00	5.47	376.33	349.34	0.01
1	373.00	10.44	410.28	356.61	0.00
2	373.00	9.74	402.74	356.90	0.00
3	373.00	9.40	406.37	356.27	0.01
4	373.00	8.71	409.27	353.54	0.00
5	373.00	8.36	398.08	354.55	0.01
6	373.00	7.68	419.11	352.73	0.01
7	373.00	7.33	393.39	353.64	0.02
8	373.00	6.66	383.04	352.55	0.01
9	373.00	6.33	359.49	351.25	0.02
10	373.00	5.72	356.38	350.47	0.01
1	373.51	10.56	482.85	355.26	0.00
2	373.51	9.73	481.61	354.98	0.00
3	373.52	9.33	476.44	353.08	0.01
4	373.53	8.52	485.18	352.18	0.00
5	373.54	8.10	472.54	350.75	0.01
6	373.55	7.30	495.06	348.65	0.01
7	373.56	6.88	466.79	349.11	0.02
8	373.57	6.09	466.96	346.90	0.01
9	373.58	5.69	414.92	347.57	0.03
10	373.60	4.98	421.04	344.83	0.01
1	373.51	10.56	460.45	355.62	0.00
2	373.51	9.78	456.54	355.76	0.00
3	373.52	9.39	459.40	354.43	0.01
4	373.53	8.61	464.23	352.19	0.00
5	373.54	8.22	452.08	351.74	0.01
6	373.55	7.45	478.15	349.32	0.01
7	373.55	7.04	449.72	350.99	0.02
8	373.57	6.28	446.26	347.98	0.01
9	373.58	5.90	401.63	347.74	0.03
10	373.59	5.22	408.23	346.79	0.01
1	373.38	10.62	438.70	356.02	0.00
2	373.38	9.87	431.98	356.09	0.00

3	373.38	9.50	437.23	355.09	0.01
4	373.38	8.76	441.31	353.82	0.00
5	373.38	8.38	434.91	353.15	0.01
6	373.37	7.65	457.24	350.60	0.01
7	373.37	7.26	431.66	352.10	0.02
8	373.36	6.52	425.94	350.08	0.01
9	373.36	6.16	391.56	350.35	0.03
10	373.35	5.50	394.09	349.02	0.01
1	373.51	10.56	417.56	356.84	0.00
2	373.51	9.85	407.75	357.18	0.00
3	373.52	9.50	416.65	356.44	0.01
4	373.53	8.79	421.88	354.56	0.00
5	373.53	8.43	411.58	354.83	0.01
6	373.54	7.74	434.49	352.83	0.01

7	373.55	7.37	410.58	354.09	0.02
8	373.56	6.67	404.38	351.02	0.01
9	373.57	6.32	375.23	350.79	0.02
10	373.59	5.69	376.23	349.86	0.01
1	374.25	10.16	385.98	358.18	0.00
2	374.25	9.51	393.99	358.20	0.00
3	374.19	9.17	414.95	357.72	0.01
4	374.12	8.47	447.78	354.46	0.00
5	374.06	8.08	411.01	356.04	0.01
6	373.99	7.39	445.03	353.20	0.01
7	373.93	7.01	405.88	355.05	0.02
8	373.86	6.32	387.97	354.41	0.01
9	373.80	5.99	358.16	354.54	0.02
10	373.74	5.38	367.01	352.36	0.01

Run Number 2

Row No.	T_V /K	U_V/ (ms^{-1})	q/ (kW/m^2)	T_W /K	M_C / kgs^{-1}
1	373.07	8.76	493.87	353.49	0.00
2	373.07	7.92	486.58	354.12	0.00
3	373.08	7.51	488.80	352.71	0.01
4	373.08	6.68	488.21	348.89	0.00
5	373.09	6.27	479.88	350.41	0.01
6	373.10	5.45	505.41	347.89	0.01
7	373.10	5.02	467.58	347.82	0.02
8	373.12	4.23	468.98	342.52	0.01
9	373.13	3.83	411.56	344.69	0.03
10	373.15	3.13	413.47	344.03	0.01
1	373.03	8.76	452.71	353.22	0.00
2	373.03	7.99	446.03	353.81	0.00
3	373.03	7.61	448.07	352.39	0.01
4	373.03	6.85	447.52	349.06	0.00
5	373.03	6.47	439.89	350.10	0.01
6	373.03	5.73	463.29	347.56	0.01
7	373.03	5.33	428.62	347.51	0.02
8	373.04	4.60	429.90	342.21	0.01
9	373.04	4.24	377.26	344.42	0.03
10	373.04	3.60	379.01	343.76	0.01
1	373.02	8.86	430.18	354.36	0.00
2	373.02	8.13	423.46	354.77	0.00
3	373.02	7.77	426.15	353.19	0.01
4	373.02	7.05	429.07	349.57	0.00
5	373.02	6.68	421.12	350.79	0.01
6	373.02	5.97	444.85	348.78	0.01
7	373.02	5.59	413.26	350.03	0.02
8	373.01	4.89	412.21	344.19	0.01
9	373.01	4.54	366.80	345.99	0.02
10	373.01	3.91	371.33	345.41	0.01

Row No.	T_V /K	U_V/ (ms^{-1})	q/ (kW/m^2)	T_W /K	M_C / kgs^{-1}
1	373.03	8.84	414.49	355.38	0.00
2	373.03	8.13	404.43	355.54	0.00
3	373.03	7.79	407.34	354.36	0.01
4	373.03	7.10	409.15	350.27	0.00
5	373.03	6.75	398.72	351.83	0.01
6	373.03	6.07	419.98	349.52	0.01
7	373.03	5.71	393.34	350.66	0.02
8	373.03	5.05	392.40	345.95	0.01
9	373.03	4.71	352.13	348.27	0.02
10	373.03	4.11	356.43	348.55	0.01
1	372.99	8.84	368.44	355.35	0.00
2	372.98	8.21	359.49	355.18	0.00
3	372.98	7.90	362.08	354.00	0.01
4	372.98	7.29	363.69	350.45	0.00
5	372.98	6.98	354.42	351.48	0.01
6	372.97	6.38	373.31	349.16	0.01
7	372.97	6.06	349.63	350.31	0.02
8	372.96	5.47	348.80	345.61	0.01
9	372.96	5.17	313.00	347.96	0.02
10	372.95	4.64	316.83	348.23	0.01
1	373.03	9.10	362.27	357.31	0.00
2	373.03	8.48	357.58	357.34	0.00
3	373.03	8.18	355.13	356.57	0.01
4	373.03	7.57	357.26	353.68	0.00
5	373.03	7.27	352.17	354.70	0.01
6	373.03	6.67	373.52	353.00	0.01
7	373.03	6.35	347.21	353.63	0.02
8	373.03	5.76	349.30	348.29	0.01
9	373.03	5.47	318.73	352.42	0.02
10	373.03	4.93	326.18	351.43	0.01

Row No.	T_V /K	U_V/ (ms^{-1})	q/ (kW/m^2)	T_W /K	M_C / kgs^{-1}
1	373.03	9.10	362.27	357.31	0.00
2	373.03	8.48	357.58	357.34	0.00
3	373.03	8.18	355.13	356.57	0.01
4	373.03	7.57	357.26	353.68	0.00
5	373.03	7.27	352.17	354.70	0.01
6	373.03	6.67	373.52	353.00	0.01
7	373.03	6.35	347.21	353.63	0.02
8	373.03	5.76	349.30	348.29	0.01
9	373.03	5.47	318.73	352.42	0.02
10	373.03	4.93	326.18	351.43	0.01
1	373.05	9.14	336.27	359.07	0.00
2	373.05	8.56	344.56	357.85	0.00
3	373.05	8.27	331.74	357.88	0.00
4	373.05	7.71	344.84	354.58	0.00
5	373.06	7.41	328.92	357.13	0.01

Row No.	T_V /K	U_V/ (ms^{-1})	q/ (kW/m^2)	T_W /K	M_C / kgs^{-1}
6	373.06	6.85	355.74	353.45	0.00
7	373.06	6.55	327.44	354.98	0.01
8	373.06	6.00	340.44	350.09	0.01
9	373.07	5.71	300.54	354.81	0.02
10	373.07	5.20	320.47	352.94	0.01
1	373.04	9.04	322.97	359.28	0.00
2	373.05	8.49	338.54	358.43	0.00
3	373.05	8.20	326.91	358.90	0.00
4	373.05	7.64	336.15	355.82	0.00
5	373.05	7.36	311.42	357.67	0.01
6	373.05	6.83	354.01	355.00	0.00
7	373.05	6.53	321.98	357.24	0.01
8	373.06	5.98	332.03	351.74	0.01
9	373.06	5.70	297.49	356.07	0.02
10	373.06	5.19	319.74	354.01	0.01

Run Number 3

Row No.	T_V /K	U_V/ (ms^{-1})	q/ (kW/m^2)	T_W /K	M_C / kgs^{-1}
1	373.05	7.29	465.28	350.76	0.00
2	373.05	6.50	460.97	351.07	0.00
3	373.05	6.11	451.43	348.94	0.01
4	373.06	5.34	457.70	346.37	0.00
5	373.06	4.95	443.03	346.47	0.01
6	373.06	4.20	464.02	342.32	0.01
7	373.07	3.81	422.77	343.61	0.02
8	373.07	3.09	419.39	338.08	0.01
9	373.08	2.73	361.12	338.81	0.03
10	373.09	2.12	352.92	334.24	0.01
1	373.05	7.29	445.29	351.68	0.00
2	373.05	6.54	438.61	351.62	0.00
3	373.05	6.16	438.01	350.90	0.01
4	373.05	5.42	445.63	346.96	0.00
5	373.06	5.04	426.42	347.32	0.01
6	373.06	4.32	451.45	345.46	0.01
7	373.06	3.93	412.63	343.90	0.02
8	373.07	3.23	407.55	339.13	0.01
9	373.07	2.88	358.63	341.73	0.02
10	373.08	2.28	351.23	337.51	0.01
1	373.02	7.30	421.00	352.49	0.00
2	373.02	6.58	412.71	352.50	0.00
3	373.02	6.23	413.98	351.51	0.01
4	373.02	5.53	420.14	348.11	0.00
5	373.02	5.17	404.27	348.99	0.01

Row No.	T_V /K	U_V/ (ms^{-1})	q/ (kW/m^2)	T_W /K	M_C / kgs^{-1}
6	373.01	4.48	430.37	346.23	0.01
7	373.01	4.12	394.45	345.97	0.02
8	373.01	3.45	393.01	340.74	0.01
9	373.00	3.11	346.43	341.63	0.02
10	373.00	2.52	340.57	340.78	0.01
1	373.01	7.37	403.36	353.93	0.00
2	373.01	6.69	392.77	353.49	0.00
3	373.01	6.35	397.96	352.89	0.01
4	373.00	5.68	401.21	349.94	0.00
5	373.00	5.34	387.85	350.48	0.01
6	373.00	4.68	414.39	348.17	0.01
7	372.99	4.32	379.55	348.36	0.02
8	372.98	3.68	376.33	343.86	0.01
9	372.98	3.36	337.70	346.70	0.02
10	372.97	2.78	334.39	343.04	0.01
1	373.05	7.40	379.35	354.73	0.00
2	373.05	6.75	369.86	354.52	0.00
3	373.05	6.44	372.46	354.71	0.01
4	373.05	5.81	379.08	351.49	0.00
5	373.05	5.48	368.54	351.44	0.01
6	373.06	4.86	391.37	348.45	0.01
7	373.06	4.53	360.93	349.29	0.02
8	373.06	3.91	354.93	345.58	0.01
9	373.06	3.61	331.90	348.78	0.02
10	373.07	3.05	343.26	349.36	0.01

1	373.07	7.49	352.01	356.14	0.00
2	373.08	6.89	342.23	355.63	0.00
3	373.08	6.60	344.60	355.88	0.01
4	373.09	6.01	347.62	352.40	0.00
5	373.09	5.72	340.90	352.86	0.01
6	373.10	5.14	366.16	350.44	0.00
7	373.11	4.82	335.96	351.30	0.02
8	373.12	4.25	336.02	347.93	0.01
9	373.13	3.97	304.27	349.84	0.02
10	373.15	3.45	307.40	349.38	0.01
1	373.05	7.52	326.25	357.55	0.00
2	373.05	6.97	336.98	356.53	0.00
3	373.05	6.68	322.18	357.32	0.00
4	373.06	6.14	336.90	352.85	0.00
5	373.06	5.85	318.57	354.94	0.01

6	373.06	5.31	355.36	351.71	0.00
7	373.06	5.01	314.15	354.10	0.01
8	373.06	4.47	327.86	349.49	0.01
9	373.07	4.19	286.94	352.02	0.02
10	373.07	3.71	302.07	352.40	0.01
1	373.03	7.49	308.85	357.92	0.00
2	373.03	6.96	319.15	357.31	0.00
3	373.03	6.69	309.24	357.98	0.00
4	373.03	6.16	320.26	353.64	0.00
5	373.03	5.89	299.85	356.04	0.01
6	373.03	5.38	341.59	352.38	0.00
7	373.03	5.09	305.43	354.44	0.01
8	373.03	4.57	319.11	349.87	0.01
9	373.03	4.30	281.87	353.91	0.02
10	373.02	3.82	299.26	352.22	0.01

Run Number 4

Row No.	T_V /K	U_V/ (ms^{-1})	q/ (kW/m^2)	T_W /K	M_C / kgs^{-1}
1	373.17	5.81	451.46	351.05	0.00
2	373.17	5.04	446.31	350.99	0.00
3	373.17	4.66	443.52	350.27	0.01
4	373.18	3.91	450.73	347.02	0.00
5	373.18	3.53	424.10	345.44	0.01
6	373.18	2.81	442.13	342.22	0.01
7	373.18	2.43	395.93	341.45	0.02
8	373.19	1.76	383.71	335.37	0.01
9	373.20	1.43	328.38	335.51	0.02
10	373.22	0.87	316.98	333.33	0.01
1	373.17	5.79	431.39	351.48	0.00
2	373.17	5.06	425.78	351.89	0.00
3	373.17	4.70	427.49	349.76	0.01
4	373.18	3.97	434.29	350.48	0.00
5	373.18	3.60	407.32	346.78	0.01
6	373.18	2.91	431.35	345.27	0.01
7	373.18	2.54	385.55	342.91	0.02
8	373.19	1.89	376.79	338.93	0.01
9	373.19	1.57	325.17	337.71	0.02
10	373.21	1.01	315.53	335.09	0.01
1	373.17	5.76	413.82	352.79	0.00
2	373.17	5.06	404.52	352.80	0.00
3	373.17	4.71	408.36	351.82	0.01
4	373.18	4.02	416.47	349.45	0.00
5	373.18	3.66	389.01	347.46	0.01
6	373.18	3.00	415.52	345.62	0.01
7	373.18	2.65	370.93	346.33	0.02

Row No.	T_V /K	U_V/ (ms^{-1})	q/ (kW/m^2)	T_W /K	M_C / kgs^{-1}
8	373.19	2.02	364.94	339.14	0.01
9	373.19	1.71	318.40	340.46	0.02
10	373.20	1.17	311.88	337.43	0.01
1	373.17	5.72	394.06	353.75	0.00
2	373.17	5.06	385.91	354.07	0.00
3	373.17	4.73	389.17	353.43	0.01
4	373.18	4.07	396.41	351.81	0.00
5	373.18	3.73	374.40	349.04	0.01
6	373.18	3.09	398.08	347.17	0.01
7	373.18	2.75	361.73	347.68	0.02
8	373.18	2.14	357.36	341.69	0.01
9	373.19	1.84	312.80	342.51	0.02
10	373.20	1.30	307.93	341.37	0.01
1	373.17	5.76	374.50	355.01	0.00
2	373.17	5.12	365.16	354.79	0.00
3	373.17	4.81	370.11	353.27	0.01
4	373.18	4.18	374.10	351.71	0.00
5	373.18	3.86	357.63	351.80	0.01
6	373.18	3.25	383.16	348.05	0.01
7	373.18	2.93	345.01	348.69	0.02
8	373.18	2.34	339.87	343.83	0.01
9	373.19	2.05	305.04	345.09	0.02
10	0.00	1.53	0.00	0.00	0.01
1	373.17	5.78	348.99	356.31	0.00
2	373.17	5.18	338.78	355.78	0.00
3	373.17	4.89	343.29	355.46	0.01
4	373.17	4.31	348.04	353.44	0.00

5	373.17	4.02	332.97	353.07	0.01
6	373.18	3.45	361.07	351.67	0.00
7	373.18	3.14	327.36	352.70	0.01
8	373.18	2.59	326.60	345.28	0.01
9	373.18	2.31	290.01	348.34	0.02
10	373.19	1.82	290.36	346.36	0.01
1	373.17	5.77	326.76	357.51	0.00
2	373.17	5.22	335.13	356.56	0.00
3	373.17	4.93	324.72	356.26	0.00
4	373.17	4.38	343.14	354.88	0.00
5	373.17	4.09	318.66	355.02	0.01
6	373.17	3.55	354.73	354.01	0.00
7	373.18	3.25	311.85	353.11	0.01
8	373.18	2.72	322.54	348.73	0.01
9	373.18	2.44	277.25	350.88	0.02
10	373.18	1.97	293.69	349.27	0.01
1	373.17	5.80	318.13	358.36	0.00
2	373.17	5.26	322.76	357.31	0.00
3	373.17	4.98	320.18	358.79	0.00
4	373.17	4.44	328.13	355.78	0.00
5	373.18	4.16	303.61	356.33	0.01
6	373.18	3.65	342.53	352.88	0.00
7	373.18	3.35	307.06	355.01	0.01
8	373.18	2.83	315.46	350.53	0.01
9	373.18	2.56	276.10	353.10	0.02
10	373.19	2.10	289.84	350.12	0.01

Run Number 5

Row No.	T_V /K	U_V/ (ms^{-1})	q/ (kW/m^2)	T_W /K	M_C / kgs^{-1}
1	373.37	4.43	445.70	349.79	0.00
2	373.37	3.67	446.57	349.33	0.00
3	373.37	3.29	431.14	346.42	0.00
4	373.37	2.56	440.39	345.87	0.00
5	373.37	2.19	402.74	340.90	0.01
6	373.38	1.50	410.59	339.08	0.00
7	373.38	1.15	349.70	335.19	0.01
8	373.39	0.56	321.14	329.68	0.00
9	373.42	0.28	183.85	317.09	0.01
10	373.18	-0.03	90.81	303.03	0.01
1	373.37	4.46	429.39	352.69	0.00
2	373.37	3.73	426.20	350.95	0.00
3	373.37	3.37	415.30	347.67	0.00
4	373.37	2.66	426.41	349.91	0.00
5	373.37	2.30	391.17	343.77	0.01
6	373.38	1.64	407.30	340.08	0.00
7	373.38	1.29	354.54	339.36	0.01
8	373.39	0.69	331.45	333.26	0.00
9	373.40	0.41	217.96	324.74	0.01
10	367.16	0.03	130.07	310.67	0.01
1	373.37	4.49	411.32	351.54	0.00
2	373.37	3.79	406.34	351.77	0.00
3	373.37	3.44	400.86	349.97	0.00
4	373.37	2.76	412.44	348.67	0.00
5	373.37	2.41	378.14	345.40	0.01
6	373.38	1.77	396.31	343.24	0.00
7	373.38	1.43	347.96	340.66	0.01
8	373.38	0.84	332.38	334.94	0.00
9	373.39	0.56	245.51	327.89	0.01
10	373.49	0.14	186.81	317.10	0.01

Row No.	T_V /K	U_V/ (ms^{-1})	q/ (kW/m^2)	T_W /K	M_C / kgs^{-1}
1	373.36	4.49	394.76	352.61	0.00
2	373.36	3.82	389.51	352.84	0.00
3	373.36	3.49	385.07	350.25	0.00
4	373.36	2.84	395.78	350.59	0.00
5	373.36	2.50	363.98	347.35	0.01
6	373.35	1.88	386.62	345.57	0.00
7	373.35	1.55	343.65	342.49	0.01
8	373.34	0.97	332.07	338.66	0.00
9	373.33	0.69	269.57	335.42	0.01
10	373.23	0.23	245.77	330.19	0.01
1	373.37	4.48	375.32	353.40	0.00
2	373.37	3.84	370.23	353.55	0.00
3	373.37	3.53	364.55	352.85	0.00
4	373.37	2.91	372.83	352.02	0.00
5	373.37	2.59	343.01	347.69	0.01
6	373.37	2.01	373.85	347.44	0.00
7	373.38	1.69	328.81	345.63	0.01
8	373.38	1.13	321.85	340.75	0.00
9	373.38	0.86	279.22	340.97	0.01
10	373.40	0.38	268.83	336.83	0.01
1	373.37	4.45	345.12	354.35	0.00
2	373.37	3.86	354.02	354.53	0.00
3	373.37	3.56	339.64	353.54	0.00
4	373.37	2.98	357.61	353.86	0.00
5	373.37	2.68	326.16	350.34	0.01
6	373.37	2.12	359.74	349.27	0.00
7	373.37	1.82	311.83	348.34	0.01
8	373.38	1.29	311.25	342.86	0.01
9	373.38	1.02	268.44	344.07	0.01
10	373.39	0.57	267.95	339.76	0.01

1	373.37	4.47	329.72	356.86	0.00
2	373.37	3.91	338.06	354.91	0.00
3	373.37	3.63	328.22	355.54	0.00
4	373.37	3.07	340.87	355.04	0.00
5	373.37	2.78	315.27	351.47	0.01
6	373.37	2.24	353.45	350.08	0.00
7	373.37	1.94	302.49	350.08	0.01
8	373.38	1.43	303.72	345.32	0.01
9	373.38	1.17	267.33	346.08	0.01
10	373.39	0.72	269.93	343.31	0.01
1	373.37	4.40	320.19	356.47	0.00
2	373.37	3.85	333.78	355.63	0.00
3	373.37	3.57	320.09	356.43	0.00
4	373.37	3.02	334.29	353.31	0.00
5	373.37	2.74	307.34	353.75	0.01
6	373.37	2.22	345.88	350.63	0.00
7	373.37	1.92	299.82	351.84	0.01
8	373.38	1.41	300.84	345.93	0.01
9	373.38	1.16	258.66	347.85	0.01
10	373.38	0.72	270.89	344.67	0.01

Appendix C. Experimental Data for non-steam condensing on a bank of Plain Tubes.

C.1. Gogonin (1971).

Fluid	R-21
Outer Diameter / m	0.017
Inner Diameter / m	0.0146
Length / m	0.52
Width / m	0.027
Horizontal Pitch / m	0.027
Vertical Pitch / m	0.0233
Number of odd tubes	1
Number of even tubes	0

Row No.	T_V /K	U_V/ (ms^{-1})	q/ (kW/m^2)	T_W /K	M_C / kgs^{-1}
1	333.15	0.00	5.50	331.10	0.00
1	333.15	0.00	7.50	329.91	0.00
1	333.15	0.00	8.10	329.61	0.00
1	333.15	0.00	10.10	328.50	0.00
1	333.15	0.00	13.90	326.56	0.00
1	333.15	0.00	14.60	326.07	0.00
1	333.15	0.00	15.80	325.17	0.00
1	333.15	0.00	17.20	324.23	0.00
1	333.15	0.00	19.50	322.64	0.00
1	333.15	0.00	20.60	322.14	0.00
1	333.15	0.00	20.50	321.81	0.00
1	333.15	0.00	21.70	321.13	0.00
1	333.15	0.00	24.80	318.74	0.00
1	333.15	0.00	28.50	316.09	0.00
1	333.15	0.00	28.30	315.79	0.00
1	333.15	0.00	29.60	314.96	0.00
1	333.15	0.00	33.20	312.26	0.00
1	333.15	0.04	35.90	312.09	0.00
1	333.15	0.04	27.10	318.92	0.00
1	333.15	0.04	26.30	319.53	0.00
1	333.15	0.04	24.10	321.12	0.00
1	333.15	0.04	19.50	323.57	0.00
1	333.15	0.04	14.70	326.49	0.00
1	333.15	0.04	16.90	325.68	0.00
1	333.15	0.04	15.60	326.51	0.00
1	333.15	0.04	11.30	328.66	0.00
1	333.15	0.04	9.70	329.36	0.00
1	333.15	0.08	7.70	330.42	0.00
1	333.15	0.08	8.70	330.11	0.00
1	333.15	0.08	11.20	328.87	0.00
1	333.15	0.08	14.40	327.74	0.00
1	333.15	0.08	15.70	326.90	0.00

Row No.	T_V /K	U_V/ (ms^{-1})	q/ (kW/m^2)	T_W /K	M_C / kgs^{-1}
1	333.15	0.08	17.60	325.92	0.00
1	333.15	0.08	18.80	325.47	0.00
1	333.15	0.08	19.80	324.84	0.00
1	333.15	0.08	23.20	323.05	0.00
1	333.15	0.08	26.20	321.37	0.00
1	333.15	0.08	25.90	321.09	0.00
1	333.15	0.08	24.50	321.30	0.00
1	333.15	0.08	29.50	318.74	0.00
1	333.15	0.08	31.40	318.74	0.00
1	333.15	0.08	35.40	315.50	0.00
1	333.15	0.08	38.20	313.53	0.00
1	333.15	0.08	41.20	312.33	0.00
1	333.15	0.14	8.40	330.53	0.00
1	333.15	0.14	12.40	328.79	0.00
1	333.15	0.14	13.20	328.46	0.00
1	333.15	0.14	16.00	326.95	0.00
1	333.15	0.14	16.90	326.63	0.00
1	333.15	0.14	17.80	326.42	0.00
1	333.15	0.14	20.20	325.76	0.00
1	333.15	0.14	19.90	325.53	0.00
1	333.15	0.14	21.70	324.72	0.00
1	333.15	0.14	22.80	324.43	0.00
1	333.15	0.14	22.50	323.68	0.00
1	333.15	0.14	25.20	322.81	0.00
1	333.15	0.14	32.70	319.09	0.00
1	333.15	0.14	34.70	317.83	0.00
1	333.15	0.14	34.90	316.57	0.00
1	333.15	0.14	36.50	316.00	0.00
1	333.15	0.14	38.70	315.22	0.00
1	333.15	0.14	43.60	312.71	0.00
1	333.15	0.21	46.80	312.15	0.00
1	333.15	0.21	44.50	313.63	0.00

1	333.15	0.21	44.90	313.77	0.00
1	333.15	0.21	43.10	314.13	0.00
1	333.15	0.21	35.40	318.15	0.00
1	333.15	0.21	36.60	318.11	0.00
1	333.15	0.21	34.40	319.41	0.00
1	333.15	0.21	32.50	320.45	0.00
1	333.15	0.21	28.80	321.89	0.00
1	333.15	0.21	24.40	323.72	0.00

1	333.15	0.21	24.70	324.10	0.00
1	333.15	0.21	21.50	325.22	0.00
1	333.15	0.21	18.80	326.35	0.00
1	333.15	0.21	19.00	326.47	0.00
1	333.15	0.21	16.70	327.33	0.00
1	333.15	0.21	18.90	326.71	0.00
1	333.15	0.21	12.80	328.98	0.00
1	333.15	0.21	12.40	329.29	0.00

C.2. Gogonin (1976).

Fluid	R-21
Outer Diameter / m	0.017
Inner Diameter / m	0.0146
Length / m	0.52
Width / m	0.027
Horizontal Pitch / m	0.027
Vertical Pitch / m	0.0233
Number of odd tubes	1
Number of even tubes	0

Row No.	T_V /K	U_V/ (ms^{-1})	q/ (kW/m^2)	T_W /K	M_C / kgs^{-1}
1	333.15	0.00	5.90	330.91	0.00
1	333.15	0.00	8.20	329.55	0.00
1	333.15	0.00	10.30	328.42	0.00
1	333.15	0.00	11.70	327.52	0.00
1	333.15	0.00	13.90	326.18	0.00
1	333.15	0.00	16.00	324.58	0.00
1	333.15	0.00	17.40	323.65	0.00
1	333.15	0.00	18.90	322.75	0.00
1	333.15	0.00	25.60	317.04	0.00
1	333.15	0.00	33.90	310.46	0.00
1	333.15	0.00	37.20	307.23	0.00
1	333.15	0.00	39.20	305.85	0.00
1	333.15	0.00	44.00	301.53	0.00
1	333.15	0.15	16.00	327.25	0.00
1	333.15	0.15	20.80	324.32	0.00
1	333.15	0.15	20.30	324.16	0.00
1	333.15	0.15	21.80	323.21	0.00
1	333.15	0.15	25.70	320.84	0.00
1	333.15	0.15	26.10	320.26	0.00
1	333.15	0.15	27.90	319.74	0.00
1	333.15	0.15	28.40	319.13	0.00
1	333.15	0.15	30.30	317.02	0.00
1	333.15	0.15	31.90	316.18	0.00
1	333.15	0.15	33.90	315.15	0.00
1	333.15	0.15	38.60	311.36	0.00
1	333.15	0.15	41.60	309.81	0.00
1	333.15	0.15	41.30	308.94	0.00
1	333.15	0.67	11.30	330.00	0.00
1	333.15	0.67	11.00	329.93	0.00
1	333.15	0.67	11.40	329.72	0.00
1	333.15	0.67	17.40	327.27	0.00
1	333.15	0.67	17.70	327.07	0.00
1	333.15	0.67	24.10	324.24	0.00
1	333.15	0.67	25.60	323.34	0.00
1	333.15	0.67	29.20	321.95	0.00
1	333.15	0.67	42.00	313.48	0.00

Row No.	T_V /K	U_V/ (ms^{-1})	q/ (kW/m^2)	T_W /K	M_C / kgs^{-1}
1	333.15	0.67	53.00	307.99	0.00
1	333.15	0.67	55.20	304.27	0.00
1	333.15	0.67	59.90	303.30	0.00
1	333.15	1.04	12.40	330.02	0.00
1	333.15	1.04	12.90	329.89	0.00
1	333.15	1.04	13.90	329.37	0.00
1	333.15	1.04	20.00	326.90	0.00
1	333.15	1.04	22.50	326.18	0.00
1	333.15	1.04	24.40	325.79	0.00
1	333.15	1.04	29.00	323.73	0.00
1	333.15	1.04	31.30	323.32	0.00
1	333.15	1.04	31.30	322.13	0.00
1	333.15	1.04	34.20	320.96	0.00
1	333.15	1.04	38.20	319.66	0.00
1	333.15	1.04	43.10	319.14	0.00
1	333.15	1.04	47.00	315.65	0.00
1	333.15	1.04	51.00	314.38	0.00
1	333.15	1.04	53.90	312.01	0.00
1	333.15	1.04	60.10	310.48	0.00
1	333.15	1.04	65.80	308.33	0.00
1	333.15	1.04	65.90	306.70	0.00
1	333.15	1.04	67.00	306.49	0.00
1	333.15	1.89	20.30	327.96	0.00
1	333.15	1.89	21.60	327.36	0.00
1	333.15	1.89	24.20	326.87	0.00
1	333.15	1.89	24.40	326.38	0.00
1	333.15	1.89	28.80	325.17	0.00
1	333.15	1.89	34.00	323.85	0.00
1	333.15	1.89	34.20	323.50	0.00
1	333.15	1.89	43.20	320.73	0.00
1	333.15	1.89	46.00	320.26	0.00
1	333.15	1.89	48.30	319.85	0.00
1	333.15	1.89	55.90	317.17	0.00
1	333.15	1.89	53.80	317.02	0.00
1	333.15	1.89	61.30	315.44	0.00
1	333.15	1.89	74.30	312.06	0.00

1	333.15	1.89	76.20	310.84	0.00
1	333.15	1.89	82.70	308.94	0.00
1	333.15	1.89	81.80	308.41	0.00
1	333.15	2.04	15.90	329.56	0.00
1	333.15	2.04	17.40	328.85	0.00
1	333.15	2.04	19.80	328.25	0.00
1	333.15	2.04	21.30	327.89	0.00
1	333.15	2.04	22.90	327.48	0.00

1	333.15	2.04	27.20	326.57	0.00
1	333.15	2.04	39.50	323.30	0.00
1	333.15	2.04	43.60	322.03	0.00
1	333.15	2.04	49.10	320.33	0.00
1	333.15	2.04	61.30	317.81	0.00
1	333.15	2.04	68.50	314.31	0.00
1	333.15	2.04	73.10	313.81	0.00
1	333.15	2.04	73.90	312.97	0.00

C.3. Shah (1978).

Fluid	Iso-propanol
Outer Diameter / m	0.0127
Inner Diameter / m	0.0109
Length / m	0.18
Width / m	0.1524
Horizontal Pitch / m	0.0254
Vertical Pitch / m	0.022
Number of odd tubes	6
Number of even tubes	5

Row No.	T_V /K	U_V/ (ms^{-1})	q/ (kW/m^2)	T_W /K	M_C / kgs^{-1}
1	358.69	0.43	52.00	334.46	0.00
2	358.69	0.38	55.60	335.91	0.00
3	358.69	0.33	39.70	331.42	0.00
4	358.69	0.29	47.80	335.23	0.00
5	358.69	0.25	32.60	330.64	0.01
6	358.69	0.22	41.50	334.91	0.01
7	358.69	0.18	26.40	329.93	0.01
8	358.69	0.16	38.20	335.64	0.01
9	358.69	0.13	30.50	334.38	0.01
1	359.07	0.42	44.40	332.97	0.00
2	359.07	0.38	48.90	335.22	0.00
3	359.07	0.34	40.80	334.74	0.00
4	359.07	0.30	47.00	338.02	0.00
5	359.07	0.26	35.60	335.42	0.01
6	359.07	0.22	39.60	337.55	0.01
7	359.07	0.19	22.20	330.87	0.01
8	359.07	0.17	32.10	336.22	0.01
9	359.07	0.14	25.70	338.33	0.01
1	360.09	0.43	54.20	330.97	0.00
2	360.09	0.38	58.20	332.45	0.00
3	360.09	0.33	44.00	328.96	0.00
4	360.09	0.29	50.20	331.60	0.00
5	360.09	0.25	38.00	328.71	0.01
6	360.09	0.21	39.70	329.30	0.01
7	360.09	0.18	28.50	326.28	0.01
8	360.09	0.15	41.90	332.32	0.01
9	360.09	0.12	38.60	333.34	0.01
1	360.56	0.43	55.30	332.08	0.00
2	360.56	0.37	60.10	333.93	0.00
3	360.56	0.33	42.80	328.96	0.00
4	360.56	0.29	50.60	332.41	0.00
5	360.56	0.25	36.90	328.76	0.01
6	360.56	0.21	40.00	330.02	0.01
7	360.56	0.18	26.70	325.97	0.01
8	360.56	0.15	43.10	333.46	0.01
9	360.56	0.12	37.40	333.42	0.01

Row No.	T_V /K	U_V/ (ms^{-1})	q/ (kW/m^2)	T_W /K	M_C / kgs^{-1}
1	359.75	0.43	47.80	330.12	0.00
2	359.75	0.38	56.80	334.36	0.00
3	359.75	0.33	41.70	330.25	0.00
4	359.75	0.29	47.60	333.02	0.00
5	359.75	0.25	36.70	330.61	0.01
6	359.75	0.22	34.20	329.25	0.01
7	359.75	0.19	29.70	329.37	0.01
8	359.75	0.16	40.50	334.64	0.01
9	359.75	0.13	36.30	335.38	0.01
1	369.70	0.30	52.10	343.30	0.00
2	369.70	0.27	56.90	345.44	0.00
3	369.70	0.23	40.70	340.74	0.00
4	369.70	0.21	45.80	342.87	0.00
5	369.70	0.18	33.10	339.65	0.01
6	369.70	0.16	37.00	341.55	0.01
7	369.70	0.14	28.20	339.60	0.01
8	369.70	0.12	38.40	344.73	0.01
9	369.70	0.09	34.40	345.52	0.01
1	361.68	0.38	40.10	340.51	0.00
2	361.68	0.34	46.00	343.92	0.00
3	361.68	0.31	33.80	340.87	0.00
4	361.68	0.28	34.20	341.16	0.00
5	361.68	0.25	25.30	339.12	0.00
6	361.68	0.23	25.60	339.44	0.00
7	361.68	0.21	20.20	338.76	0.01
8	361.68	0.19	32.40	345.62	0.01
9	361.68	0.16	30.00	347.39	0.01
1	361.75	0.37	57.60	334.34	0.00
2	361.75	0.32	55.50	332.79	0.00
3	361.75	0.28	41.30	329.09	0.00
4	361.75	0.24	45.80	330.58	0.00
5	361.75	0.21	37.90	330.24	0.01
6	361.75	0.17	40.70	331.45	0.01
7	361.75	0.14	32.80	330.23	0.01
8	361.75	0.11	31.90	329.70	0.01
9	361.75	0.09	40.90	336.80	0.01

1	362.81	0.38	50.30	336.14	0.00
2	362.81	0.33	56.80	339.18	0.00
3	362.81	0.29	34.10	331.05	0.00
4	362.81	0.26	44.00	335.90	0.00
5	362.81	0.23	33.90	333.81	0.01
6	362.81	0.20	31.40	332.53	0.01
7	362.81	0.18	29.70	334.00	0.01
8	362.81	0.15	34.80	336.51	0.01
9	362.81	0.13	35.80	339.67	0.01
1	362.73	0.37	43.80	334.00	0.00
2	362.73	0.34	55.90	340.35	0.00
3	362.73	0.29	34.40	332.51	0.00
4	362.73	0.26	44.90	338.06	0.00
5	362.73	0.23	32.60	334.78	0.01
6	362.73	0.20	38.40	337.84	0.01
7	362.73	0.18	24.00	332.92	0.01
8	362.73	0.15	29.50	335.82	0.01
9	362.73	0.13	32.60	340.13	0.01
1	362.17	0.37	38.10	339.84	0.00
2	362.17	0.33	47.60	344.95	0.00
3	362.17	0.30	28.40	338.02	0.00
4	362.17	0.27	40.90	344.68	0.00
5	362.17	0.24	26.20	339.87	0.00
6	362.17	0.22	27.80	340.85	0.00
7	362.17	0.20	22.20	340.15	0.01
8	362.17	0.18	31.00	344.82	0.01
9	362.17	0.16	23.70	343.44	0.01
1	362.85	0.35	38.90	338.54	0.00
2	362.85	0.31	49.00	343.32	0.00
3	362.85	0.28	26.60	335.28	0.00
4	362.85	0.25	38.80	341.07	0.00
5	362.85	0.23	25.70	337.13	0.00
6	362.85	0.20	29.60	339.02	0.00
7	362.85	0.18	21.50	337.00	0.01
8	362.85	0.16	33.50	342.66	0.01
9	362.85	0.14	24.10	340.28	0.01
1	363.09	0.36	31.90	339.07	0.00
2	363.09	0.33	51.50	347.96	0.00
3	363.09	0.29	29.40	340.55	0.00
4	363.09	0.27	43.40	346.89	0.00
5	363.09	0.24	19.70	338.25	0.00
6	363.09	0.22	34.60	344.92	0.01
7	363.09	0.19	18.40	339.39	0.01
8	363.09	0.18	35.80	347.19	0.01
9	363.09	0.15	20.90	342.37	0.01

C.4. Shah (1981).

Fluid	Methanol
Outer Diameter / m	0.0127
Inner Diameter / m	0.0109
Length / m	0.18
Width / m	0.1524
Horizontal Pitch / m	0.0254
Vertical Pitch / m	0.022
Number of odd tubes	6
Number of even tubes	5

Row No.	T_V /K	U_V/ (ms^{-1})	q/ (kW/m^2)	T_W /K	M_C / kgs^{-1}
1	341.60	0.40	41.30	328.93	0.00
2	341.60	0.35	38.70	327.14	0.00
3	341.60	0.32	36.20	329.85	0.00
4	341.60	0.28	33.60	328.66	0.00
5	341.60	0.25	31.00	330.86	0.00
6	341.60	0.22	28.40	329.80	0.00
7	341.60	0.20	25.80	331.48	0.00
8	341.60	0.17	23.30	330.49	0.00
9	341.60	0.15	20.70	331.67	0.01
1	341.10	0.41	37.50	322.76	0.00
2	341.10	0.37	35.30	326.85	0.00
3	341.10	0.33	33.10	329.49	0.00
4	341.10	0.30	31.00	328.60	0.00
5	341.10	0.27	28.80	330.80	0.00
6	341.10	0.24	26.70	329.99	0.00
7	341.10	0.22	24.50	331.76	0.00
8	341.10	0.19	22.40	331.02	0.00
9	341.10	0.17	20.20	332.36	0.01
1	341.00	0.45	35.50	330.15	0.00
2	341.00	0.41	33.80	328.93	0.00
3	341.00	0.38	32.10	331.60	0.00
4	341.00	0.35	30.40	331.07	0.00
5	341.00	0.32	28.70	333.41	0.00
6	341.00	0.29	27.00	332.95	0.00
7	341.00	0.26	25.30	334.96	0.00
8	341.00	0.24	23.60	334.54	0.00
9	341.00	0.22	21.90	336.22	0.00
1	341.70	0.42	27.20	333.66	0.00
2	341.70	0.39	25.30	332.55	0.00
3	341.70	0.37	23.40	334.37	0.00
4	341.70	0.34	21.50	333.83	0.00
5	341.70	0.32	19.60	335.26	0.00
6	341.70	0.30	17.70	334.74	0.00
7	341.70	0.29	15.80	335.80	0.00
8	341.70	0.27	13.90	335.28	0.00
9	341.70	0.26	12.00	335.96	0.00

Row No.	T_V /K	U_V/ (ms^{-1})	q/ (kW/m^2)	T_W /K	M_C / kgs^{-1}
1	340.50	0.50	48.30	325.10	0.00
2	340.50	0.45	45.80	323.22	0.00
3	340.50	0.41	43.20	326.06	0.00
4	340.50	0.36	40.60	324.72	0.00
5	340.50	0.32	31.00	329.57	0.00
6	340.50	0.29	35.40	325.92	0.00
7	340.50	0.26	32.80	327.87	0.00
8	340.50	0.22	30.20	326.78	0.00
9	340.50	0.19	27.70	328.29	0.01
1	340.60	0.51	48.10	326.43	0.00
2	340.60	0.46	45.50	324.71	0.00
3	340.60	0.42	42.90	329.16	0.00
4	340.60	0.38	40.40	326.11	0.00
5	340.60	0.34	37.80	328.36	0.00
6	340.60	0.30	35.20	327.20	0.00
7	340.60	0.27	32.60	329.03	0.01
8	340.60	0.23	30.10	327.97	0.00
9	340.60	0.20	27.50	329.37	0.01
1	340.60	0.58	43.00	327.13	0.00
2	340.60	0.53	40.90	325.77	0.00
3	340.60	0.50	38.80	328.35	0.00
4	340.60	0.46	36.70	327.37	0.00
5	340.60	0.42	34.60	329.58	0.00
6	340.60	0.38	32.50	328.70	0.00
7	340.60	0.36	30.40	330.56	0.00
8	340.60	0.32	28.30	329.74	0.00
9	340.60	0.30	26.20	331.25	0.01
1	340.50	0.57	41.90	330.01	0.00
2	340.50	0.52	39.40	328.51	0.00
3	340.50	0.48	36.80	330.79	0.00
4	340.50	0.44	34.30	329.70	0.00
5	340.50	0.41	31.80	331.52	0.00
6	340.50	0.38	29.20	326.06	0.00
7	340.50	0.35	26.70	331.90	0.00
8	340.50	0.32	24.10	330.94	0.00
9	340.50	0.30	21.60	331.91	0.01

1	340.70	0.47	40.00	331.30	0.00
2	340.70	0.42	37.40	329.80	0.00
3	340.70	0.39	34.70	331.90	0.00
4	340.70	0.35	32.10	330.85	0.00
5	340.70	0.32	29.40	332.50	0.00
6	340.70	0.29	26.80	331.52	0.00
7	340.70	0.27	24.10	332.72	0.00
8	340.70	0.24	21.50	331.78	0.00
9	340.70	0.22	18.90	332.53	0.01
1	340.70	0.50	33.10	332.85	0.00
2	340.70	0.47	30.90	331.74	0.00
3	340.70	0.44	28.70	333.49	0.00
4	340.70	0.41	26.50	332.71	0.00
5	340.70	0.39	24.40	334.09	0.00
6	340.70	0.36	22.20	333.35	0.00
7	340.70	0.34	20.00	334.36	0.00
8	340.70	0.32	15.10	334.74	0.00
9	340.70	0.31	15.70	334.28	0.00
1	340.70	0.54	26.90	334.34	0.00
2	340.70	0.51	25.20	333.53	0.00
3	340.70	0.49	23.50	335.09	0.00
4	340.70	0.46	21.90	334.59	0.00
5	340.70	0.44	20.20	335.85	0.00
6	340.70	0.42	18.60	335.36	0.00
7	340.70	0.40	16.90	336.34	0.00
8	340.70	0.38	15.20	335.86	0.00
9	340.70	0.37	13.60	336.54	0.00
1	340.60	0.62	32.80	335.47	0.00
2	340.60	0.59	30.10	334.28	0.00
3	340.60	0.56	27.40	335.55	0.00
4	340.60	0.53	24.70	334.62	0.00
5	340.60	0.51	22.10	335.48	0.00
6	340.60	0.49	19.40	334.57	0.00
7	340.60	0.47	16.70	335.01	0.00
8	340.60	0.45	14.00	334.11	0.00
9	340.60	0.44	11.40	334.14	0.00
1	340.70	0.60	32.30	333.54	0.00
2	340.70	0.57	30.10	332.47	0.00
3	340.70	0.54	27.90	334.05	0.00
4	340.70	0.51	25.70	333.26	0.00
5	340.70	0.49	23.50	334.47	0.00
6	340.70	0.46	21.20	333.72	0.00
7	340.70	0.44	19.00	334.56	0.00
8	340.70	0.42	16.80	333.82	0.00
9	340.70	0.41	14.60	334.31	0.00

C.5. Kutateladze (1981).

Fluid	R-21
Outer Diameter / m	0.016
Inner Diameter / m	0.014
Length / m	0.585
Width / m	0.026
Horizontal Pitch / m	0.026
Vertical Pitch / m	0.0225
Number of odd tubes	1
Number of even tubes	0

Row No.	T_V /K	U_V/ (ms^{-1})	q/ (kW/m^2)	T_W /K	M_C / kgs^{-1}
1	333.15	0.22	51.40	310.65	0.00
3	333.15	0.20	46.40	307.35	0.01
5	333.15	0.18	44.80	306.15	0.01
7	333.15	0.16	43.00	305.75	0.02
9	333.15	0.14	46.20	307.75	0.03
11	333.15	0.12	43.80	307.15	0.03
13	333.15	0.10	42.70	308.65	0.04
15	333.15	0.08	47.80	307.35	0.05
17	333.15	0.00	43.70	308.35	0.05
1	333.15	0.22	51.70	310.15	0.00
3	333.15	0.20	47.60	306.85	0.01
5	333.15	0.18	45.30	305.75	0.01
7	333.15	0.16	43.00	305.45	0.02
9	333.15	0.14	46.40	307.65	0.03
11	333.15	0.12	44.30	307.15	0.03
13	333.15	0.10	41.20	308.65	0.04
15	333.15	0.08	46.80	307.25	0.05
17	333.15	0.00	41.60	308.55	0.05
1	333.15	0.22	34.10	319.65	0.00
3	333.15	0.20	35.00	314.65	0.00
5	333.15	0.19	32.70	317.05	0.01
7	333.15	0.18	28.60	316.75	0.01
9	333.15				
11	333.15				
13	333.15				
15	333.15				
17	333.15				
1	333.15	0.22	24.90	325.15	0.00
3	333.15	0.21	26.60	322.75	0.00
5	333.15	0.20	24.40	322.25	0.01
7	333.15				
9	333.15				
11	333.15				
13	333.15				
15	333.15				
17	333.15				

Row No.	T_V /K	U_V/ (ms^{-1})	q/ (kW/m^2)	T_W /K	M_C / kgs^{-1}
1	333.15	0.22	19.60	326.95	0.00
3	333.15	0.21	19.70	326.25	0.00
5	333.15	0.20	17.80	326.25	0.01
7	333.15	0.19	11.40	325.55	0.01
9	333.15				
11	333.15				
13	333.15				
15	333.15				
17	333.15				
1	333.15	0.22	11.90	330.25	0.00
3	333.15	0.21	11.30	329.75	0.00
5	333.15	0.21	9.20	329.85	0.00
7	333.15				
9	333.15				
11	333.15				
13	333.15				
15	333.15				
17	333.15				
1	333.15	0.22	47.00	309.55	0.00
3	333.15	0.20	45.50	309.65	0.01
5	333.15	0.18	43.10	307.65	0.01
7	333.15	0.16	43.10	307.15	0.02
9	333.15	0.14	42.80	306.85	0.03
11	333.15	0.12	43.80	307.55	0.03
13	333.15	0.11	43.20	308.05	0.04
15	333.15	0.09	40.70	308.85	0.04
17	333.15	0.00	45.80	307.75	0.05
1	333.15	0.22	44.60	310.85	0.00
3	333.15	0.20	41.30	310.65	0.01
5	333.15	0.18	40.60	308.85	0.01
7	333.15	0.17	36.30	308.45	0.02
9	333.15	0.15	38.40	308.55	0.02
11	333.15	0.13	40.70	309.45	0.03
13	333.15	0.12	40.70	309.75	0.03
15	333.15	0.10	37.40	310.15	0.04
17	333.15	0.00	44.10	308.95	0.05

1	333.15	0.22	41.30	313.85	0.00
3	333.15	0.20	37.40	313.85	0.01
5	333.15	0.19	36.70	311.85	0.01
7	333.15	0.17	35.10	311.65	0.02
9	333.15	0.15	35.10	312.25	0.02
11	333.15	0.14	36.90	312.95	0.03
13	333.15	0.12	36.90	313.15	0.03
15	333.15	0.11	34.40	313.65	0.04
17	333.15				
1	333.15	0.22	38.40	315.25	0.00
3	333.15	0.20	36.30	315.75	0.01
5	333.15	0.19	35.10	313.75	0.01
7	333.15	0.17	33.30	313.65	0.02
9	333.15	0.16	32.60	313.75	0.02
11	333.15	0.14	33.50	314.65	0.03
13	333.15	0.13	34.30	314.95	0.03
15	333.15	0.12	30.50	315.25	0.03
17	333.15				
1	333.15	0.22	36.10	316.55	0.00
3	333.15	0.20	34.20	317.35	0.01
5	333.15	0.19	32.90	315.35	0.01
7	333.15	0.18	31.70	314.95	0.01
9	333.15	0.16	31.30	314.95	0.02
11	333.15	0.15	32.70	315.65	0.02
13	333.15				
15	333.15				
17	333.15				
1	333.15	0.22	25.60	322.35	0.00
3	333.15	0.21	24.30	322.95	0.00
5	333.15	0.20	23.80	321.25	0.01
7	333.15	0.19	22.70	320.95	0.01
9	333.15	0.18	21.90	320.95	0.01
11	333.15				
13	333.15				
15	333.15				
17	333.15				
1	333.15	0.22	30.20	319.35	0.00
3	333.15	0.21	29.00	319.75	0.00
5	333.15	0.19	27.50	318.15	0.01
7	333.15	0.18	27.10	317.45	0.01
9	333.15	0.17	27.70	317.55	0.02
11	333.15	0.16	29.00	318.05	0.02
13	333.15				
15	333.15				
17	333.15				
1	333.15	0.22	13.50	328.15	0.00
3	333.15	0.21	12.70	328.95	0.00
5	333.15	0.21	12.50	327.85	0.00
7	333.15	0.20	11.40	327.75	0.01
9	333.15	0.20	10.10	328.25	0.01
11	333.15	0.19	11.20	328.55	0.01
13	333.15				
15	333.15				
17	333.15				
1	333.15	0.22	14.40	328.35	0.00
3	333.15	0.21	11.90	328.85	0.00
5	333.15	0.21	12.00	327.75	0.00
7	333.15	0.20	12.10	327.75	0.01
9	333.15	0.20	11.30	327.55	0.01
11	333.15				
13	333.15				
15	333.15				
17	333.15				
1	333.15	0.44	52.70	309.55	0.00
3	333.15	0.42	52.30	309.25	0.01
5	333.15	0.39	51.40	307.75	0.02
7	333.15	0.37	48.00	307.45	0.02
9	333.15	0.35	48.70	306.85	0.03
11	333.15	0.33	47.60	307.75	0.04
13	333.15	0.31	48.20	307.15	0.04
15	333.15	0.29	45.90	308.55	0.05
17	333.15	0.27	41.30	307.95	0.06
1	333.15	0.44	43.30	315.75	0.00
3	333.15	0.42	38.70	316.45	0.01
5	333.15	0.40	40.70	314.05	0.01
7	333.15	0.39	37.60	313.75	0.02
9	333.15	0.37	37.70	313.45	0.02
11	333.15	0.35	36.20	313.45	0.03
13	333.15	0.34	35.80	313.25	0.03
15	333.15	0.32	32.70	315.15	0.04
17	333.15	0.31	31.20	314.35	0.04
1	333.15	0.44	26.80	324.15	0.00
3	333.15	0.43	24.80	325.45	0.00
5	333.15	0.42	25.20	322.65	0.01
7	333.15	0.41	24.10	322.75	0.01
9	333.15	0.40	23.30	322.65	0.01
11	333.15	0.39	24.80	322.25	0.02
13	333.15	0.37	23.60	322.45	0.02
15	333.15	0.36	22.20	322.85	0.02
17	333.15				
1	333.15	0.44	15.40	328.65	0.00
3	333.15	0.43	14.00	328.75	0.00
5	333.15	0.43	14.70	327.95	0.00
7	333.15	0.42	15.20	328.15	0.01
9	333.15	0.41	12.70	328.35	0.01
11	333.15				

13	333.15				
15	333.15				
17	333.15				
1	333.15	0.44	11.50	329.95	0.00
3	333.15	0.43	9.70	330.15	0.00
5	333.15	0.43	10.40	329.45	0.00
7	333.15	0.42	11.30	329.45	0.00
9	333.15	0.42	8.30	329.85	0.01
11	333.15	0.42	10.70	329.55	0.01
13	333.15				
15	333.15				
17	333.15				
1	333.15	0.44	34.60	319.95	0.00
3	333.15	0.42	33.50	321.15	0.00
5	333.15	0.41	33.20	317.95	0.01
7	333.15	0.40	31.40	318.65	0.01
9	333.15	0.38	30.60	318.05	0.02
11	333.15	0.37	31.40	318.35	0.02
13	333.15	0.36	30.10	319.15	0.03
15	333.15	0.34	27.40	319.05	0.03
17	333.15				
1	333.15	0.44	9.10	331.25	0.00
3	333.15	0.43	8.20	331.35	0.00
5	333.15	0.43	9.00	330.75	0.00
7	333.15				
9	333.15				
11	333.15				
13	333.15				
15	333.15				
17	333.15				
1	333.15	0.44	21.10	326.65	0.00
3	333.15				
5	333.15				
7	333.15				
9	333.15				
11	333.15				
13	333.15				
15	333.15				
17	333.15				
1	333.15	0.44	59.10	309.95	0.00
3	333.15	0.41	55.30	307.45	0.01
5	333.15	0.39	51.40	306.75	0.02
7	333.15	0.37	48.20	306.65	0.02
9	333.15	0.35	51.60	306.65	0.03
11	333.15	0.32	47.70	307.55	0.04
13	333.15	0.30	45.50	309.05	0.04
15	333.15				
17	333.15				

1	333.15	0.44	57.60	311.25	0.00
3	333.15	0.41	54.30	308.95	0.01
5	333.15	0.39	49.80	308.55	0.02
7	333.15	0.37	49.40	308.15	0.02
9	333.15	0.35	52.50	307.45	0.03
11	333.15	0.33	48.00	308.55	0.04
13	333.15				
15	333.15				
17	333.15				
1	333.15	0.44	46.00	316.45	0.00
3	333.15	0.42	43.20	314.85	0.01
5	333.15	0.40	39.80	314.55	0.01
7	333.15	0.38	38.20	314.45	0.02
9	333.15	0.37	41.10	313.95	0.02
11	333.15	0.35	37.60	314.55	0.03
13	333.15	0.33	35.30	315.45	0.04
15	333.15				
17	333.15				
1	333.15	0.44	45.50	316.25	0.00
3	333.15	0.42	43.00	314.55	0.01
5	333.15	0.40	40.30	314.35	0.01
7	333.15	0.38	38.40	314.15	0.02
9	333.15	0.37	41.10	313.65	0.02
11	333.15	0.35	36.70	314.25	0.03
13	333.15	0.33	35.20	315.45	0.03
15	333.15				
17	333.15				
1	333.15	0.44	35.50	321.15	0.00
3	333.15	0.42	33.30	319.65	0.01
5	333.15	0.41	32.10	319.55	0.01
7	333.15	0.40	29.70	319.35	0.01
9	333.15	0.38	33.00	319.05	0.02
11	333.15	0.37	29.20	319.55	0.02
13	333.15	0.36	28.00	320.15	0.03
15	333.15				
17	333.15				
1	333.15	0.44	34.80	321.35	0.00
3	333.15	0.42	32.70	320.15	0.01
5	333.15	0.41	31.50	319.85	0.01
7	333.15	0.40	28.50	319.35	0.01
9	333.15				
11	333.15				
13	333.15				
15	333.15				
17	333.15				
1	333.15	0.43	66.00	303.15	0.00
3	333.15	0.41	59.80	302.15	0.01
5	333.15	0.38	62.00	298.95	0.02

7	333.15	0.35	68.40	300.15	0.03
9	333.15	0.33	64.20	298.65	0.04
11	333.15	0.30	58.70	297.75	0.05
13	333.15	0.27	63.30	298.45	0.05
15	333.15				
17	333.15				
1	333.15	0.43	66.00	302.75	0.00
3	333.15				
5	333.15				
7	333.15				
9	333.15				
11	333.15				
13	333.15				
15	333.15				
17	333.15				
1	333.15	0.88	77.70	310.95	0.00
3	333.15	0.84	70.70	308.85	0.01
5	333.15	0.81	65.50	311.15	0.02
7	333.15	0.79	64.10	310.35	0.03
9	333.15	0.76	62.90	308.45	0.04
11	333.15	0.73	60.80	307.45	0.05
13	333.15	0.71	51.20	306.85	0.06
15	333.15				
17	333.15				
1	333.15	0.88	21.80	328.35	0.00
3	333.15	0.87	18.90	327.45	0.00
5	333.15				
7	333.15				
9	333.15				
11	333.15				
13	333.15				
15	333.15				
17	333.15				
1	333.15				
3	333.15				
5	333.15				
7	333.15				
9	333.15				
11	333.15				
13	333.15				
15	333.15				
17	333.15				
1	333.15	0.88	55.80	314.95	0.00
3	333.15	0.85	49.50	315.35	0.01
5	333.15	0.83	52.40	311.75	0.02
7	333.15	0.81	49.80	314.55	0.02
9	333.15	0.79	47.70	314.25	0.03
11	333.15	0.77	50.10	312.75	0.04
13	333.15	0.75	46.20	313.25	0.04
15	333.15	0.73	43.70	310.85	0.05
17	333.15	0.71	45.90	313.75	0.06
1	333.15				
3	333.15				
5	333.15				
7	333.15				
9	333.15				
11	333.15				
13	333.15				
15	333.15				
17	333.15				
1	333.15	0.88	19.40	328.15	0.00
3	333.15	0.87	19.10	328.65	0.00
5	333.15	0.86	18.60	327.85	0.01
7	333.15	0.85	16.60	328.65	0.01
9	333.15	0.85	14.60	328.45	0.01
11	333.15	0.84	16.40	328.15	0.01
13	333.15	0.83	16.30	328.25	0.01
15	333.15	0.83	15.10	328.15	0.02
17	333.15				
1	333.15	0.88	37.50	323.05	0.00
3	333.15	0.86	36.70	323.55	0.01
5	333.15	0.85	40.00	320.95	0.01
7	333.15	0.83	38.50	322.15	0.02
9	333.15	0.81	37.90	322.25	0.02
11	333.15	0.80	37.60	320.75	0.03
13	333.15	0.78	35.10	320.55	0.03
15	333.15	0.76	33.00	319.85	0.04
17	333.15				
1	333.15	0.88	43.90	319.15	0.00
3	333.15	0.86	39.30	320.05	0.01
5	333.15	0.84	42.10	316.55	0.01
7	333.15	0.82	40.60	319.55	0.02
9	333.15	0.81	39.90	319.85	0.02
11	333.15	0.79	39.30	318.65	0.03
13	333.15	0.77	37.40	318.05	0.03
15	333.15	0.76	34.30	317.35	0.04
17	333.15	0.74	36.80	319.45	0.05
1	333.15	0.88	43.80	319.25	0.00
3	333.15	0.86	38.80	320.55	0.01
5	333.15	0.84	41.70	317.05	0.01
7	333.15	0.82	39.70	319.55	0.02
9	333.15	0.81	39.40	319.75	0.02
11	333.15	0.79	38.90	318.45	0.03
13	333.15	0.77	37.10	318.05	0.03
15	333.15	0.76	34.10	317.55	0.04
17	333.15	0.74	34.90	320.15	0.04

1	333.15				
3	333.15				
5	333.15				
7	333.15				
9	333.15				
11	333.15				
13	333.15				
15	333.15				
17	333.15				
1	333.15				
3	333.15				
5	333.15				
7	333.15				
9	333.15				
11	333.15				
13	333.15				
15	333.15				
17	333.15				
1	333.15	0.88	16.00	329.75	0.00
3	333.15	0.87	13.50	329.55	0.00
5	333.15	0.86	16.10	328.95	0.00
7	333.15	0.86	15.50	329.15	0.01
9	333.15				
11	333.15				
13	333.15				
15	333.15				
17	333.15				
1	333.15	0.88	12.20	330.45	0.00
3	333.15	0.87	13.90	330.35	0.00
5	333.15	0.87	12.40	330.15	0.00
7	333.15	0.86	12.70	330.25	0.01
9	333.15	0.85	9.40	330.95	0.01
11	333.15				
13	333.15				
15	333.15				
17	333.15				
1	333.15	0.88	11.90	331.05	0.00
3	333.15				
5	333.15				
7	333.15				
9	333.15				
11	333.15				
13	333.15				
15	333.15				
17	333.15				
1	333.15	0.88	24.70	327.25	0.00
3	333.15	0.87	21.40	327.55	0.00
5	333.15	0.86	24.80	325.55	0.01
7	333.15	0.85	23.90	326.75	0.01
9	333.15	0.84	22.50	327.05	0.01
11	333.15	0.83	22.80	326.45	0.02
13	333.15				
15	333.15				
17	333.15				
1	333.15	0.88	33.40	323.55	0.00
3	333.15	0.86	31.60	323.85	0.00
5	333.15	0.85	34.30	321.45	0.01
7	333.15	0.83	32.80	322.65	0.01
9	333.15	0.82	32.00	323.05	0.02
11	333.15	0.81	27.60	321.85	0.02
13	333.15	0.79	31.40	321.75	0.03
15	333.15	0.78	28.10	321.15	0.03
17	333.15				
1	333.15	0.85	81.20	306.15	0.00
3	333.15	0.82	64.80	303.45	0.01
5	333.15	0.79	67.50	303.05	0.02
7	333.15				
9	333.15				
11	333.15				
13	333.15				
15	333.15				
17	333.15				
1	333.15	0.85	80.80	307.25	0.00
3	333.15	0.82	74.60	303.45	0.01
5	333.15	0.79	73.70	303.75	0.02
7	333.15				
9	333.15				
11	333.15				
13	333.15				
15	333.15				
17	333.15				
1	333.15				
3	333.15				
5	333.15				
7	333.15				
9	333.15				
11	333.15				
13	333.15				
15	333.15				
17	333.15				
1	333.15				
3	333.15				
5	333.15				
7	333.15				
9	333.15				
11	333.15				

13	333.15				
15	333.15				
17	333.15				
1	333.15				
3	333.15				
5	333.15				
7	333.15				
9	333.15				
11	333.15				
13	333.15				
15	333.15				
17	333.15				
1	333.15	1.61	25.80	328.65	0.00
3	333.15	1.60	24.80	328.15	0.00
5	333.15				
7	333.15				
9	333.15				
11	333.15				
13	333.15				
15	333.15				
17	333.15				
1	333.15	1.61	25.10	328.55	0.00
3	333.15	1.60	25.00	328.45	0.00
5	333.15				
7	333.15				
9	333.15				
11	333.15				
13	333.15				
15	333.15				
17	333.15				
1	333.15	1.61	19.80	330.55	0.00
3	333.15	1.60	20.00	329.35	0.00
5	333.15				
7	333.15				
9	333.15				
11	333.15				
13	333.15				
15	333.15				
17	333.15				
1	333.15	1.61	17.60	330.85	0.00
3	333.15	1.60	17.90	329.95	0.00
5	333.15				
7	333.15				
9	333.15				
11	333.15				
13	333.15				
15	333.15				
17	333.15				

1	333.15				
3	333.15				
5	333.15				
7	333.15				
9	333.15				
11	333.15				
13	333.15				
15	333.15				
17	333.15				
1	333.15	1.61	85.70	318.35	0.00
3	333.15	1.57	81.40	318.85	0.01
5	333.15	1.54	75.60	318.35	0.02
7	333.15	1.50	74.10	315.45	0.03
9	333.15	1.47	73.30	316.35	0.05
11	333.15	1.44	69.80	311.45	0.06
13	333.15	1.41	62.20	314.05	0.07
15	333.15	1.38	73.70	318.05	0.07
17	333.15	1.35	68.70	315.75	0.08
1	333.15				
3	333.15				
5	333.15				
7	333.15				
9	333.15				
11	333.15				
13	333.15				
15	333.15				
17	333.15				
1	333.15	1.61	64.20	322.05	0.00
3	333.15	1.58	60.10	318.45	0.01
5	333.15	1.55	62.30	320.75	0.02
7	333.15	1.53	63.30	320.55	0.03
9	333.15	1.50	62.30	319.95	0.04
11	333.15	1.47	63.20	315.65	0.04
13	333.15	1.45	56.60	317.75	0.05
15	333.15				
17	333.15				
1	333.15	1.61	56.80	323.75	0.00
3	333.15	1.58	54.30	320.85	0.01
5	333.15				
7	333.15				
9	333.15				
11	333.15				
13	333.15				
15	333.15				
17	333.15				
1	333.15				
3	333.15				
5	333.15				

7	333.15				
9	333.15				
11	333.15				
13	333.15				
15	333.15				
17	333.15				
1	333.15	1.68	76.40	315.05	0.00
3	333.15				
5	333.15				
7	333.15				
9	333.15				
11	333.15				
13	333.15				
15	333.15				
17	333.15				
1	333.15	1.68	51.00	321.95	0.00
3	333.15				
5	333.15				
7	333.15				
9	333.15				
11	333.15				
13	333.15				
15	333.15				
17	333.15				
1	333.15	1.68	37.70	325.95	0.00
3	333.15				
5	333.15				
7	333.15				
9	333.15				
11	333.15				
13	333.15				
15	333.15				
17	333.15				
1	333.15	1.68	23.30	328.95	0.00
3	333.15				
5	333.15				
7	333.15				
9	333.15				
11	333.15				
13	333.15				
15	333.15				
17	333.15				
1	333.15	1.68	17.30	330.05	0.00
3	333.15				
5	333.15				
7	333.15				
9	333.15				
11	333.15				

13	333.15				
15	333.15				
17	333.15				
1	333.15	1.68	38.60	325.35	0.00
3	333.15				
5	333.15				
7	333.15				
9	333.15				
11	333.15				
13	333.15				
15	333.15				
17	333.15				
1	333.15	1.68	76.80	314.95	0.00
3	333.15				
5	333.15				
7	333.15				
9	333.15				
11	333.15				
13	333.15				
15	333.15				
17	333.15				
1	333.15	1.62	100.40	308.65	0.00
3	333.15	1.57	93.90	312.15	0.01
5	333.15	1.53	134.10	299.05	0.03
7	333.15	1.47	95.70	310.45	0.05
9	333.15	1.43	101.20	308.35	0.06
11	333.15	1.39	85.90	309.65	0.07
13	333.15				
15	333.15				
17	333.15				
1	333.15	1.62	101.80	308.25	0.00
3	333.15	1.57	92.20	312.05	0.01
5	333.15	1.53	100.00	307.85	0.03
7	333.15	1.49	112.60	301.05	0.04
9	333.15	1.44	99.40	307.85	0.06
11	333.15	1.40	82.10	309.25	0.07
13	333.15				
15	333.15				
17	333.15				
1	333.15	1.62	107.10	312.45	0.00
3	333.15	1.57	98.30	310.05	0.02
5	333.15	1.53	93.50	310.45	0.03
7	333.15	1.49	118.20	309.45	0.04
9	333.15	1.44	98.20	310.75	0.06
11	333.15	1.39	85.00	307.45	0.07
13	333.15				
15	333.15				
17	333.15				

C.6. Cavallini (1985).

Fluid	R-11
Outer Diameter / m	0.01
Inner Diameter / m	0.006
Length / m	0.25
Width / m	0.0266
Horizontal Pitch / m	0.0133
Vertical Pitch / m	0.0115
Number of odd tubes	1
Number of even tubes	2

Row No.	T_V /K	U_V/ (ms^{-1})	q/ (kW/m^2)	T_W /K	M_C / kgs^{-1}
1	306.69	1.01	38.10	290.38	0.00
3	306.69	0.92	36.10	289.96	0.01
5	306.67	0.83	33.30	289.03	0.01
7	306.69	0.75	30.70	288.94	0.01
1	307.14	1.00	38.20	290.67	0.00
3	307.14	0.91	36.70	290.11	0.01
5	307.14	0.82	33.50	289.31	0.01
7	307.14	0.74	31.60	288.92	0.01
1	299.06	0.54	25.90	286.96	0.00
3	299.06	0.46	23.60	287.13	0.00
5	299.06	0.39	21.90	286.70	0.01
7	299.06	0.32	20.80	286.25	0.01
1	300.82	0.75	29.40	287.98	0.00
3	300.80	0.67	26.60	287.68	0.00
5	300.80	0.59	24.80	287.12	0.01
7	300.82	0.52	23.60	286.76	0.01
1	300.46	1.00	29.70	288.17	0.00
3	300.46	0.91	27.70	287.75	0.00
5	300.46	0.83	25.70	287.24	0.01
7	300.46	0.76	24.20	286.94	0.01
1	308.61	0.78	38.00	290.93	0.00
3	308.61	0.69	34.30	290.39	0.00
5	308.61	0.61	31.80	290.01	0.01
7	308.62	0.54	30.00	289.56	0.01
1	318.46	0.71	48.70	294.22	0.00
3	318.46	0.62	45.20	293.68	0.01
5	318.46	0.54	40.60	293.35	0.01
7	318.47	0.47	38.30	292.93	0.02
1	297.54	1.39	27.20	287.45	0.00
3	297.52	1.30	25.60	287.60	0.00
5	297.51	1.22	24.00	286.69	0.01
7	297.49	1.14	23.20	286.11	0.01
1	297.95	1.66	28.50	287.75	0.00
3	297.93	1.57	26.90	288.14	0.00
5	297.91	1.48	25.40	287.07	0.01
7	297.90	1.40	24.30	286.37	0.01

Row No.	T_V /K	U_V/ (ms^{-1})	q/ (kW/m^2)	T_W /K	M_C / kgs^{-1}
1	296.66	2.02	28.00	287.53	0.00
3	296.66	1.93	26.60	287.98	0.00
5	296.66	1.84	25.00	286.96	0.01
7	296.67	1.76	24.00	285.91	0.01
1	297.38	2.14	30.20	287.96	0.00
3	297.35	2.05	28.60	288.62	0.00
5	297.33	1.95	26.90	287.45	0.01
7	297.33	1.87	25.20	286.20	0.01
1	317.82	0.87	49.40	294.41	0.00
3	317.82	0.78	46.90	294.93	0.01
5	317.82	0.69	41.80	293.89	0.01
7	317.82	0.62	38.70	293.07	0.02
1	309.33	1.15	41.20	291.88	0.00
3	309.32	1.06	39.50	293.08	0.01
5	309.32	0.97	35.60	291.05	0.01
7	309.32	0.89	33.30	290.40	0.02
1	308.85	1.34	41.20	291.92	0.00
3	308.84	1.24	39.70	293.36	0.01
5	308.84	1.15	35.90	291.29	0.01
7	308.84	1.07	34.30	290.34	0.02
1	317.51	1.03	50.50	294.56	0.00
3	317.49	0.94	48.60	296.36	0.01
5	317.48	0.85	42.90	293.99	0.01
7	317.48	0.78	40.30	293.04	0.02
1	317.68	1.15	51.20	294.94	0.00
3	317.67	1.06	50.20	297.23	0.01
5	317.66	0.97	45.20	294.47	0.01
7	317.65	0.89	42.10	293.33	0.02
1	317.66	1.46	56.30	296.64	0.00
3	317.64	1.36	55.10	298.93	0.01
5	317.62	1.26	49.90	296.38	0.01
7	317.61	1.17	45.90	294.16	0.02
1	309.40	1.51	42.90	292.54	0.00
3	309.38	1.41	41.70	293.96	0.01
5	309.38	1.31	38.80	292.00	0.01
7	309.39	1.23	35.80	290.77	0.02

1	297.09	2.72	31.30	288.75	0.00
3	297.03	2.62	28.80	289.32	0.00
5	296.99	2.53	27.30	288.02	0.01
7	296.96	2.45	26.20	286.69	0.01
1	297.51	3.28	34.30	289.76	0.00
3	297.42	3.18	31.00	290.47	0.00
5	297.36	3.09	29.50	288.95	0.01
7	297.33	3.00	28.60	287.76	0.01
1	309.45	1.86	47.20	293.90	0.00
3	309.41	1.75	44.30	295.33	0.01
5	309.40	1.65	41.90	293.33	0.01
7	309.40	1.56	38.80	291.07	0.02
1	308.76	2.28	49.90	294.64	0.00
3	308.73	2.17	46.10	296.18	0.01
5	308.71	2.06	43.40	293.99	0.01
7	308.70	1.96	40.60	291.98	0.02
1	308.28	2.73	50.60	295.41	0.00
3	308.22	2.62	46.60	296.81	0.01
5	308.19	2.51	43.70	294.59	0.01
7	308.17	2.41	41.70	293.02	0.02
1	317.57	1.79	60.30	298.42	0.00
3	317.55	1.68	56.90	300.61	0.01
5	317.53	1.58	51.80	297.82	0.02
7	317.54	1.48	48.30	295.20	0.02
1	317.11	2.14	63.80	299.22	0.00
3	317.07	2.02	59.50	301.23	0.01
5	317.06	1.91	54.60	298.31	0.02
7	317.05	1.81	51.60	296.00	0.02
1	316.40	2.51	66.40	299.98	0.00
3	316.34	2.39	61.40	301.08	0.01
5	316.31	2.28	56.00	298.73	0.02
7	316.30	2.18	53.90	296.84	0.02
1	307.54	3.28	52.70	295.78	0.00
3	307.44	3.16	48.10	297.18	0.01
5	307.39	3.05	44.30	294.95	0.01
7	307.38	2.94	42.60	293.66	0.02
1	306.34	3.82	52.30	295.68	0.00
3	306.22	3.70	47.50	297.04	0.01
5	306.16	3.59	43.70	294.92	0.01
7	306.14	3.48	42.10	293.74	0.02
1	306.09	4.25	53.30	296.00	0.00
3	305.95	4.14	48.60	297.41	0.01
5	305.86	4.03	44.60	295.41	0.01
7	305.82	3.92	42.80	294.15	0.02
1	316.10	2.89	69.30	300.59	0.00
3	316.04	2.76	67.00	301.65	0.01
5	316.03	2.63	63.00	298.05	0.02
7	316.01	2.51	62.20	296.17	0.03

1	316.17	3.21	70.90	301.48	0.00
3	316.10	3.08	68.40	302.33	0.01
5	316.08	2.95	64.30	298.57	0.02
7	316.06	2.83	63.30	297.06	0.03
1	316.44	2.90	69.70	301.17	0.00
3	316.37	2.78	67.40	301.91	0.01
5	316.35	2.65	62.80	298.25	0.02
7	316.34	2.53	62.00	296.51	0.03
9	297.15	1.44	23.00	285.67	0.01
11	297.13	1.37	21.70	286.18	0.02
13	297.13	1.29	21.50	286.79	0.02
15	297.13	1.22	22.30	286.87	0.02
9	297.31	1.98	25.10	286.03	0.01
11	297.30	1.89	24.00	286.54	0.02
13	297.28	1.82	23.70	287.54	0.02
15	297.28	1.74	25.50	287.71	0.02
9	306.60	1.04	29.40	288.51	0.02
11	306.60	0.97	28.50	289.11	0.02
13	306.59	0.90	27.80	288.67	0.03
15	306.57	0.82	29.30	289.45	0.03
9	308.98	1.34	34.60	289.50	0.02
11	308.98	1.26	33.30	290.26	0.02
13	308.97	1.19	32.00	290.90	0.03
15	308.96	1.11	34.00	291.16	0.03
9	318.00	0.73	37.20	292.01	0.02
11	318.00	0.67	36.40	292.57	0.03
13	318.00	0.60	36.20	292.31	0.03
15	318.00	0.53	37.50	291.67	0.04
9	317.16	1.07	40.70	292.13	0.02
11	317.14	1.00	38.20	292.75	0.03
13	317.14	0.93	37.50	293.18	0.04
15	317.14	0.85	40.30	293.15	0.04
9	298.32	2.11	26.60	286.64	0.01
11	298.30	2.02	25.20	287.12	0.02
13	298.28	1.94	25.30	288.34	0.02
15	298.26	1.86	27.60	288.55	0.02
9	309.10	1.52	36.00	289.99	0.02
11	309.09	1.43	34.20	290.62	0.03
13	309.08	1.35	33.50	291.60	0.03
15	309.06	1.27	36.70	291.78	0.04
9	309.33	1.87	39.30	290.84	0.02
11	309.32	1.78	37.00	291.33	0.03
13	309.31	1.69	37.20	292.63	0.03
15	309.29	1.60	41.30	293.09	0.04
9	296.96	2.84	26.80	287.01	0.01
11	296.92	2.75	25.50	287.23	0.02
13	296.89	2.67	26.10	289.06	0.02
15	296.87	2.58	28.90	289.01	0.03

9	298.05	3.27	29.40	288.16	0.02
11	298.00	3.18	27.90	288.29	0.02
13	297.94	3.09	28.70	290.33	0.02
15	297.91	3.00	31.80	290.11	0.03
9	308.52	2.34	41.80	291.72	0.02
11	308.50	2.24	39.00	292.03	0.03
13	308.47	2.15	40.10	293.59	0.03
15	308.46	2.05	44.30	294.05	0.04
9	317.40	1.79	49.60	294.26	0.03
11	317.38	1.70	46.30	294.78	0.04
13	317.37	1.62	47.10	296.21	0.04
15	317.37	1.52	52.40	296.95	0.05
9	317.84	1.17	42.40	292.70	0.03
11	317.84	1.09	39.60	293.47	0.03
13	317.83	1.02	39.10	294.17	0.04
15	317.82	0.94	42.40	294.27	0.04
9	317.68	1.47	45.90	293.42	0.03
11	317.68	1.38	42.60	293.98	0.03
13	317.67	1.31	42.20	295.04	0.04
15	317.66	1.22	47.00	295.54	0.05
9	300.31	0.80	22.00	286.53	0.01
11	300.31	0.73	21.50	287.03	0.02
13	300.31	0.67	21.00	287.38	0.02
15	300.31	0.60	22.30	287.14	0.02
9	299.07	1.10	22.80	286.37	0.01
11	299.07	1.03	21.70	286.92	0.02
13	299.07	0.96	21.00	287.31	0.02
15	299.07	0.90	22.50	287.44	0.02
9	308.57	0.80	29.40	289.39	0.02
11	308.57	0.74	28.50	289.96	0.02
13	308.57	0.67	28.00	290.22	0.03
15	308.57	0.60	29.50	290.02	0.03
9	308.76	1.18	33.00	289.63	0.02
11	308.76	1.11	31.10	290.32	0.02
13	308.76	1.04	29.80	291.06	0.03
15	308.76	0.96	31.90	291.36	0.03
9	297.52	1.69	23.90	286.17	0.01
11	297.50	1.61	22.80	286.60	0.02
13	297.47	1.54	21.90	287.60	0.02
15	297.45	1.47	24.50	287.52	0.02
9	317.45	0.90	37.90	292.24	0.02
11	317.45	0.83	35.90	293.09	0.03
13	317.45	0.76	35.60	293.26	0.03
15	317.45	0.69	38.30	292.57	0.04
9	297.85	0.66	19.50	285.83	0.01
11	297.85	0.59	18.80	286.25	0.01
13	297.83	0.53	18.70	286.37	0.02
15	297.81	0.47	20.30	285.82	0.02

9	297.78	0.51	18.80	285.78	0.01
11	297.78	0.45	18.70	286.21	0.01
13	297.78	0.39	18.30	286.26	0.02
15	297.78	0.33	19.50	285.60	0.02
9	307.92	2.76	42.50	292.35	0.02
11	307.89	2.66	40.60	292.53	0.03
13	307.86	2.57	40.60	294.64	0.04
15	307.85	2.46	46.50	294.65	0.04
9	308.08	3.15	44.40	293.14	0.03
11	308.05	3.05	42.40	293.17	0.03
13	308.03	2.95	42.40	295.51	0.04
15	308.00	2.84	48.90	295.48	0.04
9	306.29	3.76	44.10	292.98	0.02
11	306.24	3.66	42.40	293.07	0.03
13	306.18	3.55	42.40	295.56	0.04
15	306.13	3.45	48.70	295.41	0.04
9	306.84	4.14	45.90	293.80	0.03
11	306.78	4.04	44.50	293.86	0.03
13	306.71	3.93	44.60	296.70	0.04
15	306.65	3.82	51.70	296.19	0.04
9	317.38	2.04	51.30	295.44	0.03
11	317.36	1.95	48.30	295.73	0.04
13	317.34	1.86	48.80	297.81	0.04
15	317.33	1.76	56.00	298.10	0.05
9	316.44	2.46	53.40	296.42	0.03
11	316.42	2.37	50.70	296.43	0.04
13	316.40	2.27	51.40	298.81	0.05
15	316.37	2.17	58.80	299.05	0.05
9	316.74	2.79	56.30	297.26	0.04
11	316.71	2.69	53.50	297.32	0.04
13	316.69	2.59	54.20	299.76	0.05
15	316.67	2.48	62.40	300.00	0.06
9	315.81	3.20	57.00	297.84	0.04
11	315.78	3.10	54.30	297.88	0.04
13	315.73	2.99	55.80	300.26	0.05
15	315.70	2.88	62.70	300.53	0.06
9	317.71	1.16	41.30	293.01	0.03
11	317.71	1.08	38.90	293.94	0.03
13	317.71	1.01	38.60	294.76	0.04
15	317.71	0.94	42.20	294.66	0.04
9	301.30	0.70	22.60	287.08	0.01
11	301.30	0.64	22.00	287.64	0.02
13	301.30	0.57	21.90	287.89	0.02
15	301.30	0.51	23.60	287.59	0.02
9	300.71	0.99	23.50	287.09	0.01
11	300.71	0.92	22.40	287.61	0.02
13	300.71	0.85	22.10	287.96	0.02
15	300.71	0.78	24.10	288.07	0.02

9	308.84	0.75	28.90	289.66	0.02
11	308.84	0.68	28.20	290.31	0.02

13	308.84	0.61	28.20	290.40	0.03
15	308.84	0.55	30.30	289.89	0.03

C.7. Cavallini (1988).

Fluid	R-113
Outer Diameter / m	0.01
Inner Diameter / m	0.006
Length / m	0.25
Width / m	0.0266
Horizontal Pitch / m	0.0133
Vertical Pitch / m	0.0115
Number of odd tubes	1
Number of even tubes	2

Row No.	T_V /K	U_V/ (ms^{-1})	q/ (kW/m^2)	T_W /K	M_C / kgs^{-1}
9	321.96	4.03	27.60	314.88	0.02
11	321.83	3.96	27.20	314.53	0.02
13	321.69	3.89	25.90	314.35	0.03
15	321.62	3.82	22.90	314.97	0.03
9	323.86	1.83	24.30	311.97	0.02
11	323.84	1.76	23.60	311.87	0.02
13	323.82	1.69	22.40	311.90	0.02
15	323.80	1.63	20.50	312.81	0.03
9	321.31	3.01	23.40	313.70	0.01
11	321.23	2.94	22.70	313.63	0.02
13	321.13	2.88	21.80	313.62	0.02
15	321.10	2.81	19.50	314.26	0.03
9	323.47	0.93	16.00	312.00	0.01
11	323.45	0.88	15.00	311.89	0.01
13	323.43	0.83	14.00	311.80	0.02
15	323.43	0.79	12.50	312.37	0.02
9	321.89	4.54	33.50	313.88	0.02
11	321.74	4.45	32.60	313.46	0.03
13	321.61	4.37	31.20	313.44	0.03
15	321.53	4.28	28.40	314.05	0.04
9	321.56	4.10	51.60	307.10	0.03
11	321.45	3.95	50.50	306.60	0.04
13	321.35	3.80	49.10	306.73	0.05
15	321.28	3.65	46.70	307.86	0.06
9	322.40	0.96	25.90	299.94	0.02
11	322.40	0.88	24.90	299.69	0.02
13	322.40	0.80	24.80	300.08	0.03
15	322.40	0.73	24.40	301.05	0.03
9	323.16	1.91	38.00	303.11	0.03
11	323.15	1.79	37.00	302.75	0.03
13	323.13	1.68	35.40	302.96	0.04
15	323.11	1.58	34.10	304.31	0.05
9	321.85	2.96	46.60	305.07	0.03
11	321.80	2.82	45.50	304.56	0.04
13	321.76	2.68	43.20	305.19	0.05
15	321.72	2.55	41.20	306.40	0.05

Row No.	T_V /K	U_V/ (ms^{-1})	q/ (kW/m^2)	T_W /K	M_C / kgs^{-1}
9	322.74	4.78	57.70	308.50	0.04
11	322.61	4.63	57.00	307.60	0.05
13	322.48	4.47	54.60	308.47	0.06
15	322.39	4.32	50.50	309.34	0.07
9	320.40	1.03	34.00	288.80	0.03
11	320.40	0.92	33.30	288.53	0.03
13	320.40	0.81	33.40	289.17	0.04
15	320.40	0.70	34.60	290.67	0.04
9	321.55	2.01	51.10	293.76	0.04
11	321.55	1.85	49.40	293.16	0.05
13	321.55	1.69	47.30	293.44	0.05
15	321.53	1.54	46.30	294.80	0.06
9	321.85	3.06	64.90	297.32	0.05
11	321.81	2.86	64.40	296.19	0.06
13	321.77	2.66	60.40	297.43	0.07
15	321.73	2.47	58.70	299.11	0.08
9	321.68	4.14	73.10	300.12	0.05
11	321.60	3.91	72.80	298.68	0.06
13	321.53	3.69	69.00	299.90	0.07
15	321.45	3.48	67.50	301.60	0.08
9	321.98	5.08	79.00	302.87	0.05
11	321.85	4.85	80.20	300.43	0.07
13	321.72	4.62	74.20	302.22	0.08
15	321.64	4.40	72.60	303.36	0.09
9	321.23	5.13	27.20	315.43	0.02
11	321.03	5.07	27.70	314.71	0.02
13	320.84	5.01	25.10	315.06	0.03
15	320.71	4.96	22.20	315.31	0.03
1	323.11	4.84	31.00	317.06	0.00
3	322.83	4.79	32.70	316.83	0.01
5	322.65	4.72	30.80	316.81	0.01
7	322.47	4.64	31.70	316.82	0.02
1	322.55	3.96	28.50	316.38	0.00
3	322.39	3.89	28.60	316.02	0.00
5	322.24	3.82	28.20	316.06	0.01
7	322.12	3.74	28.90	316.01	0.01

1	322.24	4.96	30.00	316.88	0.00
3	321.96	4.91	30.10	316.52	0.00
5	321.75	4.84	29.90	316.43	0.01
7	321.55	4.78	31.00	316.46	0.01
1	323.35	0.92	18.60	313.95	0.00
3	323.35	0.86	18.80	313.10	0.00
5	323.35	0.81	17.70	313.19	0.01
7	323.36	0.75	16.80	313.03	0.01
1	321.67	2.96	22.40	315.51	0.00
3	321.56	2.90	23.40	315.25	0.00
5	321.50	2.83	23.10	315.51	0.01
7	321.43	2.76	23.40	315.43	0.01
1	323.92	1.88	25.20	313.60	0.00
3	323.91	1.80	27.40	313.64	0.00
5	323.89	1.72	27.00	313.76	0.01
7	323.86	1.64	26.70	313.52	0.01
1	322.77	4.52	32.90	316.08	0.00
3	322.56	4.45	34.20	315.97	0.01
5	322.43	4.36	33.60	315.86	0.01
7	322.25	4.28	34.10	315.81	0.02
1	321.95	0.99	33.40	303.27	0.00
3	321.95	0.89	33.10	302.19	0.01
5	321.95	0.78	30.00	301.72	0.01
7	321.94	0.69	28.10	300.95	0.02
1	322.08	3.04	48.10	307.89	0.00
3	321.99	2.89	51.40	307.62	0.01
5	321.93	2.73	50.40	307.54	0.02
7	321.88	2.58	50.30	307.65	0.02
1	322.22	2.97	72.10	301.01	0.00
3	322.13	2.75	73.40	301.01	0.01
5	322.09	2.53	69.90	301.21	0.02
7	322.06	2.31	69.80	300.55	0.03
1	320.16	1.04	45.00	293.09	0.00
3	320.16	0.89	45.10	291.86	0.01
5	320.16	0.75	39.30	291.21	0.01
7	320.17	0.62	36.40	289.71	0.02

1	321.68	1.99	57.80	297.16	0.00
3	321.62	1.81	60.40	297.76	0.01
5	321.60	1.62	56.80	297.94	0.02
7	321.59	1.44	55.00	296.70	0.03
1	321.68	1.99	57.70	297.16	0.00
3	321.62	1.81	60.60	297.76	0.01
5	321.60	1.62	56.80	297.94	0.02
7	321.59	1.44	57.10	295.68	0.03
1	321.68	1.99	56.90	297.16	0.00
3	321.62	1.81	59.90	297.76	0.01
5	321.60	1.62	56.50	297.94	0.02
7	321.59	1.45	49.80	298.95	0.03
1	322.05	4.02	76.60	303.73	0.00
3	321.88	3.80	79.20	303.65	0.01
5	321.79	3.56	76.00	303.93	0.03
7	321.66	3.33	76.40	303.18	0.04
1	322.85	4.92	83.00	305.42	0.00
3	322.61	4.69	86.70	305.89	0.01
5	322.39	4.46	83.40	305.49	0.03
7	322.21	4.22	84.00	304.73	0.04
1	323.29	1.91	41.80	305.37	0.00
3	323.24	1.78	44.40	305.69	0.01
5	323.22	1.65	42.40	306.09	0.01
7	323.22	1.52	41.70	305.31	0.02
1	322.05	4.04	51.90	309.70	0.00
3	321.88	3.90	54.90	309.58	0.01
5	321.73	3.74	52.40	309.90	0.02
7	321.60	3.59	53.20	309.41	0.03
1	323.20	4.69	58.20	310.93	0.00
3	322.97	4.55	60.80	310.95	0.01
5	322.76	4.39	58.20	310.95	0.02
7	322.59	4.23	59.50	310.55	0.03
1	322.41	3.91	28.40	316.05	0.00
3	322.22	3.85	28.90	315.91	0.00
5	322.11	3.77	28.00	316.17	0.01
7	322.02	3.69	28.10	315.90	0.01

C.8. Honda-1 (1989).

Fluid	R-113
Outer Diameter / m	0.0159
Inner Diameter / m	0.0149
Length / m	0.1
Width / m	0.066
Horizontal Pitch / m	0.022
Vertical Pitch / m	0.022
Number of odd tubes	3
Number of even tubes	3

Row No.	T_V /K	U_V/ (ms^{-1})	q/ (kW/m^2)	T_W /K	M_C / kgs^{-1}
1	324.70	3.09	63.50	300.50	0.00
2	324.68	2.97	65.00	300.00	0.01
3	324.65	2.85	63.60	300.26	0.01
4	324.63	2.74	56.80	300.89	0.02
5	324.61	2.63	57.90	299.40	0.03
6	324.59	2.53	57.60	298.33	0.03
7	324.57	2.42	54.70	297.59	0.04
8	324.56	2.32	47.40	298.48	0.04
9	324.54	2.23	49.80	297.37	0.05
10	324.53	2.14	45.00	296.74	0.05
11	324.51	2.05	43.90	297.81	0.06
12	324.50	1.97	46.50	295.90	0.06
13	324.49	1.88	46.10	297.49	0.07
14	324.48	1.80	51.70	295.55	0.07
15	324.47	1.70	46.60	299.62	0.08
1	324.43	3.04	54.40	304.12	0.00
2	324.41	2.94	55.10	304.13	0.01
3	324.38	2.84	53.60	304.25	0.01
4	324.36	2.74	49.20	304.28	0.02
5	324.34	2.65	50.20	303.09	0.02
6	324.32	2.55	49.10	302.26	0.03
7	324.30	2.46	47.20	301.75	0.03
8	324.28	2.38	41.60	302.39	0.04
9	324.27	2.30	42.10	301.98	0.04
10	324.25	2.22	39.40	301.48	0.05
11	324.24	2.15	39.80	301.41	0.05
12	324.23	2.07	40.50	300.94	0.05
13	324.22	1.99	39.60	302.53	0.06
14	324.21	1.92	44.50	301.21	0.06
15	324.20	1.84	42.30	303.44	0.07
1	324.68	3.02	43.80	308.85	0.00
2	324.65	2.94	43.30	309.04	0.00
3	324.63	2.86	41.10	309.19	0.01
4	324.60	2.79	38.80	308.92	0.01
5	324.58	2.72	39.30	308.02	0.02

Row No.	T_V /K	U_V/ (ms^{-1})	q/ (kW/m^2)	T_W /K	M_C / kgs^{-1}
6	324.56	2.64	38.80	307.56	0.02
7	324.54	2.57	37.20	307.15	0.03
8	324.53	2.50	34.20	307.25	0.03
9	324.51	2.44	33.40	307.41	0.03
10	324.49	2.38	32.10	307.12	0.04
11	324.48	2.32	32.70	306.83	0.04
12	324.46	2.26	32.60	306.73	0.04
13	324.45	2.20	32.00	308.08	0.05
14	324.43	2.14	35.20	307.21	0.05
15	324.42	2.07	34.70	308.44	0.05
1	324.21	3.01	32.70	313.47	0.00
2	324.19	2.95	31.50	313.65	0.00
3	324.16	2.89	29.40	313.68	0.01
4	324.14	2.84	27.10	313.51	0.01
5	324.12	2.79	27.10	313.06	0.01
6	324.10	2.74	27.40	312.56	0.02
7	324.08	2.69	26.40	312.30	0.02
8	324.06	2.64	25.00	312.40	0.02
9	324.04	2.59	23.80	312.58	0.02
10	324.02	2.55	24.20	312.39	0.03
11	324.00	2.51	24.10	312.13	0.03
12	323.99	2.46	24.40	312.17	0.03
13	323.97	2.42	23.50	313.18	0.03
14	323.95	2.37	26.20	312.61	0.04
15	323.94	2.32	25.80	313.20	0.04
1	324.24	3.00	25.00	316.29	0.00
2	324.21	2.96	24.40	316.38	0.00
3	324.19	2.91	22.70	316.40	0.01
4	324.17	2.87	21.00	316.18	0.01
5	324.15	2.83	20.90	316.01	0.01
6	324.12	2.79	21.00	315.68	0.01
7	324.10	2.76	20.50	315.36	0.01
8	324.08	2.72	19.30	315.62	0.02
9	324.06	2.68	18.10	315.71	0.02
10	324.04	2.65	18.60	315.47	0.02

11	324.02	2.62	18.50	315.38	0.02
12	324.00	2.58	18.70	315.33	0.02
13	323.99	2.55	18.40	316.14	0.03
14	323.97	2.52	20.00	315.70	0.03
15	323.95	2.48	20.00	316.03	0.03
1	324.59	3.05	18.90	318.91	0.00
2	324.57	3.02	18.00	318.85	0.00
3	324.54	2.99	16.70	318.94	0.00
4	324.52	2.96	15.20	318.90	0.01
5	324.50	2.93	15.80	318.45	0.01
6	324.47	2.90	16.00	318.19	0.01
7	324.45	2.87	15.30	318.16	0.01
8	324.43	2.85	14.40	318.44	0.01
9	324.41	2.82	13.60	318.29	0.01
10	324.38	2.80	13.80	318.58	0.01
11	324.36	2.77	13.60	318.48	0.02
12	324.34	2.75	14.30	318.10	0.02
13	324.32	2.72	13.40	318.64	0.02
14	324.30	2.70	15.30	318.41	0.02
15	324.28	2.67	15.30	318.72	0.02
1	324.46	3.09	13.30	320.86	0.00
2	324.43	3.07	12.80	320.80	0.00
3	324.41	3.05	12.00	320.89	0.00
4	324.38	3.03	10.70	320.82	0.00
5	324.36	3.01	12.00	320.96	0.01
6	324.33	2.99	11.60	320.60	0.01
7	324.31	2.97	11.10	320.34	0.01
8	324.29	2.95	9.80	320.83	0.01
9	324.26	2.93	9.60	320.74	0.01
10	324.24	2.92	10.40	320.51	0.01
11	324.22	2.90	9.80	320.65	0.01
12	324.19	2.88	10.60	320.29	0.01
13	324.17	2.86	10.00	320.75	0.01
14	324.15	2.85	11.30	320.37	0.01
15	324.13	2.83	10.90	320.67	0.02
1	324.43	4.16	68.50	303.49	0.00
2	324.38	4.04	72.20	302.67	0.01
3	324.34	3.91	69.40	303.36	0.01
4	324.30	3.78	63.40	303.99	0.02
5	324.26	3.66	65.20	302.47	0.03
6	324.22	3.55	67.10	300.93	0.03
7	324.19	3.42	63.40	300.26	0.04
8	324.15	3.31	56.00	301.21	0.05
9	324.12	3.20	57.90	300.31	0.05
10	324.10	3.09	54.20	299.93	0.06
11	324.07	2.99	53.90	300.75	0.07
12	324.05	2.89	56.90	299.20	0.07
13	324.02	2.79	52.60	301.99	0.08
14	324.00	2.69	60.30	300.13	0.08
15	323.98	2.57	55.30	303.19	0.09
1	324.57	4.24	60.10	306.73	0.00
2	324.52	4.13	63.20	306.58	0.01
3	324.47	4.02	62.00	306.67	0.01
4	324.43	3.91	56.10	306.95	0.02
5	324.38	3.81	57.70	305.94	0.02
6	324.34	3.70	58.20	304.95	0.03
7	324.31	3.60	55.60	304.40	0.04
8	324.27	3.50	50.70	304.74	0.04
9	324.24	3.40	50.80	304.36	0.05
10	324.21	3.31	48.00	304.20	0.05
11	324.18	3.22	49.30	304.22	0.06
12	324.15	3.13	50.40	303.67	0.06
13	324.12	3.04	46.70	306.08	0.07
14	324.10	2.95	53.10	304.68	0.07
15	324.08	2.85	51.50	306.23	0.08
1	324.62	4.32	47.40	311.15	0.00
2	324.57	4.24	49.00	311.05	0.00
3	324.52	4.15	47.50	311.11	0.01
4	324.47	4.07	43.50	311.44	0.01
5	324.43	3.99	44.50	310.54	0.02
6	324.39	3.91	43.80	310.08	0.02
7	324.35	3.84	42.80	309.48	0.03
8	324.31	3.76	40.20	309.60	0.03
9	324.27	3.69	38.80	309.40	0.04
10	324.23	3.62	38.30	309.39	0.04
11	324.20	3.55	39.10	309.34	0.05
12	324.16	3.48	39.70	309.08	0.05
13	324.13	3.41	36.50	310.94	0.05
14	324.10	3.34	41.80	309.93	0.06
15	324.07	3.26	41.20	310.86	0.06
1	324.38	4.34	40.10	313.45	0.00
2	324.32	4.27	41.30	313.39	0.00
3	324.27	4.20	40.60	313.44	0.01
4	324.23	4.13	36.50	313.63	0.01
5	324.18	4.07	37.50	312.95	0.02
6	324.14	4.00	36.30	312.67	0.02
7	324.09	3.94	36.40	312.09	0.02
8	324.05	3.87	33.90	312.15	0.03
9	324.01	3.81	33.00	312.11	0.03
10	323.97	3.75	31.50	312.06	0.03
11	323.93	3.70	33.50	311.99	0.04
12	323.90	3.64	34.00	311.81	0.04
13	323.86	3.58	30.80	313.36	0.04
14	323.83	3.52	36.10	312.54	0.05
15	323.79	3.46	35.50	313.20	0.05
1	324.46	4.37	32.00	315.97	0.00

2	324.41	4.32	32.90	315.88	0.00
3	324.36	4.26	31.20	316.05	0.01
4	324.31	4.21	28.60	316.04	0.01
5	324.26	4.16	29.20	315.48	0.01
6	324.21	4.11	28.90	315.26	0.02
7	324.17	4.06	27.90	315.00	0.02
8	324.12	4.02	26.00	315.23	0.02
9	324.08	3.97	25.50	314.95	0.02
10	324.04	3.93	24.70	315.38	0.03
11	324.00	3.88	26.50	314.78	0.03
12	323.96	3.84	26.80	314.66	0.03
13	323.92	3.79	24.50	315.92	0.04
14	323.88	3.75	27.90	315.27	0.04
15	323.84	3.70	28.00	315.64	0.04
1	324.18	4.23	25.10	317.81	0.00
2	324.14	4.19	25.20	317.83	0.00
3	324.09	4.15	24.20	317.69	0.01
4	324.04	4.11	22.50	317.59	0.01
5	324.00	4.07	22.40	317.45	0.01
6	323.95	4.03	22.50	317.25	0.01
7	323.91	3.99	21.50	317.07	0.01
8	323.87	3.96	20.40	317.09	0.02
9	323.82	3.92	19.20	317.23	0.02
10	323.78	3.89	19.60	317.10	0.02
11	323.74	3.86	20.40	316.90	0.02
12	323.70	3.83	21.00	316.62	0.03
13	323.66	3.79	19.60	317.43	0.03
14	323.63	3.76	21.90	317.11	0.03
15	323.59	3.72	22.10	317.18	0.03
1	324.57	4.12	18.60	320.21	0.00
2	324.52	4.09	17.60	320.13	0.00
3	324.48	4.06	16.40	320.17	0.00
4	324.43	4.04	14.70	320.22	0.01
5	324.39	4.02	14.80	320.06	0.01
6	324.34	3.99	15.30	319.80	0.01
7	324.30	3.97	15.70	319.67	0.01
8	324.26	3.95	13.80	319.88	0.01
9	324.22	3.92	12.60	320.00	0.01
10	324.18	3.90	14.00	319.78	0.01
11	324.14	3.88	13.90	319.61	0.02
12	324.10	3.86	14.20	319.52	0.02
13	324.06	3.84	13.50	319.97	0.02
14	324.02	3.82	14.90	319.82	0.02
15	323.98	3.79	14.40	319.96	0.02
1	324.35	4.17	18.40	320.09	0.00
2	324.30	4.14	17.80	319.87	0.00
3	324.26	4.11	16.10	320.09	0.00
4	324.21	4.09	15.00	319.95	0.01
5	324.16	4.07	15.00	319.88	0.01
6	324.12	4.04	15.60	319.57	0.01
7	324.08	4.02	15.00	319.34	0.01
8	324.03	4.00	13.90	319.58	0.01
9	323.99	3.97	12.90	319.82	0.01
10	323.95	3.95	13.90	319.50	0.01
11	323.91	3.93	13.90	319.40	0.02
12	323.87	3.91	14.20	319.36	0.02
13	323.83	3.89	13.50	319.83	0.02
14	323.79	3.87	14.60	319.39	0.02
15	323.75	3.84	15.00	319.59	0.02
1	324.29	4.16	19.20	319.90	0.00
2	324.25	4.13	19.00	319.71	0.00
3	324.20	4.10	17.00	319.93	0.00
4	324.15	4.07	15.80	319.95	0.01
5	324.11	4.05	15.70	319.59	0.01
6	324.07	4.02	16.50	319.06	0.01
7	324.02	4.00	15.90	319.16	0.01
8	323.98	3.97	14.40	319.47	0.01
9	323.94	3.95	13.50	319.30	0.01
10	323.90	3.93	14.80	319.32	0.02
11	323.86	3.91	14.60	319.26	0.02
12	323.81	3.88	15.10	319.20	0.02
13	323.78	3.86	14.30	319.64	0.02
14	323.74	3.84	16.10	319.21	0.02
15	323.70	3.81	15.70	319.44	0.02
1	324.32	1.23	36.20	298.80	0.00
2	324.32	1.16	33.50	298.28	0.00
3	324.31	1.10	32.60	298.17	0.01
4	324.31	1.04	31.80	298.23	0.01
5	324.31	0.98	29.80	297.24	0.01
6	324.30	0.92	26.70	297.32	0.02
7	324.30	0.87	27.00	295.63	0.02
8	324.30	0.82	25.10	294.82	0.02
9	324.30	0.77	24.50	296.33	0.03
10	324.30	0.73	22.40	295.68	0.03
11	324.29	0.68	23.70	295.81	0.03
12	324.29	0.64	23.50	295.53	0.03
13	324.29	0.59	24.30	296.18	0.03
14	324.29	0.55	25.20	295.49	0.04
15	324.29	0.50	24.50	296.32	0.04
1	324.51	1.22	31.90	303.31	0.00
2	324.51	1.16	28.40	302.86	0.00
3	324.50	1.11	27.50	302.72	0.01
4	324.50	1.06	27.40	302.80	0.01
5	324.50	1.00	26.00	302.18	0.01
6	324.50	0.96	23.10	302.42	0.01
7	324.49	0.91	22.80	300.82	0.02

8	324.49	0.87	22.20	299.98	0.02
9	324.49	0.83	20.80	301.48	0.02
10	324.49	0.79	19.60	300.78	0.02
11	324.48	0.75	20.60	300.55	0.03
12	324.48	0.71	20.20	300.61	0.03
13	324.48	0.68	20.70	301.23	0.03
14	324.48	0.64	21.30	300.67	0.03
15	324.48	0.60	21.10	301.03	0.03
1	324.62	1.18	26.30	308.20	0.00
2	324.62	1.13	23.00	307.83	0.00
3	324.61	1.09	21.80	307.79	0.01
4	324.61	1.05	22.10	307.86	0.01
5	324.61	1.01	21.10	307.34	0.01
6	324.60	0.97	20.10	306.64	0.01
7	324.60	0.93	18.60	306.28	0.01
8	324.60	0.89	17.70	306.15	0.02
9	324.60	0.86	16.80	306.59	0.02
10	324.60	0.83	16.10	306.31	0.02
11	324.59	0.80	16.80	305.98	0.02
12	324.59	0.77	16.40	306.09	0.02
13	324.59	0.74	16.70	306.57	0.02
14	324.59	0.71	17.50	306.21	0.03
15	324.59	0.67	17.70	306.31	0.03
1	324.29	1.24	20.90	312.53	0.00
2	324.29	1.20	17.80	312.25	0.00
3	324.29	1.17	16.80	312.28	0.00
4	324.28	1.14	17.20	312.49	0.01
5	324.28	1.10	16.40	311.99	0.01
6	324.28	1.07	15.80	311.34	0.01
7	324.27	1.04	14.50	311.20	0.01
8	324.27	1.01	12.30	311.01	0.01
9	324.27	0.99	13.10	311.24	0.01
10	324.26	0.97	13.90	311.12	0.02
11	324.26	0.94	13.20	310.84	0.02
12	324.26	0.92	12.70	311.00	0.02
13	324.26	0.89	13.00	311.37	0.02
14	324.25	0.87	13.60	311.12	0.02
15	324.25	0.84	14.20	311.03	0.02
1	324.62	1.20	17.60	315.40	0.00
2	324.62	1.17	15.10	315.30	0.00
3	324.61	1.14	14.10	315.32	0.00
4	324.61	1.11	14.30	315.46	0.00
5	324.61	1.09	13.90	314.98	0.01
6	324.60	1.06	13.60	314.46	0.01
7	324.60	1.03	12.60	314.35	0.01
8	324.60	1.01	11.90	314.50	0.01
9	324.59	0.99	11.20	314.51	0.01
10	324.59	0.97	11.30	314.34	0.01
11	324.59	0.95	11.40	314.27	0.01
12	324.59	0.93	11.20	314.14	0.02
13	324.58	0.90	11.30	314.57	0.02
14	324.58	0.88	12.10	314.23	0.02
15	324.58	0.86	12.60	314.12	0.02
1	324.65	1.19	13.50	318.11	0.00
2	324.64	1.17	11.30	317.98	0.00
3	324.64	1.14	10.40	317.95	0.00
4	324.64	1.12	10.30	318.07	0.00
5	324.63	1.11	10.20	318.18	0.00
6	324.63	1.09	10.00	317.45	0.01
7	324.63	1.07	9.30	317.29	0.01
8	324.62	1.05	9.00	317.49	0.01
9	324.62	1.03	8.20	317.60	0.01
10	324.62	1.02	8.60	317.33	0.01
11	324.62	1.00	8.70	317.20	0.01
12	324.61	0.99	8.40	317.12	0.01
13	324.61	0.97	8.40	317.43	0.01
14	324.61	0.95	9.00	317.22	0.01
15	324.60	0.94	9.40	317.08	0.01
1	324.51	1.22	10.30	320.10	0.00
2	324.51	1.20	8.50	319.93	0.00
3	324.50	1.19	7.90	319.72	0.00
4	324.50	1.17	7.70	319.90	0.00
5	324.50	1.16	7.60	319.81	0.00
6	324.49	1.14	7.70	319.50	0.00
7	324.49	1.13	7.30	319.34	0.01
8	324.49	1.11	7.10	319.48	0.01
9	324.48	1.10	6.20	319.50	0.01
10	324.48	1.09	6.90	319.36	0.01
11	324.48	1.08	6.80	319.27	0.01
12	324.47	1.06	6.60	319.22	0.01
13	324.47	1.05	6.50	319.57	0.01
14	324.47	1.04	7.00	319.23	0.01
15	324.46	1.03	7.20	319.17	0.01
1	324.51	1.23	40.40	294.70	0.00
2	324.51	1.15	37.60	294.23	0.00
3	324.50	1.08	36.70	295.18	0.01
4	324.50	1.01	35.10	294.27	0.01
5	324.50	0.95	33.00	292.80	0.02
6	324.50	0.89	30.00	292.41	0.02
7	324.49	0.83	29.90	290.98	0.02
8	324.49	0.77	26.20	291.86	0.03
9	324.49	0.73	28.00	291.71	0.03
10	324.49	0.67	23.70	291.76	0.03
11	324.49	0.63	27.40	291.33	0.03
12	324.49	0.58	26.60	291.16	0.04
13	324.49	0.53	27.30	292.41	0.04

14	324.48	0.48	28.90	290.85	0.04
15	324.48	0.42	28.20	291.89	0.04
1	324.13	2.09	46.10	300.67	0.00
2	324.12	2.00	45.70	301.23	0.00
3	324.11	1.92	43.50	301.67	0.01
4	324.10	1.83	41.50	300.95	0.01
5	324.09	1.76	39.90	299.79	0.02
6	324.08	1.68	38.70	298.77	0.02
7	324.07	1.61	36.90	297.91	0.03
8	324.06	1.54	32.80	298.33	0.03
9	324.06	1.48	33.00	297.52	0.03
10	324.05	1.41	28.60	297.95	0.04
11	324.04	1.36	30.70	296.90	0.04
12	324.04	1.30	30.20	296.58	0.04
13	324.03	1.24	30.30	297.93	0.05
14	324.03	1.19	32.70	296.56	0.05
15	324.03	1.12	32.30	298.13	0.05
1	324.49	1.99	39.00	305.29	0.00
2	324.47	1.92	38.80	305.76	0.00
3	324.46	1.85	36.90	306.08	0.01
4	324.45	1.78	34.80	305.63	0.01
5	324.45	1.71	34.00	304.71	0.02
6	324.44	1.65	32.50	303.87	0.02
7	324.43	1.59	31.10	303.22	0.02
8	324.42	1.53	28.50	303.53	0.03
9	324.42	1.47	27.70	303.17	0.03
10	324.41	1.42	25.70	303.00	0.03
11	324.41	1.37	26.70	302.48	0.03
12	324.40	1.32	26.20	302.32	0.04
13	324.40	1.28	25.90	303.60	0.04
14	324.39	1.23	27.80	302.65	0.04
15	324.39	1.17	27.20	304.10	0.05
1	324.65	1.98	32.10	309.11	0.00
2	324.64	1.92	30.70	309.42	0.00
3	324.63	1.86	29.40	309.87	0.01
4	324.62	1.81	27.70	309.35	0.01
5	324.61	1.76	27.10	308.85	0.01
6	324.60	1.71	26.70	308.35	0.02
7	324.59	1.66	25.50	307.62	0.02
8	324.58	1.61	23.90	307.84	0.02
9	324.58	1.57	22.70	307.86	0.02
10	324.57	1.52	21.90	307.48	0.03
11	324.56	1.48	22.30	307.08	0.03
12	324.56	1.44	21.90	306.99	0.03
13	324.55	1.40	21.60	308.02	0.03
14	324.55	1.36	23.10	307.25	0.03
15	324.54	1.32	22.90	308.31	0.04
1	324.46	2.00	24.80	312.79	0.00
2	324.45	1.95	23.00	312.97	0.00
3	324.44	1.91	23.30	313.19	0.00
4	324.43	1.87	22.00	312.96	0.01
5	324.42	1.83	21.10	312.86	0.01
6	324.41	1.79	21.10	312.25	0.01
7	324.40	1.75	20.70	311.62	0.01
8	324.39	1.71	18.80	312.05	0.02
9	324.38	1.68	18.30	311.97	0.02
10	324.37	1.64	16.90	312.16	0.02
11	324.37	1.61	17.80	311.81	0.02
12	324.36	1.58	17.70	311.40	0.02
13	324.35	1.54	17.60	312.31	0.03
14	324.35	1.51	18.80	311.34	0.03
15	324.34	1.47	18.50	312.39	0.03
1	324.49	2.05	20.60	315.48	0.00
2	324.47	2.01	19.00	315.54	0.00
3	324.46	1.98	19.30	315.74	0.00
4	324.45	1.94	18.20	315.66	0.01
5	324.44	1.91	17.60	315.43	0.01
6	324.43	1.88	17.60	314.89	0.01
7	324.42	1.84	17.00	314.65	0.01
8	324.41	1.81	16.00	314.90	0.01
9	324.40	1.78	15.50	314.75	0.02
10	324.40	1.75	14.50	315.04	0.02
11	324.39	1.73	15.40	314.74	0.02
12	324.38	1.70	15.40	314.45	0.02
13	324.37	1.67	15.00	315.18	0.02
14	324.36	1.64	16.20	314.39	0.02
15	324.36	1.61	15.90	315.24	0.02
1	324.62	2.00	15.30	318.36	0.00
2	324.61	1.97	13.90	318.15	0.00
3	324.60	1.95	11.60	318.55	0.00
4	324.59	1.93	13.00	318.54	0.00
5	324.58	1.90	12.50	318.31	0.01
6	324.57	1.88	12.80	317.89	0.01
7	324.56	1.86	12.30	317.73	0.01
8	324.55	1.83	11.60	318.01	0.01
9	324.54	1.81	11.00	317.78	0.01
10	324.53	1.79	10.70	318.16	0.01
11	324.52	1.77	11.40	317.70	0.01
12	324.52	1.75	11.30	317.63	0.01
13	324.51	1.73	10.90	318.21	0.02
14	324.50	1.71	12.00	317.51	0.02
15	324.49	1.69	11.80	318.00	0.02
1	324.10	2.01	13.60	318.58	0.00
2	324.09	1.98	12.20	318.38	0.00
3	324.08	1.96	12.10	318.66	0.00
4	324.07	1.94	11.10	319.05	0.00

5	324.06	1.92	10.20	318.85	0.01
6	324.05	1.90	11.30	318.17	0.01
7	324.04	1.88	10.90	318.06	0.01
8	324.03	1.86	10.30	318.28	0.01
9	324.02	1.84	9.60	318.05	0.01
10	324.01	1.82	9.50	318.51	0.01
11	324.00	1.80	10.10	318.11	0.01
12	323.99	1.79	10.00	318.07	0.01
13	323.98	1.77	9.90	318.50	0.01
14	323.98	1.75	10.60	317.95	0.01
15	323.97	1.73	10.30	318.36	0.02
1	324.21	2.00	10.60	320.58	0.00
2	324.20	1.98	9.50	320.36	0.00
3	324.19	1.96	9.20	320.63	0.00
4	324.18	1.95	8.40	320.87	0.00
5	324.17	1.93	8.10	320.53	0.00
6	324.16	1.92	8.60	320.30	0.00
7	324.15	1.90	8.30	320.17	0.01
8	324.14	1.89	3.00	320.27	0.01
9	324.13	1.88	7.30	320.34	0.01
10	324.12	1.87	7.60	320.49	0.01
11	324.11	1.85	7.90	320.27	0.01
12	324.10	1.84	7.80	320.15	0.01
13	324.09	1.82	7.50	320.54	0.01
14	324.08	1.81	8.20	320.11	0.01
15	324.07	1.80	8.00	320.35	0.01
1	324.54	2.03	18.50	316.43	0.00
2	324.53	2.00	17.80	316.06	0.00
3	324.52	1.96	17.90	316.56	0.00
4	324.51	1.93	15.80	316.97	0.01
5	324.50	1.90	16.40	315.94	0.01
6	324.49	1.87	16.50	315.57	0.01
7	324.48	1.84	15.70	315.51	0.01
8	324.47	1.81	14.90	315.72	0.01
9	324.46	1.78	13.90	315.76	0.01
10	324.45	1.76	13.70	315.73	0.02
11	324.44	1.73	14.90	315.15	0.02
12	324.43	1.71	14.20	315.28	0.02
13	324.43	1.68	14.10	315.87	0.02
14	324.42	1.65	15.00	315.23	0.02
15	324.41	1.63	15.40	315.54	0.02
1	324.29	5.25	77.50	304.56	0.00
2	324.22	5.11	79.90	304.92	0.01
3	324.15	4.97	78.10	305.25	0.02
4	324.08	4.84	72.70	305.20	0.02
5	324.01	4.71	72.80	303.97	0.03
6	323.95	4.58	73.20	303.08	0.04
7	323.90	4.44	71.20	302.09	0.05
8	323.84	4.32	61.60	303.11	0.05
9	323.79	4.20	62.70	302.71	0.06
10	323.75	4.09	59.00	302.48	0.07
11	323.70	3.98	62.30	302.09	0.07
12	323.66	3.87	62.30	302.24	0.08
13	323.62	3.75	58.30	304.80	0.09
14	323.58	3.64	67.70	302.82	0.09
15	323.55	3.52	64.70	304.57	0.10
1	324.46	5.34	50.80	312.58	0.00
2	324.38	5.26	51.50	313.02	0.01
3	324.31	5.17	50.10	313.19	0.01
4	324.23	5.09	46.40	313.09	0.02
5	324.16	5.01	47.20	312.22	0.02
6	324.10	4.93	46.80	311.46	0.03
7	324.03	4.85	45.30	311.29	0.03
8	323.97	4.78	41.00	311.69	0.03
9	323.91	4.71	40.90	311.40	0.04
10	323.85	4.64	38.40	312.09	0.04
11	323.79	4.57	41.80	311.28	0.05
12	323.74	4.50	41.40	311.33	0.05
13	323.68	4.43	38.40	313.05	0.06
14	323.63	4.36	45.60	311.72	0.06
15	323.58	4.28	43.80	312.54	0.06
1	325.08	5.35	62.30	309.78	0.00
2	325.00	5.25	64.90	310.03	0.01
3	324.93	5.14	62.80	310.38	0.01
4	324.85	5.03	58.20	310.35	0.02
5	324.79	4.93	59.10	309.32	0.03
6	324.72	4.83	58.60	308.53	0.03
7	324.66	4.73	56.50	308.10	0.04
8	324.60	4.64	50.80	308.61	0.04
9	324.54	4.55	51.50	308.36	0.05
10	324.49	4.46	49.30	308.18	0.05
11	324.43	4.38	51.00	308.08	0.06
12	324.38	4.29	51.50	308.10	0.06
13	324.33	4.20	47.60	310.20	0.07
14	324.29	4.11	56.40	308.65	0.07
15	324.24	4.01	53.90	309.75	0.08
1	324.81	5.24	41.10	314.99	0.00
2	324.74	5.17	43.30	315.10	0.00
3	324.66	5.11	42.30	315.08	0.01
4	324.59	5.04	38.40	315.31	0.01
5	324.52	4.98	38.90	314.62	0.02
6	324.46	4.91	39.30	313.88	0.02
7	324.39	4.85	37.80	313.74	0.03
8	324.33	4.79	34.10	314.17	0.03
9	324.27	4.73	35.20	313.67	0.03
10	324.21	4.67	30.30	314.97	0.04

11	324.15	4.62	34.80	313.85	0.04
12	324.10	4.56	34.80	313.80	0.04
13	324.04	4.51	32.70	315.04	0.05
14	323.99	4.45	37.80	314.17	0.05
15	323.94	4.39	37.80	314.46	0.05
1	324.81	5.37	32.00	317.38	0.00
2	324.73	5.32	34.00	317.56	0.00
3	324.66	5.27	33.10	317.49	0.01
4	324.58	5.22	30.30	317.66	0.01
5	324.51	5.18	30.60	317.04	0.01
6	324.44	5.13	30.40	316.41	0.02
7	324.37	5.08	29.90	316.36	0.02
8	324.30	5.04	26.60	316.89	0.02
9	324.23	5.00	27.30	316.29	0.03
10	324.16	4.96	23.30	317.59	0.03
11	324.10	4.92	27.70	316.48	0.03
12	324.04	4.88	27.60	316.40	0.03
13	323.98	4.83	25.70	317.40	0.04
14	323.91	4.80	30.10	316.71	0.04
15	323.86	4.75	29.30	317.05	0.04
1	324.73	5.31	23.60	319.32	0.00
2	324.65	5.28	25.50	319.40	0.00
3	324.58	5.24	23.50	319.51	0.01
4	324.50	5.21	21.20	319.53	0.01
5	324.43	5.18	21.30	319.30	0.01
6	324.36	5.15	23.10	318.56	0.01
7	324.29	5.12	21.20	318.66	0.01
8	324.22	5.09	19.20	318.97	0.02
9	324.15	5.07	19.70	318.66	0.02
10	324.08	5.04	18.40	319.08	0.02
11	324.02	5.01	19.70	318.75	0.02
12	323.95	4.99	20.30	318.51	0.02
13	323.89	4.96	19.50	319.01	0.03
14	323.82	4.93	21.50	318.87	0.03
15	323.76	4.90	20.90	318.96	0.03
1	324.65	5.29	16.60	320.91	0.00
2	324.57	5.27	17.30	320.93	0.00
3	324.50	5.25	16.10	321.04	0.00
4	324.42	5.23	14.70	321.17	0.01
5	324.35	5.22	14.40	320.79	0.01
6	324.28	5.20	15.10	320.16	0.01
7	324.21	5.18	14.60	320.40	0.01
8	324.13	5.17	13.30	320.68	0.01
9	324.06	5.15	13.10	320.28	0.01
10	323.99	5.14	12.50	320.82	0.01
11	323.93	5.13	13.40	320.55	0.02
12	323.86	5.11	13.60	320.34	0.02
13	323.79	5.10	12.80	320.73	0.02
14	323.72	5.08	14.10	320.56	0.02
15	323.66	5.06	13.60	320.56	0.02
1	324.35	0.61	5.50	321.58	0.00
2	324.35	0.60	5.20	321.20	0.00
3	324.35	0.59	4.70	321.05	0.00
4	324.35	0.58	4.20	321.08	0.00
5	324.34	0.57	4.00	321.17	0.00
6	324.34	0.57	4.20	321.04	0.00
7	324.34	0.56	4.00	320.81	0.00
8	324.34	0.55	4.20	320.87	0.00
9	324.34	0.54	3.60	321.08	0.00
10	324.34	0.54	4.10	320.88	0.00
11	324.34	0.53	4.10	320.80	0.00
12	324.34	0.52	3.80	320.81	0.00
13	324.34	0.51	3.60	321.05	0.01
14	324.34	0.51	3.80	320.95	0.01
15	324.34	0.50	3.90	320.67	0.01
1	324.40	0.61	7.70	320.14	0.00
2	324.40	0.60	7.80	319.66	0.00
3	324.40	0.58	6.70	319.37	0.00
4	324.40	0.57	6.00	319.56	0.00
5	324.40	0.56	5.80	319.45	0.00
6	324.40	0.55	6.00	319.14	0.00
7	324.40	0.53	5.70	319.04	0.00
8	324.40	0.52	5.60	319.18	0.00
9	324.40	0.51	5.30	319.27	0.01
10	324.40	0.50	5.60	319.14	0.01
11	324.39	0.49	5.70	319.03	0.01
12	324.39	0.48	5.30	319.06	0.01
13	324.39	0.47	5.10	319.35	0.01
14	324.39	0.46	5.50	319.09	0.01
15	324.39	0.45	5.40	318.88	0.01
1	324.18	0.61	10.80	317.50	0.00
2	324.18	0.59	9.50	317.36	0.00
3	324.18	0.57	8.60	317.11	0.00
4	324.18	0.56	7.80	317.31	0.00
5	324.18	0.54	7.70	317.11	0.00
6	324.18	0.53	7.80	316.69	0.00
7	324.18	0.51	7.50	316.72	0.01
8	324.18	0.50	7.40	316.80	0.01
9	324.18	0.48	6.80	316.93	0.01
10	324.18	0.47	7.10	316.81	0.01
11	324.18	0.46	7.50	316.37	0.01
12	324.18	0.44	7.00	316.47	0.01
13	324.17	0.43	6.80	316.81	0.01
14	324.17	0.42	7.10	316.59	0.01
15	324.17	0.40	7.10	316.26	0.01
1	324.62	0.61	13.80	315.09	0.00

2	324.62	0.58	11.80	314.87	0.00
3	324.62	0.56	10.90	314.64	0.00
4	324.62	0.54	10.20	314.78	0.00
5	324.62	0.52	9.80	314.67	0.00
6	324.62	0.50	10.10	314.07	0.01
7	324.62	0.49	9.60	314.12	0.01
8	324.62	0.47	9.40	314.28	0.01
9	324.61	0.45	9.00	314.35	0.01
10	324.61	0.43	9.00	314.24	0.01
11	324.61	0.42	9.60	313.66	0.01
12	324.61	0.40	9.10	313.82	0.01
13	324.61	0.38	8.90	314.21	0.01
14	324.61	0.36	9.10	313.92	0.01
15	324.61	0.35	9.20	313.64	0.01
1	324.32	0.62	18.00	310.91	0.00
2	324.32	0.59	15.90	310.34	0.00
3	324.32	0.56	15.00	310.03	0.00
4	324.32	0.53	14.10	310.20	0.01
5	324.32	0.50	13.80	309.67	0.01
6	324.32	0.47	13.70	309.21	0.01
7	324.32	0.45	13.40	308.93	0.01
8	324.32	0.42	13.30	308.78	0.01

9	324.32	0.40	12.60	309.29	0.01
10	324.31	0.37	12.20	309.24	0.01
11	324.31	0.35	12.90	309.02	0.01
12	324.31	0.33	12.50	308.81	0.02
13	324.31	0.30	12.30	309.54	0.02
14	324.31	0.28	12.50	309.46	0.02
15	324.31	0.26	12.70	308.94	0.02
1	322.98	0.66	22.90	304.61	0.00
2	322.98	0.62	20.40	303.88	0.00
3	322.98	0.58	19.00	303.57	0.00
4	322.98	0.54	18.00	303.71	0.01
5	322.98	0.50	17.90	302.98	0.01
6	322.98	0.47	17.80	302.49	0.01
7	322.98	0.43	17.50	301.93	0.01
8	322.97	0.40	16.90	301.95	0.01
9	322.97	0.37	16.50	302.72	0.02
10	322.97	0.33	15.30	302.51	0.02
11	322.97	0.30	16.70	302.31	0.02
12	322.97	0.27	16.50	302.14	0.02
13	322.97	0.24	16.30	302.93	0.02
14	322.97	0.21	17.10	302.90	0.02
15	322.97	0.17	16.60	302.31	0.03

C.9. Honda-2 (1989).

Fluid	R-113
Outer Diameter / m	0.0159
Inner Diameter / m	0.0149
Length / m	0.1
Width / m	0.066
Horizontal Pitch / m	0.022
Vertical Pitch / m	0.0191
Number of odd tubes	3
Number of even tubes	2

Row No.	T_V /K	U_V/ (ms^{-1})	q/ (kW/m^2)	T_W /K	M_C / kgs^{-1}
1	323.92	3.03	31.10	312.22	0.00
2	323.90	2.97	31.80	312.90	0.00
3	323.87	2.93	30.70	312.27	0.00
4	323.85	2.88	26.40	312.85	0.00
5	323.83	2.85	29.30	311.73	0.01
6	323.81	2.79	26.40	311.51	0.00
7	323.78	2.76	24.00	312.38	0.01
8	323.76	2.72	24.30	312.06	0.01
9	323.74	2.69	26.70	311.14	0.01
10	323.72	2.64	24.00	311.72	0.01
11	323.71	2.61	24.40	311.71	0.01
12	323.69	2.56	26.30	310.99	0.01
13	323.67	2.53	27.80	310.97	0.02
14	323.65	2.48	26.60	311.05	0.01
15	323.64	2.44	26.90	312.54	0.02
1	323.34	3.12	28.00	312.74	0.00
2	323.31	3.07	28.90	313.51	0.00
3	323.28	3.03	27.70	312.68	0.00
4	323.26	2.98	23.90	313.26	0.00
5	323.23	2.95	26.50	312.33	0.01
6	323.21	2.90	24.80	311.81	0.00
7	323.19	2.87	21.30	313.09	0.01
8	323.17	2.83	22.00	312.57	0.01
9	323.14	2.81	23.90	311.84	0.01
10	323.12	2.76	21.50	312.22	0.01
11	323.10	2.74	21.90	312.50	0.01
12	323.08	2.69	24.30	311.78	0.01
13	323.06	2.66	25.20	311.66	0.02
14	323.04	2.62	24.50	311.74	0.01
15	323.02	2.59	24.40	313.22	0.02
1	323.53	2.77	62.80	298.73	0.00
2	323.51	2.65	61.60	301.31	0.00
3	323.49	2.57	61.40	298.79	0.01
4	323.47	2.46	54.20	300.27	0.00
5	323.46	2.39	58.10	297.66	0.01

Row No.	T_V /K	U_V/ (ms^{-1})	q/ (kW/m^2)	T_W /K	M_C / kgs^{-1}
6	323.44	2.27	53.90	296.84	0.01
7	323.43	2.21	50.80	297.33	0.02
8	323.41	2.11	50.20	297.11	0.01
9	323.40	2.04	49.30	296.20	0.02
10	323.39	1.95	45.50	296.79	0.02
11	323.38	1.89	44.30	296.68	0.03
12	323.37	1.81	44.80	295.67	0.02
13	323.36	1.75	48.80	294.96	0.03
14	323.35	1.65	46.50	295.85	0.02
15	323.34	1.59	45.30	298.24	0.04
1	323.36	2.86	51.20	303.66	0.00
2	323.34	2.76	53.70	304.74	0.00
3	323.32	2.69	50.90	303.32	0.01
4	323.30	2.60	46.00	304.10	0.00
5	323.28	2.54	47.20	302.58	0.01
6	323.26	2.45	43.30	301.86	0.01
7	323.25	2.39	40.50	302.55	0.02
8	323.23	2.32	41.30	302.33	0.01
9	323.22	2.26	39.50	302.32	0.02
10	323.20	2.19	37.50	302.20	0.01
11	323.19	2.14	36.90	302.19	0.02
12	323.18	2.07	36.10	301.58	0.02
13	323.17	2.02	40.80	300.87	0.03
14	323.15	1.94	38.80	301.65	0.02
15	323.14	1.89	42.40	303.24	0.03
1	323.56	2.82	36.40	308.96	0.00
2	323.54	2.75	38.40	310.14	0.00
3	323.52	2.70	38.90	308.42	0.00
4	323.50	2.63	34.60	309.30	0.00
5	323.48	2.59	35.70	308.08	0.01
6	323.46	2.52	32.90	307.86	0.01
7	323.44	2.48	31.00	308.04	0.01
8	323.43	2.42	32.20	308.13	0.01
9	323.41	2.38	31.10	308.21	0.01
10	323.39	2.32	29.10	307.99	0.01

11	323.38	2.28	28.20	308.08	0.02
12	323.37	2.23	28.60	307.37	0.01
13	323.35	2.19	32.40	307.25	0.02
14	323.34	2.13	29.30	308.34	0.01
15	323.33	2.09	31.80	308.93	0.02
1	324.01	2.75	23.00	314.41	0.00
2	323.98	2.71	27.80	314.48	0.00
3	323.96	2.68	25.80	313.96	0.00
4	323.94	2.63	23.00	314.44	0.00
5	323.93	2.60	26.10	313.23	0.01
6	323.91	2.55	25.20	312.31	0.00
7	323.89	2.52	22.40	313.19	0.01
8	323.87	2.48	21.00	313.97	0.01
9	323.86	2.45	24.50	312.36	0.01
10	323.84	2.41	22.70	312.54	0.01
11	323.82	2.38	24.30	313.22	0.01
12	323.81	2.33	22.30	312.21	0.01
13	323.79	2.31	24.70	312.59	0.02
14	323.78	2.26	22.60	312.38	0.01
15	323.77	2.23	21.50	314.47	0.02
1	324.06	2.76	22.40	316.16	0.00
2	324.04	2.72	23.60	316.24	0.00
3	324.02	2.69	21.10	315.92	0.00
4	324.00	2.65	18.90	316.60	0.00
5	323.98	2.63	21.40	315.38	0.00
6	323.96	2.59	20.80	314.96	0.00
7	323.94	2.57	18.00	315.64	0.01
8	323.93	2.53	18.60	315.83	0.00
9	323.91	2.51	20.00	314.81	0.01
10	323.89	2.47	18.40	314.79	0.01
11	323.88	2.45	17.30	315.68	0.01
12	323.86	2.42	18.70	314.96	0.01
13	323.84	2.40	20.60	314.84	0.01
14	323.83	2.36	19.10	315.03	0.01
15	323.81	2.33	17.80	316.51	0.01
1	324.28	4.10	15.60	319.58	0.00
2	324.24	4.08	18.10	319.94	0.00
3	324.19	4.06	15.10	319.59	0.00
4	324.15	4.04	14.10	320.15	0.00
5	324.10	4.02	17.00	318.70	0.00
6	324.06	4.00	14.10	319.36	0.00
7	324.02	3.98	12.50	319.62	0.00
8	323.97	3.97	13.40	319.17	0.00
9	323.93	3.95	15.60	318.33	0.01
10	323.89	3.93	13.10	319.19	0.00
11	323.85	3.92	13.10	318.95	0.01
12	323.81	3.90	14.70	318.81	0.01
13	323.77	3.88	17.20	318.47	0.01
14	323.73	3.85	15.50	319.73	0.01
15	323.69	3.84	12.60	319.89	0.01
1	323.53	4.21	17.60	318.33	0.00
2	323.48	4.18	19.90	318.58	0.00
3	323.44	4.16	16.50	318.24	0.00
4	323.39	4.14	15.90	318.79	0.00
5	323.34	4.12	18.30	317.44	0.00
6	323.30	4.09	15.80	318.00	0.00
7	323.25	4.08	14.50	318.05	0.01
8	323.21	4.05	15.50	317.81	0.00
9	323.16	4.04	16.80	317.06	0.01
10	323.12	4.01	15.90	317.42	0.00
11	323.08	4.00	15.20	317.38	0.01
12	323.04	3.97	15.70	317.74	0.01
13	322.99	3.96	18.30	317.29	0.01
14	322.95	3.93	17.60	318.25	0.01
15	322.91	3.91	15.10	318.01	0.01
1	323.64	4.17	25.60	315.84	0.00
2	323.60	4.13	26.80	316.60	0.00
3	323.55	4.10	23.90	316.05	0.00
4	323.50	4.06	22.20	316.60	0.00
5	323.46	4.03	26.20	314.86	0.01
6	323.42	3.99	23.20	315.12	0.00
7	323.37	3.96	20.30	315.77	0.01
8	323.33	3.93	22.40	315.13	0.01
9	323.29	3.91	22.30	314.69	0.01
10	323.25	3.87	23.00	314.35	0.01
11	323.21	3.84	22.30	314.61	0.01
12	323.17	3.80	23.00	314.77	0.01
13	323.13	3.78	25.70	314.43	0.01
14	323.09	3.73	23.60	315.79	0.01
15	323.06	3.70	21.50	315.96	0.02
1	323.25	4.16	43.30	309.75	0.00
2	323.20	4.08	45.20	311.00	0.00
3	323.16	4.03	39.30	310.86	0.00
4	323.11	3.96	36.30	311.31	0.00
5	323.07	3.92	40.00	309.47	0.01
6	323.03	3.84	34.00	309.83	0.01
7	322.99	3.80	34.60	309.59	0.01
8	322.95	3.74	34.80	309.45	0.01
9	322.91	3.70	38.50	308.01	0.02
10	322.88	3.63	36.30	308.08	0.01
11	322.84	3.58	33.60	309.04	0.02
12	322.81	3.52	35.00	308.91	0.01
13	322.78	3.48	61.70	311.28	0.02
14	322.74	3.36	36.80	309.64	0.02
15	322.71	3.31	37.50	309.61	0.03
1	323.92	4.14	60.00	305.72	0.00

2	323.87	4.03	63.10	306.97	0.00
3	323.83	3.96	61.40	305.43	0.01
4	323.79	3.84	55.00	305.99	0.00
5	323.75	3.78	55.60	304.55	0.01
6	323.71	3.68	45.10	305.91	0.01
7	323.67	3.62	51.40	304.47	0.02
8	323.64	3.53	48.00	304.74	0.01
9	323.60	3.47	50.20	304.00	0.02
10	323.57	3.37	49.30	302.77	0.01
11	323.54	3.31	44.60	304.64	0.03
12	323.51	3.23	48.30	303.61	0.02
13	323.48	3.17	53.50	303.28	0.03
14	323.45	3.07	52.40	303.85	0.02
15	323.43	3.01	51.40	305.13	0.04
1	323.42	4.11	64.30	303.22	0.00
2	323.37	3.99	66.50	295.27	0.00
3	323.33	3.91	66.10	302.93	0.01
4	323.29	3.79	53.90	305.39	0.00
5	323.25	3.72	59.60	302.25	0.01
6	323.21	3.61	51.30	303.01	0.01
7	323.18	3.55	56.40	301.88	0.02
8	323.14	3.44	53.40	301.94	0.01
9	323.11	3.37	56.60	300.51	0.03
10	323.08	3.27	55.50	299.28	0.02
11	323.05	3.20	49.60	301.65	0.03
12	323.02	3.10	56.00	299.72	0.02
13	323.00	3.03	55.40	300.80	0.04
14	322.97	2.93	57.10	300.87	0.02
15	322.95	2.85	55.30	302.15	0.04
1	322.97	2.03	46.20	299.87	0.00
2	322.96	1.94	50.60	301.36	0.00
3	322.95	1.87	45.70	300.15	0.00
4	322.94	1.78	41.70	300.74	0.00
5	322.93	1.73	46.90	297.33	0.01
6	322.92	1.64	42.70	297.52	0.01
7	322.91	1.58	38.40	298.21	0.01
8	322.90	1.51	37.70	298.10	0.01
9	322.90	1.46	38.80	296.40	0.02
10	322.89	1.38	38.20	295.99	0.01
11	322.89	1.33	38.30	296.79	0.02
12	322.88	1.26	38.90	294.78	0.01
13	322.88	1.21	36.70	295.78	0.03
14	322.87	1.14	36.20	295.27	0.02
15	322.87	1.09	34.80	297.87	0.03
1	323.62	2.02	13.70	318.22	0.00
2	323.60	1.99	14.30	317.70	0.00
3	323.59	1.98	13.30	317.99	0.00
4	323.58	1.95	12.40	317.78	0.00

5	323.57	1.94	13.50	317.47	0.00
6	323.56	1.91	13.50	317.16	0.00
7	323.55	1.89	11.70	317.55	0.00
8	323.54	1.87	11.30	317.54	0.00
9	323.53	1.86	12.60	317.33	0.01
10	323.52	1.83	10.80	317.72	0.00
11	323.51	1.82	12.40	317.41	0.01
12	323.51	1.80	12.20	317.41	0.00
13	323.50	1.78	12.50	317.80	0.01
14	323.49	1.76	12.50	317.19	0.01
15	323.48	1.74	12.00	317.98	0.01
1	323.81	2.03	11.10	320.01	0.00
2	323.80	2.01	11.90	319.30	0.00
3	323.79	1.99	10.80	319.79	0.00
4	323.78	1.97	9.70	319.48	0.00
5	323.77	1.96	11.10	319.37	0.00
6	323.76	1.94	12.30	318.56	0.00
7	323.75	1.93	9.90	319.15	0.00
8	323.74	1.91	10.00	319.14	0.00
9	323.73	1.90	10.30	319.13	0.00
10	323.72	1.88	10.10	319.22	0.00
11	323.71	1.86	10.40	319.21	0.01
12	323.70	1.85	9.80	319.40	0.00
13	323.69	1.83	10.60	319.59	0.01
14	323.68	1.81	10.70	319.28	0.00
15	323.67	1.80	10.10	319.87	0.01
1	323.17	1.94	46.20	298.77	0.00
2	323.16	1.85	50.50	300.96	0.00
3	323.15	1.79	46.60	299.15	0.00
4	323.14	1.69	41.80	300.94	0.00
5	323.13	1.64	42.70	298.03	0.01
6	323.12	1.56	40.00	298.22	0.01
7	323.11	1.51	37.80	298.21	0.01
8	323.11	1.43	38.10	297.51	0.01
9	323.10	1.38	36.80	296.50	0.02
10	323.10	1.31	35.00	296.90	0.01
11	323.09	1.27	33.30	297.09	0.02
12	323.09	1.20	35.30	295.89	0.01
13	323.08	1.15	34.60	296.18	0.03
14	323.08	1.09	34.60	297.18	0.02
15	323.08	1.04	35.40	296.18	0.03
1	322.88	2.08	40.30	302.68	0.00
2	322.87	2.00	43.00	304.37	0.00
3	322.86	1.95	40.90	303.06	0.00
4	322.85	1.87	37.90	303.35	0.00
5	322.84	1.82	36.50	302.14	0.01
6	322.83	1.74	33.80	302.13	0.01
7	322.82	1.70	33.70	302.12	0.01

8	322.81	1.64	32.90	301.51	0.01
9	322.81	1.59	31.70	301.11	0.02
10	322.80	1.53	30.50	301.00	0.01
11	322.79	1.49	30.20	300.39	0.02
12	322.79	1.43	30.10	300.79	0.01
13	322.78	1.39	30.60	300.88	0.02
14	322.78	1.33	30.20	301.88	0.01
15	322.77	1.29	30.50	301.77	0.03
1	323.50	1.97	33.80	306.40	0.00
2	323.49	1.91	37.00	307.79	0.00
3	323.48	1.86	34.30	306.58	0.00
4	323.47	1.79	33.20	306.87	0.00
5	323.46	1.75	31.70	305.76	0.01
6	323.46	1.69	29.00	305.96	0.00
7	323.45	1.65	29.20	306.05	0.01
8	323.44	1.60	28.90	305.34	0.01
9	323.43	1.56	27.80	304.93	0.01
10	323.43	1.50	27.10	304.93	0.01
11	323.42	1.47	26.20	304.62	0.02
12	323.42	1.42	26.60	304.92	0.01
13	323.41	1.39	27.00	304.91	0.02
14	323.40	1.33	27.00	306.00	0.01
15	323.40	1.30	26.90	305.80	0.02
1	322.97	1.98	25.70	310.37	0.00
2	322.96	1.93	27.30	311.66	0.00
3	322.95	1.90	25.10	310.65	0.00
4	322.94	1.85	24.00	311.24	0.00
5	322.93	1.82	23.40	310.13	0.01
6	322.92	1.77	20.90	310.52	0.00
7	322.91	1.74	21.60	310.61	0.01
8	322.90	1.70	21.00	310.00	0.01
9	322.89	1.67	21.30	309.39	0.01
10	322.89	1.63	20.60	309.59	0.01
11	322.88	1.61	19.80	309.58	0.01
12	322.87	1.57	20.00	309.77	0.01
13	322.87	1.54	21.10	309.27	0.01
14	322.86	1.50	20.80	310.96	0.01
15	322.85	1.47	20.40	310.45	0.02
1	322.94	1.93	20.00	313.84	0.00
2	322.93	1.89	20.30	315.03	0.00
3	322.92	1.87	19.20	313.92	0.00
4	322.91	1.83	18.10	314.71	0.00
5	322.90	1.80	18.10	313.80	0.00
6	322.89	1.77	16.00	314.39	0.00
7	322.88	1.75	17.00	314.38	0.01
8	322.87	1.72	16.40	313.67	0.00
9	322.87	1.70	16.30	313.47	0.01
10	322.86	1.66	16.00	313.36	0.00
11	322.85	1.64	15.30	313.35	0.01
12	322.84	1.61	15.90	313.44	0.01
13	322.84	1.59	18.90	312.64	0.01
14	322.83	1.56	16.50	314.53	0.01
15	322.82	1.53	14.70	314.42	0.01
1	322.83	1.98	19.90	313.73	0.00
2	322.81	1.94	20.00	314.81	0.00
3	322.80	1.92	19.20	313.80	0.00
4	322.79	1.88	18.10	314.59	0.00
5	322.78	1.86	18.00	313.58	0.00
6	322.78	1.82	16.00	314.18	0.00
7	322.77	1.80	16.90	314.17	0.01
8	322.76	1.77	16.70	313.56	0.00
9	322.75	1.75	16.30	313.25	0.01
10	322.74	1.71	16.00	313.14	0.00
11	322.73	1.69	15.40	313.33	0.01
12	322.73	1.66	16.00	313.33	0.01
13	322.72	1.64	17.90	312.52	0.01
14	322.71	1.61	16.40	314.41	0.01
15	322.70	1.59	15.90	314.30	0.01
1	323.76	1.99	17.10	316.36	0.00
2	323.74	1.96	17.80	317.64	0.00
3	323.73	1.94	15.80	316.73	0.00
4	323.72	1.91	14.20	317.82	0.00
5	323.71	1.89	15.70	316.31	0.00
6	323.70	1.86	14.10	316.90	0.00
7	323.69	1.84	14.70	316.99	0.01
8	323.69	1.81	14.50	316.29	0.00
9	323.68	1.80	14.70	316.18	0.01
10	323.67	1.77	14.00	315.97	0.00
11	323.66	1.75	13.40	316.06	0.01
12	323.65	1.73	13.90	316.15	0.01
13	323.64	1.71	15.10	315.74	0.01
14	323.63	1.68	14.40	317.33	0.01
15	323.63	1.66	13.70	317.03	0.01
1	323.53	1.14	29.70	303.43	0.00
2	323.53	1.08	34.00	303.93	0.00
3	323.52	1.04	28.30	303.72	0.00
4	323.52	0.98	27.50	304.12	0.00
5	323.52	0.95	26.80	302.12	0.01
6	323.52	0.90	25.20	302.02	0.00
7	323.51	0.86	24.70	302.91	0.01
8	323.51	0.82	25.60	301.21	0.01
9	323.51	0.78	25.30	300.51	0.01
10	323.51	0.74	24.70	300.01	0.01
11	323.51	0.70	23.30	301.31	0.01
12	323.51	0.66	23.80	300.61	0.01
13	323.50	0.63	25.50	299.70	0.02

14	323.50	0.58	24.20	300.50	0.01
15	323.50	0.55	24.30	300.70	0.02
1	321.64	1.29	24.70	307.34	0.00
2	321.63	1.24	27.60	307.83	0.00
3	321.63	1.20	23.70	307.33	0.00
4	321.62	1.15	23.70	307.52	0.00
5	321.62	1.12	22.70	306.12	0.01
6	321.62	1.08	21.30	305.92	0.00
7	321.61	1.05	20.30	307.01	0.01
8	321.61	1.01	21.70	305.11	0.01
9	321.61	0.98	21.50	304.51	0.01
10	321.61	0.93	21.40	304.11	0.01
11	321.60	0.90	19.50	305.20	0.01
12	321.60	0.86	20.10	305.00	0.01
13	321.60	0.84	21.60	304.20	0.01
14	321.60	0.79	20.60	305.00	0.01
15	321.60	0.76	20.10	305.30	0.02
1	322.16	1.29	22.20	309.76	0.00
2	322.16	1.25	26.90	310.26	0.00
3	322.15	1.21	21.00	309.75	0.00
4	322.15	1.17	20.50	310.05	0.00
5	322.15	1.14	20.10	308.75	0.00
6	322.14	1.10	18.60	308.74	0.00
7	322.14	1.08	17.90	309.64	0.01
8	322.14	1.04	19.30	307.94	0.00
9	322.13	1.01	19.30	307.33	0.01
10	322.13	0.97	19.10	306.83	0.01
11	322.13	0.95	17.30	308.13	0.01
12	322.13	0.91	17.60	307.83	0.01
13	322.12	0.89	19.40	306.92	0.01
14	322.12	0.85	18.70	308.12	0.01
15	322.12	0.83	17.80	308.22	0.01
1	323.53	1.21	19.50	311.93	0.00
2	323.53	1.17	21.00	312.33	0.00
3	323.52	1.15	18.30	312.02	0.00
4	323.52	1.11	17.90	312.32	0.00
5	323.52	1.09	17.70	311.12	0.00
6	323.51	1.05	16.20	311.31	0.00
7	323.51	1.03	15.80	312.01	0.01
8	323.51	1.00	16.60	310.51	0.00
9	323.51	0.98	16.80	310.01	0.01
10	323.50	0.95	16.80	309.60	0.01
11	323.50	0.93	15.10	310.60	0.01
12	323.50	0.90	15.60	310.40	0.01
13	323.50	0.88	17.00	309.70	0.01
14	323.49	0.84	16.20	310.89	0.01
15	323.49	0.82	15.40	310.89	0.01
1	323.59	1.20	17.10	313.99	0.00
2	323.58	1.17	18.30	314.38	0.00
3	323.58	1.14	15.70	314.18	0.00
4	323.58	1.11	15.40	314.58	0.00
5	323.57	1.09	15.10	313.37	0.00
6	323.57	1.07	13.80	313.57	0.00
7	323.57	1.05	13.40	314.07	0.00
8	323.56	1.02	14.10	312.76	0.00
9	323.56	1.00	14.60	312.36	0.01
10	323.56	0.98	14.40	311.96	0.00
11	323.56	0.96	13.00	312.76	0.01
12	323.55	0.93	13.30	312.75	0.01
13	323.55	0.91	14.70	312.15	0.01
14	323.55	0.89	13.90	313.35	0.01
15	323.55	0.87	13.30	313.15	0.01
1	323.70	1.19	14.10	316.30	0.00
2	323.70	1.16	15.10	316.60	0.00
3	323.69	1.14	13.20	316.49	0.00
4	323.69	1.12	13.00	316.89	0.00
5	323.69	1.10	13.10	315.39	0.00
6	323.68	1.08	11.70	315.88	0.00
7	323.68	1.06	11.40	316.38	0.00
8	323.68	1.04	12.10	314.88	0.00
9	323.67	1.02	12.30	314.87	0.01
10	323.67	1.00	12.60	314.67	0.00
11	323.67	0.98	10.90	315.17	0.01
12	323.66	0.96	11.30	315.36	0.00
13	323.66	0.95	12.90	314.76	0.01
14	323.66	0.92	11.90	315.96	0.01
15	323.66	0.91	11.20	315.76	0.01
1	323.39	1.20	12.30	317.69	0.00
2	323.39	1.18	13.20	317.89	0.00
3	323.38	1.16	11.40	317.78	0.00
4	323.38	1.14	11.20	318.28	0.00
5	323.38	1.12	11.10	317.28	0.00
6	323.37	1.10	10.10	317.57	0.00
7	323.37	1.09	10.10	317.97	0.00
8	323.37	1.07	10.30	316.97	0.00
9	323.36	1.06	10.90	316.56	0.00
10	323.36	1.03	10.80	316.26	0.00
11	323.36	1.02	9.30	316.86	0.01
12	323.35	1.00	9.60	316.95	0.00
13	323.35	0.99	10.90	316.35	0.01
14	323.35	0.97	10.30	317.55	0.00
15	323.35	0.96	9.40	317.25	0.01
1	323.53	1.21	39.80	295.63	0.00
2	323.53	1.13	47.50	295.83	0.00
3	323.52	1.07	38.50	295.72	0.00
4	323.52	1.00	36.10	296.92	0.00

5	323.52	0.95	37.40	292.22	0.01
6	323.52	0.88	33.20	294.12	0.01
7	323.51	0.84	32.90	293.91	0.01
8	323.51	0.77	33.80	292.81	0.01
9	323.51	0.73	33.20	291.51	0.02
10	323.51	0.67	32.90	291.41	0.01
11	323.51	0.62	36.20	293.91	0.02
12	323.51	0.55	31.80	291.01	0.01
13	323.51	0.51	33.70	290.61	0.02
14	323.50	0.45	31.60	291.50	0.01
15	323.50	0.41	30.50	292.90	0.03
1	323.48	5.60	61.80	309.28	0.00
2	323.39	5.50	65.10	309.99	0.00
3	323.31	5.42	65.10	309.11	0.01
4	323.23	5.31	55.30	309.33	0.00
5	323.15	5.25	60.60	308.35	0.01
6	323.08	5.15	55.70	307.78	0.01
7	323.01	5.08	55.50	307.71	0.02
8	322.94	4.99	57.20	307.04	0.01
9	322.87	4.92	54.80	306.97	0.03
10	322.81	4.82	51.50	306.71	0.02
11	322.75	4.76	51.10	307.45	0.03
12	322.69	4.67	53.90	306.79	0.02
13	322.63	4.61	55.90	306.93	0.04
14	322.58	4.50	54.10	306.88	0.02
15	322.52	4.44	54.80	308.92	0.04
1	323.39	5.28	49.90	311.59	0.00
2	323.32	5.19	49.50	312.32	0.00
3	323.24	5.14	50.20	311.64	0.01
4	323.17	5.06	41.20	311.87	0.00
5	323.10	5.01	45.40	311.30	0.01
6	323.03	4.93	46.20	309.83	0.01
7	322.97	4.88	41.40	310.67	0.02
8	322.91	4.81	40.50	310.21	0.01
9	322.84	4.77	42.80	309.94	0.02
10	322.78	4.69	38.90	309.78	0.01
11	322.73	4.65	38.00	310.63	0.02
12	322.67	4.58	41.90	309.37	0.01
13	322.62	4.53	42.60	310.52	0.03
14	322.56	4.46	42.40	309.36	0.02
15	322.51	4.41	41.20	311.51	0.03
1	323.62	5.26	42.40	313.92	0.00
2	323.54	5.19	42.20	314.24	0.00
3	323.47	5.15	42.70	313.97	0.00
4	323.40	5.08	34.50	314.20	0.00
5	323.33	5.04	38.70	313.63	0.01
6	323.26	4.98	38.70	312.36	0.01
7	323.19	4.94	34.40	313.09	0.01
8	323.13	4.88	35.80	312.73	0.01
9	323.06	4.84	36.10	312.56	0.02
10	323.00	4.78	33.20	312.60	0.01
11	322.94	4.75	31.80	313.14	0.02
12	322.88	4.69	35.50	311.98	0.01
13	322.83	4.65	34.00	313.13	0.02
14	322.77	4.60	35.70	312.17	0.02
15	322.71	4.56	34.60	313.81	0.03
1	323.34	5.27	33.20	315.74	0.00
2	323.26	5.22	32.00	316.16	0.00
3	323.19	5.19	32.70	315.99	0.00
4	323.11	5.14	25.50	316.31	0.00
5	323.04	5.11	29.70	315.74	0.01
6	322.97	5.07	28.40	314.97	0.00
7	322.91	5.04	25.00	315.21	0.01
8	322.84	5.00	28.70	314.74	0.01
9	322.77	4.97	26.70	315.07	0.01
10	322.71	4.93	26.80	314.61	0.01
11	322.64	4.91	24.40	315.14	0.02
12	322.58	4.87	27.40	314.48	0.01
13	322.52	4.84	25.50	315.62	0.02
14	322.46	4.80	26.30	314.86	0.01
15	322.40	4.77	23.10	316.50	0.02
1	323.53	5.43	23.40	318.23	0.00
2	323.45	5.40	22.60	318.35	0.00
3	323.37	5.38	22.90	318.37	0.00
4	323.30	5.35	19.20	318.10	0.00
5	323.22	5.34	21.30	318.02	0.00
6	323.14	5.31	19.90	317.74	0.00
7	323.07	5.29	16.80	317.87	0.01
8	323.00	5.27	19.30	317.60	0.00
9	322.92	5.26	19.50	317.42	0.01
10	322.85	5.23	18.30	317.25	0.01
11	322.78	5.22	17.50	317.58	0.01
12	322.71	5.20	17.60	317.71	0.01
13	322.64	5.19	19.40	317.84	0.01
14	322.57	5.16	21.20	317.47	0.01
15	322.50	5.14	18.90	318.10	0.01
1	323.22	5.32	73.40	305.12	0.00
2	323.14	5.19	76.40	306.74	0.00
3	323.07	5.10	74.50	305.47	0.01
4	323.00	4.97	62.20	305.80	0.01
5	322.93	4.90	70.30	304.43	0.02
6	322.87	4.77	67.30	303.07	0.01
7	322.81	4.69	61.50	303.71	0.02
8	322.75	4.57	61.30	303.55	0.01
9	322.70	4.50	63.00	302.80	0.03
10	322.64	4.38	61.80	301.04	0.02

11	322.59	4.31	57.00	303.79	0.04
12	322.54	4.20	62.00	301.54	0.02
13	322.50	4.12	61.20	302.30	0.04
14	322.45	4.01	59.70	302.55	0.03
15	322.41	3.93	62.70	304.01	0.05
1	323.92	5.50	60.70	308.22	0.00
2	323.84	5.40	59.40	310.04	0.00
3	323.76	5.33	60.40	308.86	0.01
4	323.68	5.23	53.10	309.08	0.00
5	323.61	5.17	57.20	308.51	0.01
6	323.54	5.08	50.40	307.84	0.01
7	323.47	5.02	52.60	307.77	0.02
8	323.40	4.93	50.20	307.60	0.01
9	323.34	4.87	52.20	306.64	0.02
10	323.27	4.78	49.20	306.67	0.01
11	323.21	4.73	49.70	307.41	0.03
12	323.16	4.64	51.40	306.56	0.02
13	323.10	4.58	53.80	307.10	0.03
14	323.04	4.48	51.30	306.84	0.02
15	322.99	4.42	55.40	308.19	0.04
1	323.39	5.45	53.10	309.79	0.00
2	323.31	5.36	50.80	311.61	0.00
3	323.23	5.31	56.00	309.73	0.01
4	323.16	5.21	46.90	310.36	0.00
5	323.08	5.16	49.80	309.88	0.01
6	323.01	5.07	47.70	308.91	0.01
7	322.94	5.02	44.20	309.74	0.02
8	322.88	4.95	44.40	309.18	0.01
9	322.81	4.90	45.60	308.31	0.02
10	322.75	4.82	42.70	308.45	0.01
11	322.69	4.77	43.40	309.09	0.03
12	322.63	4.69	45.70	308.33	0.02
13	322.57	4.64	46.90	308.67	0.03
14	322.52	4.55	44.40	308.72	0.02
15	322.46	4.50	49.10	309.96	0.04
1	323.78	5.38	36.60	314.48	0.00
2	323.70	5.32	36.10	315.50	0.00
3	323.63	5.29	37.50	314.63	0.00
4	323.55	5.23	29.30	315.35	0.00
5	323.48	5.20	34.80	314.28	0.01
6	323.41	5.15	33.30	313.51	0.00
7	323.34	5.11	33.10	313.74	0.01
8	323.27	5.06	29.70	314.07	0.01
9	323.20	5.03	32.50	313.20	0.01
10	323.13	4.98	29.00	313.63	0.01
11	323.07	4.95	29.00	313.97	0.02
12	323.00	4.91	28.90	314.00	0.01
13	322.94	4.88	33.50	313.34	0.02
14	322.88	4.82	32.30	313.18	0.01
15	322.82	4.79	32.60	314.92	0.02
1	323.87	5.51	29.40	316.57	0.00
2	323.78	5.47	29.20	317.38	0.00
3	323.70	5.44	30.10	316.60	0.00
4	323.62	5.40	23.60	317.22	0.00
5	323.55	5.38	27.90	316.45	0.01
6	323.47	5.34	26.70	315.77	0.00
7	323.39	5.32	26.30	316.09	0.01
8	323.32	5.28	23.50	316.22	0.01
9	323.25	5.26	26.00	315.55	0.01
10	323.17	5.22	22.70	315.97	0.01
11	323.10	5.20	23.30	316.20	0.01
12	323.03	5.17	25.60	315.73	0.01
13	322.96	5.15	27.80	315.46	0.02
14	322.90	5.10	25.60	315.70	0.01
15	322.83	5.08	26.20	316.93	0.02
1	323.98	5.51	23.20	318.68	0.00
2	323.90	5.48	23.00	319.30	0.00
3	323.81	5.46	23.20	318.71	0.00
4	323.73	5.43	18.10	319.03	0.00
5	323.66	5.42	21.20	318.56	0.00
6	323.58	5.39	20.60	317.98	0.00
7	323.50	5.38	20.10	318.30	0.01
8	323.42	5.36	18.50	318.42	0.00
9	323.35	5.34	19.90	317.95	0.01
10	323.28	5.32	17.40	318.18	0.01
11	323.20	5.31	17.70	318.30	0.01
12	323.13	5.28	19.60	318.13	0.01
13	323.06	5.27	21.50	317.96	0.01
14	322.99	5.24	19.40	318.19	0.01
15	322.92	5.22	20.10	319.02	0.02
1	324.17	0.60	15.70	314.57	0.00
2	324.17	0.57	16.90	313.77	0.00
3	324.17	0.55	14.50	313.87	0.00
4	324.17	0.52	13.60	313.67	0.00
5	324.17	0.50	14.60	312.97	0.00
6	324.17	0.48	13.60	312.57	0.00
7	324.17	0.46	13.20	312.87	0.00
8	324.17	0.43	13.60	312.47	0.00
9	324.17	0.42	13.60	312.57	0.01
10	324.16	0.39	12.90	312.46	0.00
11	324.16	0.38	12.80	312.86	0.01
12	324.16	0.35	12.50	312.66	0.00
13	324.16	0.33	13.30	312.86	0.01
14	324.16	0.31	13.10	312.46	0.01
15	324.16	0.29	12.90	313.36	0.01
1	323.98	0.56	12.40	316.88	0.00

2	323.98	0.54	12.60	316.68	0.00
3	323.98	0.52	11.20	316.48	0.00
4	323.98	0.50	10.40	316.28	0.00
5	323.97	0.49	11.40	315.77	0.00
6	323.97	0.46	10.40	315.37	0.00
7	323.97	0.45	11.10	315.77	0.00
8	323.97	0.43	10.70	315.37	0.00
9	323.97	0.42	10.60	315.47	0.00
10	323.97	0.40	10.20	315.27	0.00
11	323.97	0.38	9.90	315.67	0.01
12	323.97	0.36	9.90	315.57	0.00
13	323.97	0.35	10.30	315.77	0.01
14	323.97	0.33	9.60	315.47	0.00
15	323.97	0.32	9.90	316.17	0.01
1	323.98	0.59	10.00	318.78	0.00
2	323.98	0.57	10.20	318.28	0.00
3	323.98	0.56	9.20	318.38	0.00
4	323.97	0.54	8.50	318.17	0.00
5	323.97	0.53	9.20	317.97	0.00
6	323.97	0.51	8.30	317.77	0.00
7	323.97	0.50	8.40	317.77	0.00
8	323.97	0.49	8.70	317.67	0.00
9	323.97	0.47	8.70	317.57	0.00
10	323.97	0.46	8.50	317.47	0.00
11	323.97	0.45	8.20	317.77	0.00
12	323.97	0.43	8.80	317.27	0.00
13	323.97	0.42	8.40	317.97	0.01
14	323.97	0.40	8.00	317.67	0.00
15	323.97	0.39	8.10	318.27	0.01
1	323.98	0.59	8.80	319.58	0.00
2	323.98	0.57	8.80	319.38	0.00
3	323.98	0.56	8.00	319.18	0.00
4	323.97	0.55	7.50	319.07	0.00
5	323.97	0.54	8.10	318.97	0.00
6	323.97	0.52	7.10	318.87	0.00
7	323.97	0.51	7.40	318.77	0.00
8	323.97	0.50	7.20	318.87	0.00
9	323.97	0.49	7.80	318.67	0.00
10	323.97	0.48	7.40	318.47	0.00
11	323.97	0.47	7.20	318.77	0.00
12	323.97	0.45	7.60	318.47	0.00
13	323.97	0.44	7.40	318.97	0.00
14	323.97	0.43	6.90	318.77	0.00
15	323.97	0.42	7.10	319.27	0.01
1	323.02	0.61	14.70	313.82	0.00
2	323.02	0.58	14.70	313.92	0.00
3	323.02	0.56	13.60	313.02	0.00
4	323.02	0.54	13.10	313.02	0.00
5	323.02	0.52	13.60	312.42	0.00
6	323.02	0.49	12.30	312.62	0.00
7	323.02	0.48	12.40	312.22	0.00
8	323.02	0.45	13.10	311.82	0.00
9	323.02	0.43	12.90	311.82	0.01
10	323.02	0.41	12.30	311.62	0.00
11	323.02	0.39	12.10	312.12	0.01
12	323.02	0.37	12.80	311.02	0.00
13	323.02	0.35	12.60	312.12	0.01
14	323.02	0.33	11.90	311.62	0.01
15	323.02	0.31	11.90	312.72	0.01
1	322.48	0.62	18.60	309.38	0.00
2	322.48	0.58	17.90	310.58	0.00
3	322.48	0.56	18.10	307.98	0.00
4	322.48	0.52	17.40	308.08	0.00
5	322.48	0.50	17.70	307.38	0.00
6	322.48	0.46	15.50	307.78	0.00
7	322.48	0.44	16.40	307.08	0.01
8	322.48	0.41	16.40	307.18	0.00
9	322.48	0.39	16.60	306.78	0.01
10	322.47	0.36	16.10	306.37	0.00
11	322.47	0.34	15.70	307.07	0.01
12	322.47	0.30	17.10	305.27	0.01
13	322.47	0.28	16.70	306.87	0.01
14	322.47	0.25	15.50	306.57	0.01
15	322.47	0.23	16.00	307.67	0.01

C.10. Briggs (1995).

Fluid	R-113
Outer Diameter / m	0.0187
Inner Diameter / m	0.0127
Length / m	0.272
Width / m	0.0143
Horizontal Pitch / m	0.0262
Vertical Pitch / m	0.0227
Number of odd tubes	4
Number of even tubes	5

Row No.	T_V /K	U_V/ (ms^{-1})	q/ (kW/m^2)	T_W /K	M_C / kgs^{-1}
1	320.50	0.13	30.70	299.40	0.00
2	320.50	0.11	28.60	299.00	0.00
3	320.50	0.08	26.40	298.10	0.00
4	320.50	0.07	23.40	297.40	0.00
5	320.50	0.05	21.60	296.70	0.00
6	320.50	0.03	18.70	296.00	0.00
7	320.40	0.02	16.90	295.30	0.00
8	320.30	0.01	14.10	294.50	0.00
9	320.30	0.00	11.10	293.50	0.00
10	320.30	0.00	10.20	293.40	0.00
1	320.50	0.13	31.60	298.30	0.00
2	320.50	0.11	29.40	298.00	0.00
3	320.50	0.08	26.80	297.10	0.00
4	320.50	0.06	23.60	296.40	0.00
5	320.50	0.05	21.40	295.70	0.00
6	320.50	0.03	18.40	295.00	0.00
7	320.40	0.02	16.80	294.50	0.00
8	320.30	0.01	14.00	293.80	0.00
9	320.30	0.00	10.80	292.90	0.00
10	320.30	0.00	10.10	292.80	0.00
1	320.50	0.13	31.80	297.50	0.00
2	320.50	0.11	29.60	297.20	0.00
3	320.50	0.08	26.60	296.30	0.00
4	320.50	0.07	23.40	295.70	0.00
5	320.40	0.05	21.30	295.00	0.00
6	320.40	0.03	18.50	294.50	0.00
7	320.40	0.02	16.50	293.90	0.00
8	320.20	0.01	13.80	293.40	0.00
9	320.20	0.00	10.70	292.60	0.00
10	320.20	0.00	10.00	292.50	0.00
1	320.50	0.13	32.60	296.90	0.00
2	320.50	0.10	30.00	296.60	0.00
3	320.50	0.08	26.80	295.70	0.00
4	320.50	0.06	23.60	295.10	0.00
5	320.40	0.04	21.40	294.60	0.00

Row No.	T_V /K	U_V/ (ms^{-1})	q/ (kW/m^2)	T_W /K	M_C / kgs^{-1}
6	320.40	0.03	18.30	294.10	0.00
7	320.40	0.02	16.40	293.50	0.00
8	320.10	0.01	13.70	293.00	0.00
9	320.10	0.00	10.60	292.20	0.00
10	320.10	0.00	9.90	292.20	0.00
1	320.50	0.13	33.10	296.50	0.00
2	320.50	0.11	30.40	296.20	0.00
3	320.50	0.08	27.40	295.40	0.00
4	320.50	0.06	23.80	294.90	0.00
5	320.40	0.04	21.70	294.40	0.00
6	320.40	0.03	18.70	293.90	0.00
7	320.40	0.02	16.70	293.40	0.00
8	320.40	0.00	13.90	292.90	0.00
9	320.40	0.00	10.70	292.20	0.00
10	320.40	0.00	10.00	292.20	0.00
1	320.50	0.13	33.60	296.20	0.00
2	320.50	0.10	30.90	295.80	0.00
3	320.50	0.08	27.50	295.10	0.00
4	320.40	0.06	23.90	294.50	0.00
5	320.40	0.04	21.90	294.10	0.00
6	320.40	0.03	18.60	293.60	0.00
7	320.30	0.01	16.50	293.10	0.00
8	319.80	0.00	13.80	292.70	0.00
9	319.80	0.00	10.60	292.10	0.00
10	319.80	0.00	10.00	292.00	0.00
1	320.50	0.13	34.10	295.90	0.00
2	320.50	0.11	31.40	295.60	0.00
3	320.50	0.08	28.00	294.90	0.00
4	320.50	0.06	24.20	294.40	0.00
5	320.40	0.04	22.40	294.00	0.00
6	320.40	0.03	19.10	293.60	0.00
7	320.30	0.01	17.10	293.10	0.00
8	319.30	0.00	14.40	292.70	0.00
9	319.30	0.00	11.10	292.10	0.00
10	319.30	0.00	10.30	292.00	0.00

1	320.50	0.13	34.20	295.60	0.00
2	320.50	0.11	31.50	295.30	0.00
3	320.50	0.08	27.80	294.60	0.00
4	320.40	0.06	24.30	294.10	0.00
5	320.40	0.04	22.40	293.70	0.00
6	320.40	0.03	19.00	293.30	0.00
7	320.40	0.01	17.00	292.90	0.00
8	319.30	0.00	14.30	292.50	0.00
9	319.30	0.00	10.90	291.90	0.00
10	319.30	0.00	10.20	291.90	0.00
1	320.50	0.23	31.80	299.80	0.00
2	320.50	0.21	32.50	300.20	0.00
3	320.50	0.18	29.00	299.00	0.00
4	320.50	0.16	28.40	299.00	0.00
5	320.50	0.14	26.00	298.10	0.00
6	320.40	0.12	26.40	298.40	0.00
7	320.40	0.10	25.70	298.10	0.00
8	320.40	0.08	25.70	298.20	0.00
9	320.40	0.06	23.10	297.30	0.00
10	320.40	0.05	23.30	297.60	0.00
1	320.50	0.22	32.60	298.80	0.00
2	320.50	0.20	33.30	299.20	0.00
3	320.50	0.17	29.50	298.00	0.00
4	320.50	0.15	28.90	298.00	0.00
5	320.50	0.13	26.30	297.10	0.00
6	320.50	0.11	26.80	297.50	0.00
7	320.40	0.09	26.20	297.10	0.00
8	320.40	0.08	26.00	297.20	0.00
9	320.40	0.05	23.40	296.40	0.00
10	320.40	0.04	23.40	296.60	0.00
1	320.50	0.22	33.40	298.10	0.00
2	320.50	0.20	34.00	298.40	0.00
3	320.50	0.17	29.90	297.30	0.00
4	320.50	0.15	29.40	297.30	0.00
5	320.40	0.13	27.00	296.60	0.00
6	320.40	0.11	27.30	296.90	0.00
7	320.40	0.09	26.60	296.50	0.00
8	320.40	0.07	26.00	296.50	0.00
9	320.40	0.05	23.40	295.80	0.00
10	320.30	0.04	22.60	295.80	0.00
1	320.50	0.22	34.20	297.50	0.00
2	320.50	0.20	34.70	297.80	0.00
3	320.50	0.17	30.50	296.70	0.00
4	320.50	0.15	29.80	296.70	0.00
5	320.50	0.13	27.40	296.10	0.00
6	320.40	0.11	27.70	296.40	0.00
7	320.40	0.09	26.90	296.00	0.00
8	320.40	0.07	26.20	296.00	0.00
9	320.40	0.05	23.40	295.30	0.00
10	320.40	0.03	22.40	295.20	0.00
1	320.50	0.22	34.50	297.00	0.00
2	320.50	0.20	35.10	297.30	0.00
3	320.50	0.17	30.70	296.30	0.00
4	320.50	0.15	30.20	296.40	0.00
5	320.50	0.12	27.70	295.70	0.00
6	320.40	0.11	28.00	295.90	0.00
7	320.40	0.08	27.20	295.60	0.00
8	320.40	0.07	26.40	295.60	0.00
9	320.40	0.04	23.50	294.90	0.00
10	320.30	0.03	22.00	294.80	0.00
1	320.50	0.22	34.90	296.70	0.00
2	320.50	0.20	35.60	296.90	0.00
3	320.50	0.17	31.10	296.00	0.00
4	320.50	0.15	30.40	295.90	0.00
5	320.50	0.13	28.20	295.40	0.00
6	320.40	0.11	28.40	295.60	0.00
7	320.40	0.08	27.60	295.30	0.00
8	320.40	0.07	26.50	295.20	0.00
9	320.40	0.04	23.60	294.60	0.00
10	320.30	0.03	22.10	294.50	0.00
1	320.50	0.22	35.40	296.40	0.00
2	320.50	0.20	35.90	296.60	0.00
3	320.50	0.17	31.30	295.60	0.00
4	320.50	0.15	30.60	295.70	0.00
5	320.50	0.12	28.40	295.20	0.00
6	320.40	0.11	28.70	295.40	0.00
7	320.40	0.08	27.90	295.10	0.00
8	320.40	0.06	26.70	295.00	0.00
9	320.40	0.04	23.50	294.40	0.00
10	320.30	0.03	22.00	294.30	0.00
1	320.50	0.22	35.80	296.00	0.00
2	320.50	0.20	36.30	296.20	0.00
3	320.50	0.17	31.60	295.30	0.00
4	320.50	0.15	30.70	295.30	0.00
5	320.40	0.13	28.70	294.90	0.00
6	320.40	0.11	28.80	295.00	0.00
7	320.40	0.08	28.10	294.80	0.00
8	320.40	0.07	27.00	294.70	0.00
9	320.40	0.04	23.80	294.10	0.00
10	320.30	0.03	22.20	294.00	0.00
1	320.70	0.32	32.90	299.60	0.00
2	320.70	0.30	34.50	300.30	0.00
3	320.70	0.27	31.30	299.10	0.00
4	320.70	0.25	30.50	299.10	0.00
5	320.70	0.22	27.20	297.90	0.00
6	320.70	0.21	27.50	298.20	0.00

7	320.70	0.18	26.80	297.80	0.00
8	320.70	0.17	26.70	298.00	0.00
9	320.70	0.15	23.80	296.90	0.00
10	320.70	0.13	25.10	297.60	0.00
1	320.70	0.32	34.10	298.90	0.00
2	320.70	0.30	35.50	299.60	0.00
3	320.70	0.27	31.90	298.40	0.00
4	320.70	0.25	31.10	298.40	0.00
5	320.70	0.23	27.90	297.30	0.00
6	320.70	0.21	28.30	297.60	0.00
7	320.70	0.19	27.50	297.20	0.00
8	320.70	0.17	27.40	297.40	0.00
9	320.70	0.15	24.30	296.40	0.00
10	320.70	0.13	25.70	297.00	0.00
1	320.70	0.32	34.70	298.10	0.00
2	320.70	0.30	36.40	298.70	0.00
3	320.70	0.27	32.30	297.50	0.00
4	320.70	0.25	31.70	297.60	0.00
5	320.70	0.23	28.40	296.60	0.00
6	320.70	0.21	28.70	296.90	0.00
7	320.70	0.18	27.80	296.50	0.00
8	320.70	0.17	27.50	296.60	0.00
9	320.70	0.14	24.50	295.70	0.00
10	320.70	0.13	25.90	296.20	0.00
1	320.70	0.32	35.50	297.60	0.00
2	320.70	0.30	37.20	298.20	0.00
3	320.70	0.27	32.90	297.00	0.00
4	320.70	0.25	32.10	297.00	0.00
5	320.70	0.22	28.50	296.20	0.00
6	320.70	0.20	29.10	296.40	0.00
7	320.70	0.18	28.00	296.10	0.00
8	320.70	0.16	28.00	296.20	0.00
9	320.70	0.14	24.80	295.30	0.00
10	320.70	0.13	26.30	295.90	0.00
1	320.70	0.33	36.00	297.00	0.00
2	320.70	0.30	38.00	297.50	0.00
3	320.70	0.27	33.30	296.50	0.00
4	320.70	0.25	32.50	296.50	0.00
5	320.70	0.22	29.00	295.70	0.00
6	320.70	0.21	29.40	295.90	0.00
7	320.70	0.18	28.40	295.60	0.00
8	320.70	0.16	28.30	295.70	0.00
9	320.70	0.14	25.00	294.90	0.00
10	320.70	0.13	26.50	295.40	0.00
1	320.70	0.33	36.40	296.70	0.00
2	320.70	0.30	38.40	297.20	0.00
3	320.70	0.27	33.60	296.20	0.00
4	320.70	0.25	32.80	296.20	0.00
5	320.70	0.22	29.40	295.40	0.00
6	320.70	0.21	29.70	295.60	0.00
7	320.70	0.18	28.50	295.30	0.00
8	320.70	0.16	28.50	295.40	0.00
9	320.70	0.14	25.20	294.70	0.00
10	320.70	0.13	26.70	295.10	0.00
1	320.70	0.33	36.80	296.30	0.00
2	320.70	0.31	39.00	296.80	0.00
3	320.70	0.27	33.80	295.80	0.00
4	320.70	0.25	33.10	295.80	0.00
5	320.70	0.23	29.60	295.10	0.00
6	320.70	0.21	30.00	295.30	0.00
7	320.70	0.18	28.90	295.00	0.00
8	320.70	0.17	28.80	295.10	0.00
9	320.70	0.14	25.60	294.40	0.00
10	320.70	0.13	27.00	294.80	0.00
1	320.70	0.32	37.00	296.10	0.00
2	320.70	0.30	39.00	296.50	0.00
3	320.70	0.27	33.70	295.50	0.00
4	320.70	0.25	33.20	295.50	0.00
5	320.70	0.22	29.70	294.90	0.00
6	320.70	0.20	30.10	295.10	0.00
7	320.70	0.18	29.00	294.80	0.00
8	320.70	0.16	28.90	294.90	0.00
9	320.70	0.13	25.60	294.30	0.00
10	320.70	0.12	26.80	294.60	0.00
1	320.60	0.42	34.90	300.70	0.00
2	320.60	0.40	37.10	301.60	0.00
3	320.60	0.37	34.00	300.40	0.00
4	320.60	0.35	32.80	300.30	0.00
5	320.60	0.32	28.80	298.80	0.00
6	320.60	0.30	29.40	299.20	0.00
7	320.60	0.28	28.40	298.70	0.00
8	320.60	0.26	28.00	298.80	0.00
9	320.60	0.24	24.80	297.70	0.00
10	320.60	0.22	25.60	298.10	0.00
1	320.60	0.43	35.90	299.50	0.00
2	320.60	0.40	38.60	300.40	0.00
3	320.60	0.37	34.90	299.10	0.00
4	320.60	0.35	33.40	299.00	0.00
5	320.60	0.32	29.50	297.80	0.00
6	320.60	0.30	30.00	298.20	0.00
7	320.60	0.28	28.90	297.70	0.00
8	320.60	0.26	28.60	297.80	0.00
9	320.60	0.24	25.20	296.70	0.00
10	320.60	0.22	25.90	297.10	0.00
1	320.60	0.43	37.00	298.80	0.00
2	320.60	0.40	39.60	299.60	0.00

3	320.60	0.37	35.50	298.40	0.00
4	320.60	0.35	34.20	298.30	0.00
5	320.60	0.32	30.20	297.20	0.00
6	320.60	0.30	30.50	297.40	0.00
7	320.60	0.28	29.50	297.00	0.00
8	320.60	0.26	29.20	297.10	0.00
9	320.60	0.23	25.40	296.00	0.00
10	320.60	0.22	26.40	296.50	0.00
1	320.60	0.43	38.10	298.20	0.00
2	320.60	0.41	40.70	298.90	0.00
3	320.60	0.37	36.40	297.80	0.00
4	320.60	0.35	35.00	297.60	0.00
5	320.60	0.32	30.90	296.60	0.00
6	320.60	0.30	31.20	296.90	0.00
7	320.60	0.28	29.90	296.40	0.00
8	320.60	0.26	29.60	296.50	0.00
9	320.60	0.23	25.90	295.60	0.00
10	320.60	0.22	26.80	295.90	0.00
1	320.60	0.43	38.90	297.70	0.00
2	320.60	0.41	41.60	298.40	0.00
3	320.60	0.37	37.10	297.20	0.00
4	320.60	0.35	35.60	297.20	0.00
5	320.60	0.32	31.40	296.20	0.00
6	320.60	0.30	31.80	296.40	0.00
7	320.60	0.28	30.30	296.00	0.00
8	320.60	0.26	30.20	296.10	0.00
9	320.60	0.23	26.20	295.20	0.00
10	320.60	0.21	27.20	295.60	0.00
1	320.60	0.43	39.60	297.50	0.00
2	320.60	0.40	42.20	298.10	0.00
3	320.60	0.37	37.50	297.10	0.00
4	320.60	0.34	35.70	296.90	0.00
5	320.60	0.31	31.90	296.10	0.00
6	320.60	0.29	32.20	296.30	0.00
7	320.60	0.27	30.70	295.90	0.00
8	320.60	0.25	30.60	296.00	0.00
9	320.60	0.22	26.50	295.10	0.00
10	320.60	0.21	27.20	295.40	0.00
1	320.60	0.43	40.90	297.30	0.00
2	320.60	0.41	43.60	297.90	0.00
3	320.60	0.37	38.50	296.90	0.00
4	320.60	0.35	36.60	296.70	0.00
5	320.60	0.32	32.90	296.00	0.00
6	320.60	0.30	32.90	296.10	0.00
7	320.60	0.27	31.60	295.70	0.00
8	320.60	0.25	31.30	295.80	0.00
9	320.60	0.23	27.30	295.00	0.00
10	320.60	0.21	28.20	295.30	0.00

1	320.60	0.44	42.50	297.30	0.00
2	320.60	0.42	45.10	297.80	0.00
3	320.60	0.38	39.90	296.90	0.00
4	320.60	0.35	37.80	296.70	0.00
5	320.60	0.32	34.10	296.00	0.00
6	320.60	0.30	34.20	296.10	0.00
7	320.60	0.27	32.70	295.70	0.00
8	320.60	0.25	32.60	295.80	0.00
9	320.60	0.23	28.60	295.10	0.00
10	320.60	0.21	29.00	295.30	0.00